DETERIORATION OF A FILLED GLASS FIBRE REINFORCED POLYESTER COMPOSITE IN AQUEOUS ENVIRONMENTS

By

DAVID L. WOYTOWICH

A Thesis
Submitted to the Faculty of Graduate Studies
in Partial Fulfilment of the Requirements
for the Degree of

Doctor of Philosophy

Department of Civil Engineering
University of Manitoba
Winnipeg, Manitoba

ISBN 0-315-76942-4

DETERIORATION OF A FILLED GLASS FIBRE REINFORCED POLYESTER COMPOSITE IN AQUEOUS ENVIRONMENTS

BY

DAVID L. WOYTOWICH

A thesis submitted to the Faculty of Graduate Studies of the University of Manitoba in partial fulfillment of the requirements of the degree of

DOCTOR OF PHILOSOPHY

DETERIORATION OF A FILLED GLASS FIBRE REINFORCED POLYESTER COMPOSITE IN AQUEOUS ENVIRONMENTS

ABSTRACT

Glass fibre reinforced plastics (FRP) are used extensively in the fabrication of underground piping and storage vessels for water and sewage applications. For reasons of economy, these composites are manufactured with fillers such as calcium carbonate and aluminum trihydrate (ATH), which may compromise their long-term durability in the field.

Preliminary laboratory tests were conducted (52 weeks) at room temperature (25°C) and elevated temperatures (45°C) to evaluate the long-term deterioration behaviour of an experimental filled filament wound (FFW) polyester composite in various simulated aqueous field environments. Acidic environments were identified as having the most deleterious effect on postcured FFW composites.

The latter phases of the experimental research program focused on extreme acidic field environments. One particular application of interest to engineers is the low pH conditions (pH 2.2 to 2.5) found in the collection and storage of sewage. Deterioration was measured in terms of changes in specimen weight, the loss of composite material, changes in flexural and hardness properties, increases in the concentration of calcium and aluminum ion in the leachate, the depth of penetration of a visible boundary through the thickness of the composite, and changes in diffusion characteristics. To monitor changes in diffusion characteristics, a new fluorescent-dye solvent exchange (FDSE) method was developed.

An Acid Deterioration (AD) model was developed to quantify the rate of

deterioration of FFW composites exposed to acidic environments. The AD model, which claims that the rate of deterioration, as measured by the depth of penetration, is proportional to the square root of immersion time, was verified in different acidic environments. The primary chemical reaction associated with the sulfuric acid (pH 2.23) and acetic acid (pH 2.22) was the dissolution of calcium carbonate. The rate of deterioration of the acetic acid specimens was found to be 1.6 to 3.9 times greater than the sulfuric acid specimens under accelerated temperature conditions (45°C). The intrinsic diffusion coefficients in the degraded layer of these specimens were estimated to be 5.02×10^{-5} and 5.07×10^{-6} $mm^2.sec^{-1}$, respectively.

Based on the findings of this work, it is suggested that the CSA Standard CAN3-B66-M85 for the manufacturing of prefabricated septic tanks be revised to include an accelerated laboratory test procedure to quantify the rate of deterioration of materials exposed to acidic (sewage) environments.

To God and my Family

(Marguerite, Jenna, Jonathon, and John)

ACKNOWLEDGEMENTS

Sincere gratitude and appreciation are extended to members of my thesis advisory committee: Dr. Jan A. Oleszkiewicz and Dr. Arthur B. Sparling, Department of Civil Engineering; Dr. Martin W. King, Department of Clothing & Textiles, and Dr. Myron G. Britton, Department of Agricultural Engineering, the University of Manitoba, for their assistance, guidance and wisdom during the investigative, and analytical phases of this research.

Special appreciation goes to Dr. Walter Michalyna, Agriculture Canada; Dr. Emmanuel Attiogbe, Master Builders USA, and Mr. Hector Poggi-Varaldo, Department of Civil Engineering, the University of Manitoba, for their commentary contributions and assistance in testing and the use of laboratory equipment.

Special thanks goes to Mr. Fred Champagne and Mr. Fred Olynk of Fibre West Industries for their support and financial assistance. Their contribution regarding the supply of materials is much appreciated.

The financial support for graduate research provided by the National Research Council Canada (IRAP-M) and by the Canada Mortgage and Housing Corporation (CMHC University Scholarship Program) is gratefully acknowledged.

The analysis of laboratory data by three undergraduate students: Mr. Derek Belsham, Mr. Charles Boulet, and Ms. Agatha Yu is much appreciated. Thanks go to Ms. Judy Teerhuis, Department of Textiles and Clothing, and Mr. Gary Burgess, Department of Botany, the University of Manitoba, for their assistance in the analyses of (visual and fluorescent) photomacrographs.

Analytical testing of mechanical properties by Mr. S. Welsh and

Ms. D. Meagher of FiberGlas Canada Inc. is gratefully acknowledged. Thanks are also extended to Mr. A. Jakilazek and Ms. T. Paton of the Manitoba Department of the Environment (WM Ward Technical Services Lab.) for their assistance in chemical analyses.

Very special thanks go to Judy Tingley, Department of Civil Engineering, the University of Manitoba for her daily invaluable assistance, her attention to standards of high quality research, and her dedication to students. Thanks go to my fellow students: Mr. Daryl McCartney and Mr. Hector Poggi-Varalda for their advice and friendship during the difficult times.

Special gratitude is especially extended to Ingrid Trestrail for editing and typing this manuscript under very demanding time constraints.

Love, gratitude and appreciation go to my family over the last seven years. Special love and gratitude goes to my wife Marguerite for her support, understanding, patience and confidence in me to complete this work. To my children (Jenna, Jonathon and John) for their personal sacrifices during the completion and writing of this thesis. I look forward to spending more time with them.

Gratitude and appreciation go to my mom, dad (passed away December 24th, 1989), dad and mom (Lapka), and numerous relatives and friends. Without their encouragement and support it would have been difficult to complete this work. I would especially like to thank Wesley and Marianne for the use of their personal computer during the writing of this thesis.

Lastly, I would like to thank God for giving me the courage, guidance, health and spiritual strength to complete this work.

TABLE OF CONTENTS

LIST OF TABLES

LIST OF FIGURES

LIST OF ABBREVIATIONS

AA	Atomic absorption
AASHTO	American Association of State Highway and Transportation Officials
AC	Acid comparison
ACPA	American Concrete Pipe Association
AD	Acid deterioration
AISI	American Iron and Steel Institute
ASTM	American Society for Testing of Materials
ATH	Aluminum trihydrate (raw material: Solem Industries) FRP Glass fibre-reinforced plastics
CGSB	Canadian Government Specifications Board
CSA	Canadian Standards Association
CSP	Corrugated steel pipe
CRC	Chemical Rubber Company
FVC	Filler-volume-concentration
FD	Fluorescent dye
FDSE	Fluorescent-dye solvent exchange
FFW	Filled filament wound
FRP	Glass fibre-reinforced plastics
GS	Galvanized (zinc-coated) steel
HC	Heat cure
IA	Image analysis
MDH	Moisture desorption heat

MEK	Methyl ethyl ketone
meq	Milli-equivalents
MIC	Microbial induced corrosion
MIP	Mercury intrusion porosimetry
MS	Mild steel
PA	Postcure acid
PS	Preliminary screening
PVC	Polyvinyl chloride
RPM	Reinforced plastic mortar
SA	Solvent absorption
SCL	Sandy clay loam
SD	Standard deviation
SE	Solvent exchange
SEM	Scanning electron microscopy
SMC	Sheet moulding compounds
TEM	Transmission electron microscope
WPCF	Water Pollution Control Federation

LIST OF SYMBOLS

A	Rate of deterioration (regression coefficient)
A_{ac}	Rate of deterioration in acetic acid
A_r	Relative rate of deterioration ratio, A_{ac}/A_s
A_s	Rate of deterioration in sulfuric acid
B	ml of EDTA titrant to determine Ca^{++} as mgL^{-1} of $CaCO_3$
b	Beam width, mm
b_1	Chemical reaction constant
C	Concentration of the diffusing species, moles·cm^{-3}
C_i	Initial concentration of diffusing species, moles·cm^{-3}
C_e	Concentration of diffusing species at equilibrium, moles·cm^{-3}
C_f	Correction factor for partially cured FFW specimens, constant
C_A	Concentration of the diffusing species A, moles·cm^{-3}
C_{AB}	Concentration of H^+ ions in bulk solution, moles·cm^{-3}
D	Diffusion coefficient, $mm^2.sec^{-1}$
D_1	Deflection lag factor, dimensionless
D_d	Diffusion coefficient in the acid-degraded layer, $mm^2.sec^{-1}$
D_e	Effective (one-dimensional) diffusion coefficient, $mm^2.sec^{-1}$
D_o	Pre-exponential factor, constant
d	Beam depth, mm
E_1	Flexural modulus of pipe material, MPa
E	Flexural modulus of FFW specimens, GPa
E'	Modulus of soil reaction, MPa

E_d	Activation energy, kcaL.G-mole^{-1}
E_{fo}	Initial dry flexural modulus of large FFW specimens, GPa
E_{to}	Initial dry tensile modulus of large FFW specimens, GPa
E_f	Dry flexural modulus of large FFW specimens, GPa
E_o	Initial dry flexural modulus of small FFW specimens, GPa
F	Constant, mm^2
G_1	Gram - molecular weight of $Al_2O_3 \cdot 3H_2O$
G_2	Gram - molecular weight of two moles of Al^{+++}
G	Time dependent parameter, dimensionless
H	Wet Barcol hardness of small FFW specimens
H_o	Dry Barcol hardness of small FFW specimens
H_o	Initial Barcol hardness of non-lined surface of FFW specimens
h	Depth of acid penetration, mm
h_1	Depth of concrete carbonation, cm
I	Moment of inertia, mm^4
J	One dimensional flux of diffusing species, moles.mm^2.sec
K	Acid coefficient of proportionability, sec.mm^{-2}
K_b	Bedding constant, dimensionless
K_1	Carbonation coefficient, mm.sec$^{-1/2}$
L	Original thickness of FFW specimen, mm
L_1	Support span, mm
l	Thickness of a plane sheet or specimen, mm
M_e	Maximum moisture content at saturation, %
M_L	Percent moisture loss, %

$M_{(t)}$	Percent weight gain, %
m	Slope of the tangent from load deflection curve, $N.mm^{-1}$
m_e	Weight of diffusing species at equilibrium (saturation), g
m_i	Initial weight of diffusing species, g
m_l	Weight of moisture lost at drying time t_1, c
$m_{(t)}$	Weight of diffusing species at immersion time (t), g
N_A	Mass of hydrogen, moles
N_B	Mass of calcium carbonate, moles
P_1	Corrosion rate of metal coupons, $mm.year^{-1}$
P	Load at a given point on the load-deflection curve, N.
ρ	Density of solid reactant (B) in composite, $g.cm^{-3}$
Q_a	Molar flux of H^+ within the degraded layer, $mole.m^{-2}.s^{-1}$
R	Mean pipe radius, mm
R	Universal gas constant
S	Wet flexural strength of small FFW specimens, Mpa
S_1	Ultimate stress at failure, MPa
S_a	Absorption slope of the linear portion of the absorption isotherm plot, $(t)^{-½}$
S_d	Desorption slope of the linear portion of the desorptions isotherm plot, $(t')^{½}$
S_f	Dry flexural strength of large FFW specimens, Mpa
S_{fo}	Initial dry flexural strength of large FFW specimens, Mpa
S_t	Tensile strength of large FFW specimens, Mpa
S_{to}	Initial tensile strength of large FFW specimens, Mpa

S_u	Initial dry flexural strength of small FFW specimens, Mpa
T_1	Absolute temperature in degrees Kelvin
t	Immersion time period, (weeks)
t′	Drying time period, min.
∀	Volume of unreacted core, cm^3
W_1	Weight of metal coupon after immersion time = t_1, g
W_2	Weight of metal coupon after immersion time = t_2, g
W_c	Vertical earth load on pipe, $N.mm^{-1}$
W_f	Weight of oven dried (112°C at 36 h) immersed specimen, g
W_i	Initial weight of dry specimen, grams
W_L	Vertical live load on pipe, $N.mm^{-1}$
W_m	Dry material weight loss, %
W_t	Weight of moist specimen, grams
$W_{t'}$	Weight of degraded specimen at drying time t_1, s
X	Direction of space coordinate, mm
X_1	Horizontal deflection of flexible pipe, mm
Y	Deterioration test parameter

LIST OF SPECIMENS

Specimen Type	Environment Type	Temp. (°C)	FFW Postcure Conditions	Metal Type
(A) FFW Deterioration				
D25	Deionized water	25°C	112°C, 36 h	N/A
D45	" "	45°C	112°C, 36 h	N/A
B25	NaOH (buffered)	25°C	112°C, 36 h	N/A
B45	" "	45°C	112°C, 36 h	N/A
1A45	H_2SO_4 (pH 3.5-4.5)	45°C	112°C, 36 h	N/A
2A45	HCl (pH 3.5-4.5)	45°C	112°C, 36 h	N/A
3A45	CH_3COOH (pH 3.5-4.5)	45°C	112°C, 36 h	N/A
S45	Mg SO_4	45°C	112°C, 36 h	N/A
R45	MIC soil	45°C	112°C, 36 h	N/A
(B) Metal Corrosion Experiment				
DS25	Deionized water	25°C	N/A	MS*
DS45	" "	45°C	N/A	MS
DG25	" "	25°C	N/A	GS**
DG45	" "	45°C	N/A	GS
BS25	NaOH (buffered)	25°C	N/A	MS
BS45	" "	45°C	N/A	MS
BG25	" "	25°C	N/A	GS
BG45	" "	45°C	N/A	GS
AS25	H_2SO_4 (ph 3.5-4.5)	25°C	N/A	MS
AS45	" "	45°C	N/A	MS
AG25	" "	25°C	N/A	GS
AG45	" "	45°C	N/A	GS
RS45	MIC soil	45°C	N/A	MS
RG45	" "	45°C	N/A	GS
(C) Post-cure Acid Experiment				
S55-18	H_2SO_4 (ph 2.2-2.5)	45°C	55°C, 18 h	N/A
S55-36	" "	45°C	55°C, 36 h	N/A
S112-18	" "	45°C	112°C, 18 h	N/A
S112-36	" "	45°C	112°C, 36 h	N/A
(D) Acid Comparison Experiment				
D112	Deionized water	45°C	112°C, 36 h	N/A
D25	" "	45°C	room temp.	N/A
S25	H_2SO_4 (pH 2.2-2.5)	45°C	room temp.	N/A
A25	CH_3 COOH (pH 2.2-2.5)	45°C	room temp.	N/A

CHAPTER 1

INTRODUCTION

In the past, the selection of a material for a specific engineering application was based primarily on structural requirements such as strength and stiffness. Today more research is being focused on factors such as durability and the need to develop more corrosion-resistant materials. One reason for the interest in this area of research is the significant increase in costs associated with the replacement and maintenance of engineered structures in the field. Glass fibre reinforced plastics (FRP) are used extensively in the fabrication of underground piping and storage vessels for water and sewage applications. Blaga (1982) reported that reinforced polyester tubular composites are replacing steel for water distribution systems and concrete for sewage systems due to their improved resistance to corrosion or deterioration.

The utilization of fillers such as calcium carbonate is a new technique incorporated into the manufacturing of FRP structures to lower the cost of the product. Sheet moulding compounds (SMC) consisting primarily of chopped glass fibres, polyester resin and calcium carbonate fillers are widely used in commercial, space, and military applications (Springer, 1983). In Canada, filled FRP septic tanks are manufactured in accordance with the Canadian Standard Association (CSA) Standard CAN3-B66-M85 (1985) to meet initial strength requirements. The two most common fillers used in filled FRP structures are calcium carbonate ($CaCO_3$) and aluminum trihydrate ($AL_2O_3.3H_2O$).

Penn (1979) has stressed the importance of testing FRP composites under simulated service or real life conditions. Unfortunately, under such conditions, tests are often impractical and accelerated test procedures must be developed to reduce the time

required to evaluate changes in material properties. (Ciriscioli et al., 1987). For example, Craigie et al. (1986) conducted accelerated tests at elevated temperature (38° to 48°C) to quantify the effects of long-term methane exposure on FRP storage tanks. There is no standard procedure to evaluate in a stressed or unstressed state, the accelerated deterioration behaviour of filled FRP composites exposed to natural aqueous environments. It is hoped that this work will facilitate the establishment of a standard accelerated test procedure for materials exposed to such environments.

The experimental research program was designed to evaluate the long term deterioration behaviour of an FRP composite exposed to various aqueous environments. To this end an experimental filled filament wound (FFW) composite for underground tubular structural applications such as culvert piping and septic tanks was developed and is presented in Section 2.2. The structural layer of the FFW composite, consisting of continuous glass fibre reinforcement and a filled polyester-resin matrix, was designed on the basis of optimizing the flexural properties in the hoop direction so as to limit deflections in the field due to loading. A 750 mm diameter FFW pipe was fabricated (Fibre West Industries Ltd.) for test purposes. The filler materials used in the construction of the test pipe consisted of an equal proportion by weight of calcium carbonate (Snowhite) and aluminum oxide trihydrate (Solem ATH).

Prior to the start of the research program, a literature review was conducted to delineate aggressive aqueous environments which occurred naturally in the field (see section 2.3). This review included field studies related to the corrosion of galvanized corrugated steel pipe (CSP) culverts and the deterioration of concrete sewage structures. The information was used as a basis of selecting the laboratory environments for the experimental research program.

A flow diagram of the different phases (Phases 1, 2, 3, and 4) of the experimental research program is shown in Figure 1.0. Phase 1, which is referred to as the Preliminary Screening (PS) study, consisted of a field investigation and two laboratory experiments. The purpose of the field investigation was to characterize and obtain samples from an in situ aggressive soil for the two PS experiments. The soil samples were collected from a failed CSP culvert site near Harding, Manitoba.

The primary objective of the PS experiments (Chapter 3) was to evaluate and compare the deterioration behaviour of postcured[1] FFW composites and metals (steel and galvanized steel) following immersion in various laboratory aqueous (25°and 45°C) environments in order to identify the environment which would have the most deleterious effect on each material. Changes in weight loss, mechanical properties, and increases in the concentrations of calcium and aluminum ions in the leachate were monitored. A moisture desorption heat (MDH) method was also developed and used to monitor changes in the diffusion characteristics of wet-attacked, postcured FFW specimens.

New test methods were developed in Phase 2 (Chapter 4) in order to quantify more accurately the deterioration behaviour of FFW composites exposed to extreme acidic environments. The methods that were developed include: a gravimetric method to measure material weight loss, a fluorescent-dye solvent exchange (FDSE) desorption method to monitor changes in diffusion characteristics and two visual methods to measure the depth of penetration. These methods were used in a third experiment, the Postcure Acid (PA) experiment, to determine the effects of various postcuring conditions on the deterioration behaviour of FFW composites exposed to low pH (2.2 to 2.5) sulfuric acid

---

1 Postcured denotes specimens which were cured at 112°C for 36 hours prior to immersion.

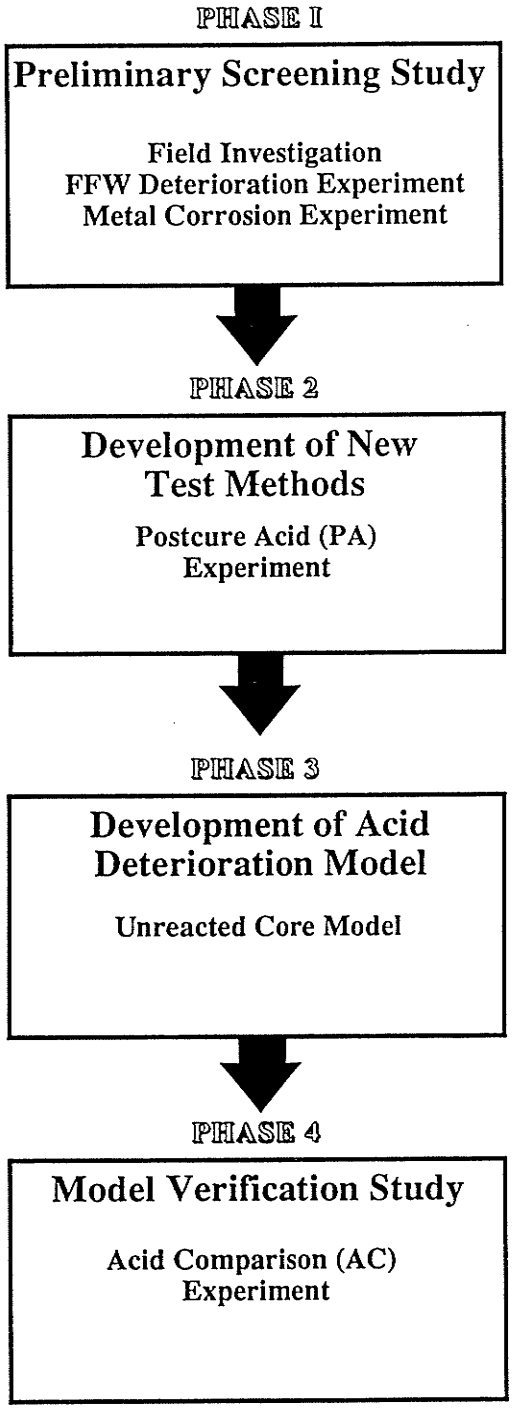

Figure 1.0 Flow diagram of experimental research program

environments.

An Acid Deterioration model, based on a special case of the moving boundary diffusion problem, was developed in Chapter 5 to quantify the rate of deterioration of FFW composites exposed to acidic environments. The model assumed that the resistance to acid diffusion through the degraded layer controls the rate of deterioration and claims that the advancing boundary of deterioration is proportional to the square root of time.

A fourth experiment, the acid comparison (AC) experiment, was designed to verify the model by comparing the rates of deterioration of virgin[2] FFW composites exposed to low pH (2.2 to 2.3) sulfuric and acetic acid environments, under accelerated temperature conditions (45°C). Model parameters and experimental data from the AC experiment were used to predict the intrinsic diffusion coefficients in the degraded layer of such composites.

---

2 Virgin denotes specimens that are cured at room temperature.

CHAPTER 2

BACKGROUND AND RESEARCH OBJECTIVES

2.1 GLASS FIBRE REINFORCED PLASTICS (FRP)

This section provides background information on the structural function and properties of the components of a glass fibre reinforced plastic (FRP) composite. The two primary structural components in FRP composites are the glass fibre reinforcement and the matrix.

The structural behaviour of FRP materials is normally based on two criteria. First, the initial strength and modulus properties are highly dependent on the nature and quantity of reinforcement used and secondly the majority of the applied load is carried by the fibres. It is known that the matrix does not provide strength and serves only to bond the glass fibre reinforcement and to transfer the loads to and between fibres (Blaga, 1979).

The matrix structure can be considered the "weak link" of the composite since it is more influenced by the environment or service condition (Reinhart and Clement, 1987). The properties of the matrix are important, however, since they may control the long term chemical resistance properties of the composite. It was assumed prior to start of the research program that the uncertainty in the long term performance of the filled FRP composite would be associated with the deterioration of the filler constituents.

2.1.1 Glass Fibre Reinforcement

Shackelford (1988) classified glass fibre reinforced composites as those containing discontinuous (chopped strand mat), cloth (woven fabrics) and continuous (rovings) glass fibres. FRP composites reinforced with chopped strand mat are isotropic in the plane of the lamina. Examples of isotropic composites are sheet moulding compounds (SMC) which are widely used for panel substitution in the automotive industry (Weng and Sun, 1979). Filled and unfilled SMC are fabricated using chopped strand mat. Generally, composites reinforced with chopped strand mat have lower load carrying capacity than those reinforced with glass rovings. This is because the loads applied to such composites must be transferred in shear to the randomly distributed fibres through interfacial bonding between the matrix and the glass (Reinhart and Clements, 1987).

Composites reinforced with woven glass fabric exhibit mechanical properties in only two orthogonal directions. These composites are referred to as having "orthogonally anisotropic" or "orthotropic" properties (Holmes and Just, 1983).

Filament winding is a manufacturing process whereby continuous glass rovings are impregnated with a resin admixture and wound on a mandrel in either the hoop and longitudinal (biaxial) directions or laid at an helix angle. One advantage of filament wound composites is that the orientation of the glass rovings can be aligned in different directions to optimize their anisotropic properties. The technique is often used in the fabrication of tubular FRP structures such as storage tanks and lightweight piping (McCarvill, 1987).

2.1.2. Filled Polyester-Matrix

Polyester resins are one of the most widely used commercial resin matrix systems (Updegraff, 1982). There are two forms of polyester resins; saturated and unsaturated polyesters. Saturated polyesters are resins that contain single carbon-carbon atoms and are usually prepared by the condensation polymerization of dibasic acids with dihydric alcohols. Unsaturated polyesters are the group of polyesters in which the dibasic acid component, consists of an unsaturated acid such as fumaric acid resulting in weak double bonds between the carbon atoms (Dudgeon, 1987). Consequently, the polymer is easily dissolved in a reactive vinyl monomer such as styrene to assist in cross-linking of the polyester chains (see Figure 2.0).

Inorganic filler particles are usually added to the unsaturated polyester and cross-linking monomer to extend rather than reinforce the matrix. Common cost-reducing fillers used in SMC materials include calcium carbonate and aluminum trihydrate (ATH). The SMC formulation first involves mixing the filler particles with the polyester resin admixture to form a paste. The addition of a catalyst or free radical initiator, such as an organic peroxide, results in the formation of a three dimensional thermoset plastic by cross-linking the unsaturated polymer to the monomer, filler particles and reinforcement. It is known that calcium carbonate fillers assist in reducing shrinkage of molded parts while ATH fillers provide improved flame retardancy characteristics (McCluskey and Doherty, 1987). Dudgeon (1987) reported data from Grayson and Eckroth (1982) which showed that while calcium carbonate (20 percent by weight) in unreinforced cured polyester resin improved matrix stiffness properties, the filler had little effect on strength characteristics.

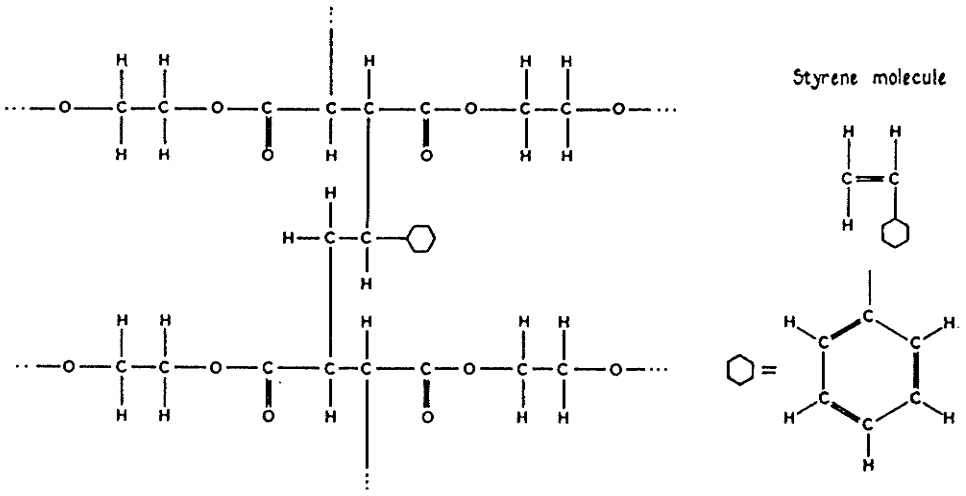

Figure 2.0 Cross-linking of polyester chains with styrene
(from Holmes and Just, 1983)

2.2 DEVELOPMENT OF AN EXPERIMENTAL COMPOSITE

Tsai (1979) has recognized that the construction of a structure from FRP composites is highly dependent on its specific application. There is a lack of research on the long-term durability of filled FRP structures exposed to naturally aggressive aqueous environments. To this end an experimental filled filament wound (FFW) composite for underground tubular applications such as piping (culverts) and storage (septic) tanks was developed. The FFW composite was designed on the basis of optimizing the orientation of the continuous glass fibres to ensure that the mechanical (directional) properties of the composite were fully utilized for such applications .

2.2.1 Structural: Underground Tubular Applications

Underground flexible FRP structures such as culverts and tubular septic tanks derive their ability to support earth and live loads from their inherent strength and the passive resistance of the soil as they deflect. Flexible CSP culverts are recognized as a soil-steel system in which the flexible steel conduit acts with the surrounding soil fill to support loads (AISI, 1984). As the active soil and live loads cause a decrease in the vertical diameter and an increase in the horizontal diameter the combined effects of active and passive pressures exerts relatively uniform compressive and bending stresses. These stresses occur primarily in the circumferential or hoop direction of the composite pipe wall. The structural design and underground installation procedures for plastic, polyvinyl chloride (PVC) and FRP, culverts closely parallels that of CSP culverts (AASHTO, 1988; Greenwood, 1975).

An equation developed by Spangler is recommended in ASTM D-3839 (1979), "Underground Installation of Flexible Reinforced Thermosetting Pipe and Reinforced

Plastic Motor Pipe", to estimate pipe deflections in the field. This equation relates the horizontal deflection to the load, material characteristics and properties of the soil and is expressed as follows:

[1] $$X_1 = [(D_1 W_c + W_L) K_b R^3] / (E_1 I + 0.061 E' R^3)$$

where:

X_1 = Horizontal deflection of the pipe, mm

D_1 = Deflection lag factor, dimensionless

W_C = Vertical earth load on pipe, $N.mm^{-1}$

W_L = Vertical live load on pipe, $N.mm^{-1}$

K_b = Bedding constant, dimensionless

R = Mean pipe radius, mm

I = Moment of inertia, mm^4

E′ = Modulus of soil reaction, MPa

E_1 = Flexural modulus of pipe material, MPa

It is evident from Eqn. [1] that the tubular structure should have sufficient local strength in bending and pipewall stiffness (E_1I) so as to develop and utilize the passive resistance of the soil ($0.061E'R^3$). In fact the Water Pollution Control Federation (WPCF,1970) has recommended as a practical measure that the value of E_1I should never be less than 10 to 15 percent of the term $0.061E'R^3$ and the allowable deflection in the field should not exceed five percent of the nominal diameter of the flexible pipe. It is apparent that significant loss in stiffness properties during the service life of the structure, as indicated by a decrease in the flexural modulus (E_1), could result in structural failure in the field. Accelerated laboratory testing can be used to evaluate

long-term changes in flexural properties.

2.2.2 Chopped FRP Composites

Various types of chopped FRP laminates have been recommended for tubular (water and sewage) applications. Watanabe (1979) has proposed a sandwich laminate which takes into account the resistance to acid attack and the required distribution of mechanical stresses. The laminate, shown in Figure 2.1a, consists of a layered core structure of unfilled polyester resin reinforced with chopped strand mat, sandwiched between woven glass fabric and corrosion-resistant surface mat layers. The reinforcing roving cloth is placed on both sides of the core structure so as to enhance flexural properties of the laminate. The unfilled surface mat layers contain low volumetric fibre fractions for acid resistance.

The Canadian Standard Association (CSA, 1989) has recently proposed a new filled laminate structure for FRP septic tanks. The multi-layered structure, shown in Figure 2.1b, consists of an unfilled exterior surface layer, a structural layer, and an anti-wicking barrier which is protected by an interior surface layer. The structural layer may consist of filled or unfilled chopped strand FRP layers which may be reinforced with a woven glass fabric. The structural layer in either case must be protected by an "anti-wicking barrier" of unfilled chopped FRP of at least 2.5 mm from the interior side exposed to the sewage environment. The exterior side of the structural layer must also be protected from natural aqueous environments by a corrosion liner of one or more layers of unfilled polyester resin having a range in thickness between 0.13 to 0.30 mm.

The CSA requirement for an anti-wicking barrier was based on the Canadian Government Specifications Board (CGSB, 1969) Standard 41-P-22 and the findings

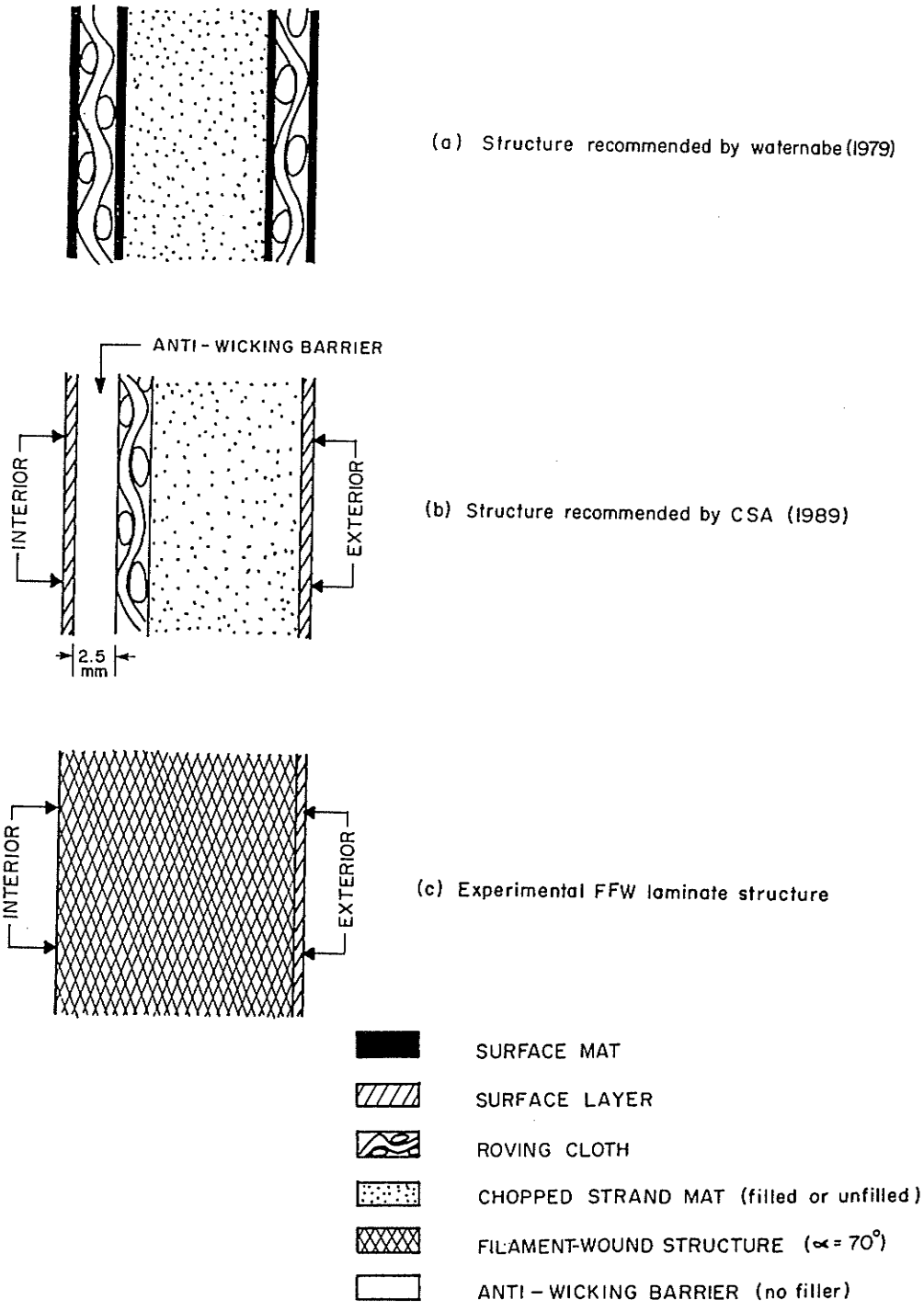

Figure 2.1 Various laminate structures for tubular applications

of an unpublished laboratory study conducted by FiberGlas Canada (1987). In this four year study, various filled and unfilled chopped GRP composites were immersed in acetic acid (initial pH 2.25) at room temperature. The experimental results showed that specimens containing calcium carbonate (33% by weight) or aluminum trihydrate (42% by weight) retained only 46 and 44 percent of their initial flexural modulus and 76 and 58 percent of their initial flexural strength properties, respectively, after four years. The CSA concluded that this reduction in flexural properties was associated with the chemical deterioration of the interfacial bond between the filled polyester-matrix and the glass fibres. It was also assumed that the primary deterioration mechanism involved the adsorption (wicking) of acetic acid along the discontinuous glass fibres.

2.2.3 Filled Filament Wound (FFW) Composite

There are two inherent disadvantages of chopped strand reinforced FRP composites. Firstly the use of short fibres prevents the composite from fully utilizing the high strength, high modulus mechanical properties of the continuous glass filaments. Instead the mechanical behaviour of the composite relies on the matrix to transfer the loads to the fibres and the integrity and efficiency of the fibre/matrix interfacial bond. If for some reasons such as fluid absorption or chemical action, the fibre/matrix bond loses its structural integrity, it follows that the mechanical properties of the composite will be impaired. Watanabe (1979) showed that for unfilled FRP composites reinforced with woven glass cloth, the bond strength at the interface was reduced by water after tensile fracture. This may not be the case when the reinforcement is provided by rovings of continuous filaments. For example, Fonda (1989) reported that the strength in filament wound laminates comes directly from the continuous filaments that can carry the

load without overloading the fibres.

The second disadvantage involves the orientation of the reinforcing phase. In most cases the design of the tubular structure may require greater mechanical properties in the hoop direction than the axial direction. However, in using orthotropic FRP materials to achieve such properties, the mechanical behaviour properties in the hoop direction cannot be controlled independently of those in the axial direction.

In this work it was decided that it was necessary to control the isotropy of the composite and to design an experimental composite that would optimize the flexural properties in the hoop direction so as to limit deflections in the field due to normal loading. This was accomplished by using a filament winding technique in which the spacing of the rovings and angle of winding were controlled to give a continuous filled structure free from discontinuities associated with fabric edges. The experimental filled filament wound (FFW) structure, shown in Figure 2.1c, is well suited to a small scale research study under controlled conditions.

2.2.4. Description of Experimental FFW Composite

The FFW laminate consists of a structural layer and an exterior surface layer. The structural layer was fabricated using continuous Type E-glass rovings, impregnated with a uniform mixture of orthophthalic unsaturated polyester resin and fillers (weight ratio; 1:1). The impregnated glass rovings were helically wound at an angle of 70° from the axis of the 750 mm diameter pipe. The two filler materials used in the resin-filler matrix were calcium carbonate and ATH (weight ratio: 1:1).

A blue pigmented polyester resin (corrosion) liner was applied to the exterior surface of the pipe during fabrication. The average thickness of the surface layer was

determined, using a visual light microscope, to be 0.253 mm (SD = 0.092 mm). The interior surface of the composite was not lined in order to quantify the rate of deterioration for a non-protected surface.

The average density of the experimental FFW composite (described in Table 2.0) was determined to be 1.88 grams·cm^{-3}. The density of the composite material was determined in accordance with ASTM-D-792 (1986). For information regarding the chemical analysis and material properties of each FFW component, the reader is referred to Appendix I. The filler constituents, Solem ATH and Snowhite $CaC0_3$, accounted for 32 percent of the total weight of the FFW composite. The volume relationship of filler to resin (FVC) is approximately 2.0. A further description of the physicochemical properties of each filler constituent is presented in the following sections.

2.2.4.1 Solem ATH Filler Properties

The Solem ATH filler particles used in the FFW composite is a material which is produced as a by-product from the Bayer chemical process (Solem, 1988) for chemical separation of pure aluminum oxide from Bauxite ore. Solem ATH is 99.5 percent by weight pure aluminum oxide trihydrate ($AL_20_3.3H_20$). The remaining 0.5 percent consists of various oxide impurities. The average diameter of each particle is 15 μm and ranges from 1 to 45 μm. Typical chemical, physical and particle size distribution properties are described in Appendices I-3, and I-4.

TABLE 2.0 Description of Experimental FFW Composite

Components	Constituents	Weight (%)	Specific Gravity ($g \cdot cm^{-3}$)
Exterior liner	pigment[1] (blue); general purpose polyester[2]	4.0	
Structural layer			
Roving	Continuous E-glass filaments[3]; silane treated (diameter 0.025 mm)	32.0	2.54
Resin	Orthophthalic unsaturated[4]; polyester-alkyd; styrene-cross linking agent	32.0	1.1-1.3
Filler	Solem ATH[5] Snowhite calcium carbonate[6]	16.0 16.0	2.4-2.6
[1] CP4000	Manufactured by FiberGlas Canada, Guelph, Ontario		
[2] F11-2000	Manufactured by FiberGlas Canada, Guelph, Ontario		
[3] Type E-CR	Manufactured by FiberGlas Canada, Guelph, Ontario		
[4] W1840	Manufactured by GWIL Industries, Burnaby, B.C.		
[5] Solem-336LV	Manufactured by Solem Industries Inc., Norcross, Georgia		
[6] Snowhite 452	Manufactured by Steep Rock Resources Inc., North York, Ontario		

Pure aluminum trihydrate consists of 34.6 percent by weight of chemically-combined water and is also chemically expressed as aluminum hydroxide (2 $AL(OH)_3$). It is recognized as a flame retardant and smoke suppressant in unsaturated polyester composites (Hindersinn and Witschard, 1978). The low endothermic heat of hydration

of aluminum trihydrate of 0.28 kcaL.g^{-1} and the diluent and cooling effect of the water vapour that is released prevents the ignition of filled polymer composites at flame temperatures (Connolly and Thornton, 1965; Solem 1988). The thermodynamic flame retardancy properties of ATH filler materials are beneficial to culvert structures in that they are often subject to ditch fires.

Aluminum hydroxide compounds also have amphoteric properties, in that the solubility of its solid phase increases for both acidic and basic conditions (Weber, 1972; Benefield, 1982). The maximum theoretical concentrations of soluble aluminum species which can exist in water at equilibrium with the aluminum hydroxide precipitate at 25°C are presented as a function of pH in Figure 2.2. According to solubility equilibrium criteria, there is no tendency for a precipitate to occur at pH levels below 4.0. Typical chemical dissolution expressions for basic and acidic reactions are described below:

[2] $$\textit{Base Reaction:}\quad 2AL(OH)_3 + 2OH^- \rightarrow 2AL(OH)_4^-$$

[3] $$\textit{Acid Reaction:}\quad 2AL(OH)_3 + 6H^+ \rightarrow 2AL^{+++} + 6H_2O$$

The complete characterization of a reaction requires not only an evaluation of the equilibrium condition but more importantly the rate of the reaction. Unfortunately, there is little information available on the rate of dissolution of Solem ATH in acids or bases.

Because of the lack of information, an eight week preliminary laboratory experiment was conducted at room temperature (20.5°C) conditions to obtain a better understanding of the dissolution properties of Solem ATH particles in acidic environments. The experiment was designed to compare the acid dissolution behaviour

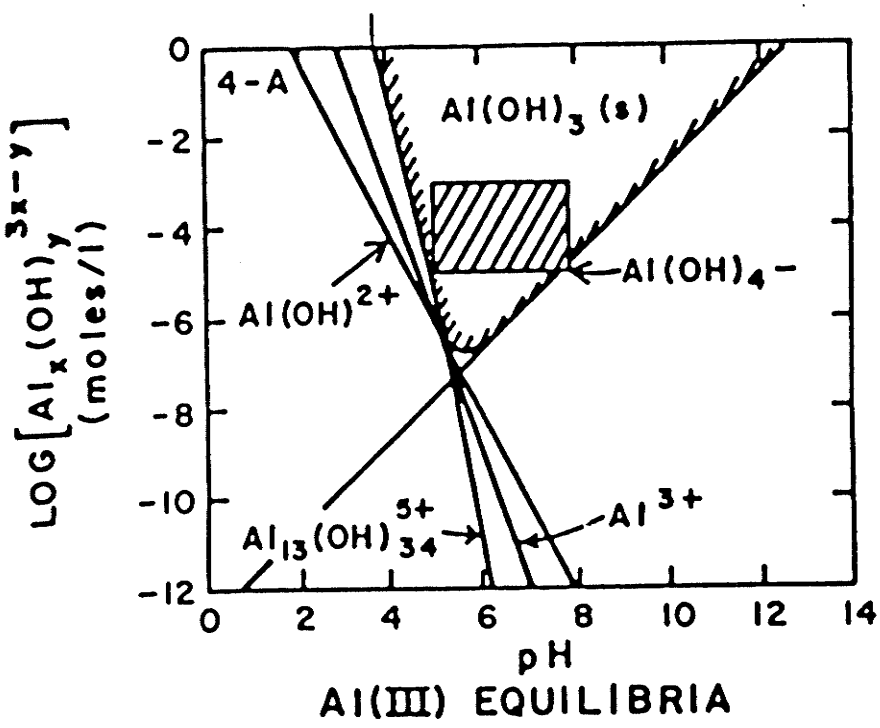

Figure 2.2 Solubility equilibria diagram for aluminum hydroxide at 25°C (from Weber, 1972)

of Solem ATH and commercial grade $2AL(OH)_3$. Forty grams of Solem ATH and $2AL(OH)_3$ were added to a two-L solution of sulfuric acid at two pH levels. This represented an initial concentration of approximately 6,915 $mg.L^{-1}$ as aluminum (AL^{+++}) ion. The AL^{+++} concentration in solution was subsequently measured on a weekly basis in accordance with Standard 303 C (1985) using an atomic absorption (SpectrAA-20; Varian) spectrophotometer. A summary of test results for pH and dissolved Al^{+++} concentrations are presented in Appendices I-5 and I-6.

It is evident from Figure 2.3 that increases in the AL^{+++} concentration, although slightly higher for Solem ATH, were similar for each pH condition. The experimental data also shows that the rate of dissolution is dependent on pH and is much greater for the lower pH (1.33-1.34) condition. The aluminum ion concentration appears to reach an asymptote between 100 and 150 $mg.L^{-1}$ for the higher pH (2.09-2.15) condition. The theoretical saturation concentration of Al^{+++}, based on a k_{sp} of $10^{-32.34}$ (Benefield, 1982) for aluminum hydroxide at 25°C, was determined to be 5.5 x 10^7 $mg.L^{-1}$ at pH 2.12 (see Appendix I-7). The experimental results suggest that both Solem ATH and aluminum hydroxide could be effective fillers in FRP structures exposed to low pH acidic (sulfuric acid) field environments. Further research is required to explain the difference between theoretical and observed results. The effectiveness of these fillers in low pH sulfuric acid environments is, associated with their low rates of dissolution.

2.2.4.2 Snowhite ($CaC0_3$) Filler Properties

The Snowhite ($CaC0_3$) filler used in the fabrication of the composite consists of untreated natural ground limestone. Snowhite is only 95.0 percent by weight pure

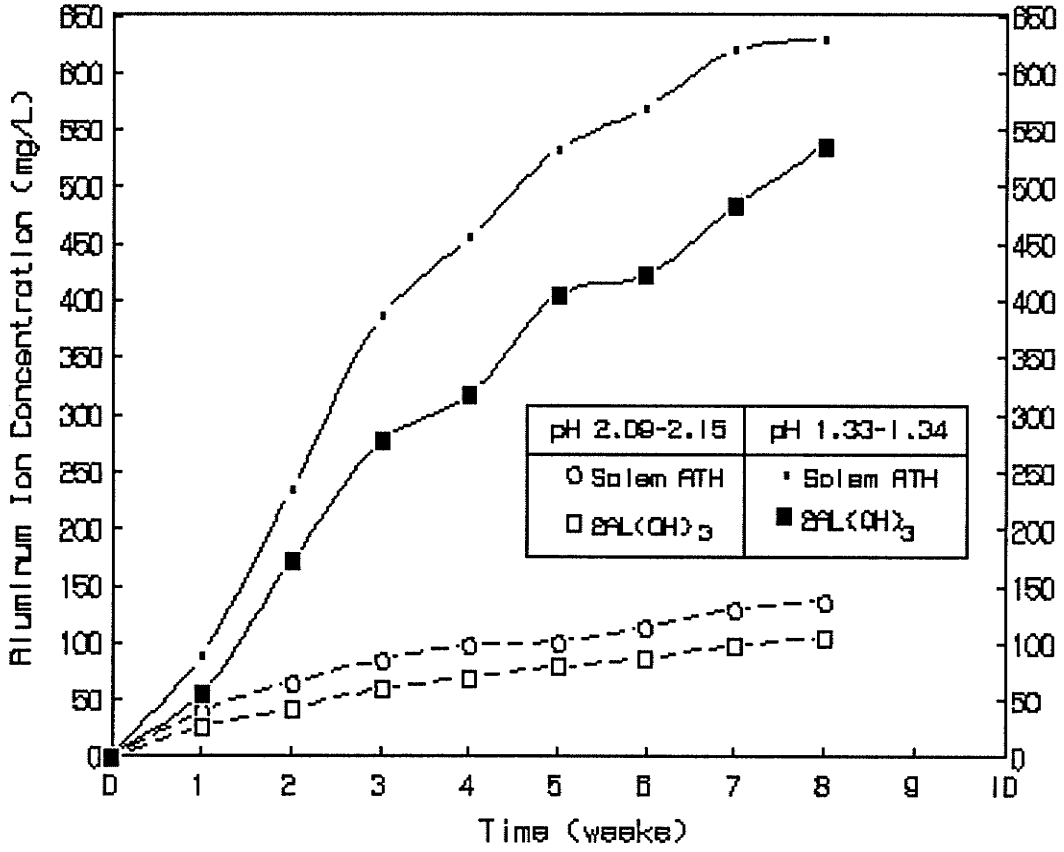

Figure 2.3 Dissolved Al^{+++} concentration as a function of time for Solem ATH and $2Al(OH)_3$ in sulfuric acid

calcium carbonate. The remaining 5 percent consists of various oxide impurities (see Appendix I-8). The mean filler particle size is 17 μm. It was reported (CRC, 1973) that the saturation concentration of natural limestone ranges from 14.25 to 18.75 mg/L for cold and hot water, respectively. Calcium carbonate because of its low solubility is more resistant to leaching in water environments. It is, however, readily dissolved in low pH acidic environments.

[4] $$CaCO_3 + 2H^+ \rightarrow Ca^{++} + CO_2 + H_2O$$

One advantage of calcium carbonate is that large amounts of this filler can be added while still maintaining a processable paste (McCluskey and Doherty, 1987). However, Monte and Sugerman (1986) showed that untreated $CaC0_3$ particles in FRP materials contain many latent areas for composite failure due to entrapped air and moisture. In such cases the interfacial bond between calcium carbonate fillers and resins can be improved by surface treatment with stearic acid and titanium coupling agents (Seymour and Carrahers, 1981).

2.2.4.3 Inorganic Microstructural Characteristics

Scanning electron microscopy (SEM) was utilized in this work to characterize the inorganic microstructural features of the experimental FFW composite. A SEM (JEOL-JSM 840) combined with a dispersive x-ray analyzer (Tracor Northern 5500) was used for this purpose. The function of the x-ray analyzer was to evaluate the microstructural distribution of inorganic elemental atoms, expressed as a percentage by weight, in a given scanning area.

SEM measurements were taken at various locations along the thickness of post-

cured virgin specimens (8 mm x 8 mm x 4.8 mm). It was found that a minimum scanning area of 0.0625 mm^2 (0.25 mm x 0.25 mm) or 500x magnification was effective in minimizing localized effects. The average microstructural characteristics of the laminate was determined from elemental-dispersive spectrums conducted at 17 different locations along the thickness of the specimen. A typical elemental-dispersive spectrum is shown in Figure 2.4.

A summary of the average percent of calcium, aluminum, and silica, expressed as a percentage by weight of the total weight of inorganic elements, is shown in Table 2.1 . The SEM results compared well with the estimated weights of calcium, aluminum and silicon used in the fabrication of the experimental FFW test pipe. A combination of these elements is present in the glass reinforcement (Type E) and filler components (Solem ATH, and Snowhite $CaCO_3$).

Table 2.1 SEM Analysis of Inorganic Microstructural Characteristics of Experimental FFW Composite

Inorganic Element	Average Percent by Weight	
	SEM Analysis	FFW Pipe*
Calcium	40.0 (5.1)	34
Aluminum	29.1 (5.9)	30
Silicon	21.1 (5.6)	25
Other	9.8 (6.4)	11

* Estimated

Brackets: standard deviation.

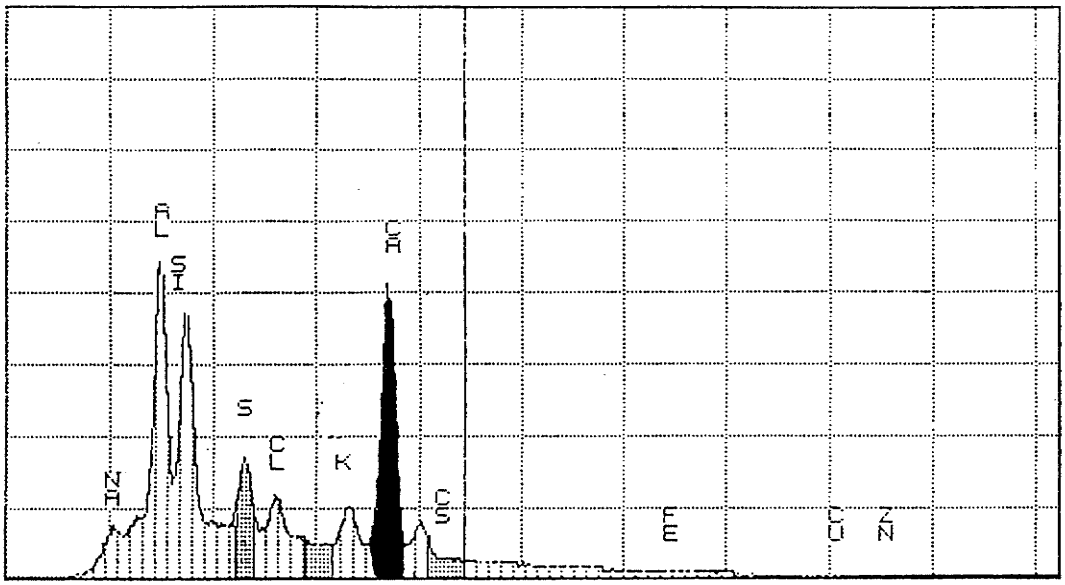

Figure 2.4 A typical elemental-dispersive spectrum along the thickness of an experimental FFW specimen

2.3 NATURAL AGGRESSIVE AQUEOUS ENVIRONMENTS

This section describes natural aqueous field environments that have resulted in the aggressive deterioration of concrete and metal structures. Field studies related to CSP culvert corrosion were also reviewed in order to delineate a typical aggressive *in situ* soil environment.

2.3.1 Soft Water

Soft waters, such as those draining from mountain regions and rainwater, are low in total dissolved solids. These waters have been found to be aggressive to concrete due to leaching of calcium hydroxide from the hardened cement pastes (Hoff, 1979). Such waters have been referred to as pure or carbonic species deficient waters (Benefield, 1982).

2.3.2 Acids

Groundwater acidity is due primarily to the presence of carbon dioxide (carbonic acid) and organic acids (humic acid) resulting from decaying organic matter. Biczok (1967) reported that the pH in the zone of humus formation may range from 3.6 to 4.0. Similar low pH environments were observed in peat and marsh soil when high concentrations of the sulfate ion (2000 $mg.L^{-1}$) and low buffering conditions (lack of lime) are present. The latter conditions resulted from the oxidation of reduced sulfur compounds such as hydrogen sulfide gas or pyrite into sulfuric or sulfurous acid. Holt (1967) in a corrosion study of CSP culverts identified strong acidic conditions in Podsol soils located in North-Eastern Minnesota. Smith and Ehrlich (1967) identified acidic (Sphagnum moss) surface soils in Eastern Manitoba where the pH range of the ground

water ranged from 3.5 to 4.0.

Starkey (1986) and Fontana (1986) reported that the chemical nature of the soil may also increase in acidity where conditions change seasonally from anaerobic to aerobic. It is known that in nutrient-rich environments such as sulfur fields, oil fields, and sewage, anaerobic microorganisms can produce large amounts of reduced sulfur compounds which may in turn be oxidized by other bacteria to sulfuric acid. Gaudy and Gaudy (1988) also noted that the sulfur oxidizing bacteria were responsible for the low pH conditions in acid drainage water from mines.

The US Environmental Protection Agency (EPA, 1985) identified sulfur oxidizing bacteria such as *Thiobacillus thioxidans* and *Thiobacillus concretivorous* as being the primary microorganisms responsible for the production of sulfuric acid and the deterioration of structures in contact with sewage. These bacteria oxidize sulfur compounds such as hydrogen sulfide to sulfuric acid, often reducing pH values to below 2.0, and are considered responsible for corrosion of concrete structures exposed to air (ASCE, 1980). Thus, surfaces above the liquid level in an anaerobic septic tank will be subject to sulfuric acid attack.

It is also known that anaerobic sulfate-reducing bacteria may outcompete methanogens for hydrogen gas (H_2) and produce acetate as an end product which could accumulate (Oleszkiewicz et al., 1989). This process could potentially subject the submerged surfaces in an anaerobic septic tank to acetic acid attack. Corrosion associated with anaerobic conditions is expected to be less severe than sulfuric acid (crown) corrosion since the generation of acetic acid usually stops below pH 5.0 (Postgate, 1984).

Others have reported the accumulation of total volatile acids (as measured by

acetic acid) in simulated landfill leachate (Chian et al., 1985). The pH of this leachate was observed to drop to a minimum value of 5.0.

2.3.3 Bases

Holt (1967) identified Chernozemic soils as having a pH range of between 8.0 and 10.0. Others reported that the pH in most soils and groundwaters normally do not exceed 9.5 (Haviland, 1966; Noyce and Ritchie, 1979). The basicity of natural groundwater is normally not deleterious to concrete since the material is chemically basic.

2.3.4 High Sulfate

Common soluble sulfate salts found in aqueous soil environments include: sodium sulfate, potassium sulfate, calcium sulfate (gypsum), and magnesium sulfate (Hoff, 1979). According to the U.S. Bureau of Reclamation, sulfate ion concentrations in water samples ranging from 1,500 to 10,000 $mg.L^{-1}$ have shown to result in severe concrete attack (ACPA, 1980). The primary mechanism of concrete deterioration involves the formation of gypsum and ettingrite which in turn induces swelling and cracking due to expansion stresses. It is recognized that magnesium sulfate which is common in seawater in concentrations of 2,000 $mg.L^{-1}$ is more deleterious to concrete than the other sulfate salts (Soroka and Itzhak, 1979).

2.3.5 Microbial Induced Corrosion (MIC) Soil

Numerous field studies have had limited success in establishing meaningful relationships between CSP culvert corrosion and specific factors related to the

characteristics of the *in situ* soil (Noyce and Ritchie, 1979; Holt, 1967; Patenaude, 1986). However, the factors identified in these studies which contributed to extensive CSP corrosion rates (0.07 to 0.14 $mm.y^{-1}$) included the chemical nature of the soil, the presence of sulfates and sulfate reducing bacteria (SRB) and the frequency of wetting and degree of submergence. Others identified SRB as the most causative organism of microbiologically induced corrosion (MIC) of metals at coastal and offshore marine sites and recommend that corrosion tests should be conducted in their *in situ* natural environment (Hamilton and Maxwell, 1986; Starkey, 1986).

Tiller (1986) presented criteria developed by Booth et al. (1967) to categorize the potential soil aggressiveness by determination of three soil parameters: electrical resistivity, redox potential, and water content (see Table 2.2).

Table 2.2 System to Assess Soil Aggressiveness

Soil Parameter	Property	
	Aggressive	Non-aggressive
Soil resistivity (ohm.cm)	<2,000	>2,000
Redox potential (volts) at pH 7.0	<0.40	>0.40
Water content (wt %)	>20	<20

2.4 EXISTING TEST PROCEDURES AND METHODS TO QUANTIFY DETERIORATION AND DIFFUSION COEFFICIENTS

2.4.1 Background

Presently, there is no standard test procedure to evaluate, in a stressed or unstressed state, the chemical resistance of a filled FRP composite. The only comparable

test practice for determining the chemical resistance of thermosetting resins used in unfilled FRP structures intended for liquid service is ASTM Standard C-581 (1983). Unfilled FRP laminate sheets are first prepared according to a standard procedure and subsequently immersed in a liquid service environment to determine the rate of deterioration or chemical resistance. The rate of deterioration is based on measuring changes in specimen dimensions, visual appearance, and mechanical properties (Barcol hardness; ASTM D-2583, flexural strength and modulus; ASTM D-790, tensile strength and modulus ASTM D-638).

The test procedure described in Standard C-581 is often impractical for room temperature service conditions, consequently, accelerated testing is often required. As well, some of the test methods recommended have limited application. For example, it has been found that FFW specimen dimensional changes cannot be measured accurately due to the curved nature of the irregularly shaped specimens. Therefore, one of the primary objectives in this work was to develop new analytical methods to quantify more accurately the rate of deterioration of FFW composites in natural aqueous environments.

Polymeric materials degrade by processes quite different than metals. In aqueous metal corrosion, the reactions occur at metal surfaces and are of an electrochemical nature. For neat (unfilled) polymers, Fontana (1986) and Bravenic (1983) reported that the deterioration mechanisms involve physicochemical processes such as swelling and dissolution. Similar mechanisms of deterioration have been reported for concrete materials exposed to low pH sulfuric acid solutions (Attiogbe and Rizkalla, 1980).

Table 2.3 lists some of the analytical methods used to evaluate the corrosion and chemical resistance of metals and cured thermoset resins. It is apparent from this table

Table 2.3 Analytical Methods for Metals and Cured Thermoset Resins (from Fenner, 1975)

Method	Alloys and Metals	Cured Thermoset Resins
Weight change:		
As penetration (loss in thickness)	Yes	No
% weight change	Rarely used	Yes
Permeation	Special gases (hydrogen blistering)	Yes
Change in hardness	Relatively few instances (graphitization, dezincification, etc.)	Yes
Dimensional changes	Yes (losses)	Yes
Tensile properties	Special case: usually not done	Generally no
Compressive properties	Special case: usually not done	Yes
Flexural properties	Special case: usually not done	Yes
Elongation	No	No
Appearance change of test sample:	Yes	Yes
Surface attach (pitting, craters, crevices, blistering, etc.)	Yes	Yes
Laminar-wall attack	Yes	Yes
Colour	Yes	Yes
Deleterious effects to environment	Yes	Yes

that the only methods that can be used to compare the corrosion/deterioration behaviour of metals and plastic materials include weight change, specimen dimensions and visual appearance.

The first laboratory test method to quantify the deterioration of a composite by measuring changes in the diffusion coefficient was developed for concrete materials using radioactive isotopes (Biczok, 1967). Unfortunately, radioactive isotope tracing techniques require stringent safety precautions and are very time-consuming. A simple and more reliable method of quantifying the pore structure and diffusion characteristics of wet attacked FRP composites is required.

Mercury intrusion porosimetry (MIP) and image analysis (IA) have been used to measure concrete structure properties such as porosity and pore-size distribution. These methods are described and evaluated in Section 2.4.2. Recently, nuclear probing methods have verified the application of classical diffusion theory by measuring the concentration of deuterium (D_2O) in graphite/epoxy composites as a function of depth of penetration (DeIasi and Schulte, 1984).

Most diffusion characterization studies in polymer systems have been associated with the transport of water vapour (moisture) and liquid water. The diffusion coefficient has been determined experimentally by the application of analytical diffusion models to the observed data. The fundamental theory of diffusion and a review of the absorption/diffusion behaviour of moisture and solvents is presented in Section 2.4.3.

2.4.2 Pore Structure Characterization Methods

2.4.2.1 MIP and IA Methods

MIP is based on the principle that the pressure required to force mercury (Hg) into the pores of a material is inversely proportional to the size of the pores. MIP techniques were employed by Wild et al. (1987) to determine the porosity and pore size distribution in cured clay-lime systems. However, Feldman (1984) reported that the injection of mercury at high pressures could disrupt the pore structure of blended cement pastes resulting in similar damage to that which would occur under severe oven-drying conditions. A second disadvantage of MIP tests is that there is no way of accurately predicting permeability/diffusion from porosity and pore size measurements. Hughes (1986) addressed this problem for cement pastes and developed an equation relating permeability to pore size, pore volume and pore tortuosity.

A method for large pore analysis using IA techniques has been developed by Parrot et al. (1984) for hydrated alite cement. Petrographic IA techniques were developed by Garychuck (1987) for carbonate rock porosity measurements. The latter technique combines vacuum evacuation with subsequent impregnation of a low viscosity epoxy resin (ER) mixed with methylene blue dye. However, difficulties were encountered in identifying the pore-solid boundary interfaces when viewing these images in black and white. Harvey's (1987) attempts to resolve the problem by using an ER mixture using a fluorescent (Rhodamine B) dye were unsuccessful.

MIP and IA techniques were not used in this work to characterize the pore structure of degraded FFW composites due to the potential risk of causing further damage (cracks) in the degraded layer of the laminate due to the high pressures required for fluid injection. Other reasons included the sensitivity to sample preparation and the

length of time required to run the tests.

2.4.3. Diffusion Characterization Methods

2.4.3.1 Theory of Diffusion

In 1855, Adolf Fick developed a mathematical model based on the same fundamental equations developed by Fourier for heat conduction. Fick developed the laws of diffusion and quantified the diffusion coefficient as a measurement of the rate at which the diffusion process occurs (Cheremisinoff, 1986; Shewmon, 1963; Schackelford, 1988). The diffusion flux for a chemical species is related to the diffusion coefficient by Fick's first law:

[5] $$J = - D \cdot (\partial C / \partial X)$$

where J is the one-dimensional flux of the diffusing species (mass$\cdot l^{-2} \cdot t^{-1}$), D is the diffusion coefficient ($l^2 \cdot t^{-1}$), C is the concentration of the diffusing species (mass$\cdot l^{-3}$), and X is the direction of the space coordinate.

In 1912, Perrin followed the movement of a spherical Brownian particle and determined experimentally that the displacement of a particle diffusing away from a central location was not proportional to time, but was proportional to the square root of time (Lavenda, 1985). The average diffusion coefficient was measured as the linear slope of the mean square displacement of the particle versus time curve.

In cases of non-steady state diffusion, such as the absorption or desorption of moisture in the thickness direction of a polymer sheet or concrete slab, the change in concentration and flux within this slab can be approximated from the one-dimensional case of Fick's second law of diffusion. The concentration gradient changes along the

diffusion path changes with time and this condition can be represented by a second order differential equation:

[6] $$(\partial C / \partial t) = \partial / \partial X \cdot (D \, \partial C / \partial X)$$

where $\partial/\partial X$ is the concentration gradient and t is the time coordinate.

Fick's Second Law is not an independent law, and is actually a modification of the first law when applied to a differential mass balance for specific boundary conditions. If the diffusion coefficient is constant and is independent of concentration, position and time, then Eqn. [6] becomes

[7] $$\partial C / \partial t = D \, \partial^2 C / \partial X^2$$

The concentration of the diffusing species through the thickness (l) of a plane sheet was determined as a function of position and time for a specific set of boundary conditions (Crank, 1965).

[8] $$C = C_i; \quad 0 < x < 1 \; t \leq 0$$

[9] $$C = C_e; \quad x = 0, \; x = 1 \; t > 0$$

The non-steady-state solution of Eqn. [7] and the initial condition [8] and the boundary condition [9] is

[10] $$\frac{C(t) - C_i}{C_e - C_i} = 1 - (4/\pi) \left\{ \sum_{n=0}^{\infty} (2n+1)^{-1} \sin [(2n+1) \, \pi \, x / l] \cdot \exp [-D(2n+1)^2 \, \pi^2 \, t / l^2] \right\}$$

The total amount of the diffusing species absorbed is obtained by the integration of Eqn. [10] through the thickness (l) of the flat sheet:

[11]
$$m(t) \int_0^l C(x,t)\, dx$$

which yields

[12]
$$\frac{m(t) - m_i}{m_e - m_i} = G = 1-(8/\pi^2)\{\sum_{n=0}^{\infty} (2n+1)^{-2} \exp\,[-(2n+1)^{-2}\, \pi^2\, (Dt/s^2)]\}$$

where

m_i, m(t) and m_e are the initial values, at time (t), and equilibrium (saturated) weights of the diffusing species in the material. G is a time-dependent parameter for a set of specific environmental conditions. For a material insulated on one side s is twice the thickness (s = 2*l*). Eqn. [12] is approximated by the expression (Shen and Springer, 1976):

[13]
$$G = 1 - \exp\,[-7.3\, (Dt/s^2)^{.75}]$$

Crank (1975) recognized that the diffusion coefficient in aniosotropic materials can vary in any direction throughout the laminate thickness and developed a simplified approach to determine the one-dimensional diffusivity of such materials. He assumed that if large, thin, flat sheets could be considered infinite in the y and z direction and the flow is arranged to be one-dimensional, then the diffusivity will be normal to the plane and will vary only in the x direction. Whitney et al. (1982) recommended that in cases where thin, flat, plastic composite specimens are not practical for moisture absorption

testing, then the edges (thickness dimension) of the specimens should be sealed to ensure that the "effective" diffusion coefficient (D_e) is one-dimensional.

2.4.3.2 Absorption/Diffusion Behaviour of Moisture and Solvents in Polymer Systems

The published literature concerning the absorption behaviour of atmospheric moisture in FRP and graphite reinforced polymer systems is voluminous. The absorption/diffusion behaviour is usually characterized by an isotherm plot of specimen weight gain (absorption) as a function of the square root of time.

Previous studies have shown cured epoxy resins absorb atmospheric moisture (water vapour) by instantaneous surface adsorption and this water is subsequently absorbed into the laminate (DeIasi and Whiteside, 1978; Shirrell, 1978; Carter, 1978; Bonniau and Bunsell, 1984). It has been recognized from tests in humid air that absorbed water is usually not in the liquid form but consists of groups of molecules linked by hydrogen bonds to the polymer. Liquid water, however, may be transported by capillary action along cracks and along fibre-matrix interfaces in composites.

The absorption of moisture in plastic composites has been extensively modelled by the one-dimensional case of Fick's Second Law. For example Shen and Springer (1976) and Whitney (1978) successfully applied the concentration-independent Fickian diffusion model to determine the moisture content and the diffusivity of graphite-epoxy aniosotropic (unattacked) composites in water vapour and liquid water environments. Bonniau and Bunsell (1984) applied two different diffusion models (single and two-phase models) for glass-epoxy composites exposed to water vapour and concluded it was

possible to describe the water vapour absorption properties of these materials using the Fickian diffusion model. The same glass-epoxy composites, however, showed different behaviour when immersed in water since whitening and cracking was observed. Miller (1984) presented a multi-media Fickian diffusion model for steady-state boundary conditions and Rao et al. (1984) for permeable fibre polymer composites. Hahn (1987) presented a unified qualitative micromechanistic model to explain observations of anomalous moisture diffusion behaviour.

The use of Fick's Second Law in describing moisture absorption/diffusion behaviour is based on the following assumptions:

1. One-dimensional diffusion that is normal to the specimen surface area.
2. A constant diffusion coefficient which depends only on temperature and is independent on moisture concentration, position and stress levels inside the material and time.
3. Isothermal and isobaric conditions on both sides of the specimen.
4. A constant moisture concentration on both sides of the specimen.
5. Initially, the temperature and moisture distributions are uniform inside the laminate.
6. No chemical reaction or material deterioration.

Shen and Springer (1976) developed an accelerated test method based on the above assumptions to determine the absorption behaviour of a series of graphite-epoxy composites exposed to humid air and to water. A parameter of practical significance defined in the test was the percent weight gain (M) (Springer, 1976):

[14] $$M(t) = (W_{(t)} - W_i)\ (W_i^{-1})\ (100)$$

where W(t) is the weight of moist specimen at time = t, and W_i is the initial weight of dry specimen at time = 0.

The weight of the absorbed moisture, m_t, is equal to the difference of the total weight of the moist material and the initial weight of the dry material.

[15] $$m_{(t)} = W_{(t)} - W_i$$

Therefore, combining [13] and [14]:

[16] $$M_{(t)} = m_{(t)} \cdot (W_i)^{-1}\ (100)$$

The effective diffusion coefficient (D_e) is derived from the initial slope of an absorption isotherm plot of percent moisture content (M_t), versus the square root of immersion time curve and the following expression:

[17] $$D_e = (\pi\ /16)\ (l \cdot M_e^{-1})^2\ (\Delta M \cdot \Delta t^{-1/2})^2$$

Where

D_e = Effective diffusion coefficient for material, two sides exposed to the environment, $mm^2.sec^{-1}$

M_e = Maximum moisture content at saturation, %

l = Thickness of specimen, mm

ΔM = Specimen weight change, %

Δt = Immersion time period (t_2-t_1)

Since the specimen thickness (l), and the maximum moisture saturation at equilibrium

(M_e), are constants, Eqn. [17] can be reduced to:

[18]
$$D_e = (F)\ (S_a)^2$$

Where:

F = $(\pi/16)\ (l \cdot M_e^{-1})^2$ or constant, mm^2

S_a = Absorption slope of the linear portion of the absorption isotherm plot, $(t)^{-1/2}$

An edge coating impermeable to moisture is recommended, otherwise, a correction factor must be made for "edge effects". One advantage of the Shen and Springer (1976) test method is that M_e can be estimated and total saturation of the specimen is not required in order to calculate the diffusion coefficient. To classify an absorption isotherm as Fickian, the initial portion of the absorption (weight gain) isotherm when plotted against the square root of immersion or drying time ($t^{1/2}$) must be linear up to 60 percent of the value of the maximum moisture content or equilibrium is reached (Crank, 1965).

Numerous studies investigating the absorption of water vapour and liquid water in graphite/glass reinforced epoxy laminates have shown the diffusion coefficient to be independent of concentration and related to temperature by the Arrhenius relationship (DeIasi and Whiteside, 1978; Whitney and Browning, 1978; Gillat and Broutman, 1978):

[19]
$$D_e = D_0 \cdot e^{-E_d/R_1T_1}$$

where D_e is the effective diffusion coefficient, D_o is the pre-exponential factor or permeability index, E_d is the activation energy, R_1 is the universal gas constant and T_1 is the absolute temperature in degrees Kelvin. The activation energies (E_d), obtained from the slope of an Arrhenius plot (log D_e versus $1/T_1$), were generally less than 10 kcal/g-mole.

It is recognized that Fickian diffusion is generally applicable to rubbery polymers, and often fails to describe the diffusion process in glassy polymers (Springer, 1984). The glass transition from temperature is defined as the temperature that a glassy hard state polymeric material turns from a glassy hard state to a soft rubbery state. The glass transition temperature ($T_{g)}$ is usually lowered by the absorption of moisture which changes the diffusion behaviour of the material by softening the resin matrix and causing it to swell. This process is known as plasticization. Whitney et al. (1982) emphasized that care should be taken in high-temperature moisture exposure environments near the wet T_g of the matrix. The rapid rate of water absorption, forced by the temperature gradient, could result in rapid swelling and induce permanent damage to the specimens in the form of stress cracks.

A "solvent" is a generic description of a liquid such as distilled water and alcohol that can dissolve solids. The diffusion of a solvent into a composite's intramolecular network may result in physical changes that cause anomalous diffusion. Anomalous diffusion which cannot be explained in terms of concentration-dependent diffusion is commonly referred to as non-Fickian diffusion. Examples of such physical changes include excessive swelling of the polymeric material and the formation of an advancing "swollen gel" boundary (Fontano, 1986). In extreme cases, such as the rapid

diffusion of toluene and methyl ethyl ketone into cured polyester resins, osmotic stresses created at the boundary between the swollen surface layer and the non-swollen surface core resulted in the formation of solvent-stress cracks (Bravenec, 1983).

It has also been shown that absorbed water can generate internal pressures around inclusions in filled polymer composites (Sargent and Ashbee, 1984) through the formation of a crystalline hydrate. The hydration process immobilizes molecules of liquid water into a lattice structure (water of crystallization) which results in an increase in volume. The increase in volume for a filler particle encapsulated by a polymer can generate a confining internal pressure from the polymer matrix that, if in excess of the tensile strength of the polymer, can cause internal cracking of the composite.

For polymer systems which exhibit swelling, the relative rates of diffusion and relaxation associated with structural changes determines whether the process is described by Fickian or non-Fickian behaviour (Crank, 1975; Springer, 1984). For example, if the rate of solvent diffusion in the laminate is slower than the change in polymer structure due to equilibrium swelling, the diffusion process is usually classified as Fickian. When relaxation processes inside the material at the boundary between the swollen and unpenetrated layers are slower compared with the rate of diffusion to that boundary, an advancing boundary or non-Fickian behaviour is observed (Crank, 1975; Bravenic, 1983).

Non-Fickian behaviour has been observed in high temperature liquid water-polymer systems. Hahn and Kim (1978) found micro-cracks in graphite/epoxy composites following exposure in distilled water at 82°C. Gillat and Broutman (1978) suggested that immersion temperatures above 63°C not only accelerated the diffusion

process of water in graphite/epoxy composites but also changed the water absorption mechanisms resulting in non-Fickian behaviour

Bonniau and Bunsell (1984) observed that the liquid water uptake in glass/epoxy composites was greater than that due to humid (100%) air. Surface whitening and cracking was observed for composites exposed to liquid water, that is, at weight gains greater than 1.0 percent. Losses in dry material were also observed at temperatures above 40°C. In other work at 50°C, the absorption of water in post-cured, unfilled, cross-linked polyester resin specimens exhibited Fickian diffusion behaviour (Bravenic, 1983). The diffusion coefficient of polyester resin specimens which were postcured for 28 h at 90°C was calculated to be 2.0×10^{-6} $mm^2.sec^{-1}$. This value was determined using the method developed by Shen and Springer (1976).

The absorption behaviour and environmental effects of post-cured polyester-E glass (SMC) specimens in distilled water, salt water, and various liquid fuels was investigated by Loos et al. (1980). Prior to immersion in each environment, the filled and unfilled SMC specimens were thermally post-cured by drying in an oven at 66°C until no additional weight loss was observed. The diffusion coefficients were determined using the gravimetric method developed by Shen and Springer (1976). The diffusion coefficients for unfilled SMC-65, filled SMC-25 (41.8% $CaC0_3$ by weight) and filled SMC-30EA (40% $CaCO_3$ by weight), immersed in distilled water at 50°C, were determined to be in the range of 1.6 to 2.1×10^{-6} $mm^2.sec^{-1}$. In most cases, a loss in weight was observed after M_e was reached. This non-Fickian behaviour was attributed to material deterioration and explained by the formation of cracks and the leaching of resin particles.

A maximum laboratory operating temperature of 45°C was used in this work to minimize potential effects associated with hygrothermal damage to the experimental FFW composite. The gravimetric method developed by Shen and Springer cannot be used to characterize diffusion properties of composites that have undergone extensive deterioration in aqueous environments. There is a need to develop other test methods to quantify the change in diffusion characteristics of such composites.

2.5 RESEARCH OBJECTIVES

Primary objectives of this experimental research program are summarized below:

1. To identify the most hostile simulated aqueous environment by comparing the effects of various laboratory environments and temperature conditions on the deterioration behaviour of large post-cured FFW specimens and metal (steel and galvanized) coupons.
2. To develop new test methods to quantify the deterioration of small FFW specimens in low pH acidic environments (hostile environment identified in 1.) and to demonstrate the usefulness of these methods in determining the effects of postcuring on deterioration behaviour in sulfuric acid (pH 2.2 to 2.5).
3. To develop a mathematical model quantifying the rate of deterioration of small (virgin) FFW specimens exposed to acidic environments.
4. To verify and use the model developed in (3), in combination with experimental data, to predict the intrinsic diffusion coefficients in the acid-degraded layers of FFW specimens exposed to sulfuric and acetic acid.

CHAPTER 3

PRELIMINARY SCREENING STUDY: PHASE 1

3.1 INTRODUCTION

The Preliminary Screening (PS) study was designed on the basis of a field investigation and two laboratory experiments. In this work, these experiments are referred to as the FFW deterioration and the metal corrosion experiments. The purpose of the field investigation was to delineate an aggressive *in situ* soil site in order to obtain soil samples to simulate an MIC environment.

The laboratory experiments were designed to assess and compare the deterioration behaviour of postcured FFW composites and metals (steel and galvanized) following exposure in various simulated aqueous field environments (see Section 2.3). A specific objective of these experiments was to identify the environment which had the most deleterious effect on each material. The experiments were conducted at room temperature (25°C) and elevated temperature (45°C) conditions. Standard test methods (Section 3.3.3) were used to measure and monitor changes in weight loss, mechanical properties, and increases in the concentrations of calcium and aluminum ion in the leachate. A moisture desorption heat (MDH) method was also developed and used to monitor changes in the diffusion characteristics of wet postcured FFW specimens.

3.2 FIELD INVESTIGATION

A culvert field site was investigated on August 26, 1987 to determine the cause of a failure of a gravelled municipal road (SW 1/4 35-12-23) near Harding, Manitoba.

The road failure resulted from a collapsed 600 mm diameter corrugated steel pipe (CSP) underground culvert structure. An alkaline meadow drained into the culvert site (see Figure 3.0). The field service life of the corroded CSP culvert was only 10 years.

The inlet of the collapsed culvert was submerged during the site investigation. Discussion with local representatives in the area indicated that water levels at the site are known to fluctuate for periods of weeks or even months. The soil at the culvert site was identified, from topographic soil maps, as belonging to the Newdale Smooth Phase soil group.

The culvert site (12 m length) was excavated and sections of the corroded CSP were inspected. Hydrogen sulfide gas was evident during the excavation and a localized area of yellow precipitate, assumed to be ferrous sulfide, was observed adjacent to the exterior of the corroded CSP and the soil. The interior and exterior of the 16 gauge (1.6 mm) CSP had corroded uniformly with perforations evident along the length of the CSP. Corroded metal specimens and soil samples were taken from the site for further analysis and laboratory testing.

A visual examination of the corroded metal specimen revealed bulky yellow corrosion products that were raised above a black hard scale that had adhered to the metal surface. The metal surface beneath the corrosion products was bright and shiny. When the black scale was immersed in a strong solution of hydrochloric acid, hydrogen sulfide gas was generated, which suggested a form of iron sulfide. The positive identification of sulfide at the site and the formation of an iron sulfide scale suggested that the observed MIC behaviour was related to the presence of anaerobic sulfate-reducing bacteria (SRB). Hamilton (1985) reported that the formation of iron sulfides

Figure 3.0 Field investigation: Photographs of culvert site near Harding, Manitoba

on buried steel pipelines in anaerobic environments, such as waterlogged clay soils, is characteristic of the action of the sulfate reducers. Similar MIC behaviour and SRB activity has been identified in a study with corroded CSP culverts in Wisconsin (Patenaude, 1986). In this work, the CSP corrosion rate at Harding was measured at 0.08 $mm.y^{-1}$. This value is based on uniform corrosion through both the interior and exterior sides of the culvert structure.

A conductivity meter (Geonex; Model No. EM 38) and a pH meter equipped with an inert platinum indicator electrode and saturated calomel reference electrode were used to make on-site measurements for pH, resistivity (R) and redox potential (E_h). The pH, R, and E_h of the surface ditch water was found to be 8.6, 233 ohm-cm, and 0.455 V, respectively. Correspondingly, the pH and R values of the soil were lower and measured at 7.6 and 170 ohm.cm, respectively. The value of E_h varied from +0.155 V near the surface of the soil (2cm) to -0.055 V at 40 cm below the surface. The average moisture content and wet and dry bulk densities of the Harding soil were determined to be 38%, 1.56 $g.cm^{-3}$ and 0.98 $g.cm^{-3}$, respectively (see Appendix II-1).

The soil texture was identified from a sieve analysis (Appendix II-2) to be a sandy clay loam (SCL). The percentage of sand, silt and clay was determined to be 48, 27 and 25 percent, respectively. A laboratory chemical analysis of the soil extract also showed that it contained approximately 3.0 percent organic carbon and 80 $meq.L^{-1}$ (3844 $mg.L^{-1}$) of the sulfate ion. The high concentration of sulfate ion was associated with the cations; calcium (20.8 $meq.L^{-1}$), magnesium (23.6 $meq.L^{-1}$) and sodium (35.6 $meq.L^{-1}$).

Using the criteria described by Booth et al. (1967) in Table 2.2, the Harding *in*

situ soil is categorized as aggressive in nature. Soil was collected from the field site and stored in a sealed plastic container for the FFW deterioration and metal corrosion experiments.

3.3 FFW DETERIORATION EXPERIMENT

3.3.1 Materials

Large test specimens, 10 x 25 cm with an average thickness of 5.00 mm (SD = 0.17 mm) and weight of 278.19 g (SD 4.43g) were cut from the FFW test pipe described in Section 2.2.4, using a diamond blade saw. A summary of the average physical dimensions of the 36 large postcured specimens is presented in Appendix II-3. One reason for using large test specimens was to ensure that a sufficient number of test coupons could be cut from each specimen for testing of flexural and tensile properties.

The test specimens were cut in the longitudinal (tensile) and hoop (flexural) directions. The location and orientation of the test specimens was controlled to ensure random stratified sampling by applying a cardboard template to the inside surface of the test pipe prior to sawing. A total of 125 longitudinal and 125 hoop test specimens, similar to those shown in Figure 3.1, were prepared. The edges of the specimens were sanded and brush-coated with a catalyzed (MEKP) corrosion resistant resin[3]. The primary reason for this coating was to ensure that the diffusion of the penetrant into the laminate was one-dimensional (Whitney et al., 1982) and so minimize "edge effects" (Shen and Springer, 1976).

---

3 DION COR-RES 7000A-Modified bisphenol polyester with maximum corrosion and temperature resistance (Fiber Glass Canada Inc.)

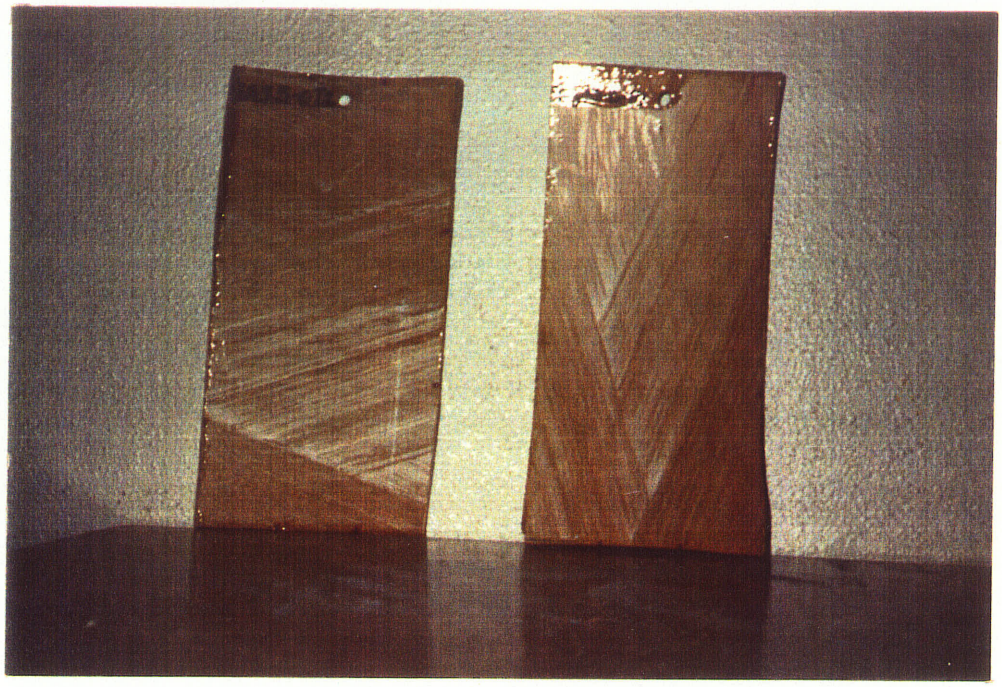

Figure 3.1 Photographs of large coated postcured FFW specimens (longitudinal and hoop)

All of the coated test specimens were postcured, prior to immersion, in a large horizontal airflow oven[4] (Manufacturer Model No. 52201-800) with an accuracy of $\pm$ 3°C. A preliminary postcured experiment was undertaken, prior to postcuring all the specimens, in order to determine the effects of thermal postcuring on material weight loss measurements. A drying temperature of 112°C was selected on the basis of recommendations made by FiberGlas Canada (1988). It was found that the orientation of the test specimens in the hot oven was an important consideration during drying. For example, minimal weight losses were observed for specimens placed with the exterior (blue) liner surface facing upward, whereas significant weight losses and styrene odours were found for specimens lying with their non-protected interior surface facing upward. These observations suggest that the liner was effective in preventing the expulsion of styrene and/or moisture through the exterior surface of the specimen. In all subsequent work, specimens were postcured and reconditioned (dried) with the interior surface of the specimen facing upward in the oven.

The relationship of percent weight loss as a function of time for a postcure temperature of 112°C is shown in Figure 3.2. It was found that minimal changes in weight loss (that is less than 0.003 grams.hr^{-1}) occurred after a postcure time period of 36 hours (see Appendix II-4). Based on these results and because of time constraints, all test specimens were postcured at a temperature of 112°C for 36 hours and stored in a desiccator. These specimens (8) were removed at random from the desiccator and immediately weighed prior to immersion in one of the seven controlled laboratory

---

[4] Accuracy determined by Shell-lab for a range of temperatures between 80°C and 235°C.

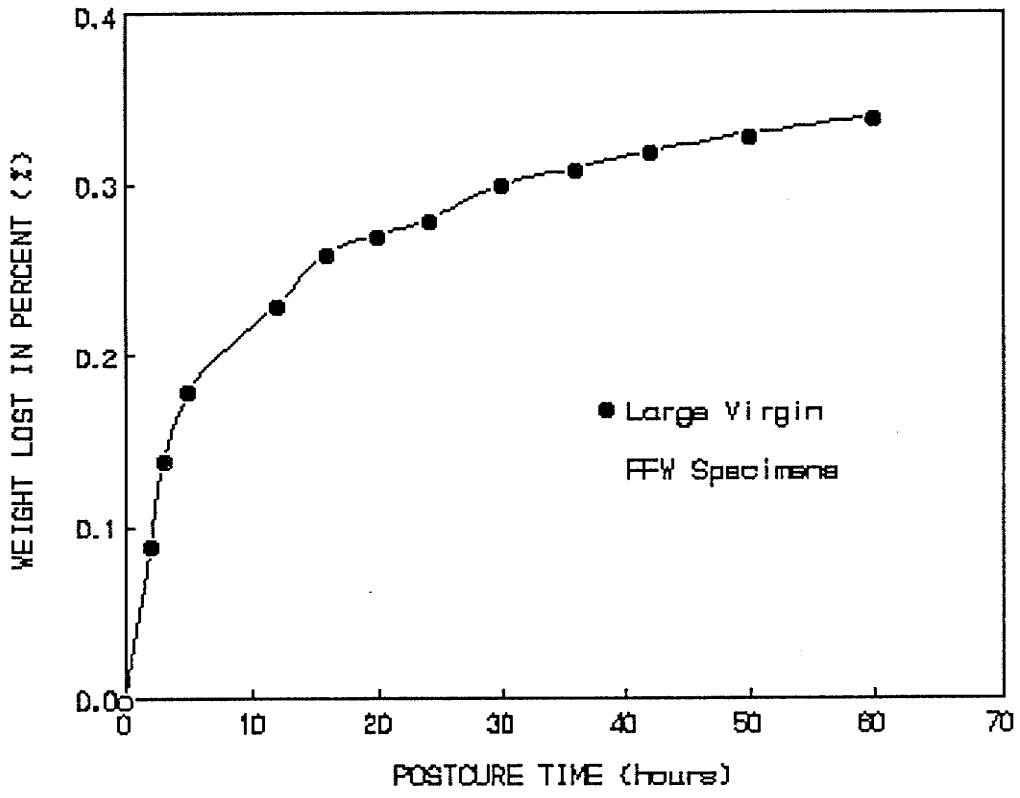

Figure 3.2 Percent weight loss versus time for large virgin specimens postcured at 112°C

environments.

3.3.2 Laboratory Procedures

The experimental design of the FFW deterioration study is summarized in Table 3.0. Laboratory control parameters were defined in the experimental program to simulate five aqueous field environments at various low (25°C) and high temperature (45°C) conditions. These include: softwater (deionized), alkaline (NaOH), acidic (inorganic and organic acids), saline (M_gSO_4), and an anaerobic/aerobic biological (MIC soil) environment.

Deionized water (D25, D45) and sodium hydroxide solutions buffered with boric acid (B25, B45) were used to simulate softwater and alkaline environments, respectively. The sodium hydroxide solution (pH 9.0-9.5) was buffered to eliminate fluctuations in pH caused by the effects of carbon dioxide from the atmosphere. Sulfuric (1A45) and hydrochloric (2A45) acid solutions were used to simulate inorganic acid environments. Acetic acid (3A45) was used to simulate an organic acid environment. The pH values used ranged from 3.5 to 4.5. These pH values are known to be highly aggressive to buried concrete pipe structures (PCA, 1989).

An average magnesium sulfate (S45) concentration used to simulate a saline environment was 1870 mg/L $S0_4^{--}$. This value is similar to the concentration of sulfates found in seawater which is known to cause deterioration of concrete structures.

The laboratory solutions were prepared using deionized water with a conductance of less than 0.2 Mhos. Sixteen postcured specimens, longitudinal (8) and tensile (8), were placed in each closed top container (Figure 3.3) and filled with 18 L of solution.

Table 3.0 Experimental Design of FFW Deterioration Study

		Laboratory Control Parameters		
Aqueous Environment	Laboratory Medium	Operating Parameter	Temp. 25°C	Temp. 45°C
1. Softwater	Deionized water (neutral)	pH: 7.0-8.0	D25	D45
2. Alkaline	NaOH (buffered)	pH: 9.0-9.5	B25	B45
3. Acidic				
- Inorganic	H_2SO_4	pH: 3.5-4.5	-	1A45
	HCl	pH: 3.5-4.5	-	2A45
- Organic	CH_3COOH	pH: 3.5-4.5	-	3A45
4. Saline	$MgSO_4$	1,500-2,000 $mg.L^{-1}$ as $SO_4^{=}$	-	S45
5. Biological	MIC soil	>2,000 $mg.L^{-1}$ as $SO_4^{=}$ anaerobic/aerobic	-	R45

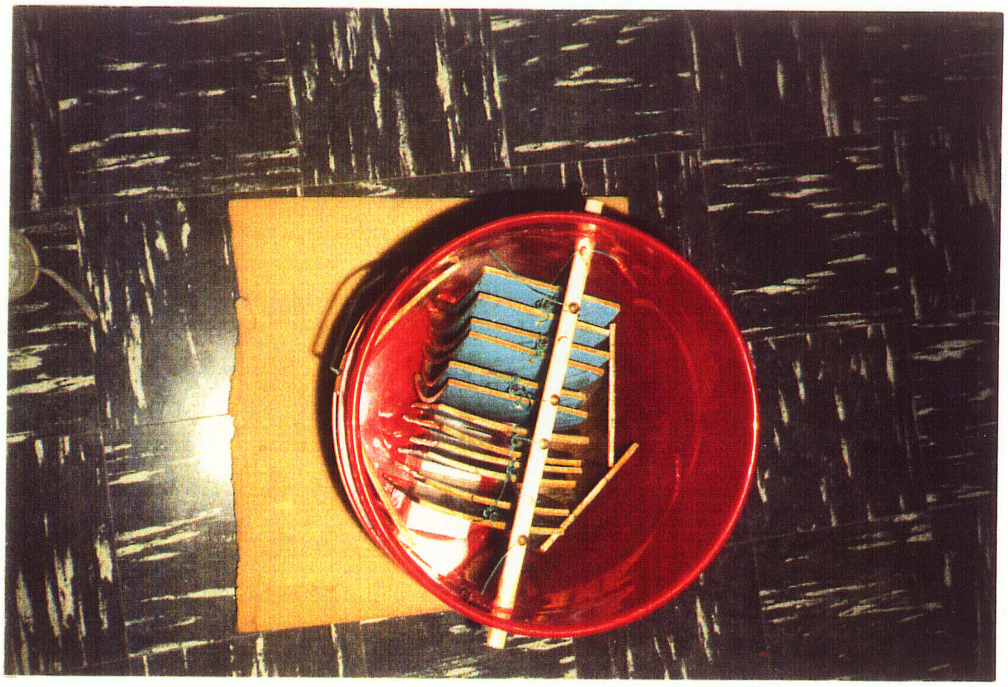

Figure 3.3 Photograph of large FFW specimens in 22.5 L plastic containers prior to immersion

A detailed description regarding the preparation of each environment is presented in Appendix II-5. The specimens were mounted on an ethafoam block in the vertical position and were separated by an equal distance of 1.25 cm using glass rods. Two containers (D25, B25) were placed in a low temperature controlled chamber at 25°C and the remaining 6 containers (D45, B45, 1A45, 2A45, 3A45, S45) were placed in a second temperature controlled chamber at 45°C.

The MIC soil samples (R45) were used to simulate an aggressive anaerobic/aerobic biological environment. Deionized water was added to the Harding soil sample to make a paste. A volume of 11 L of the wet-soil paste was placed in the temperature controlled chamber at 45°C for two weeks in order to acclimatize the microorganisms to the elevated temperature condition. The water content of the paste was measured at 45.3 percent. Sixteen postcured samples, longitudinal (8) and tensile (8), were immersed vertically in the paste to one-half the specimen length. The specimens were removed every two weeks, rotated (180°), and re-immersed in the paste to simulate one anaerobic/aerobic cycle.

The temperature and pH levels of each immersion medium were checked at 2-day intervals during the 27 week test period. Because of evaporation, deionized water was added as required to maintain the level in each container at a constant volume. Additional amounts of 1.0 N sulfuric acid and glacial acetic acid were added intermittently to the acid solutions to maintain the pH in the range of 3.5 to 4.5. The amount of acid added was measured in terms of milli-equivalents (meq). Other tests were conducted on a weekly basis to monitor changes in specimen weight (D25, D45), and calcium and aluminum ion concentration (D25, D45, 1A45, 2A45, 3A45) in the

leachate. Visual microscopic examinations and tests related to monitoring changes in specimen volume (swelling) were also conducted over the 27 week test period.

Following each period of immersion (5, 14 and 27 weeks), four test specimens, (2) hoop and (2) longitudinal were removed for testing of dry mechanical properties. One additional set of "control" specimens, hoop and longitudinal, was used to measure and compare long-term (52 weeks) changes in dry and wet mechanical properties.

3.3.3 Analytical Methods

Diffusion coefficients were measured for FFW composites immersed in deionized water using a gravimetric method. Deterioration was measured in terms of the loss in dry material weight, increases in the concentrations of calcium and aluminum ions in the leachate, changes in microscopic appearance, specimen dimensions, tensile, flexural and hardness properties. A new moisture desorption heat (MDH) method, based on gravimetric measurements, was also used to measure the extent of deterioration by monitoring changes in moisture desorption/diffusion characteristics. A new desorption slope (S_d) parameter is proposed, based on the latter method, to quantify deterioration in the degraded layer of exposed FFW specimens.

3.3.3.1 Gravimetric

Absorption Test Methods

The accelerated absorption test method developed by Shen and Springer (1976), described in Section 2.4.3.2, was used to determine the effective diffusion coefficient (D_e). The FFW composites exposed to deionized water (D25, D45) were selected for

these calculations for two reasons. First, the D_e values based on the absorption of deionized water could be compared to those of others (Bravenic, 1983; Loos et al., 1980) for similar temperature conditions. Secondly, it was believed that deionized water would result in minimum material weight loss.

The absorption test method, essentially, involved immersing the postcured FFW specimens for a period of 27 weeks in a water bath at one of two temperature conditions (25° and 45°C). Changes in specimen weight were measured as follows:

1. Each postcured specimen was weighed after drying in a desiccator (W_i).
2. The specimen was immersed in deionized water for the pre-determined time period.
3. On removal from the water, excess liquid was wiped off using a cloth towel and the specimen was reweighed (W_t).

A digital Mettler analytical balance (Mettler PE 300) with an accuracy of $\pm$ 0.01 grams was used for all weighings. The percent change in specimen weight was then calculated according to Equation [14].

Material Weight Loss

A method to evaluate the percentage of material weight lost during liquid immersion is described in Standard ASTM D 570 (1981). This standard recommends that plastic materials known to contain appreciable amounts of water-soluble ingredients should be reconditioned under the same conditions used during postcuring in order to determine losses in soluble material weight. Consequently, all postcured specimens were reconditioned at a temperature of 112°C until no further weight loss was observed.

Detailed steps used for determining the dry material weight loss were as follows:

1. The postcured specimen was weighed after drying in desiccator (W_i).
2. The specimen was immersed in the test environment for a pre-determined time.
3. On removal from the solution, excess surface liquid was wiped off using a cloth towel.
4. The specimen was reconditioned in an oven at 112°C.
5. From time to time the specimens were removed from the oven, cooled in a desiccator and weighed (W_t).
6. Step 5 was repeated until no more weight loss was observed,(W_f).
7. The material loss of the reconditioned postcured FFW specimens was determined using Equation [20].

[20] $$W_m = (W_i - W_f)\ (W_i)^{-1}\ (100)$$

Where:

W_m = dry material weight loss, %

W_f = weight of oven dried exposed specimen, g

3.3.3.2 Calcium and Aluminum Analysis

Calcium and aluminum ion concentrations were determined in accordance with Standard Methods for the Examination of Water and Wastewater (1985). The concentrations of calcium and aluminum ions were measured to estimate the quantity of soluble filler constituents, Solem ATH and Snowhite $CaCO_3$, in the leachate. This

estimate is based on the assumption that there was minimal deterioration of the glass component. Calcium was determined using an ethylenediaminetetracetic acid (EDTA) titrimetric method and aluminum was measured using an atomic absorption (AA) spectrometry method.

Calcium: EDTA Titrimetric Method

Calcium measurements were determined in accordance with the 3500-Ca D. EDTA Titrimetric Method described in Standard Methods (1984). This method involves the use of EDTA as the titrating agent. EDTA is a chelating agent that forms stable complex ions with calcium. A chemical indicator causes a colour change to occur when all of the calcium has been complexed by the EDTA at a pH of 12 to 13, as shown in the equation:

[21] $$Ca^{++} + EDTA \rightarrow [Ca^{++} \ . \ EDTA]_{complex}$$

Using a pipet, 5 N sodium hydroxide was added to ensure that the pH was sufficiently high so that the indicator combined only with calcium. The volume of the 0.01 M EDTA titrant was recorded at the endpoint when no further colour change occurred. The calcium concentration is reported in terms of $CaCO_3$ equivalent and was calculated by the following expression:

[22] $$Calcium\ ion = (B)\ (1{,}000)\ (ml\ of\ sample)^{-1}$$
$$as\ mg.L^{-1}\ CaCo_3$$

Where:

B = ml of titrant for sample; 1 mg $CaCO_3$ equivalent to 1.00 ml 0.01 M EDTA titrant at the calcium indicator endpoint

Aluminium: AA Spectrometric Method

Two methods were evaluated to determine the feasibility of measuring aluminum concentrations at low pH's. A colorimetric method using an Eriochrome Cyanine R indicator, described in the Standard Methods (1989), was evaluated using solutions of known Al concentrations and the results compared with those from AA spectrometry. The former method proved unsuccessful in low pH acetic acid due to unknown interferences.

To measure aluminum using atomic absorption spectrometry, a nitrous oxide-acetylene flame is required to atomize the liquid sample. A light beam is directed through the flame and onto a detector that measures the amount of light absorbed by the atomized element. Because aluminum has its own characteristic absorption wavelength, an aluminum source lamp is used. The amount of energy at the characteristic wavelength absorbed in the flame is proportional to the concentration of aluminum in the sample.

Aluminum measurements were determined in accordance with Standard 3111D. Direct Nitrous Oxide-Acetylene Flame Method (Standard Methods, 1989). A Perkin-Elmer (Model 2380) AA spectrophotometer was used in the analyses. Aluminum stock standards were supplied by Spex Plasma Standard Inc. Samples were diluted with a deionized water in the concentration range of 1 to 10 mg/L. Potassium chloride (KCl) was added to the samples and standards to ensure complete aluminum ionization. The

aluminum ion concentration expressed as mgL^{-1} of $Al_2O_3.3H_2O$ was calculated as follows:

[23] $$Aluminum\ ion\ as\ mg.L^{-1} = [Al^{+++}\ mgL^{-1}]\ (G_1)\ (G_2)^{-1}$$

Where:

G_1 = Gram-molecular weight of $Al_2O_3.3H_2O$

G_2 = Gram-molecular weight of two moles of Al^{+++}

3.3.3.3 Microscopic Appearance and Specimen Dimensions

The initial surface of both virgin and postcured specimens were examined at 6x magnification using a light stereo microscope (Wild Leitz Canada Ltd.). The surface of the virgin FFW specimens was opaque and white-grey, in colour. Small surface cracks (1 mm x 1 mm x 5 mm) and spherical surface flaws (1 mm in diameter) incorporated during manufacturing were evident and are shown in Figure 3.4. In comparison, the postcured specimens indicated a colour change to a translucent amber and an increase in the size of surface cracks and flaws. At a greater magnification (x 50), "volcano" shaped flaws were observed. This effect is attributed to the rapid expulsion of entrapped moisture, air, and free styrene during postcuring.

As discussed in Section 2.4.3, one of the physical changes that usually occurs during the absorption of a solvent is swelling. It is recommended in Standard ASTM C 581 (1983) that to measure the extent of swelling, the thickness of each specimen should be measured immediately following postcuring and after each exposure period.

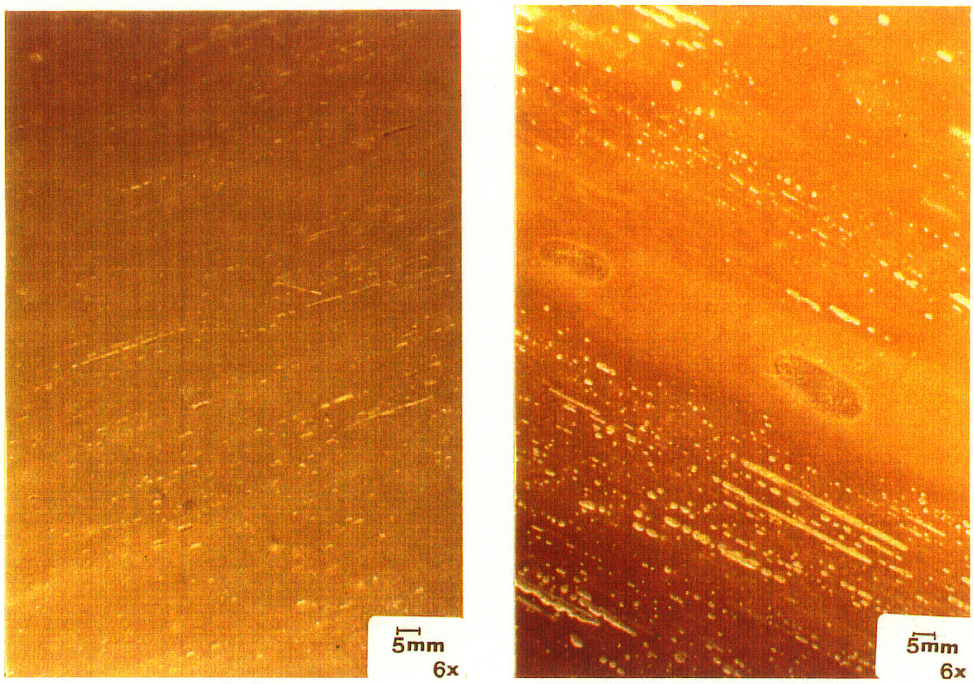

Virgin Postcured

Figure 3.4 A comparison of surface macrographs (x 6) of virgin and postcured specimens

The thickness is usually measured to the nearest 0.025 mm at the geometric centre of the specimen using a micrometer.

Thickness measurements for FFW specimens could not be done accurately using a micrometer due to the irregular exterior surface of the blue corrosion liner. To circumvent this problem the extent of swelling was determined by volumetric measurements and the volumetric measuring device shown in Figure 3.5 was designed for this purpose. The device was a thin vessel (3.25 cm x 14.25 cm x 380 cm) constructed out of plexiglass and designed to accommodate both curved (flexural) and straight (tensile) specimens.

Prior to taking the volumetric measurements, the device was first levelled using screws located at each bottom corner to ensure a constant initial water level or meniscus datum. The specimen was placed in the meter containing a known volume of water and the displaced volume was measured using pipettes to an accuracy of $\pm$ 0.2 cm^3. The average specimen volume was determined, prior to immersion, to be 151.1 cm^3 (see Appendix.II-3). Following each immersion time period, the volume of each specimen was re-measured. The increase in specimen volume, expressed as a percentage of the initial volume was determined.

3.3.3.4. Mechanical Properties

The following parameters were measured to evaluate changes in mechanical properties: flexural modulus, flexural strength, tensile modulus, tensile strength, and Barcol hardness. Following three predetermined immersion time periods (5, 14 and 27 weeks), a set of (2) hoop and (2) longitudinal test specimens was removed from each

Figure 3.5 Volumetric displacement measuring device

environment and reconditioned in a oven at 112°C until no more weight loss was observed. The oven dried specimens were placed in a sealed container with dessicant and transported by air to FiberGlas Canada's research facility in Guelph, Ontario for testing. A minimum of five flexural coupons and three tensile coupons were cut, using a diamond blade saw, from each of the reconditioned hoop and longitudinal specimens. Barcol hardness measurements were determined on both the interior and exterior sides of each specimen.

The mechanical properties of the "control" specimens were tested in both the dry and wet states. After 52 weeks of immersion, a set of control specimens were removed from each aqueous environment. Two specimens (one flexural and one tensile) were tested in their reconditioned (dry) state and the other two specimens were tested in the wet state. The reason for these tests was to compare the long term reduction in dry and wet mechanical properties.

On removal from their environment, the wet specimens were rinsed in distilled water and re-immersed in a sealed, clean, plastic container of deionized water. The wet and dry specimens were immediately transported to FiberGlas Canada's research facilities for testing of mechanical properties.

Flexural Properties: ASTM D790

Tests to measure flexural strength and modulus properties were conducted in accordance with Test Method I - Procedure A of ASTM D790 (1986). The ultimate flexural measurements are based on homogeneous beam theory for an elastic material supported at two points and loaded at the midpoint. The apparent flexural strength was

calculated by the following equation:

[24] $$S_1 = 3PL_1 / 2bd_2$$

Where:

S_1 = Ultimate stress at failure, MPa

P = load at a given point on the load-deflection curve, N

L_1 = support span, mm

b = beam width, mm

d = beam depth, mm

The flexural modulus is the ratio of stress to corresponding strain within the elastic limit and is determined as the tangent to the initial straight-line portion of the load deflection curve.

The flexural modulus (E) is calculated as follows:

[25] $$E_1 = L_1^3 m / 4bd^3$$

Where:

E_1 = modulus of elasticity, GPa

L_1 = support span, mm

m = slope of tangent from load deflection curve, N/mm

b = beam width, mm

d = beam depth, mm

A minimum of ten test coupons with dimensions (133 mm x 25 mm) were tested with the curved side in a concave orientation on the testing fixture for each immersion

condition. The support span was 10.2 cm. A cross head speed of 0.5 cm/min and a chart speed of 30 cm/min were selected on the Instron universal testing machine (Model No. PD-115). A digitizing pad (Numonics No. 2205) was used to transfer the stress-strain data to an IBM computer system for analysis.

Tensile properties: ASTM D 638

Tests to measure tensile strength and tensile modulus were conducted in accordance with ASTM D 638 (1987). This method covers the determination of tensile properties of reinforced plastics under conditions of constant temperature, humidity, and testing machine speed. A minimum of six standard "dog bone" shaped test coupons (Type-1), were tested for each immersion condition. The machine cross head speed was set at 0.5 cm/min. The tensile strength was determined by dividing the maximum load by the original minimum cross-sectional area of the coupon (measured by a micrometer to the nearest 0.025 mm). The tensile modulus was determined as the slope of the initial linear portion of the stress-strain curve.

Barcol Hardness: ASTM D2583

All of the Barcol hardness tests were performed before the coupons were cut from the test specimens. A minimum of 10 measurements were taken on the interior surface of each specimen using a Barcol Impressor (Model No. 934-1) manufactured by Barber-Colman Co.

3.3.3.5 Moisture Desorption Heat (MDH) Method

Shen and Springer (1976) showed experimentally that the expression for moisture distribution as a function of time can be derived from either moisture absorption or desorption tests. If the latter method is to be utilized, the specimen must first be exposed to a wet environment until equilibrium or saturation of the specimen is attained. Following saturation, the specimen is oven dried under controlled elevated temperature conditions (desorption). This test method is based on the assumption of no chemical reaction or material deterioration during the absorption and desorption tests.

As described in Section 2.4.3.2, there is a need to develop new test methods to quantify the changes in diffusion characteristics of plastic composites that have deteriorated following exposure in wet environments. In cases of extensive material weight loss, it is evident that the sole reliance on monitoring changes in specimen weight during absorption tests does not permit one to distinguish between the weight of the absorbed liquid and the corresponding loss of material. In this work, a new moisture desorption (MDH) method was developed to monitor changes in diffusion characteristics of exposed FFW specimens.

Development of MDH Method

A schematic of the concepts used in the development of the MDH method is shown in Figure 3.6. Deterioration was assumed to be a surface-related phenomenon resulting in the formation of a degraded layer and an advancing interface boundary .

It was postulated that the rate of moisture diffusing from the degraded layer during desorption tests (step 2), could be used to quantify the diffusion characteristics of

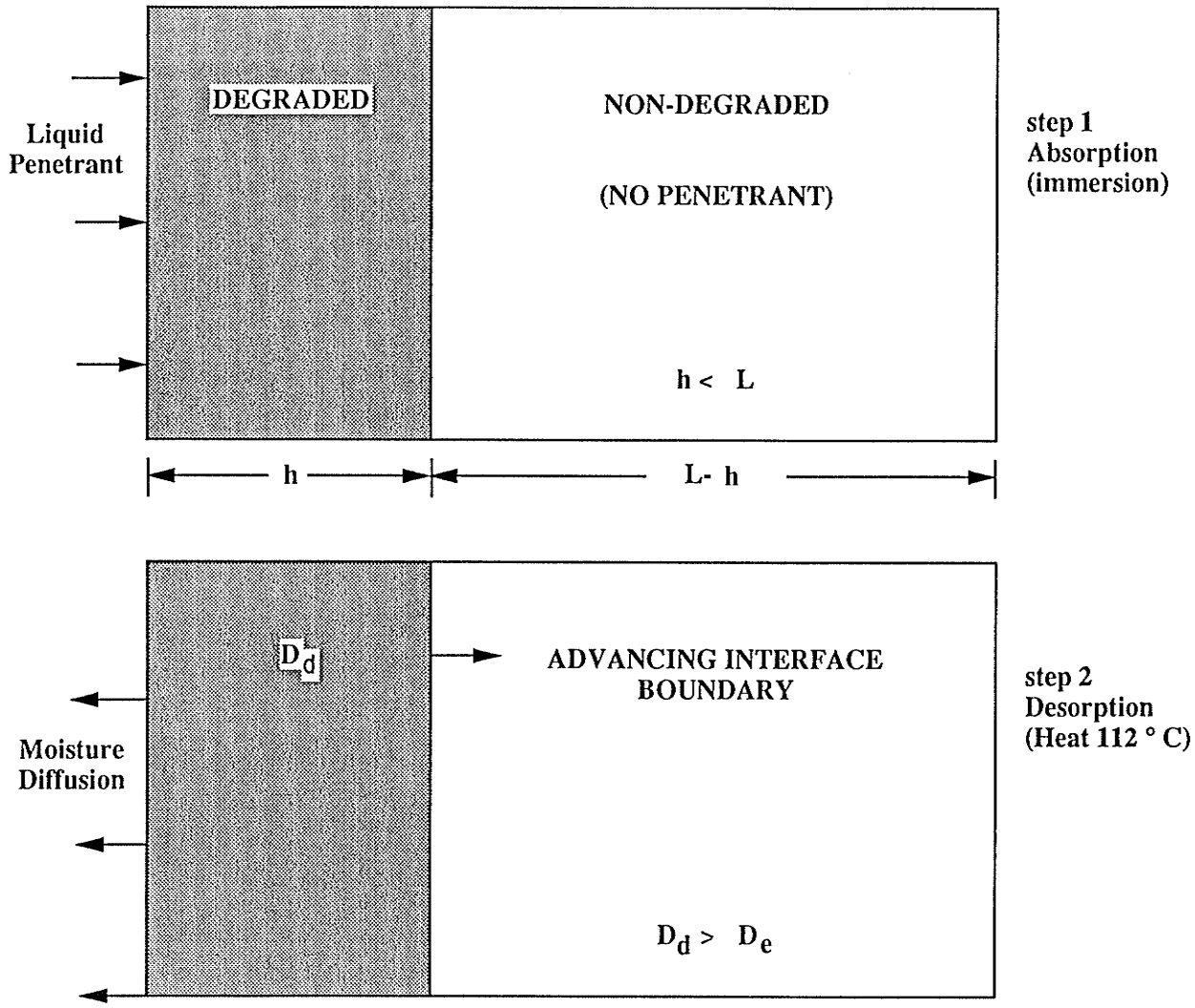

Figure 3.6 Concepts used in the development of the moisture desorption heat (MDH) method: PS Study

specimens exposed to an aqueous environment for a specific immersion time (t). Average diffusivity (D_d) in the degraded surface layer was assumed to be quasi-constant and much greater than that of the unattacked material (D_e). This assumption is based on a long immersion time period. The increase in diffusivity ($D_d > D_e$) is associated with two physical deterioration mechanisms: excessive swelling (cracks) and leaching of soluble material.

The moisture drying rate, herein referred to as the desorption slope (S_d) parameter, is expressed as the percent moisture lost (M_L) divided by the square root of the drying time $(t')^{1/2}$. S_d is essentially the initial linear portion of the desorption isotherm plot. Characteristic desorption isotherms are obtained by plotting percent moisture loss (M_L) as a function of the square root of drying time $(t')^{1/2}$. M_L is calculated from:

[26]
$$M_L = (W_{(t)} - W_{(t')}) (W_t^{-1}) (100)$$

By substituting the weight of moisture lost (m_L), which is equal to ($W_t - W_{t'}$), Eqn. [26] becomes:

[27]
$$M_L = (m_L) (W_{(t)}^{-1}) (100)$$

Where:

M_L = Percent moisture weight loss, %

$W_{(t)}$ = Weight of moist specimen at immersion time = t, g

$W_{(t')}$ = Weight of FFW specimen after drying at time = t', g

m_L = Weight of moisture lost after drying at time = t', g

Equation [26] is similar to Equation [16]. The denominator (W_t) in Eqn. [26] is, however, the total weight of the wet specimen rather than the initial weight of the dry specimen (W_i). The test method to determine M_L is essentially the same method used to determine material weight loss (see Section 3.3.3.1; steps 2-5). First, the wet specimens are removed from their environment after a predetermined immersion time (t) and weighed $W_{(t)}$. These specimens are then dried in an oven at 112°C and re-weighed intermittently $W_{(t')}$ to determine the weight of moisture lost (m_L).

In this work, the desorption slope parameter, S_d, is mathematically expressed as

[28] $$S_d = (\Delta M_L)\ (\Delta t')^{-1/2}$$

where:

S_d = Desorption slope of the linear portion of the desorption isotherm plot, $(t')^{-1/2}$

A least-square linear regression analysis was used to quantify the regression coefficient of the initial portion of the desorption slope for at least 60 percent of the desorption isotherm data.

3.3.4 Results and Discussion

Diffusivity and Temperature Effects

The effect of using temperature as a means of accelerating the rate of diffusion was evaluated using visual and gravimetric (water absorption) test methods. Photomacrographs taken of the interior surface of a D45 specimen, exposed to distilled water, showed a white discoloration (see Figure 3.7). However, no further increase in

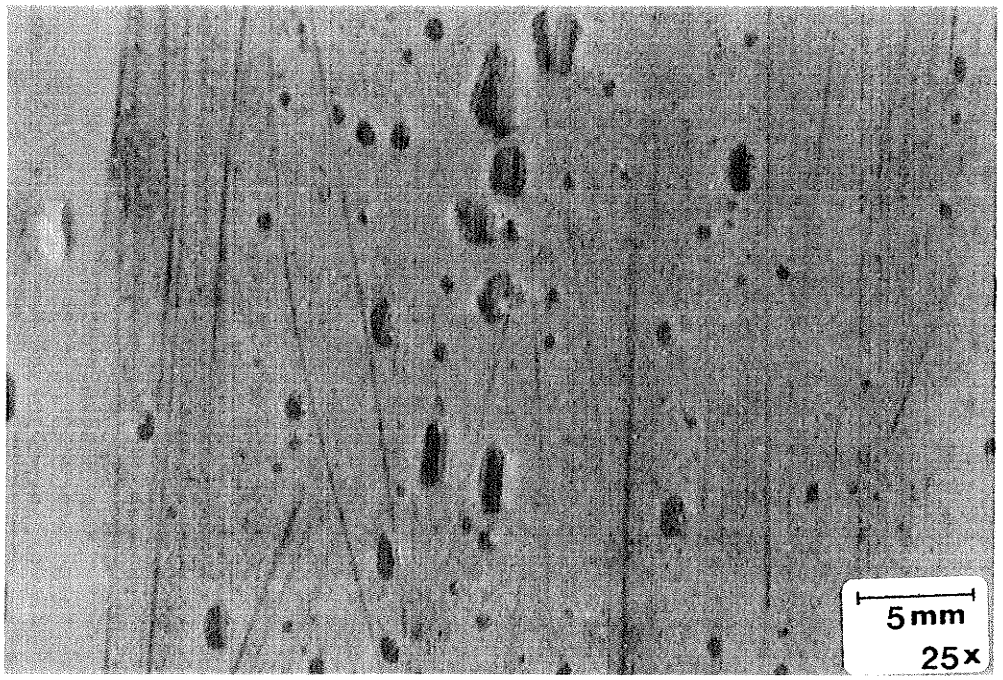

Distilled - 27 wks immersion (45°C)

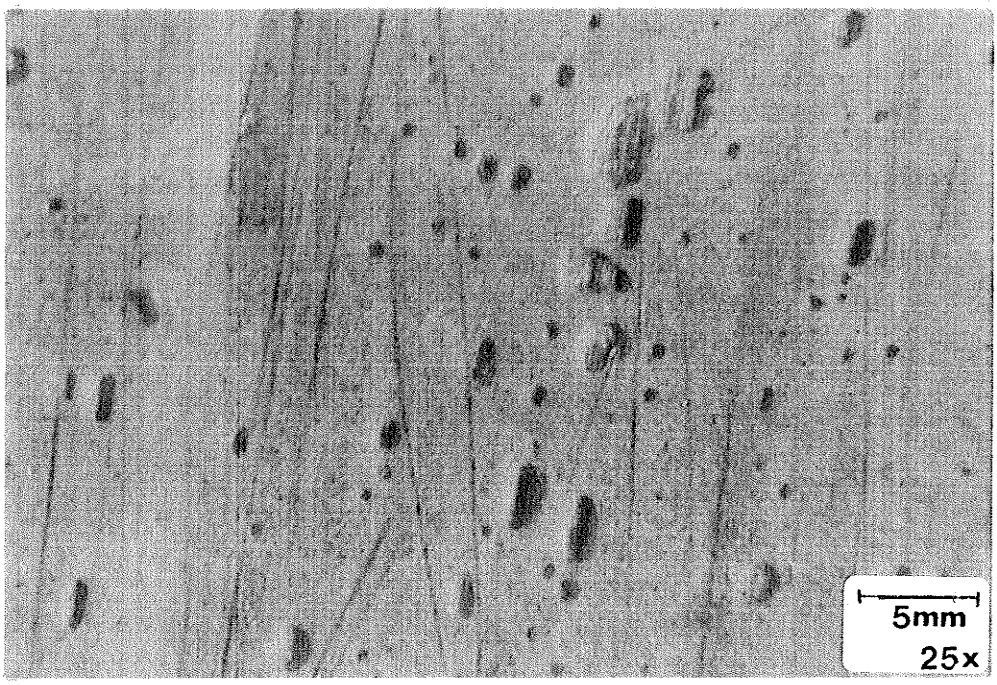

Distilled - 2 wks immersion (45°C)

Figure 3.7 Surface photomacrographs of postcured specimens in deionized water (45°C) after 2 and 27 weeks immersion

whitening or changes in surface characteristics was observed after 2 weeks exposure. Watanabe (1979) also observed surface whitening for unfilled woven glass reinforced polyester composites immersed in water. He suggested this resulted from the reduction of transparency in the specimen due to scattered light and debonding at the interface between the resin and glass fibres.

Absorption isotherms for postcured FFW specimens immersed in deionized water at 25° and 45°C are shown in Figure 3.8. The initial linear slope of each isotherm demonstrates Fickian diffusion behaviour. The test method developed by Shen and Springer (1976) was used to approximate D_e and M_e for the 45°C isotherm plot. D_e and M_e for the 25°C isotherm could not be determined since the point at which the linear slope starts to curve and become concave towards the abscissa axes (t_L) must be known (see Appendix. II-6). It is evident from the 45°C isotherm that t_L was reached after an immersion time of approximately 16 weeks.

The values of D_e and M_e were calculated from the 45°C isotherm and approximated to be 1.4 x 10^{-6} mm^2/sec and 1.61%, respectively. These values compared well with those obtained by others (Watanabe, 1979; Bravenic, 1983; Loos et al., 1980) for crosslinked polyester and SMC specimens under similar laboratory operating conditions.

A comparison of the linear slopes of both 25°C and 45°C absorption isotherms, S_a, show an increase in the latter slope by a factor (S_{a45}/S_{a25}) of 2.38. These results are in agreement with Watanabe (1979) who showed that an increase in temperature (25°C to 50°C) for unfilled polyester composites immersed in deionized water also increased S_a by a factor of 2.5. It is interesting to note that the diffusion coefficient

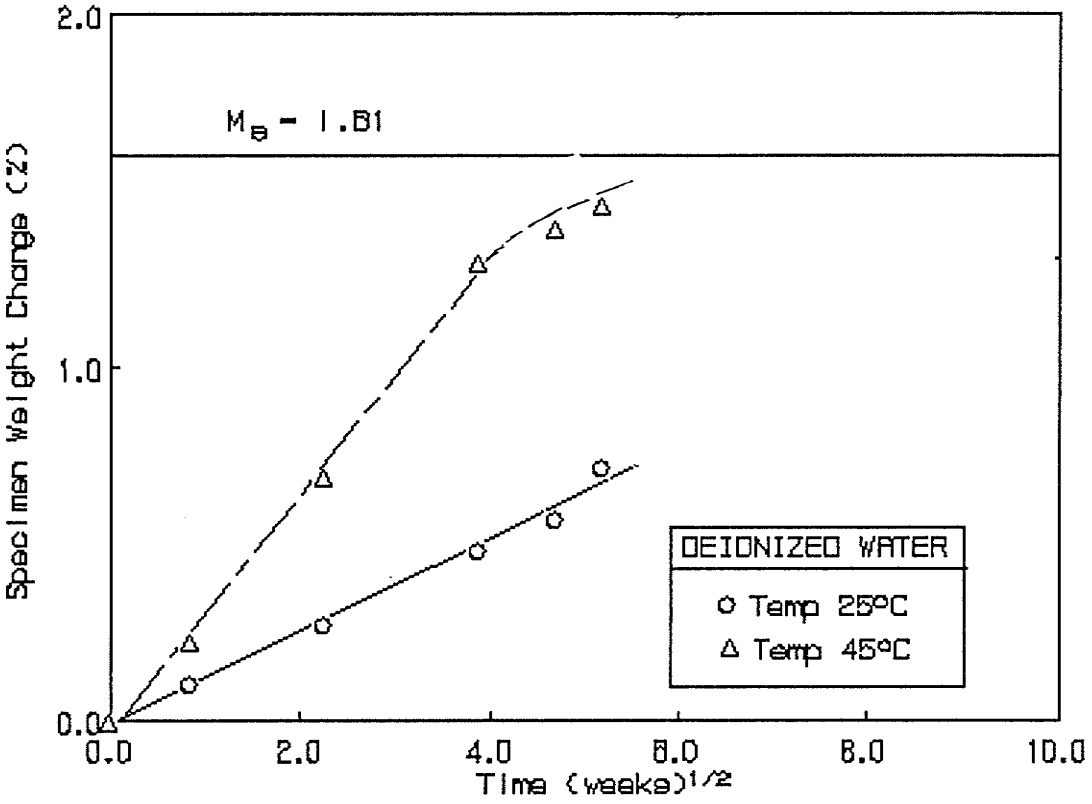

Figure 3.8 Absorption isotherms for FFW specimens immersed in deionized water at 45°C and 25°C

calculated by Watanabe (1979) also varied with an increase in temperature according to the Arrhenius relationship.

Loos and Springer (1980) showed for unfilled and filled SMC materials that M_e is relatively insensitive to liquid temperatures. Thus, the increase in diffusivity resulting from an increase in temperature (20°C) can be estimated using Equation [18] and the ratio of the absorption isotherm slopes $(S_{a45}/S_{a25})^2$. For example, if the value of M_e at 25°C is assumed to be equal to 1.61% (M_e at 45°C), the increase in diffusivity resulting from a temperature increase from 25° to 45°C is estimated at 5.7.

In summary, absorption tests conducted at a temperature of 45°C were effective in increasing the rate of diffusion of deionized water in postcured FFW specimens. No anomalies in Fickian diffusion behaviour were observed during these tests.

Deterioration Test Results

Table 3.1 shows the average pH conditions in each laboratory environment during the test period. The standard deviation was largest for the sulfuric (1A45) and hydrochloric (2A45) acidic environments. Figure 3.9 shows that most of the variation in pH occurred during the first 5 weeks of immersion. An increase in pH was observed during this period and measured amounts of concentrated acid were added to maintain a lower pH condition. The average pH in the acidic environments during the 27 week immersion time period ranged from 3.85 to 4.32 (see Appendix.II-7).

The average material weight lost per specimen (W_m), expressed as a percentage, was determined for the following environments: deionized water (D25, D45) sodium hydroxide (B25, B45), sulfuric acid (1A45), hydrochloric acid (2A45), acetic acid

Table 3.1 Average pH Conditions During the 27 Week Test Period: PS Study

Environment Type	Average pH	Standard Deviation
Deionized water		
D25	7.91	0.38
D45	7.52	0.23
NaOH (Buffered)		
B25	9.28	0.03
B45	9.23	0.04
Acids		
1A45	3.96	0.73
2A45	4.32	0.70
3A45	3.85	0.24
Sulfates		
S45	7.66	0.19
MIC Soil		
R45	7.63	0.28

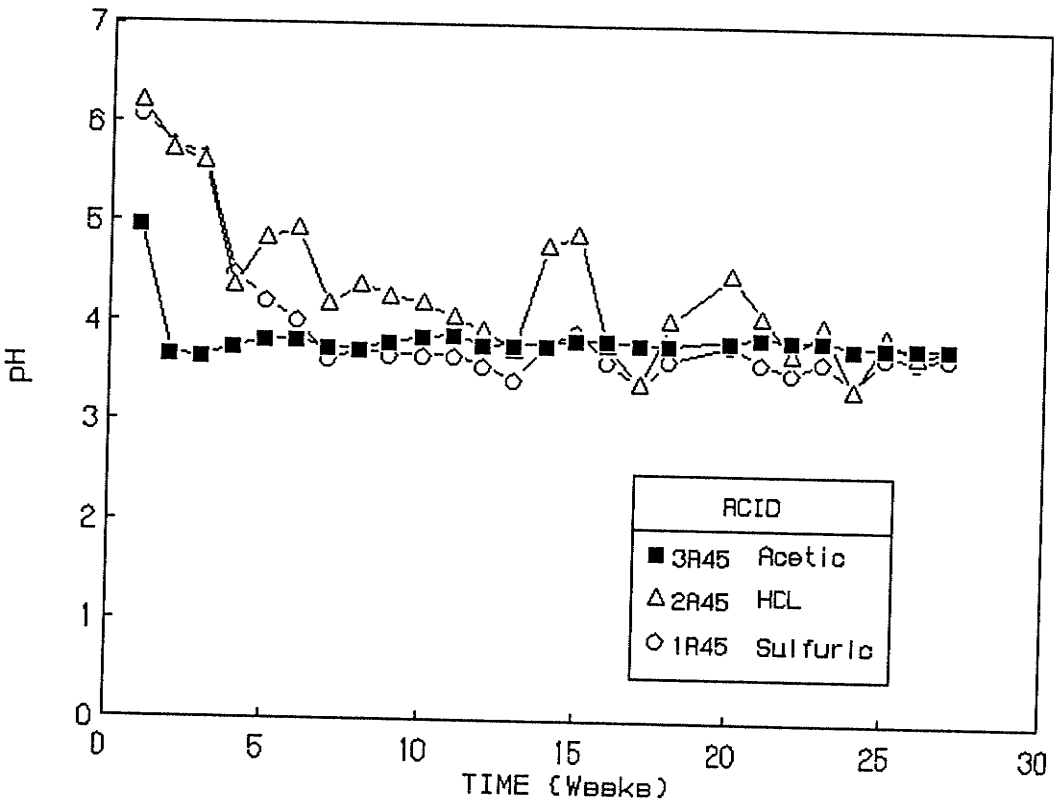

Figure 3.9 Changes in average pH versus immersion time: 1A45, 2A45 and 3A45

(3A45), and magnesium sulfate (S45). W_m, however, could not be measured for the MIC soil (R45) environment due to soil and bacteria embedded in the interior surface of the laminate. Different cleaning procedures and compounds were used to attempt to remove these particulates but proved to be unsuccessful. A surface microphotograph (Figure 3.10) shows the soil and bacteria embedded in the R45 specimens after 14 weeks immersion.

Test results showing the extent of material weight loss after 5, 14 and 27 weeks immersion are summarized in Appendix II-8. Changes in W_m for specimens immersed in deionized water and a buffered sodium hydroxide solution were similar. For example, after 27 weeks immersion (Table 3.2) the average material weight loss for D25 and B25 specimens were 0.21% and 0.16%, respectively. In comparison, the average material weight loss for D45 and B45 specimens were 0.45% and 0.45%, respectively. These results show that the effect of raising the temperature (25°C to 45°C) increases W_m by an average factor of 2.5. The average material weight loss for S45 specimens exposed to magnesium sulfate for 27 weeks was 0.57%. This value was slightly higher than the values measured for D45 and B45 specimens.

The highest W_m results were observed for the acidic environments. For example, after 27 weeks immersion the average material weight loss for 1A45, 2A45 and 3A45 specimens was measured at 0.91, 0.86, and 1.98%, respectively. Plots of W_m versus immersion time (Figure 3.11) are concave in shape which suggest that the rate of material weight loss for these specimens decreases with time . It is also evident that the highest W_m values were for specimens immersed in acetic acid. The W_m results for the sulfuric and hydrochloric acid (1A45 and 2A45) specimens are similar, which suggest

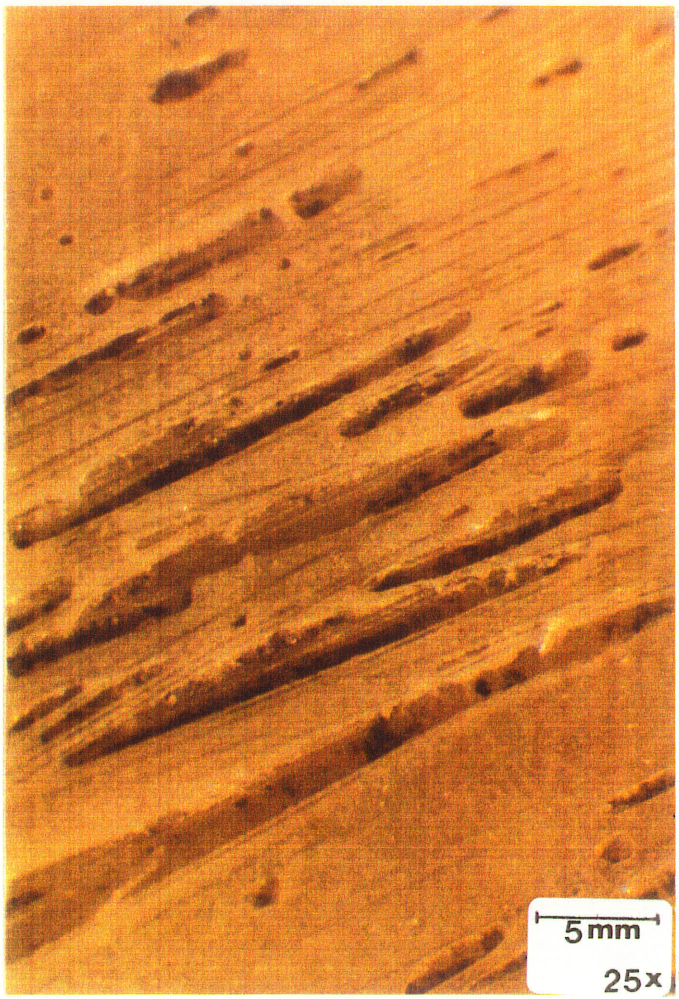

Figure 3.10 Surface photomacrograph of R45 specimens after 14 weeks immersion in MIC soil

Table 3.2 Extent of Deterioration for FFW Specimens after 27 Weeks Immersion: PS Study

Description Test Parameter	Deionized Water		NaOH (Buffered)		ACID			Sulfates	MIC
					H_2SO_4	HCl	Ch_3CO OH	$MgSO_4$	Soil
Environment	D25	D45	B25	B45	1A45	2A45	3A45	S45	R45
Gravimetric									
Average material weight loss (%)	0.21 (0.02)	0.45 (0.04)	0.16 (0.03)	0.45 (0.03)	0.91 (0.07)	0.86 (0.04)	1.98 (0.15)	0.57 (0.02)	*
Chemical									
Calcium as $CaCO_3(mgL^{-1})$	122	180	*	*	920	1,000	2,550	284	**
Aluminum as $AL_2O_3.3H_2O$ (mgL^{-1})	< 1	< 1	< 1	< 1	4	1	4	< 1	**
Dimensions									
Increase in volume (%)	0.19 (0.00)	1.59 (1.05)	0.55 (0.33)	1.53 (0.01)	1.65 (0.69)	1.67 (0.65)	1.66 (0.55)	1.26 (0.02)	1.06 (0.17)
Loss (%) in Dry Mechanical Properties									
Flexural strength $(1-S_f/S_{fo})$	4.9 (6.2)	24.0 (5.1)	10.5 (6.7)	16.4 (10.4)	20.1 (4.7)	26.7 (8.2)	23.8 (6.6)	20.8 (4.7)	15.7 (8.9)
Flexural modulus $(1-E_f/E_{fo})$	1.79 (10.3)	11.3 (6.5)	-0.6 (7.8)	7.7 (1.48)	9.5 (6.2)	14.3 (12.3)	8.3 (14.0)	1.2 (9.0)	3.6 (10.3)
Tensile strength $(1-S_t/S_{to})$	11.4 (7.0)	19.2 (11.2)	8.9 (13.5)	1.2 (9.6)	4.9 (7.3)	11.8 (15.7)	8.9 (7.6)	10.2 (10.7)	4.9 (4.2)
Tensile modulus $(1-E_t/E_{to})$	-18.8 (14.4)	7.9 (14.4)	-12.0 (21.9)	-2.0 (10.3)	3.0 (11.6)	1.0 (16.4)	4.0 (12.3)	-12.9 (29.5)	-7.9 (10.9)
Barcol hardness .../H_o)	2.0 (2.1)	2.1 (4.1)	1.8 (5.2)	0.00 (3.3)	8.9 (8.3)	12.3 (11.9)	17.9 (10.7)	7.00 (7.1)	1.9 (5.4)

Standard deviations in brackets

* Not available due to test interferences

** Not applicable

\- Negative number indicates an increase (%) in dry mechanical properties

< Less than

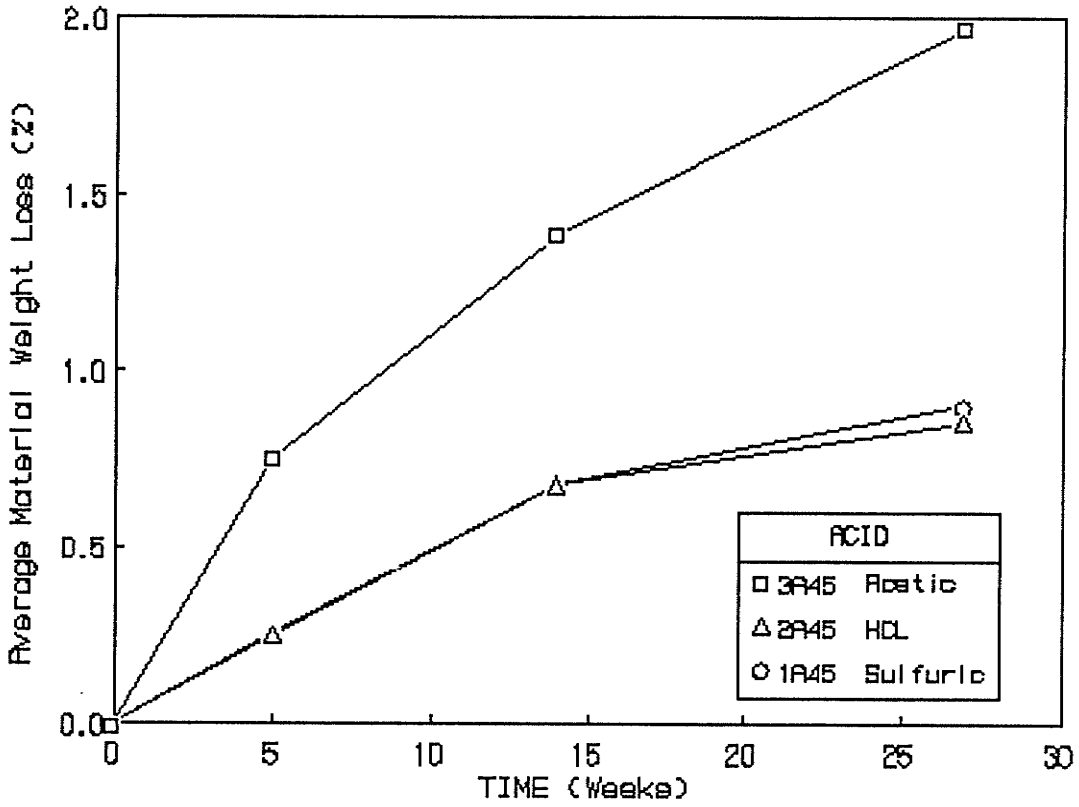

Figure 3.11 Average material weight loss (W_m) versus immersion time: 1A45, 2A45 and 3A45

that a similar deterioration mechanism occurs for each inorganic acid evnironment.

Average weekly calcium ion (Ca^{+++}) concentrations are summarized in Appendix II-9 for each environment. The Ca^{++} concentrations in deionized water (D25, D45) and magnesium sulfate (S45) environments after 27 weeks exposure (Table 3.2) ranged from 122 to 284 $mg.L^{-1}$ as $CaCO_3$. Calcium in the buffered sodium hydroxide solution, however, could not be measured due to colour interferences.

The highest Ca^{++} concentrations were measured in the acidic environments and ranged from 920 to 2550 $mg.L^{-1}$. The Ca^{++} concentration in acetic acid (3A45) was observed to be more than 2.5 times greater than for the inorganic acid (1A45, 2A45) environments. The Ca^{++} plots (Figure 3.12) are similar to the W_m plots in that they are concave in shape. A comparison of the 1A45 and 2A45 plots suggest that the calcium dissolution behaviour mechanism for specimens immersed in sulfuric and hydrochloric acids are similar.

The total aluminum ion (Al^{+++}) concentration expressed as $AL_20_3.3H_20$, was less than 4 $mg.L^{-1}$ after 27 weeks exposure (see Table 3.2). It is evident that calcium carbonate is more soluble than ATH in acidic environments. The solubility of Solem ATH does not appear to be influenced by the type of acid medium in the pH range 3.5 to 4.5. Since the FFW specimens contain an equal percentage by weight of each filler constituent, it can be concluded that the primary acid deterioration mechanism is the dissolution of calcium carbonate and not ATH particles. These results are in agreement with earlier experimental results (see Section 2.2.4.1) which suggested that Solem ATH could be an effective filler in FRP structures exposed to acidic environments due to its low rate of dissolution.

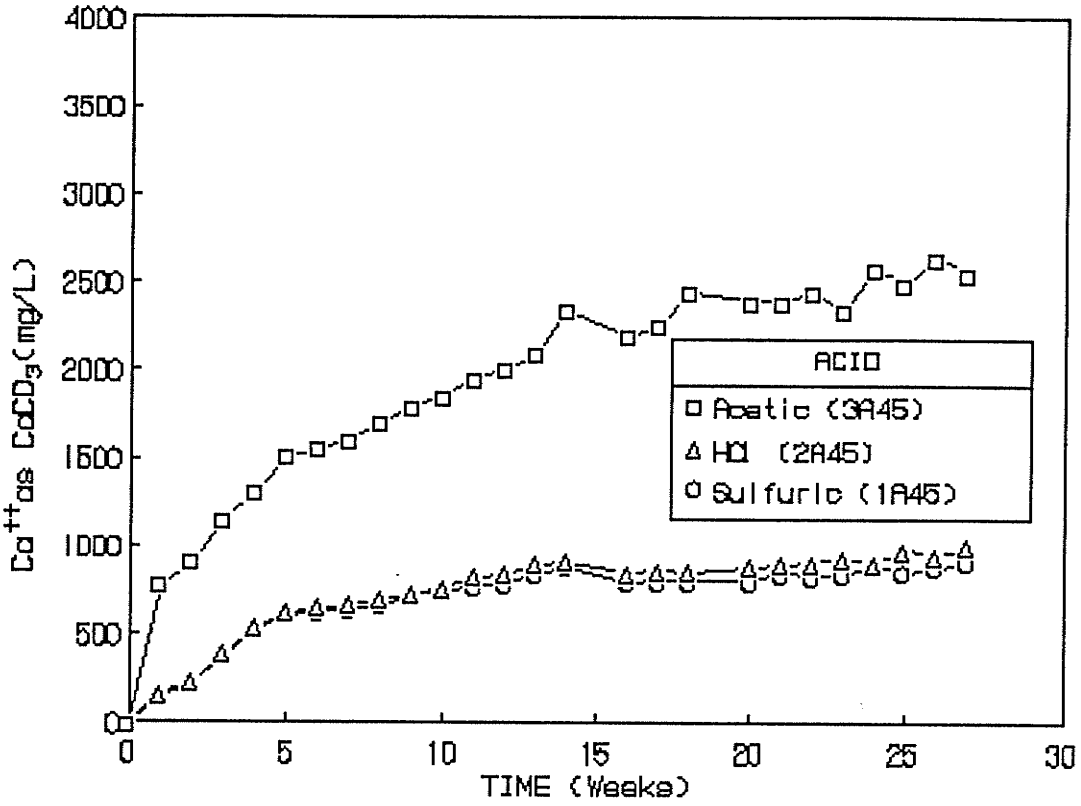

Figure 3.12 Calcium ion concentration of leachate versus immersion time: 1A45, 2A45 and 3A45

The concentration of hydrogen ions resulting from the ionization of sulfuric and acetic acid was correlated to the concentration of Ca^{++} as $CaCO_3$ (meq L^{-1}) in the leachate. The regression coefficients for the sulfuric and hydrochloric relationships (Figures 3.13 and 3.14) was determined to be 1.14 and 1.13, respectively. These results imply that the deterioration behaviour mechanisms for 1A45 and 2A45 specimens are similar. The high coefficients of determination (0.991 and 0.994) indicate that the addition of 1 meq L^{-1} of hydrogen ions (H^+) is related to the formation of 1.13 to 1.14 meq L^{-1} of calcium ions in the leachate. These results verify that the H^+ ions reacted primarily with $CaCO_3$ according to Eqn. [4]:

[4] $$\textit{Acid reaction:}\quad CaCO_3 + 2H^+ = Ca^{++} + CO_2 + H_2O$$

Surface micrograph of the same area of a 1A45 specimen after 2 and 27 weeks immersion in sulfuric acid are shown in Figures 3.15 and 3.16, respectively. Deterioration appears to be a surface phenomenon related to the enlargement of existing "flaws and cracks" in the direction of fiber reinforcement.

Surface micrographs of a 3A45 specimen (same surface area) immersed in acetic acid for 2 and 27 weeks are shown in Figures 3.17 and 3.18, respectively. A comparison of 1A45 and 3A45 specimens shows that the enlargement of the surface flaws and surface whitening were more extensive for the 3A45 specimens. These observations are in agreement with material weight loss and calcium ion leachate results which suggest that the deterioration behaviour mechanisms for 1A45 and 3A45 specimens are different.

Volumetric measurements were taken at different immersion times (5, 4 and 27 weeks) times in order to quantify the degree of swelling. The average percentage

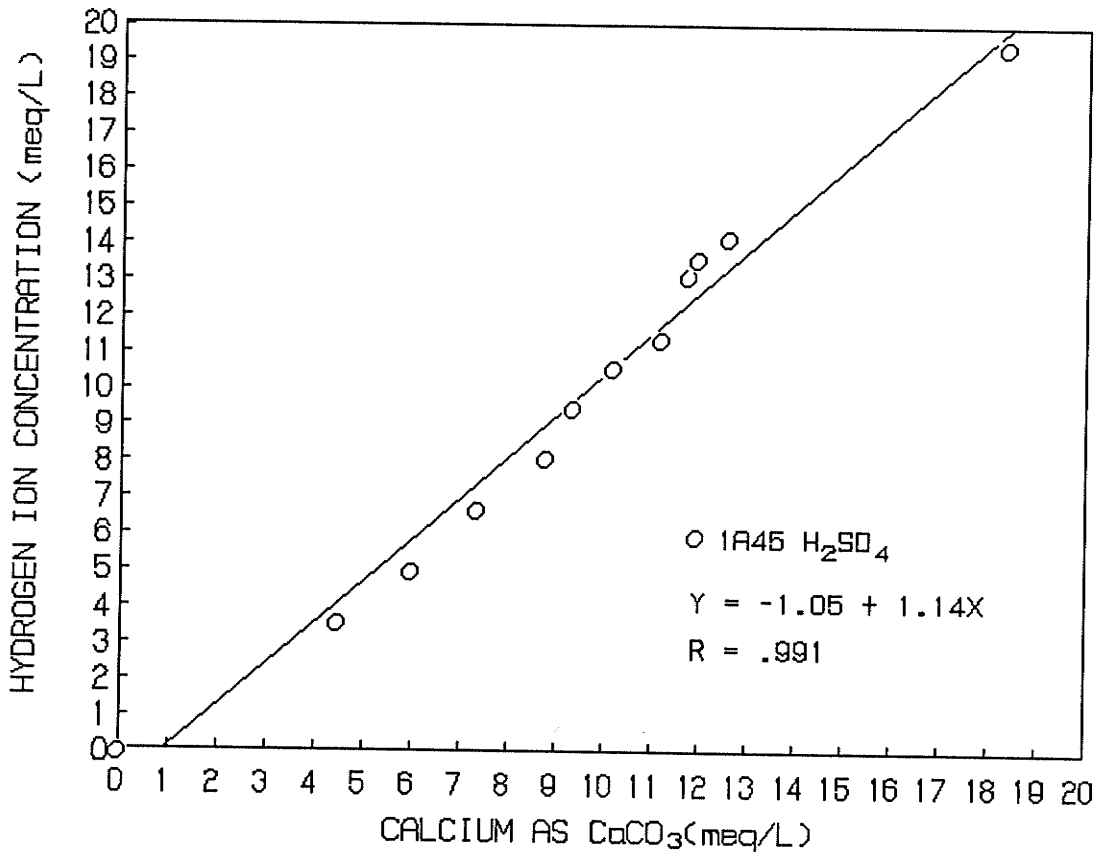

Figure 3.13 Regression analysis: hydrogen ion concentration (H_2SO_4) versus calcium as $CaCO_3$ in the leachate

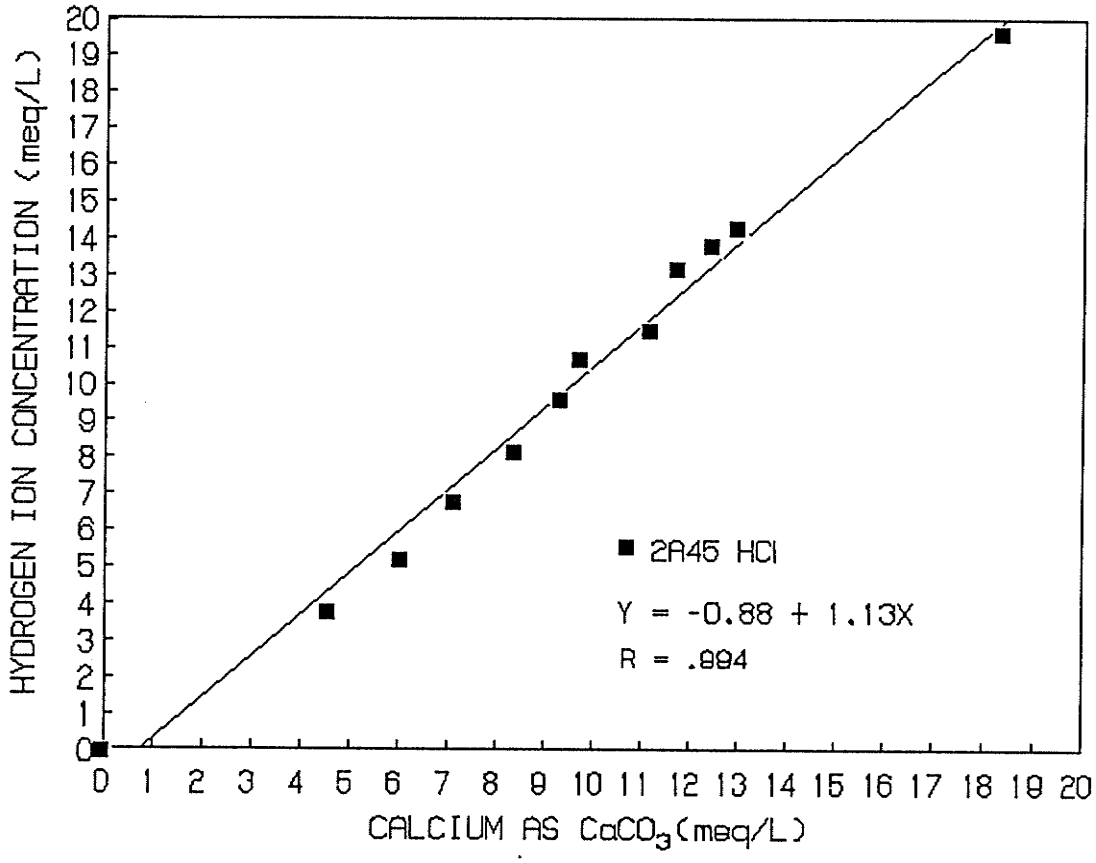

Figure 3.14 Regression analysis: hydrogen ion concentration (HCl) versus calcium as $CaCO_3$ in the leachate

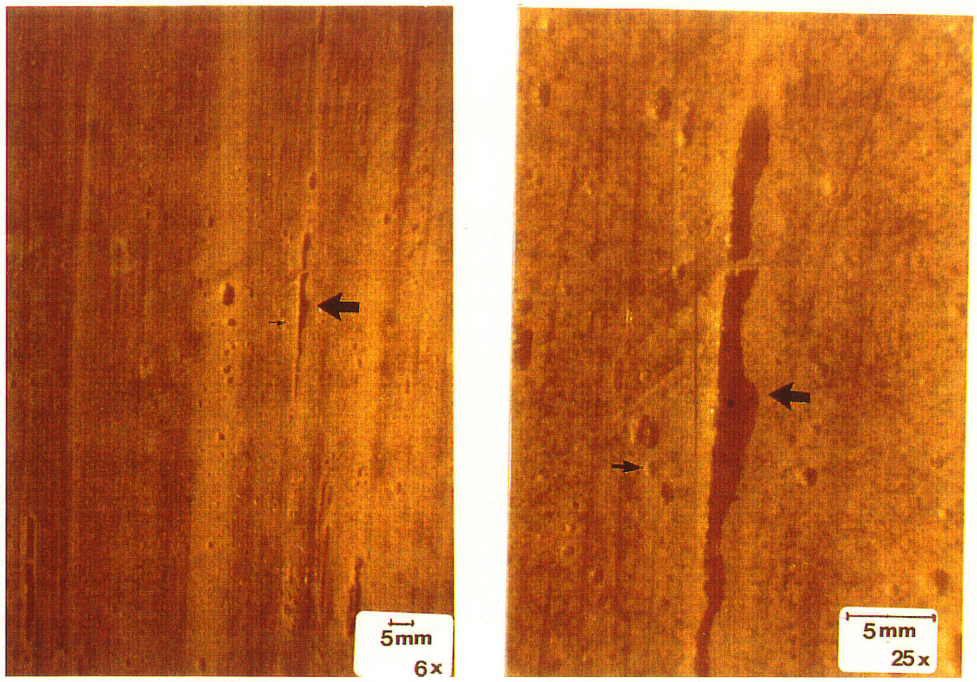

Figure 3.15 Surface photomacrographs of 1A45 specimens after 2 weeks immersion in sulfuric acid at 45°C

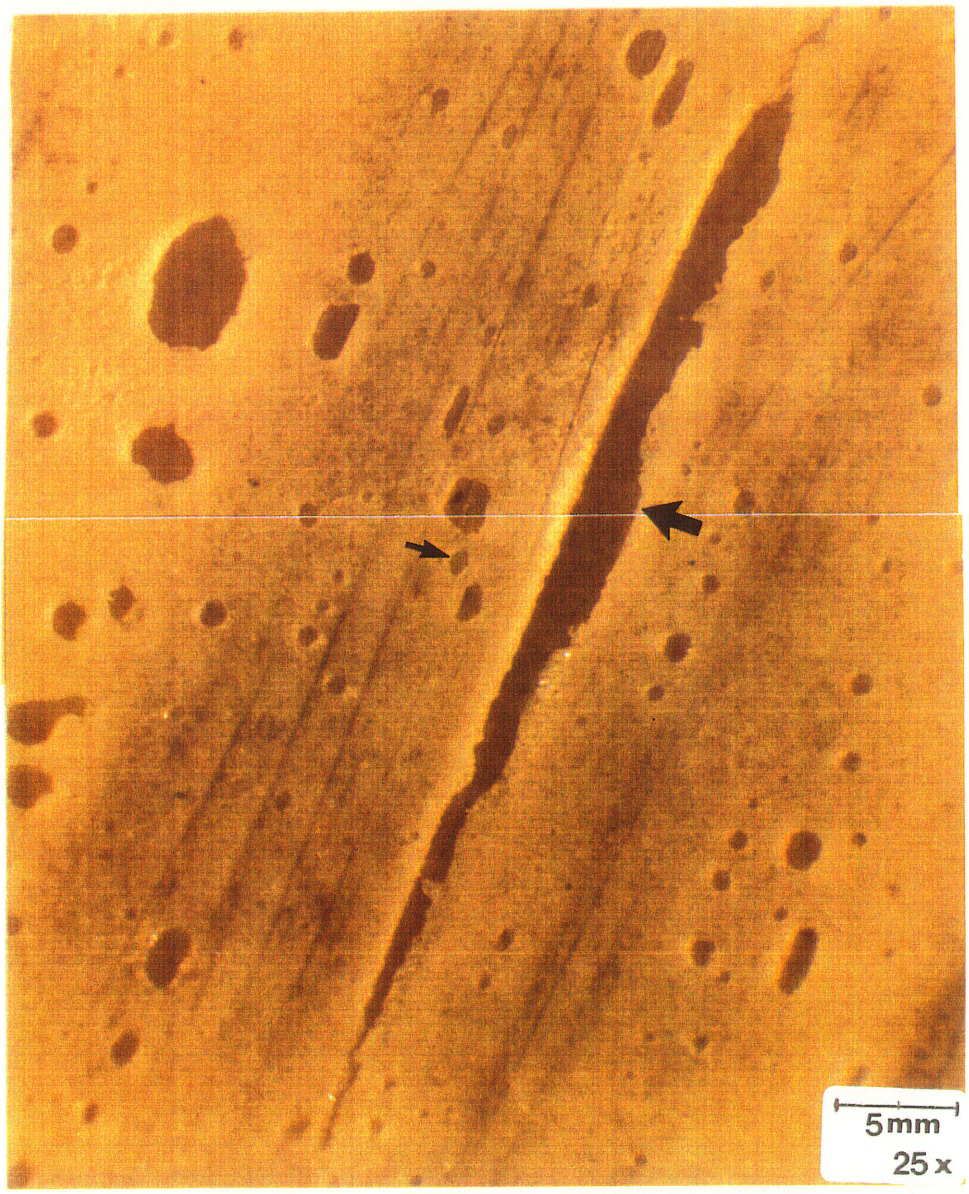

Figure 3.16 Surface photomacrographs of 1A45 specimens after 27 weeks immersion in sulfuric acid at 45°

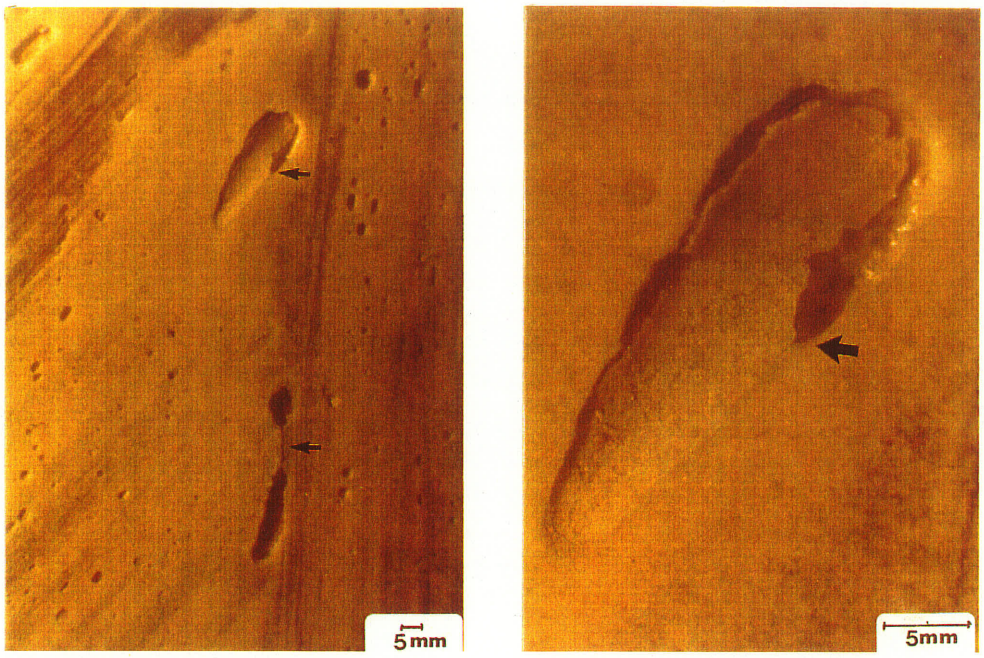

Figure 3.17 Surface photomacrographs of 3A45 specimens after 2 weeks immersion in acetic acid at 45°

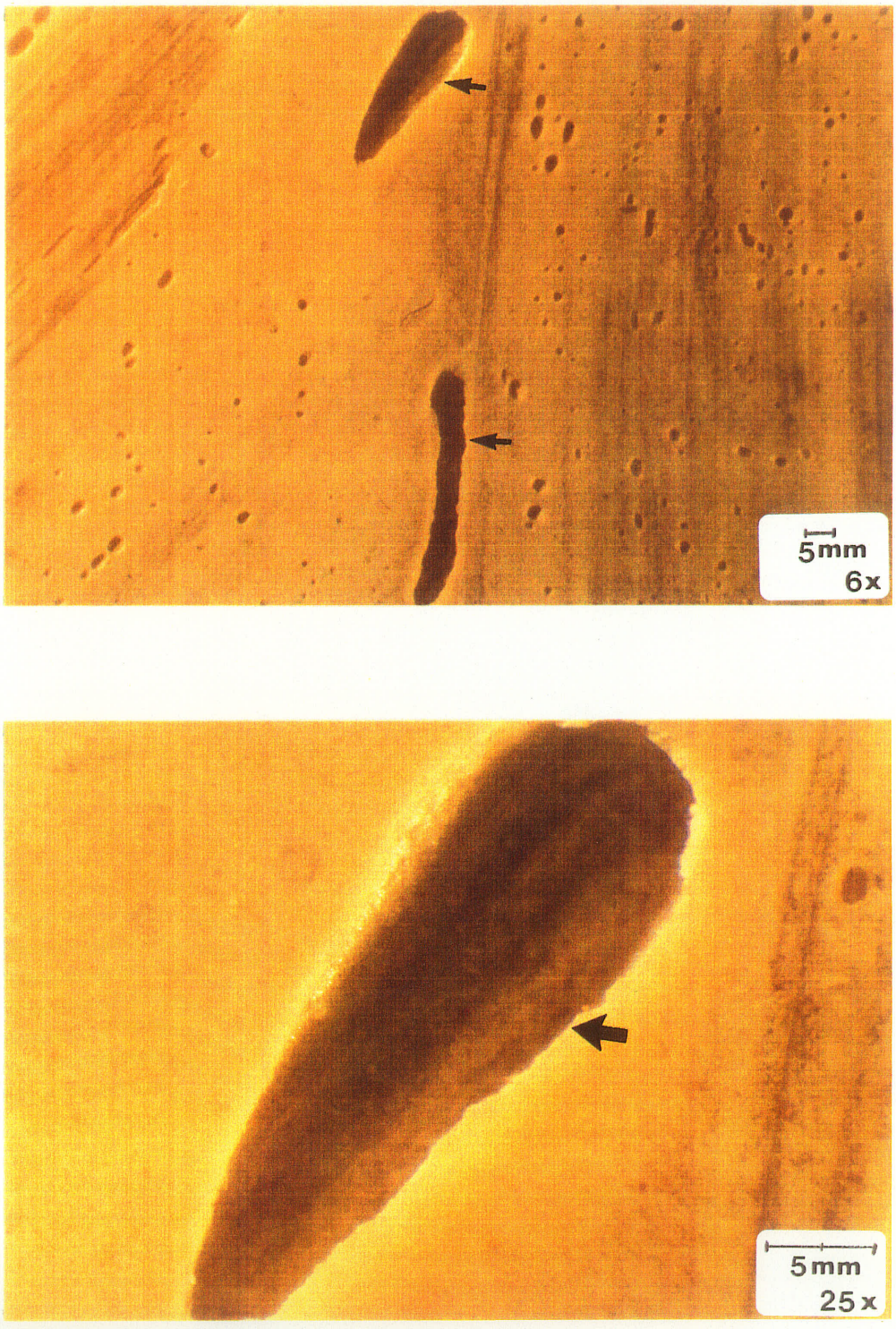

Figure 3.18 Surface photomacrographs of 3A45 specimens after 27 weeks immersion in acetic acid at 45°

increase in the volume of the FFW specimens after 27 weeks exposure is shown in Table 3.2. It is evident that the degree of swelling in the low temperature environments is less than in the high temperature environments. For example, the increase in volume for D25 and B25 specimens were 0.19 and 0.55% respectively. In comparison, the increase in volume for specimens that were totally submerged at the higher temperature (D45, B45, 1A45, 2A45, 3A45, S45) ranged from 1.26 to 1.67%. The lower value for the R45 specimens (1.06%) was attributed to the specimens being partially submerged (anaerobic/aerobic) in the MIC soil.

The average increase in specimen volume for each temperature condition is shown in Figure 3.19. The data for these plots were pooled and averaged according to the low (D25, B25) and high (D45, B45, 1A45, 2A45, 3A45, S45) temperature conditions (see Appendix II-10). The average volume increase for D25 and B25 specimens after 5, 14 and 27 weeks exposure were 0.10, 0.17 and 0.37%, respectively. In comparison, the average volume increase for the high temperature (45°C) specimens were 0.90%, 1.36% and 1.56% respectively. The concave shape of the higher temperature (45°C) plot suggests that the rate of swelling decreases with exposure time. In contrast to the above results, Bravenic (1983) observed no changes in the dimensions of unfilled crosslinked polyester specimens that were saturated in water at 50°C. The precision of his measurements, however, were limited by the resolution of his micrometer.

The average initial dry mechanical properties for postcured FFW specimens prior to immersion, are shown in Table 3.3. The initial flexural (S_{fo}) and tensile (S_{to}) strengths were determined to be 281.5 and 24.6 MPa, respectively. In comparison, the

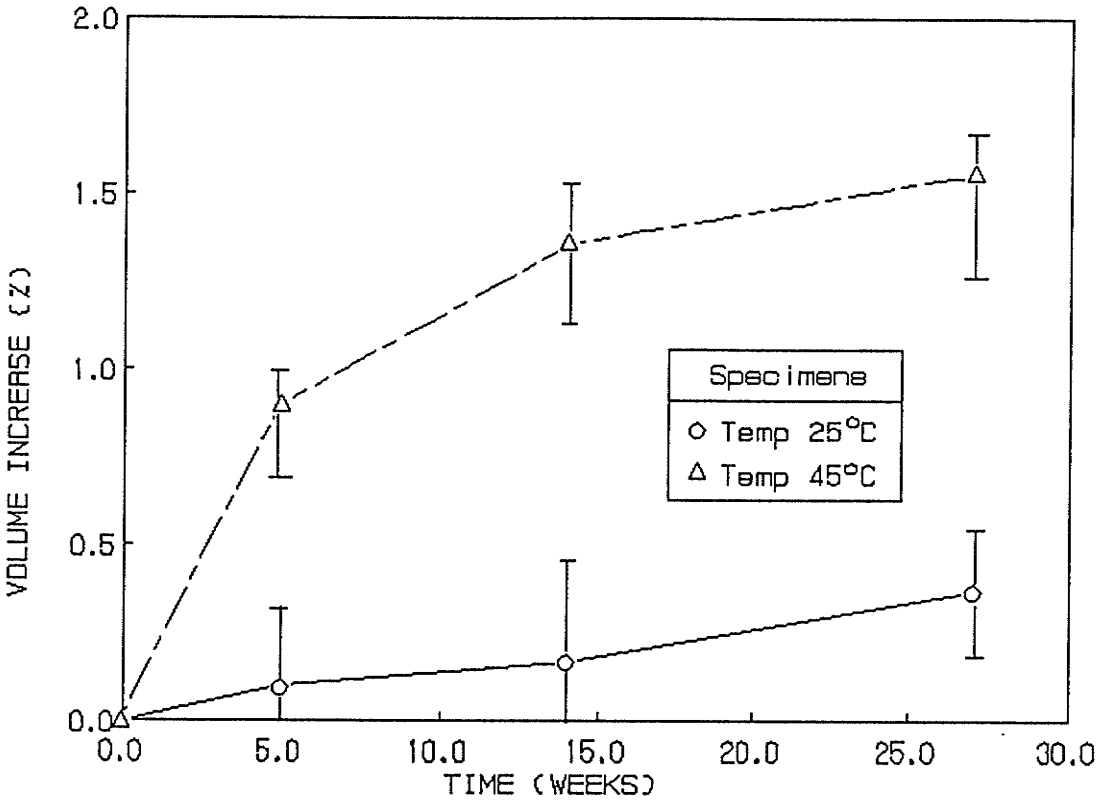

Figure 3.19 Average volume increase (%) versus immersion time: (25° and 45°C)

Table 3.3 Average initial dry mechanical properties of FFW specimens prior to immersion

Test Parameter	Number of Observations	Average Value	Standard Deviation
Flexural strength (S_{fo})	24	281.5 MPa	21.3
Flexural modulus (E_{fo})	24	16.8 GPa	1.2
Tensile strength (S_{to})	17	24.6 MPa	4.0
Tensile modulus (E_{to})	17	10.1 GPa	1.7
Barcol hardness (H_o)	15	61.6	4.1

initial flexural (E_{fo}) and tensile (E_{to}) modulus of elasticity were determined to be 16.8 and 10.1 GPa, respectively. The initial Barcol hardness (H_o) on the interior FFW surface was 61.6.

The average dry mechanical properties of exposed specimens were poor physical indicators of deterioration. The results are summarized in Appendix II-11, II-12, and II-13. Belsham (1989) conducted a statistical analysis using a two tailed Student t-Test (95% confidence limit) to compare the dry flexural and tensile properties of specimens which had been immersed in various environments after 27 weeks exposure. The results (Appendix. II-14) showed that there was no significant difference in properties for specimens immersed in different environments at the same temperature.

Losses in dry mechanical properties were normalized with respect to the "baseline" data (identified by the subscript $_0$ in Table 3.3) and expressed as a loss (%) in the initial dry mechanical property ($1\text{-}S_f/S_{fo}$, $1\text{-}E_f/E_{fo}$, $1\text{-}S_t/S_{to}$, $1\text{-}H/H_o$). The losses in dry flexural strength after 27 weeks immersion (Table 3.2) ranged from 4.9 to 10.5%

for the low temperature (25°C) environments and from 15.7 to 26.7 percent for the high temperature (45°C) environments. An increase in flexural modulus was observed for the 25°C environments, while losses in flexural modulus for the 45°C environments ranged from 1.2 to 14.3%. The losses in dry tensile strength ranged from 8.9 to 11.4% for the 25°C environments and from 1.2 to 11.8% for the 45°C environments. An increase in tensile modulus was also observed for the 25°C environments. Future testing of dry tensile strength and moduli properties (Table 3.2) is not recommended due to the large variance in the tensile data. The highest losses in dry Barcol hardness were observed for the acidic (45°C) environments and ranged from 8.9 to 17.9%.

A summary of dry and wet mechanical properties after 52 weeks immersion is shown in Appendix II-15. A comparison of the loss in dry and wet mechanical properties for each temperature condition is shown in Table 3.4. Losses in wet mechanical properties were significantly greater than corresponding losses in dry mechanical properties. Higher losses in wet mechanical properties were observed for the high temperature (45°C) condition. These results are in agreement with Gibson et al. (1984) who showed elevated temperature distilled water (49°-51°C) causes more rapid diffusion of moisture in SMC-R25 and SMC-R65 materials and, consequently, more rapid losses in flexural dynamic properties than the room temperature water environment.

In this work, the average loss in wet flexural strength ranged from 21.5% (25°C) to 41.0% (45°C). In comparison, the average loss in wet tensile strength ranged from 40.7% (25°C) to 52.8% (45°C). Losses in wet Barcol hardness ranged from 7.6% (25°C) to 21.8% (45°C) after 52 weeks exposure. Wet mechanical properties are greater at 45°C and these results indicate that these properties should be tested in the wet state.

Table 3.4 Comparison of Dry and Wet Mechanical Property Losses (%) after 52 Weeks Immersion

Mechanical Property	Low Temperature (25°C) %		High Temperature (45°C) %	
1. Flexural Strength				
Dry	6.6	(4.0)	18.0	(5.6)
Wet	21.5	(4.2)	41.0	(2.5)
2. Flexural Modulus				
Dry	1.8	(8.9)	-.6*	(3.0)
Wet	18.5	(4.2)	25.2	(3.5)
3. Tensile Strength				
Dry	17.5	(2.4)	17.5	(13.8)
Wet	40.7	(6.1)	52.8	(5.3)
4. Tensile Modulus				
Dry	-25.7*	(20.8)	-8.9*	(8.9)
Wet	24.8	(19.8)	48.5	(4.7)
5. Barcol Hardness				
Dry	0.2	(2.1)	2.4	(4.1)
Wet	7.6	(4.4)	21.8	(5.8)

* indicates an increase in value.

standard deviation in brackets.

Similar losses in wet tensile strength were observed by others for SMC-R25 specimens after immersion in salt water (93°C) for 180 days (Springer et al., 1980; Springer, 1984).

Typical desorption isotherm plots for D45 and 3A45 specimens immersed in deionized water and acetic acid are shown in Figures 3.20 and 3.21, respectively. A comparison of the plots shows the initial slopes of the 3A45 isotherms are greater than the D45 isotherms. Desorption slopes (S_d) were determined from the initial linear desorption isotherm plots for specimens immersed after 27 weeks.

The desorption slopes (Table 3.5) were based on a least-square regression analysis conducted on the initial linear portion of the isotherm which constituted 50 to 60 percent of the total moisture lost. The high correlation coefficients, ranging from 0.987 to 0.999 which suggest a strong linear relationship.

Regression coefficients (S_d) for D25 and B25 specimens were 0.030 and 0.033 $min^{-1/2}$,respectively. In comparison, S_d for the higher temperature (45°C) environments were much higher and ranged from 0.052 to 0.123 $min^{-1/2}$.

The highest desorption slope was for 3A45 specimens immersed in acetic acid. This value was approximately two times greater than S_d determined for 1A45 and 2A45 specimens. The S_d values for specimens immersed in sulfuric and hydrochloric acid were similar which suggest a similar deterioration behaviour mechanism.

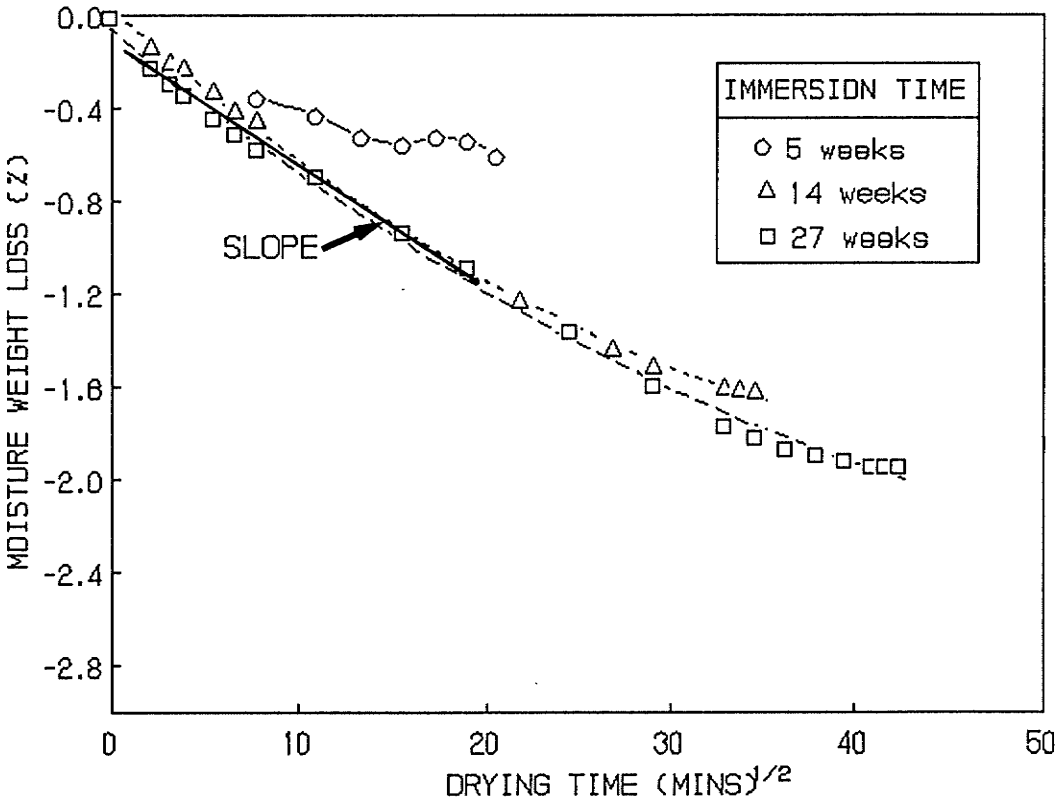

Figure 3.20 Typical desorption isotherm for D45 specimens after 27 weeks immersion: MDH method

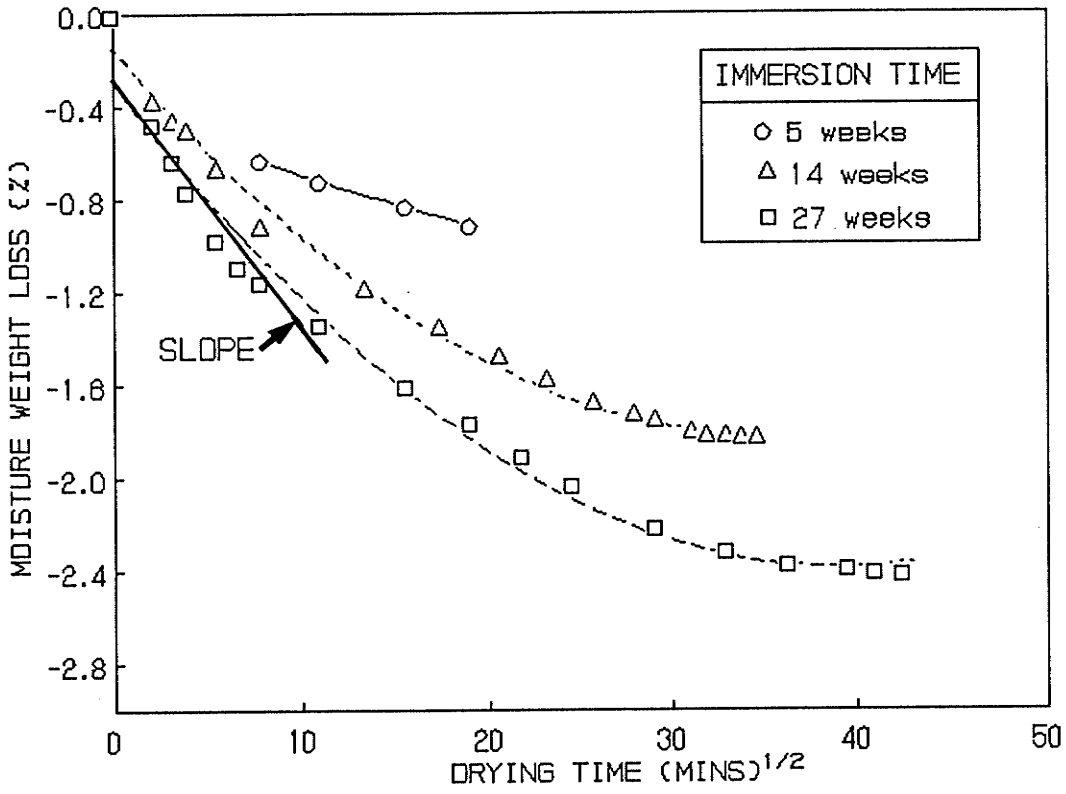

Figure 3.21 Typical desorption isotherm for 3A45 specimens after 27 weeks immersion: MDH method

Table 3.5 Desorption Slope Analyses after 27 Weeks Immersion: PS Study

Environment Type	Desorption Slope ($min^{-1/2}$)	Correlation Coefficient (R)
Deionized Water		
D25	0.030	0.995
D45	0.052	0.996
NaOH (Buffered		
B25	0.033	0.998
B45	0.055	0.997
Acids		
1A45	0.059	0.999
2A45	0.058	0.998
3A45	0.123	0.987
Sulfates		
S45	0.060	0.995
MIC Soil		
R45	0.058	0.998

The desorption slope of none of the acidic specimens passed through the origin. The intercept of the desorption plot was excluded from the desorption slope analysis since it is believed to result from surface deterioration. For example, it is believed that the acid which filled the "enlarged" surface flaws and or cracks (Figure 3.16 and 3.18) evaporated almost instantaneously with the application of heat, resulting in an initial weight loss. If this suggestion is correct, then the intercept is an indicator of the level of deterioration at the surface of acid-attacked specimens due to the "enlargement" of surface flaws and cracks.

It was postulated (Section 3.3.3.5) that S_d could be used as a deterioration test parameter to quantify the quasi-constant diffusion characteristics in the degraded layer (h) of FFW specimens. If this assumption is correct then specimens showing the greatest material weight loss (W_m) for a specific immersion time period should also show the greatest change in S_d. A comparison of S_d versus material weight lost (W_m) after 27 weeks immersion is shown in Table 3.6. A strong correlation (Figure 3.22) and a linear least-square regression analysis (Equation 29) show good correlation between S_d and W_m ($R = 0.955$) for the high temperature (45°C) environments. This relationship verifies that S_d can be used as a valid test parameter to predict the extent of material weight loss for FFW specimens immersed in aqueous environments.

[29] $$W_{m(45°)} = -0.191 + 16.53\ S_{d(45°C)}\quad R = 0.955$$

The usefulness of this relationship is demonstrated in predicting W_m for R45 specimens exposed to an MIC soil environment. It was found earlier that W_m could not be measured due to soil and bacteria embedded in the interior surface of the R45

Table 3.6 A Comparison of S_d and W_m After 27 Weeks Immersion: PS Study

Environment Type	S_d ($min^{-1/2}$)	W_m (%)
1. Low Temperature		
D25	0.030	0.16
B25	0.033	0.21
2. High Temperature		
D45	0.052	0.45
B45	0.055	0.45
1A45	0.059	0.91
2A45	0.058	0.86
3A45	0.123	1.98
S45	0.060	0.74
R45	0.058	0.77*

* Predicted from regression equation.

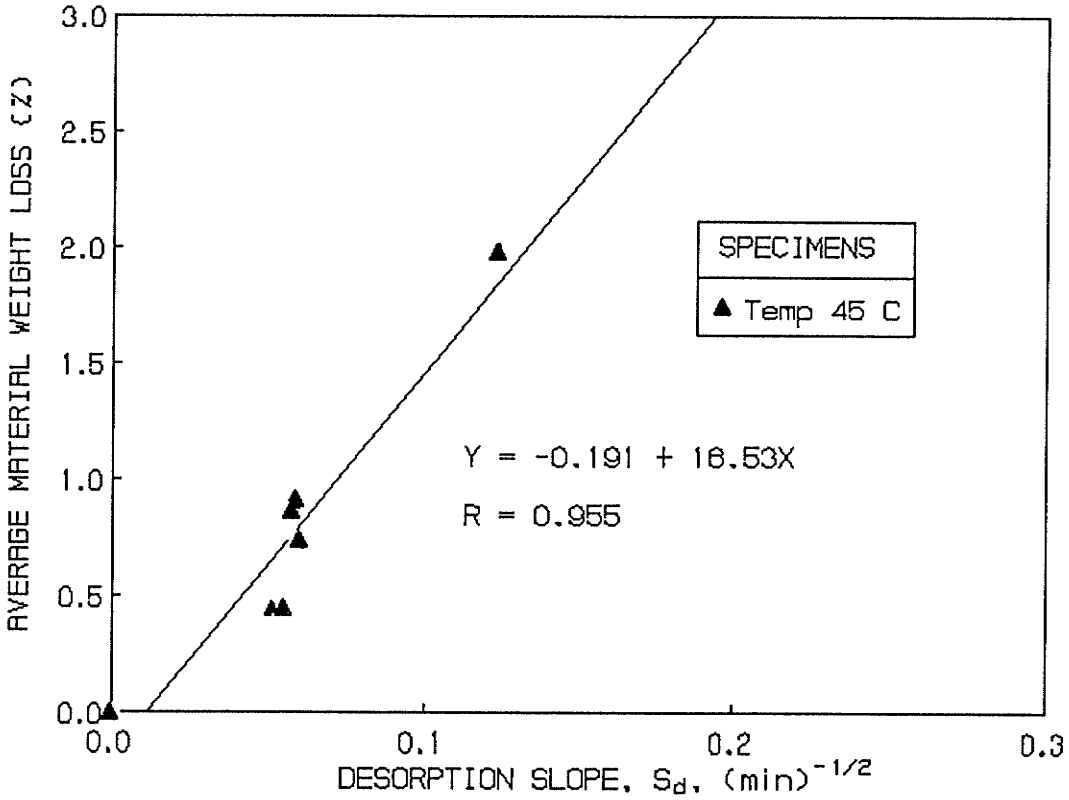

Figure 3.22 Regression analysis: material weight loss (W_m) versus desorption slope (S_d) for the 45°C environments

specimens. However, using Equation [29] and a value of S_d (0.058 $min^{-½}$), W_m is predicted to be 0.77% (Table 3.6). This value is similar in magnitude to S45 specimens immersed in $MgSO_4$ (0.74%).

3.4 METAL CORROSION EXPERIMENT

A specific objective of the metal corrosion experiment was to assess and compare the corrosion/deterioration behaviour of metals (mild and galvanized steel) and postcured FFW composites in similar laboratory environments. Laboratory control parameters were selected to simulate four field environments; softwater, alkaline (base), acid (inorganic), and an anaerobic/aerobic biological MIC environment. The experiments were conducted for low (25°C) and high (45°C) temperature conditions. The 45°C temperature condition was selected to accelerate the rate of deterioration. Weight loss methods were used to quantify and compare the corrosion/deterioration behaviour of both materials.

3.4.1 Materials

Mild steel (MS) and galvanized steel (GS) coupons (13 mm x 102 mm x 0.8 mm) were stamped from 22 gage sheet metal (supplied by Russel Steel Ltd., Wpg., Man.) and prepared according to ASTM D 2688 (1983). A 7 mm diameter hole was drilled at the top with its centre about 8 mm from the edge of each coupon. The edges of the coupons were sanded and the hole deburred with an oversized drill. A total of 130 coupons of each metal were prepared, cleaned, and identified.

In cleaning the MS coupons, oil was first removed by immersion in

trichloroethylene. The cleaned coupons were immersed in 2.4 N HCl for 30 minutes at room temperature, rinsed rapidly (three times) in deionized water, rinsed successively in isopropyl alcohol, trichloroethylene and dried with a clean cloth. The GS coupons, were, however, only cleaned with trichloroethylene and dried with a clean towel.

All cleaned dry coupons were weighed on an analytical balance to the nearest 0.1 mg and stored in a desiccator. The coupons were removed from the desiccator and reweighed immediately prior to being immersed in each environment.

3.4.2 Laboratory Procedure

The experimental design for the metal corrosion experiment is shown in Table 3.7. The laboratory environments selected for comparison included: deionized water, NaOH (initially buffered at pH 9.2), sulfuric acid (initial pH 3.5) and an MIC soil (anaerobic/aerobic). The immersion mediums were prepared according to the same procedures used in the FFW deterioration experiment (see Appendix II-5).

Sixteen coupons were mounted on a 5 mm glass horizontal rod at 9.5 mm intervals, and immersed in a filled (3 litre volume) closed top container. Metal coupons submerged in the MIC soil paste were removed every two weeks and suspended in air for a period of two weeks to simulate an anaerobic/aerobic cyclic environment. Successive cycles were conducted over the course of the test program. The metal coupons were exposed to the same number of anaerobic/aerobic cycles as the FFW specimens.

The temperature and pH levels of each immersion medium were checked at 2 day intervals during the 27 week test period. Because of evaporation, deionized water was

Table 3.7 Metal Corrosion Experiment Design Program

Laboratory Medium	Metal Type	Laboratory Control Parameter: Operating Parameter	Temp. 25°C	Temp. 45°C
Deionized water (softwater)	MS* GS**	pH range 7.0-8.0	DS25 DG25	DS45 DG45
NaOH (base)	MS GS	pH range 9.0-9.5	BS25 BG25	BS45 BG45
Sulfuric acid (inorganic)	MS GS	ph range 3.5-4.5	AS25 AG25	AS45 AG45
MIC Soil (biological)	MS GS	$SO_4^{=} > 2{,}000$ mg/L anaerobic/aerobic	-	RS45 RG45

* Mild steel.

** Galvanized steel.

added as required to maintain the level in each container at a constant volume. Additional amounts of 1.0 N sulfuric acid were added intermittently to maintain the pH in the range of 3.5 to 4.5.

Following each immersion time period (2, 5, 14 and 27 weeks), four metal coupons were removed from each environment, visually examined and cleaned for weight loss measurements.

3.4.3 Analytical Methods

Electrochemical reactions in aqueous environments are normally characterized by uniform attack over the metal surface. For example, it has been shown that a piece of steel or zinc immersed in dilute sulfuric acid will normally dissolve at a uniform rate over its entire surface (Fontana, 1986). In cases of uniform attack, the metal surface becomes thinner and eventually fails. The rate of uniform corrosion can be accurately estimated on the basis of weight loss.

Two weight loss methods (Methods B and C) are described in ASTM D 2688 (1983) to determine the corrosivity of water in distribution pipe systems. The flat coupon test (Method B) was used in this experiment since this method was simpler and less time-consuming. This method involves merely immersing metal coupons in an aqueous environment and measuring their weight loss for a specific exposure time. After removal, these coupons are cleaned using a series of acid rinses and other chemical treatments needed to remove scale and to restore the original metal surface. A "blank" coupon is subjected to the identical cleaning procedure in order to determine the "blank" correction factor. This factor is added to the weight loss to determine the actual weight

loss prior to cleaning. One disadvantage of the test method observed by Riber et al. (1989) has been the loss of precision in the results due to the cleaning preparation techniques. The average corrosion rate for a specific immersion time period is expressed as follows:

[30] $$P_1 = [(L)\ (W_2 - W_1)\ (W_1)^{-1}]\ [(t)^{-1}]\ [182.5]$$

Where:

P_1 is the corrosion rate, $mm.y^{-1}$

L is the original thickness of the coupon, mm

t is the immersion time period (t_2 - t_1), days

W_2 is the weight of the metal coupon after t_2, grams

W_1 is the weight of the metal coupon after t_1, grams

3.4.4 Results and Discussion

The average pH condition in each laboratory environment during the test period is shown in Table 3.8 (see Appendix II-16). Standard deviations were the largest for the sulfuric acid environments.

The average material weight loss for DS25 and AS25 coupons was 7.09% and 9.41%, respectively, after 27 weeks immersion (Table 3.9). In comparison, the average material weight loss for DS45 and AS45 coupons were 13.53% and 15.56%. The similarity in results between deionized water and sulfuric acid suggests that corrosion rates are independent of pH. These observations are in agreement with others (Betz, 1980) who reported that in the pH range between 4 to 10 the corrosion of iron depends

Table 3.8 Average pH Conditions During 27 Week Test Period: Metal Corrosion Experiment

Environment Type	Low Temperature (25°C)			High Temperature (45°C)		
	Specimen Type	Average pH	Standard Deviation	Specimen Type	Average pH	Standard Deviation
Deionized water	DS25	7.63	0.42	DS45	8.00	0.29
	DG25	8.38	0.39	DG45	7.96	0.35
NaOH Buffered)	BS25	9.20	0.04	BS45	9.19	0.05
	BG25	9.18	0.04	BG45	9.19	0.05
Sulfuric acid	AS25	4.03	0.34	AS45	3.80	0.21
	AG25	4.34	0.56	AG45	4.31	0.55
MIC soil	RS25	**	**	RS45	7.63	7.63
	RG25			RG45	0.28	0.28

Table 3.9 Average Material Weight Loss (W) after 27 Weeks Immersion: Metal corrosion Experiment

Environment Type	Low Temperature (25°C)		High Temperature (45°C)	
	Specimen Type	W (%)	Specimen Type	W (%)
Deionized water	DS25	7.09	DS45	13.53
	DG25	4.91	DG45	11.86
NaOH (buffered)	BS25	0.02	BS45	0.00
	BG25	0.01	BG45	0.07
Sulfuric acid	AS25	9.41	AS45	15.56
	AG25	7.59	AG45	9.27
MIC soil	RS25	**	RS45	21.13
	RG25	**	RG45	4.58

** Not available.
* Negligible.

primarily on the rate of mass transfer (diffusion) of oxygen to the cathode surface.

Test results showing the extent of material weight loss (W) after 2, 5, 14 and 27 weeks immersion are summarized in Appendix II-17. Changes in material weight loss for MS coupons immersed in deionized water and sulfuric acid as a function of immersion time are similar (Figures 3.23 and 3.24). Surface photographs of the MS coupons immersed in deionized water (DS45) and sulfuric acid (S45) after 14 and 27 weeks immersion are shown in Figure 3.25.

It is known that natural scales form as oxidation products on the surface of corroding metals (Montgomery, 1985). Hard black scales, most likely ferric hydroxide, developed on the surface of the DS45 and AS45 specimens after 2 weeks immersion . However, after 14 weeks exposure these hard scales softened and deteriorated, resulting in further increases in the rate of corrosion.

Maximum corrosion rates were calculated on the basis of weight loss measurements between 14 and 27 weeks (Table 3.10). The maximum corrosion rates for DS25 and AS25 coupons were 0.066 and 0.098 mm y^{-1}. These results are in agreement with Haviland et al. (1966) who showed, in a culvert field study, that the corrosion rates of 86% of the non-galvanized CSP culverts inspected were less than 0.05 mm y^{-1}; the maximum corrosion rate was reported at 0.13 mm y^{-1}. Most of these culverts were exposed to quiet natural waters and corrosion was confined to the interior surface and occurred below the water line.

In comparison, the maximum corrosion rates for DS45 and AS45 specimens were 0.129 and 0.159 mm y^{-1}, respectively. These results show that the effect of raising the temperature from 25° to 45°C increased the corrosion rate of mild steel in deionized

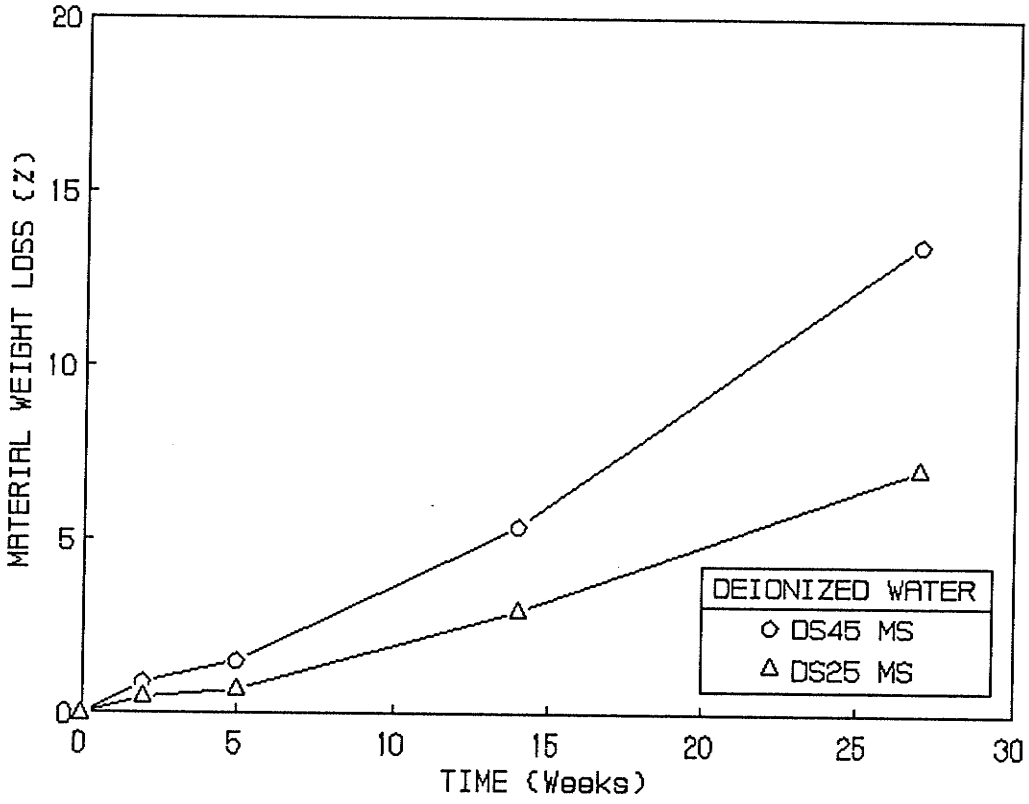

Figure 3.23 Average material weight loss versus immersion time: DS25, DS45

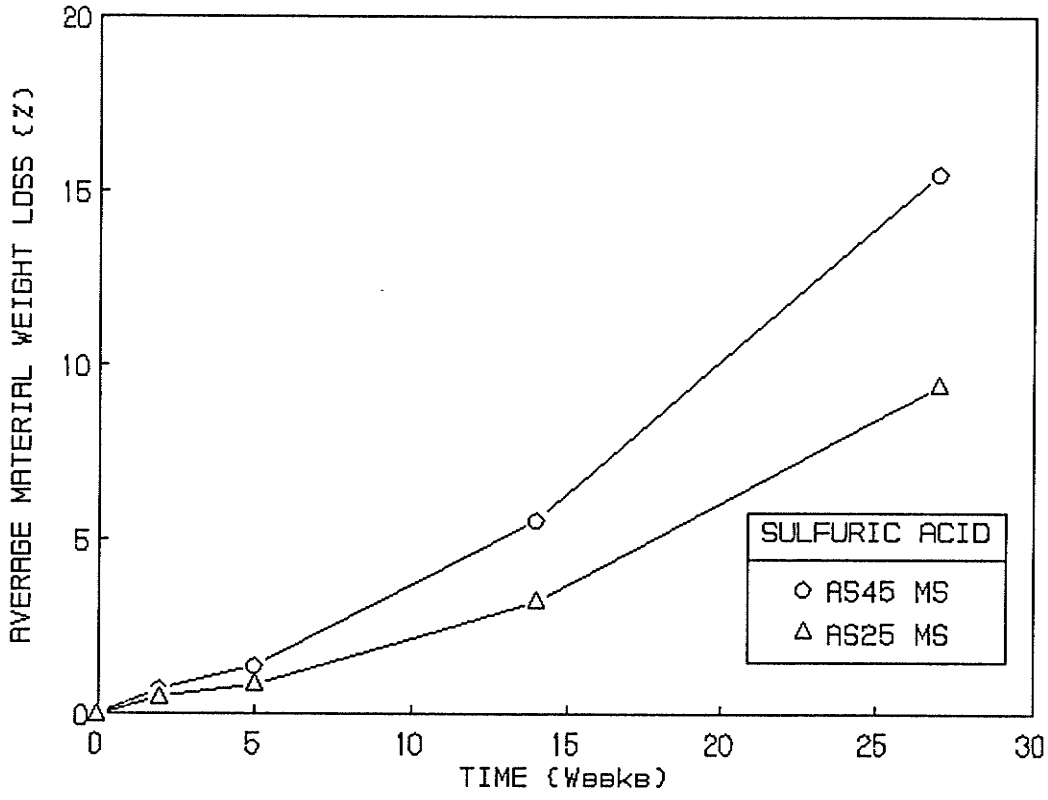

Figure 3.24 Average material weight loss versus immersion time: AS25, AS45

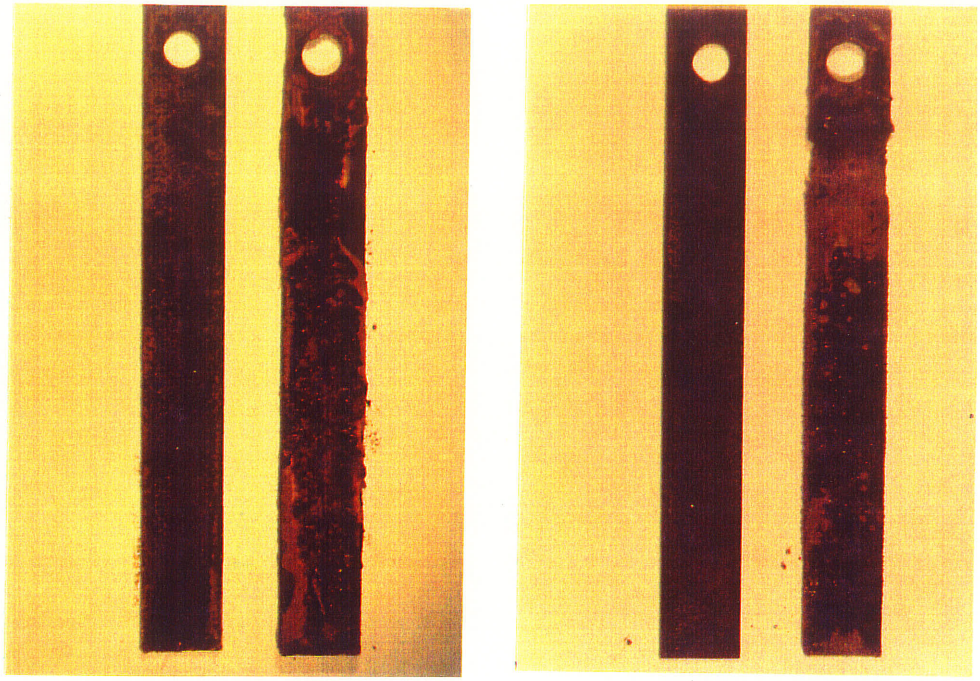

DS45
14 weeks 27 weeks

AS45
14 weeks 27 weeks

Figure 3.25 Surface photographs of DS45 and AS45 coupons after 14 and 27 weeks immersion

Table 3.10 Maximum Corrosion Rate (P) Between 14 and 27 weeks Exposure: Metal Corrosion Experiment

Environment Type	Low Temperature (25°C)		High Temperature (45°C)	
	Specimen Type	P $mm.y^{-1}$	Specimen Type	P $mm.y^{-1}$
Deionized water	DS25	0.066	DS45	0.129
	DG25	0.018	DG45	0.102
NaOH (buffered)	BS25	*	BS45	*
	BG25	*	BG45	*
Sulfuric acid	AS25	0.098	AS45	0.159
	AG25	0.063	AG45	0.081
MIC soil	RS25	**	RS45	0.183
	RG25	**	RG45	0.005

** Not available.
* Negligible.

water and sulfuric acid from 1.6 to 2.0. These results are in good agreement with those by Butler and Ison (1966) which show from an Arrhenius plot for iron coupons immersed in water (Figure 3.26), that the effect of increasing the temperature from 25°C to 45°C would increase the corrosion rate by a factor of 1.6.

It is evident that material weight losses and maximum corrosion rates for the galvanized steel coupons (Tables 3.9 and 3.10) were lower than mild steel coupons in deionized water, sulfuric acid, and MIC soil environments. Surface photographs show the formation of porous white scales on the surface of the DG45 and AG45 coupons after 14 weeks immersion (Figure 3.27). This scale, most likely a zinc hydroxide, deteriorated and turned a brown rusty colour after 27 weeks exposure.

These observations suggest that some protection is afforded to the steel by the less noble zinc, which acts as a sacrificial anode. However, once this zinc coating is oxidized, the corrosion rate is expected to be similar to the mild steel coupons. The corrosion rates of mild and galvanized steel coupons were negligible in the buffered NaOH solution and were not affected by temperature.

Changes in average material weight loss (W) for MS and GS metals immersed in the MIC soil (45°C) environment are shown in Figure 3.28. The plot for the RS45 coupons is linear in shape, which suggests a direct relationship between W and exposure time. The RG45 coupons, however, showed no significant increase in weight loss between 5 and 27 weeks exposure. During this period, W remained relatively constant at 4.4 (SD 0.2%).

Cleaning of the hard scale from the surface of the RG45 coupons revealed a protected steel surface. It is known that the weight of the zinc coating (275 $g.m^{-2}$) also

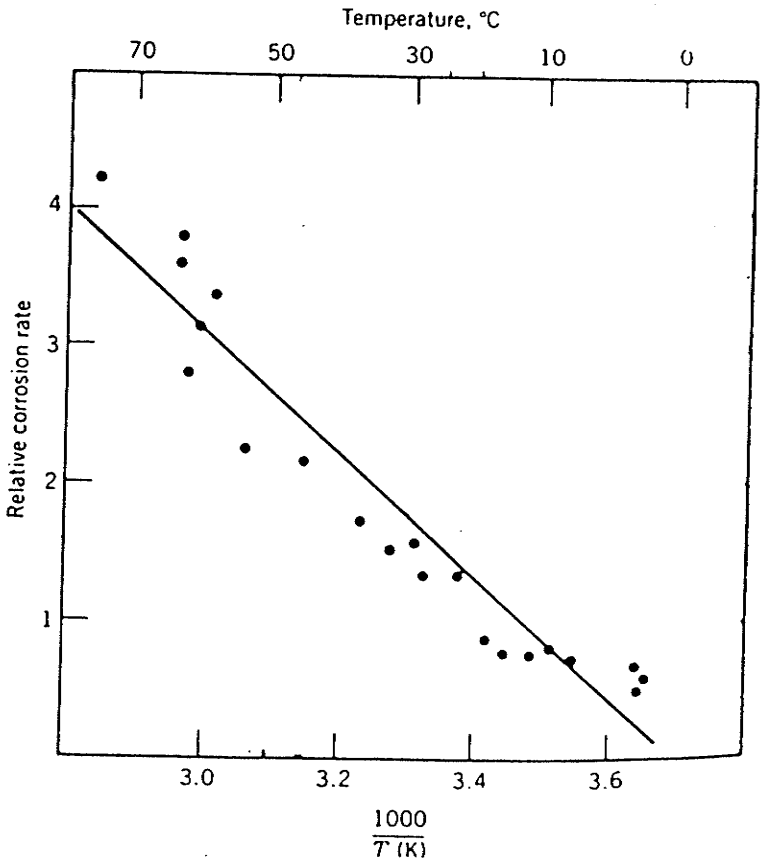

Figure 3.26 Arrhenius plot of corrosion rate versus temperature for iron immersed in water (from Butler and Ison, 1966)

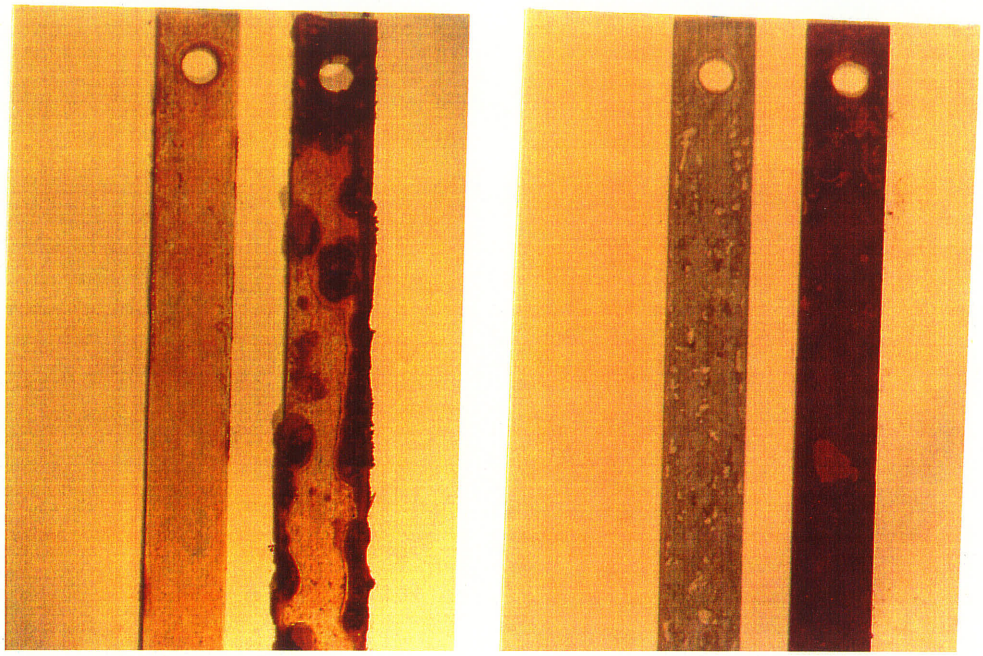

DG45
14 weeks 27 weeks

AG45
14 weeks 27 weeks

Figure 3.27 Surface photographs of AG45 and AS45 coupons after 14 and 27 weeks immersion

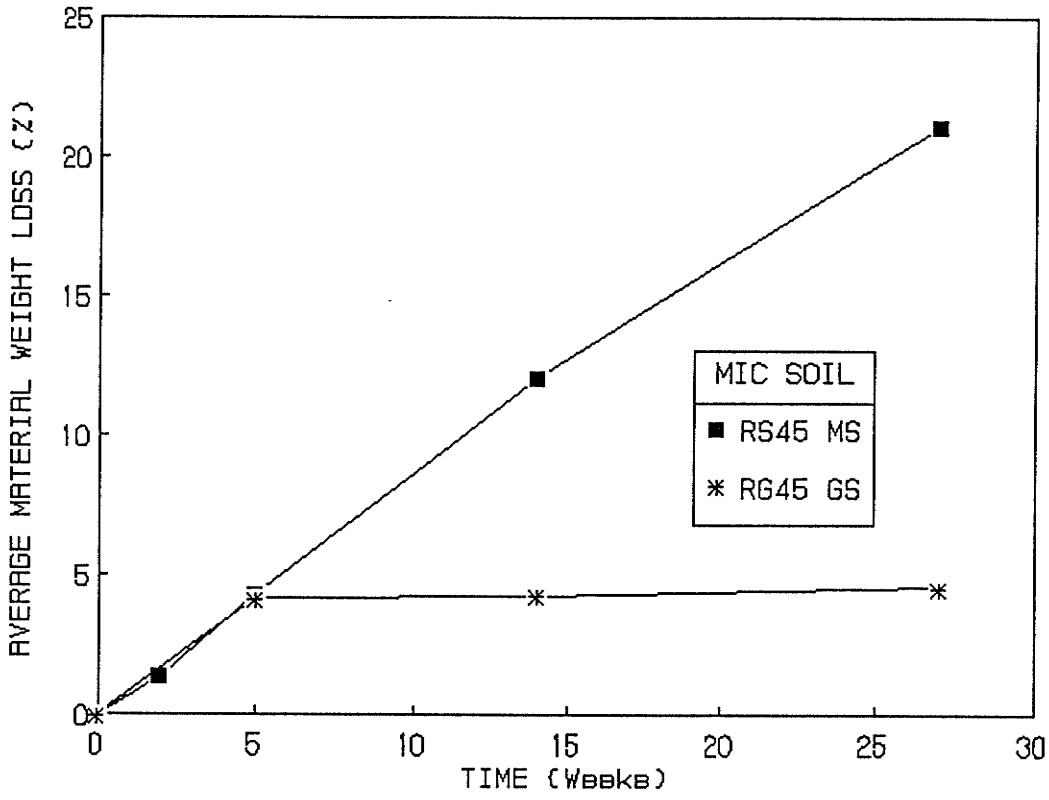

Figure 3.28 Average material weight loss versus exposure time: RS45, RG45

corresponds to 4.5 percent of the weight of the coupon (Russel Steel, 1988). These results suggest that once the zinc coating was oxidized, the protective zinc oxide scale inhibited further corrosion. It was concluded that the accelerated laboratory (45°C) testing of GS coupons in MIC soil did not simulate the corrosion behaviour exhibited at the Harding culvert site.

The highest corrosion rate in the experiment (0.183 mm $year^{-1}$) was measured for mild steel coupons exposed to an MIC soil (45°C) environment. The laboratory corrosion rate was 2.3 times greater than the corrosion rate (O.08 mm y^{-1}) observed in the *in situ* field environment. Higher laboratory corrosion rates were anticipated since the tests were conducted at elevated temperatures. Surface photographs (Figure 3.29) show that a hard black scale had formed on the surface of the RS45 coupons after only 5 weeks exposure. When the black scale was immersed in HCl, hydrogen sulfide gas was generated, suggesting a form of iron sulfide. Similar scale was found on the surface of corroded CSP specimens obtained from the Harding site. After 14 weeks, the coupons were cocooned with bulky yellow corrosion products. X-ray diffraction analyses verified that the corrosion products were of a non-crystalline structure.

Uniform corrosion, observed on the surface of cleaned RS45 coupons, suggests the formation of galvanic cells between the scale (cathode) and the unreacted steel adjacent and beneath it (anode). Similar galvanic corrosion behaviour by the action of SRB on iron has been observed by others (Dexter, 1988).

Figure 3.29 Surface photographs of RS45 coupons after 5, 14, and 27 weeks exposure

3.5 WEIGHT LOSS COMPARISON BETWEEN MS AND FFW MATERIALS

A bar diagram comparing the average material weight loss for MS and FFW materials is shown in Figure 3.30 for deionized water and NaOH environments after 27 weeks immersion. The material weight lost for MS coupons immersed in deionized water was 33.8 (25°C) to 34.5 (45°C) times higher than for FFW specimens.

The material weight losses for MS coupons and FFW specimens after 27 weeks immersion in sulfuric acid (45°C) were 15.56 and 0.91%, respectively. The highest metal weight loss was measured for MS coupons exposed to the MIC soil (Figure 3.31) environment. Unfortunately, a direct comparison with FFW specimen was not possible due to soil and bacteria which were embedded in the surface of the composite.

A comparison of materials based totally on weight loss methods is not accurate. For example, inaccurate measurements may result if some of the degraded solids remain attached to the FFW composites. New analytical methods such as determining the depth of penetration through the thickness of the FFW composite as a function of immersion time is one way to make more meaningful comparisons.

3.6 SUMMARY AND CONCLUSIONS

The primary purpose of the Preliminary Screening (PS) study was to assess and compare the deterioration behaviour of postcured FFW composites and metals (steel and galvanized) following exposure in various simulated natural aqueous field environments. A specific objective of the FFW deterioration and metal corrosion experiments was to identify the environment which had the most deleterious effect on each material. The conclusions of the PS study are summarized below:

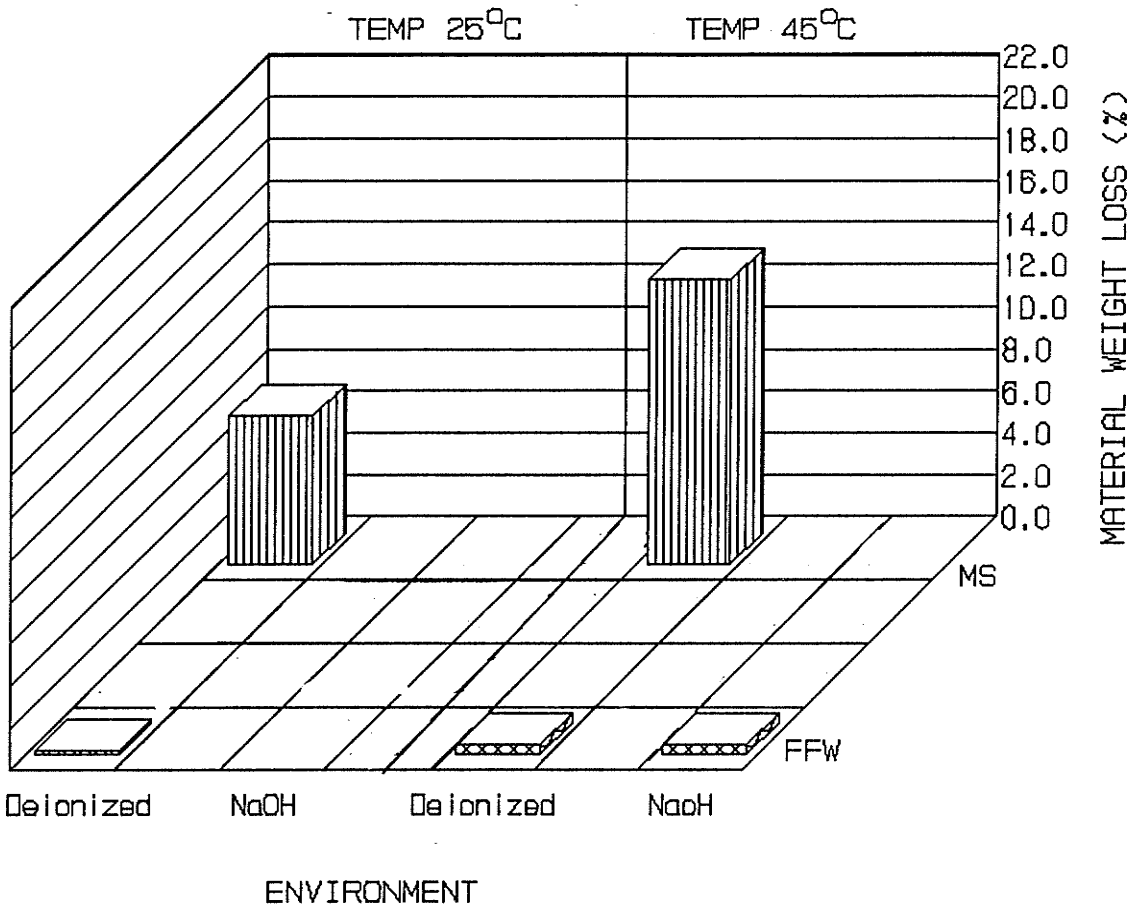

Figure 3.30 Weight loss comparison of MS and FFW materials after 27 weeks immersion in deionized water and NaOH

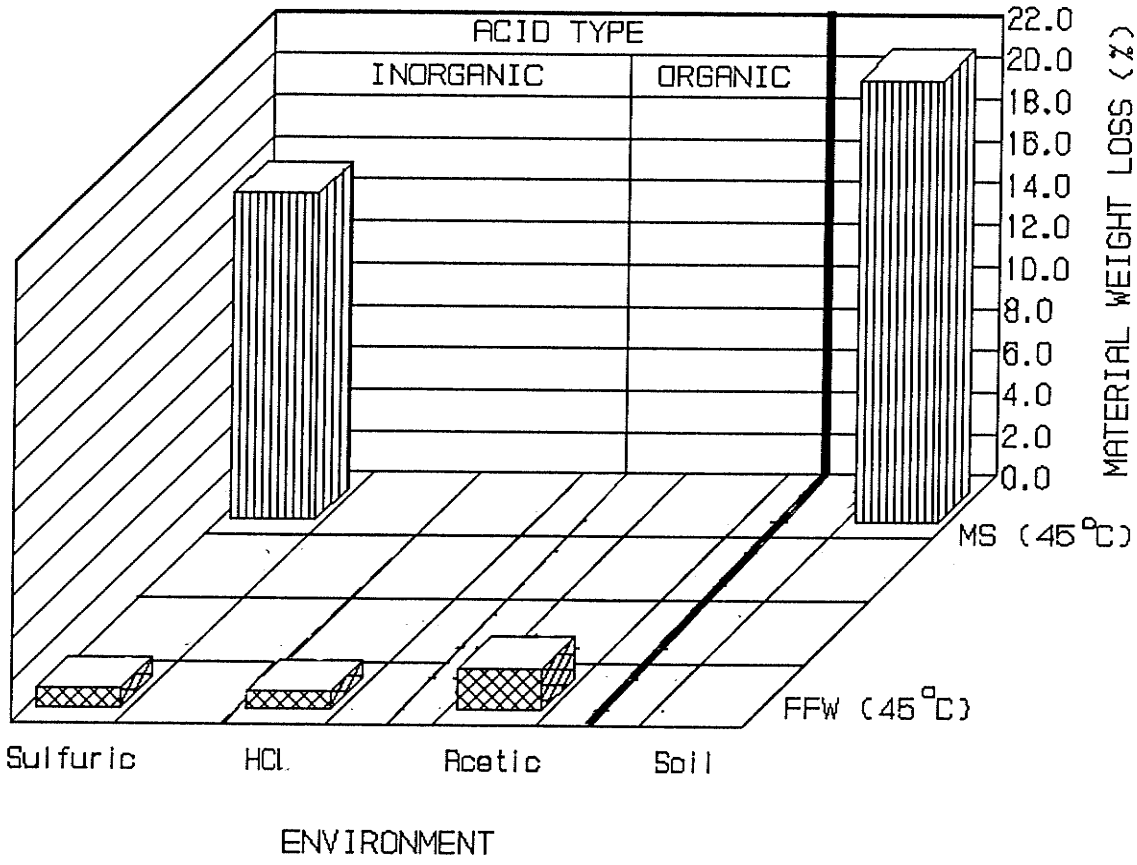

Figure 3.31 Weight loss comparison of MS and FFW materials after 27 weeks in acid and soil (45°C) environments

3.6.1 FFW Deterioration Experiment

1. Absorption tests conducted at a temperature of 45 °C were effective in increasing the rate of diffusion of deionized water in postcured FFW specimens. D_e and M_e values at this temperature were determined, based on the method developed by Shen & Springer (1976) to be 1.4×10^{-6} mm^2/sec and 1.61%, respectively.
2. The most hostile aqueous environment, based on physical, chemical and visual indicators were acidic (pH 3.5 to 4.5) environments. Preliminary results show deterioration is more extensive for postcured FFW specimens in acetic acid then in sulfuric or hydrochloric acids.
3. Springer (1984) suggested that the non-Fickian behaviour of liquid transport in SMC materials may be due to the deterioration of the material, most likely through the loss of resin particles. In this work, the chemical analyses showed that most of the material weight loss for FFW specimens exposed to acidic environments (pH 3.5 to 4.5) is in the form of calcium carbonate particles.
4. Material weight loss methods cannot accurately quantify deterioration in MIC soil environments due to soil/bacteria embedment. New analytical methods are required in order to quantify more accurately the deteriorative behaviour of FFW composites in aqueous environments.
5. Volumetric measurements did not show differences in swelling between specimens immersed in environments at the same temperature. Average increases in volume for specimens immersed at 45°C were higher than at 25°C.
6. Losses in wet mechanical properties were greater than losses in dry mechanical properties. Future testing of mechanical properties should be conducted in the

wet state to simulate actual field environments.

7. A laboratory operating temperature of 45° was effective in accelerating the deterioration behaviour of postcured FFW specimens exposed to various aqueous environments.

3.6.2 Metal Corrosion Experiment

1. The maximum corrosion rates for MS coupons immersed in deionized water and sulfuric acid at 25°C were 0.066 and 0.098 mm y^{-1}. These values are similar in magnitude to the field corrosion rates observed at the Harding culvert site.
2. The maximum corrosion rates for MS coupons immersed in deionized water and sulfuric acid (45°C) was 0.129 and 0.159 mm y^{-1}, respectively. Raising the temperature from 25° to 45°C increased the corrosion rate of mild steel in deionized water by an average factor of 1.8.
3. The corrosion behaviour of GS coupons exposed to a MIC soil, under accelerated laboratory (45°C) test conditions, did not simulate the high corrosion rates observed for galvanized CSP in the field.
4. The highest corrosion rate (0.183 mm.$year^{-1}$1) was observed for MS coupons exposed to an MIC soil. It was demonstrated that accelerated laboratory testing of MS coupons in MIC (45°C) soil, utilizing anaerobic/aerobic cycles, can simulate long-term biological corrosion behaviour in the field.

CHAPTER 4

DEVELOPMENT OF NEW TEST METHODS TO QUANTIFY FFW DETERIORATION IN EXTREME ACIDIC ENVIRONMENTS (PHASE 2)

4.1 INTRODUCTION

The most hostile aqueous environment identified in the Preliminary Screening (PS) was an acidic environment. One of the primary objectives of the experimental research program was to develop new test methods to quantify more accurately the deterioration of FFW composites exposed to extreme acidic environments. One particular application is the low pH (2.2-2.5) conditions found in the collection and storage of sewage.

The four analytical methods presented in this chapter were specifically developed for small flexural FFW specimens. One advantage of using smaller-sized specimens is that experimental results can be more easily reproduced. For example in the earlier PS study, all of the large FFW specimens were immersed in the same 18 L of solution throughout the FFW deterioration experiment. This was because of the high replacement cost of laboratory solutions required to submerge the specimens. However, with smaller specimens it is possible to complete the testing and discard the laboratory solution after each immersion time period. This procedure allows the extent of deterioration to be determined for each period and to be measured from either the leachate or the properties of the wet specimens.

The four methods developed include: a gravimetric weight loss method for partially cured specimens, a fluorescent-dye solvent exchange (FDSE) method and two

visual methods to measure the average depth of penetration[5].

The gravimetric weight loss method was developed for virgin specimens and includes a correction factor. The FDSE method was developed to overcome some of the problems associated with the moisture desorption heat (MDH) method that was developed (Section 3.3.3.5). The FDSE method is basically an extension of the MDH method and uses solvent exchange rather than thermal drying techniques to quantify the desorption slope (S_d) parameter. Two methods, the Heat Cure (HC) and Fluorescent Dye (FD) method were developed to permit accurate visual identification of the location of an advancing boundary of deterioration through the thickness of the composite in order to measure the average depth of penetration. The usefulness of the new methods in quantifying deterioration was demonstrated in the following Postcure acid (PA) experiment (Section 4.3). These methods were used to determine the effects of various postcure conditions on the deterioration of FFW composites exposed to a low pH (2.2-2.5) sulfuric acid environment. The experiment was conducted under accelerated conditions of increased temperature (45°C).

4.2 NEW TEST METHODS

4.2.1 Gravimetric Weight Loss Method

This method was developed to estimate the dry material weight loss of FFW composites that were not fully cured prior to immersion. It is known that thermal drying enhances the curing process resulting in the release of excess styrene and a material

---

5 The depth of penetration is measured from the interior surface to the boundary between the saturated and non-saturated layers.

weight loss. Cuadrado et al. (1983), who studied the curing kinetics of a general purpose unsaturated resin, showed that following complete curing, a loss of approximately ten percent of the initial mass was observed. In this work, it was apparent that a correction factor (CF) was required which would take into account weight losses associated with further curing during the reconditioning of wet specimens.

To this end, a postcure experiment was undertaken to determine the effects of temperature (112°C) on the average material weight loss of small flexural specimens. The results (Appendix III-1) are similar to those obtained in an earlier postcure experiment for large FFW specimens. The average material weight loss after 36 hours was 0.37 percent of the initial dry weight. No significant material weight loss was observed after a drying time of 36 hours.

The procedure for estimating the dry material weight loss of virgin or partially cured FFW specimens was as follows:

1. The FFW specimens were weighed after drying in a desiccator (W_i).
2. The dry specimens were immersed in a liquid environment for a predetermined time period.
3. On removal excess surface liquid was wiped off with a cloth and the wet specimens were reconditioned at 112°C for 36 hours.
4. After cooling the final weight (W_f) of each specimen was recorded.
5. The weight of dry material lost was estimated for the FFW specimens (W_m) from Equation [31].

[31] $$W_m = (W_i - W_f - C_F)\ (W_i)^{-1}\ (100)$$

Where:

W_m = Dry material weight loss per specimen (%)

CF = Correction factor for partially cured FFW specimens (e.g. C_F = 0.0037 (W_i) for the virgin FFW specimens used in this study).

It is evident that the correction factor for virgin FFW specimens postcured at 112°C for 36 hours would be zero and Equation [31] would be equivalent to Equation [20].

4.2.2. Fluorescent-Dye Solvent Exchange (FDSE) Method

Gravimetric water absorption techniques can not be used to determine the effective diffusion coefficients of filled plastic SMC materials, where extensive material weight loss occurs due to the leaching of soluble solids (Section 2.4.3). This has led to the development of the moisture desorption heat (MDH) method (Section 3.3.3.5), which is based on principles of thermally activated moisture diffusion. One disadvantage of using heat in the MDH method is that cracks may be initiated during reconditioning of wet plastic specimens at elevated temperatures. Severe drying conditions could also cause changes in the original diffusion characteristics of the material. This mechanism was suggested by Whitney et al. (1977) who showed higher diffusion coefficients for epoxy matrix composites based on moisture desorption tests than those calculated from water absorption tests, under similar temperature (71°C) conditions.

Consequently, the FDSE method has been developed to overcome some of the

problems associated with the MDH method. The development of the FDSE method was based on a literature review and a preliminary experimental investigation.

4.2.2.1 Literature Review

Solvent Exchange Desorption: Cement Pastes

Solvent exchange (SE) desorption methods have been used extensively to quantify the diffusion coefficients of water-saturated cement pastes. Parrot (1981) concluded that the less dense water miscible solvent, methanol, could replace water in saturated cement paste by a simple physical process of counter diffusion. Day (1981), however, questioned the use of methanol and showed that methanol reacted with calcium hydroxide in the cement paste to form an undesirable carbonate-silica reaction product. Feldman (1987) also observed that methanol reacts with hydrated Portland cement and was unsuitable for use when diffusion coefficients are to be measured. He concluded that 2-propanol was an acceptable solvent since no such reaction seemed to occur. He approximated the diffusion coefficient of 2-propanol in water-saturated cement paste to be in the range of 10^{-5} to 10^{-6} $mm^2.sec^{-1}$. The diffusion coefficients were based on Fick's model for unsteady diffusion in a semi-infinite solid. A similar range of values were observed for the diffusion of potassium iodide (KI) and potassium chloride (KCl) in water-saturated cement paste and bentonite clay at a temperature of 30°C (Atkinson and Nickerson, 1984).

Hughes (1987) demonstrated that methanol exchanged at a much faster rate than 2-propanol in ordinary Portland cement (OPC) pastes. He also suggested that before accepting the use of a solvent to measure diffusion coefficients, a critical appraisal should

be made of possible solvent-structure interactions.

Absorption of Methanol and 2-Propanol in FRP Composites

There are few research studies showing the effects of methanol and 2-propanol absorption on FRP composites. Craigie et al. (1986) have demonstrated that composites made from novalac based vinyl ester resin swell when immersed in methanol at temperatures between 37.8° and 48.9°C and have shown that no chemical reaction occurs. The maximum percent weight gain of these specimens was determined to be 10 percent at equilibrium with a corresponding increase in specimen thickness of 5 percent.

In other work, Bravenec (1983) has characterized the absorption of 2-propanol at 50°C in postcured (90°C for 28 hrs), unfilled styrene crosslinked polyester resins. The maximum percent weight gain at equilibrium (530 hrs) was 11.4 percent, with a corresponding increase in dry specimen dimensions averaging 4.6 percent. A gradual decrease in specimen weight was observed only after equilibrium (M_e) was attained. These results suggest that long-term exposure of cured polyester resin in 2-propanol (530 hrs at 50°C) could result in the leaching of polymer soil fractions from the composite.

In this work, a preliminary experimental investigation was used in the development of the FDSE method. The specific objectives of this investigation were to evaluate the effects of the absorption of methanol and 2-propanol in FFW composites and to select the most suitable solvent exchange medium to be used in the FDSE method.

4.2.2.2 Preliminary Experimental Investigation

The preliminary experimental investigation consisted of two experiments; a solvent absorption and a fluorescent-dye solvent exchange (FDSE) experiment. A description of materials, laboratory procedures, results and discussion is presented in Appendix III.

Problems were encountered with the weighing of the methanol saturated specimens during the solvent absorption experiment. The weights of these specimens were constantly decreasing which was felt to be attributed to high evaporation rates. This made it difficult to obtain reliable and consistent data. Severe deterioration (softening) and whitening was observed for virgin specimens immersed in methanol (45°C) after 5 days exposure (Appendix III-5). The FFW specimens exposed to 2-propanol at 45°C were not affected by weighing problems. Softening and whitening were not observed for the 2-propanol specimens. A characteristic linear isotherm plot was not obtained when methanol was used as the solvent. The reason for this was either high exchange rates or possible solvent-structure interactions. It was, however, possible to characterize the linear slope of the 2-propanol FDSE isotherm. The results showed that 2-propanol was a more suitable solvent exchange medium.

A description of the FDSE method used to quantify changes in diffusion characteristics (S_d) of wet FFW specimens is as follows:

1. A 2-propanol solution was prepared by dissolving 4 g of Fluorescent Yellow G dye in a 1 L solution of 2-propanol at 45°C. A closed top plastic container was used to prevent evaporation.
2. Following a specified immersion time period, the wet FFW specimens

were removed from their aqueous environment and excess surface moisture was wiped off with a cloth towel.

3. The wet specimens were weighed and immediately re-immersed in the 2-propanol solution at 45°C.
4. Steps 2 and 3 were repeated at specified time intervals.
5. The FDSE test was considered complete when no further losses in specimen weight were observed.

A characteristic FDSE isotherm was then obtained by plotting the changes in percent moisture loss (M_L) as a function of the square root of the immersion (exchange) time in 2-propanol. The desorption slope (S_d) parameter was measured from the initial slope of the initial portion (60%) of the FDSE isotherm plot and determined by linear regression.

4.2.3 Depth of Penetration (Visual) Methods

The location of the advancing boundary of deterioration is poorly defined for virgin FFW composites which have been exposed to aqueous environments because the natural white-grey colour offers no visual contrast to whitening associated with deterioration. As a result, two methods were developed to visually enhance the advancing boundary of deterioration and so facilitate measurement of the average depth of penetration. These methods are referred to as the Heat Cure (HC) and the Fluorescent Dye (FD) methods.

4.2.3.1 Heat Cure (HC) Method

Thermal drying (reconditioning) of wet virgin FFW specimens causes different colour changes to occur in the saturated and non-saturated layers of the laminate. It was observed in the PS study that upon reconditioning, the saturated layer of the large wet FFW specimens acquired a white haze. In contrast, the non-saturated regions remained a darker colour. Depth of penetration measurements were obtained from the same specimens that were used previously in determining the material weight loss.

A description of the Heat Cure (HC) method is as follows:

1. The wet FFW specimens are reconditioned in an oven at 112°C for 36 hours and cooled in a desiccator.
2. Six coupons were cut from each specimen (see Figure 4.0) using a diamond blade saw.
3. The edges of these coupons were sanded and cleaned with glycerine to enhance the definition of boundary location.
4. The distance between the inner surface of the coupon and the visible boundary was measured at 2.5 mm intervals around the coupon perimeter using a light stereo microscope (Wild Leitz Canada Ltd.) with a calibrated eyepiece scale at a magnification of x 50 and a maximum resolution of $\pm$ 27 μm.
5. The average depth of penetration (h) was calculated from a minimum of 100 measurements per specimen.

4.2.3.2 Fluorescent Dye (FD) Method

The FD method was based on the assumption that the fluorescent dye/alcohol solution would be exchanged with the liquid penetrant that had been adsorbed into the laminate. The adsorbed yellow colorant in the laminate could than be used to identify the advancing boundary of deterioration. One advantage of the FD method is that specimens used in the FDSE test can also be used to quantify the depth of penetration.

The FD method is similar to the HC method in that the FDSE specimens were also cut into six coupons (Figure 4.0). The edges of these coupons, however, were only sanded since glycerine caused streaking. Again the distance between the surface of the specimen and the visible boundary was measured at 2.5 mm intervals along each edge using either visible light or fluorescent (ultraviolet) microscopic techniques. In this work, ultraviolet light measurements were also taken on a Nikon OPTIPHOT microscope equipped with an EPIS Copic-Fluorescence attachment. The maximum resolution of the fluorescent microscope at x 40 was $\pm$ 19.8 μm at a wavelength range between 330 and 380 nm.

4.3 POSTCURE ACID (PA) EXPERIMENT

4.3.1 INTRODUCTION

The primary objective of the Postcure Acid (PA) experiment was to demonstrate the usefulness of the aforementioned new methods in measuring the effects of postcuring on deterioration. Sulfuric acid was selected as the immersion medium in order to simulate deterioration in extreme acidic sewage environments due to sulfur oxidizing bacteria (Section 2.3.2).

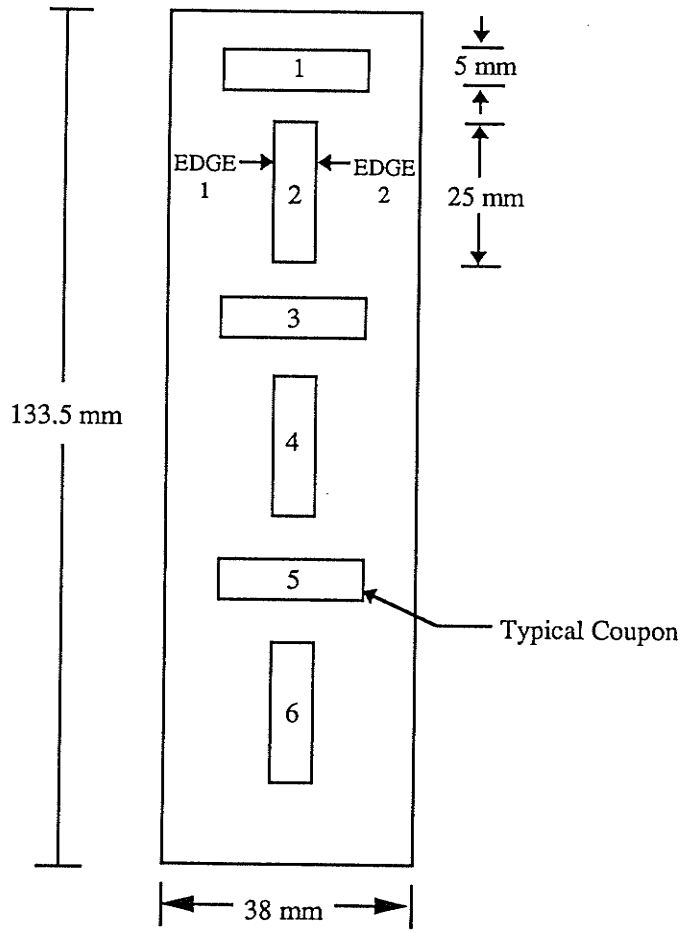

Figure 4.0 Coupon preparation to measure depth of penetration from small FFW specimens

Various types of postcured specimens were immersed for 12 weeks at 45°C. A combination of two curing temperatures (55° and 112°C) and time duration periods (18, 36 hrs) were investigated. The operating conditions for the PA experiment are shown in Table 4.0.

Table 4.0 Operating Conditions: PA Experiment

Reactor Type	Environment Type	Temp. (°C)	pH Condition	Specimen Preparation	
				Temp. (°C)	Time (hrs)
S55-18	Sulfuric acid	45	2.2-2.5	55	18
S55-36	Sulfuric acid	45	2.2-2.5	55	36
S112-18	Sulfuric acid	45	2.2-2.5	112	18
S112-36	Sulfuric acid	45	2.2-2.5	112	36

4.3.2 MATERIALS

Specimens with nominal dimensions of 133.5 mm x 38.0 mm x 4.80 mm were cut in the hoop direction from the same FFW test pipe used in the PS study (Section 2.2.4). Prior to postcuring, the edges of the specimens were sanded and coated by brush with a corrosion-resistant polyester resin (DION COR-RES 6695R)[6]. The coating was applied at room temperature using a methyl ethyl ketone peroxide (1%

6 Trademark of Koppers Company, Inc., Pittsburg, PA 15219, U.S.A.

MEKP) catalyst. The edge coating provided a visible layer of approximately 0.05 mm.

The coated specimens were postcured in a temperature controlled oven (Fisher Isotemp oven, 200 series, Model 230F). The average weight losses for virgin FFW specimens postcured at 112°C were 7 to 10 times greater than for the specimens postcured at 55°C. There was no change in weight loss after 18 hours of postcuring at 55°C. The average percent weight loss for the various postcured specimens (S55-18, S55-36, S112-18, S112-36) are shown in Table 4.1.

Four closed top plastic containers were filled with 3 L of 0.1 N sulfuric acid and placed in a temperature controlled chamber at 45°C. Eight specimens were submerged for 12 weeks in each of the four containers, each corresponding to one of the postcure conditions. The sulfuric acid solution was prepared from concentrated 36 N sulfuric acid and deionized water. The deionized water was produced with a conductance of less than 0.2 μmhos/cm using a Millipore system.

Table 4.1 Percent Weight Loss For Various Postcure Conditions: PA Experiment

Specimen Type	Postcure Conditions		Weight Loss (%)
	Temp. (°C)	Time (hr)	
S55-18	55	18	0.04
S55-36	55	36	0.04
S112-18	112	18	0.30
S112-36	112	36	0.37

4.3.3 Laboratory Procedure

The temperature and pH levels were checked at 2-day intervals. Deionized water was added as required to maintain the level in each container at a constant 3 L volume. Additional amounts of 1.0 N sulfuric acid were added intermittently to maintain the pH in the range of 2.2 to 2.3. The amount of acid added to each container was measured and recorded in meq. Test methods used in the Preliminary Screening Study (Section 3.3.3) were also used to monitor changes in specimen weight, calcium ion and aluminum ion concentrations in the leachate.

Following 12 weeks exposure, the specimens were removed from each container. Five of the test specimens were rinsed with deionized water and tested in the wet state for wet flexural properties. The testing of wet mechanical properties, was based on earlier recommendations (Section 3.6.1) and in accordance with ASTM D 790. Two other wet specimens were reconditioned at 112°C for 36 hours to determine the average value of soluble material weight loss (W_m) and the average depth of penetration (h) using the HC method according to Section 4.2.3.1. The remaining specimen was used to monitor changes in diffusion properties (FDSE method) and also to determine the average value of h by the FD method.

4.3.4 RESULTS AND DISCUSSION

The average pH was maintained between 2.2 and 2.3 during the 12 week immersion test period (Table 4.2). A summary of the test results showing the extent of deterioration after 12 weeks exposure is shown in Table 4.3.

Changes in specimen weight, when plotted against the square root of immersion

Table 4.2 Average pH During 12 week Test Period: PA Experiment

Treatment Type	Number of Observations	Average Value	Standard Deviation
S55-18	12	2.25	0.05
S55-36	12	2.22	0.05
S112-18	12	2.21	0.05
S112-36	12	2.23	0.06

Table 4.3 Extent of Deterioration of Postcured FFW Specimens After 12 Weeks (45°C) Immersion in Sulfuric Acid: PA Experiment

Deterioration Test Parameter	Postcure Condition			
	S55-18	S55-46	S112-18	S112-36
Gravimetric				
Material weight loss (%)	1.54 (0.07)	1.65 (0.01)	1.50 (0.09)	1.55 (0.11)
Chemical				
Calcium as $CaCO_3$ ($mg.L^{-1}$)	1220	1140	1120	1240
Aluminum as $Al_2O_3.3H_2O$ ($mg.L^{-1}$)	204	173	185	210
Loss in Wet Mechanical Properties (%)				
Ultimate flexural strength	31.0 (7.9)	27.3 (10.6)	30.4 (4.8)	27.5 (6.3)
Flexural modulus	30.2 (6.0)	27.8 (15.2)	28.0 (15.2)	22.7 (9.7)
Barcol hardness	31.6 (9.1)	31.6 (12.3)	35.5 (11.2)	33.3 (9.0)
Diffusion properties ($min^{-1/2}$)				
Desorption slope parameter	0.014	0.013	0.010	0.009
Depth of Penetration (μm)				
HC method (visible light)	245 (40)	248 (32)	266 (44)	285 (25)
FD method (visible light)	242 (25)	262 (36)	230 (36)	239 (23)

Standard deviations in brackets.

time (Figure 4.1), showed that the rate of specimen weight change was lower for the S112-18 and S112-36 specimens than for the S55-18 and S55-36 specimens. However, the change in specimen weight of all specimens appear to be similar and reach an asymptote after 12 weeks exposure. These results suggest that changes in weight of the various postcured specimens are not influenced by different postcure conditions after long-term exposure in sulfuric acid (see Appendix III-9).

The average material weight losses between the various postcured specimens, after 12 weeks immersion (Table 4.3) ranged between 1.50 and 1.65%. These results suggest that postcuring does not affect material weight loss in low pH sulfuric acid environments.

The calcium ion concentration in the acid leachate when plotted as a function of immersion time (Figure 4.2) also showed little difference between the various postcured specimens. The total concentration of calcium after 12 weeks of sample immersion (Table 4.3) ranged from 1,120 to 1,240 $mg.L^{-1}$ as $CaCO_3$. In comparison, the concentration of dissolved aluminum ranged from 173 to 210 $mg.L^{-1}$ as $Al_2O_3.3H_2O$. It is evident, since the FFW composite consisted of an equal percentage by weight of each filler constituent, that calcium carbonate is more soluble than ATH in low pH sulfuric acid environments. A summary of the concentrations of calcium measured in the leachate at the end of each week are presented in Appendix III-9.

It was suggested that the dissolution of calcium carbonate in sulfuric acid might have been influenced by the formation of a calcium sulfate precipitate.

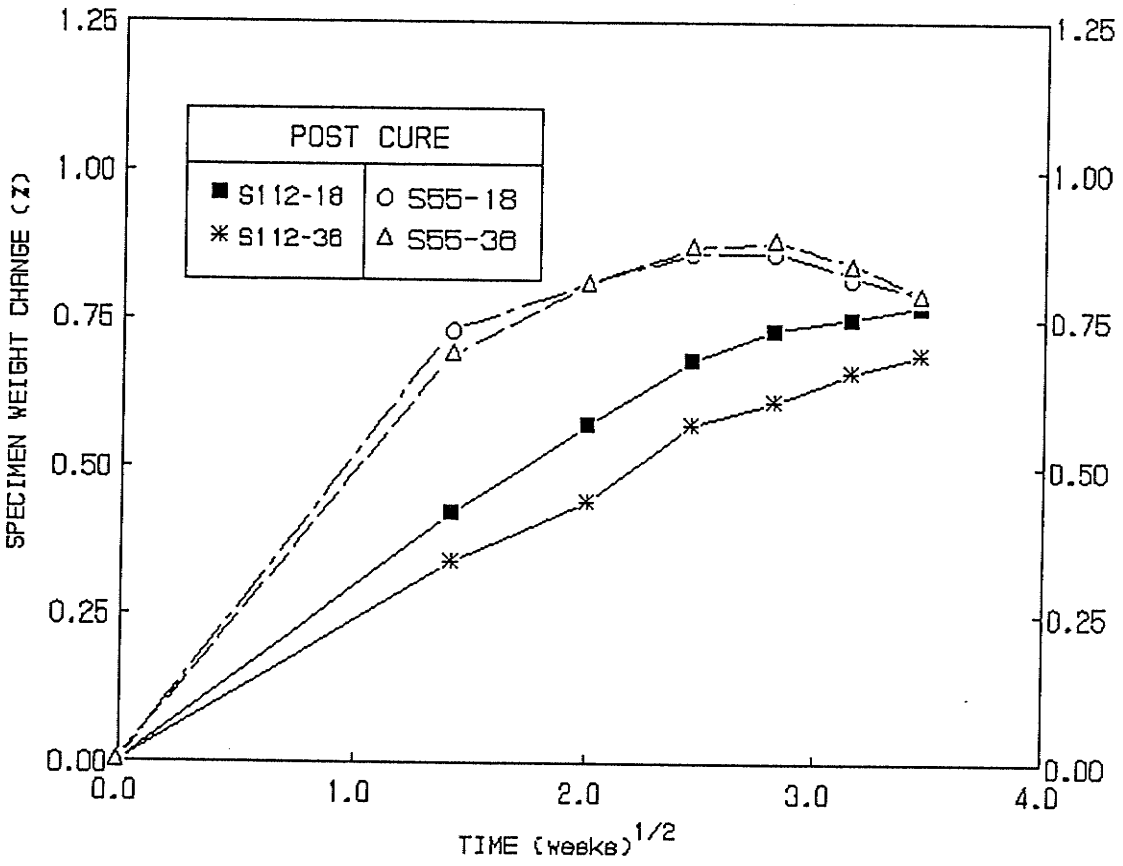

Figure 4.1 Changes in specimen weight vs. immersion time: PA experiment

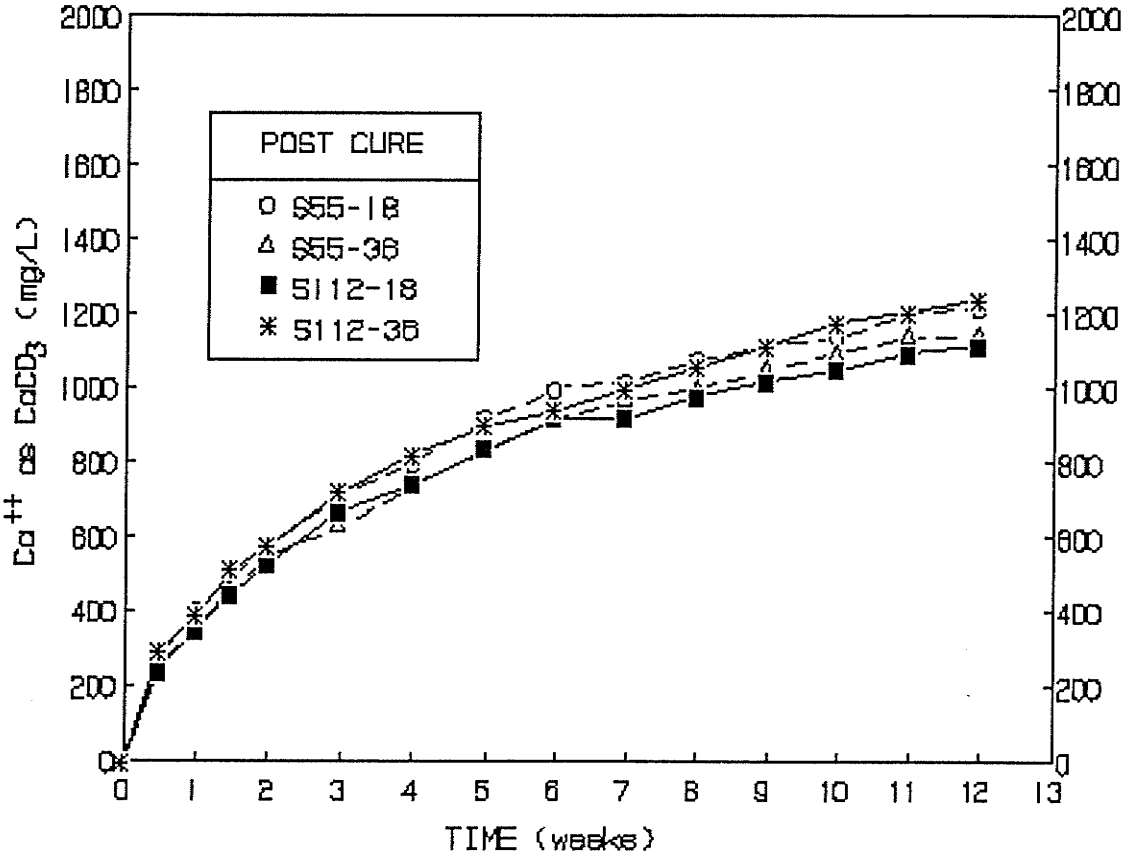

Figure 4.2 Calcium ion concentration in the leachate vs. immersion time: PA Experiment

[32] $$CaCO_3 + H_2SO_4 \rightarrow Ca^{++} + Co_2 + H_2O + SO_4^{--}$$

No precipitate was observed in the sulfuric acid leachate during the experiment. However, theoretical calculations based on ideal equilibrium acid behaviour (Appendix III-10) were carried out to confirm this. These calculations showed that the amount of available sulfate added (2.0×10^{-2} M) by the addition of sulfuric acid (pH 2.23) was insufficient to result in the formation of a calcium sulfate precipitate. The theoretical calcium ion concentration that would result in the formation of a precipitate under these conditions was estimated to be 1,915 $mg.L^{-1}$ as $CaCO_3$. Thus, it was unlikely that a calcium sulfate precipitate would have formed during the experiment since the maximum calcium concentration measured in the leachate was 1,240 $mg.L^{-1}$ as $CaCO_3$. The theoretical calculations appear to be in agreement with the experimental observations.

The average initial dry mechanical properties for the postcured specimens are shown in Table 4.4. Losses in wet flexural properties and Barcol hardness were normalized with respect to these data and were presented (Table 4.3) as a loss (%) of the initial dry mechanical properties ($1-S/S_0$, $1-E/E_0$, and $1-H/H_0$). The losses in wet flexural properties were similar for the four specimens and ranged from 22.7 to 31.0%. In comparison, the reduction in Barcol hardness ranged from 31.6 to 35.5%.

Diffusion properties were characterized for the postcured specimens from the FDSE isotherm plots shown in Figure 4.3. The desorption slope parameter (S_d) was calculated using the same linear regression techniques used in the MDH method (see Section 3.3.3.5). The values of S_d after 12 weeks immersion were similar and ranged from 0.009 to 0.014 $min^{-1/2}$ (Table 4.3). These results suggest that there is no

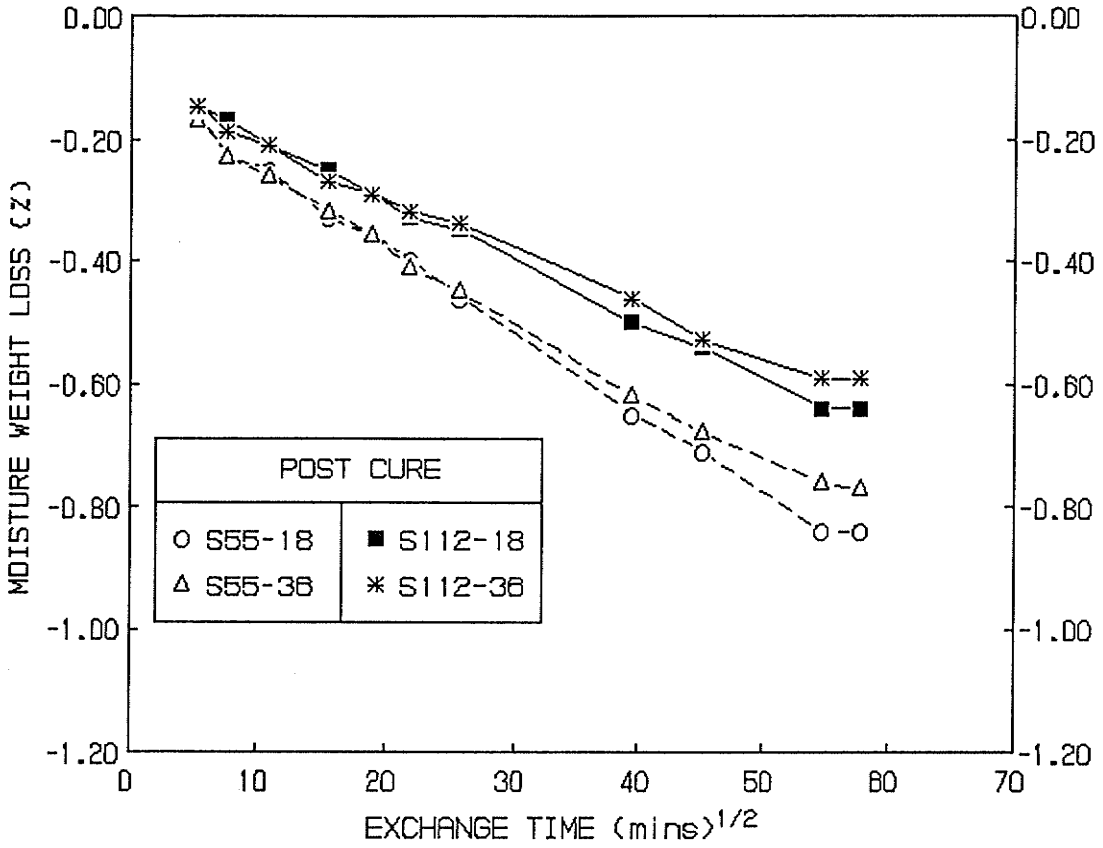

Figure 4.3 FDSE desorption isotherms for postcured specimens after 27 weeks Immersion: PA Experiment

difference in the diffusion properties of postcured specimens exposed to low pH sulfuric acid conditions.

Table 4.4 Initial Dry Mechanical Properties of Postcured Specimens: PA Experiment

Specimen Type	Flexural Strength (S_0)		Flexural Modulus (E_0)		Barcol Hardness (H_0)	
	MPa	Standard Deviation	GPa	Standard Deviation	Unit	Standard Deviation
S 55-18	297.0	(17.2)	21.2	(1.5)	58.4	(4.1)
S 55-36	286.0	(26.9)	21.6	(3.3)	56.3	(6.1)
S112-18	313.0	(12.9)	24.3	(2.0)	60.9	(6.5)
S112-36	310.0	(14.3)	23.3	(1.3)	61.6	(4.1)

The average depth of penetration, based on the HC (visible light) method ranged from 245 to 285 μm. The average values of h, based on the FD (visible light) method ranged from 230 to 262 μm. The similarity in results suggest that the depth of sulfuric acid penetration is not influenced by different postcure conditions. Fluorescent microscopy techniques utilized in the FD (ultraviolet light) method were found to be ineffective in determining the depth of penetration. This was because the technique did not identify clearly the boundary interface between the saturated (attacked) and non-saturated (non-attacked) layers.

4.4 CONCLUSIONS

1. New test methods that were developed to measure changes in diffusion characteristics (FDSE) and depth of penetration based on visible light measurements (HC and FD). These methods were effective in quantifying the extent of deterioration behaviour of small FFW specimens in an extreme sulfuric acid environment.

2. The primary chemical reaction associated with low pH sulfuric acid deterioration (2.2-2.3) was the dissolution of calcium carbonate.

3. Postcuring was found not to affect the deterioration behaviour of FFW composites in low pH sulfuric acid conditions.

CHAPTER 5

DEVELOPMENT OF AN ACID DETERIORATION MODEL (PHASE 3)

5.1 INTRODUCTION

One of the primary objectives of the research study was to develop a practical mathematical model to quantify the rate of deterioration of FFW composites exposed to acidic environments. The requirement for a good engineering model is that it is a close mathematical representation of a real situation (Levenspiel, 1972).

There is a need to develop deterioration models to quantify the rate of deterioration of materials which have been exposed to a known environmental history. The information obtained from such models can be used for design and life prediction to ensure structural integrity and reliability in the field.

Several models have been developed in the last decade to assess the behaviour of material degradation in plastic composite materials. Springer (1984) proposed an analytical model to predict the degradation in the mechanical properties of graphite-epoxy composites exposed to elevated temperatures. Ye (1989) developed a fatigue damage accumulation model for random SMC composites which can be used to predict the number of cycles required to reach a given reduction in stiffness when cycling at different fatigue levels.

In this work an acid deterioration model was developed for filled FFW composites exposed to acidic conditions. The model is based on an unreacted core model that was first presented by Yagi and Kunii (1955) for gas solid reactions. Here the

model is adapted to a physical-chemical process involving a solid-liquid interface. One advantage of the model is that it yields a comparatively simple solution which is based on a pseudo-steady state approximation of the moving boundary diffusion problem.

5.2 MODEL DEVELOPMENT

5.2.1 Background

Many important gas solid reactions are controlled by the mass transfer and diffusion of gases through a solid reactant. Weiz and Goodwin (1963) in their work on diffusion-controlled combustion of "coke" within a porous catalyst particle, noted that the progressive shell mechanism (unreacted-core model) should have general applicability in a wide variety of solid-fluid rate phenomena. Coutant et al. (1970) carried out an extensive series of experiments in which porous limestone particles were injected into hot gaseous SO_2, collected and analyzed. The data suggested that the rate of reaction was governed by a "diffusion-plus-reaction" mechanism since the quantity of sulfur picked up by the limestone particles and measured as $CaSO_4$ was proportional to the square root of the reaction time. Pigford and Sliger (1973) extended the mechanism to include an additional pore diffusion process for special cases.

Luss (1968) showed mathematically that the pseudo-steady state (PSS) approximation is valid during most stages of reaction for predicting the rate of reaction for gas-solid reactions in spherical particles. Levenspiel (1972) indicated that the PSS approximation method used for determining reaction rates when the surrounding medium is a gas applies equally well to liquids.

5.2.2 Acid Deterioration Model

The Acid Deterioration Model is based on the concept of a shrinking unreacted-core. In this work the unreacted core model was applied to FFW composite-acid reactions. Figure 5.0 illustrates a conceptual picture of the proposed model in which the resistance to acid diffusion through the "ash" or degraded layer controls the rate of deterioration.

The acid reaction is assumed to occur first at the outer surface of the FFW solid and then to progress inward. It is noteworthy that the deterioration response of concrete to sulfuric acid (pH 1) is similar. Attiogbe and Rizkalla (1988), using SEM photomicrographs, showed that concrete deterioration started from the acid-exposed surface and moved inward.

It is assumed in the proposed Acid Deterioration Model that the zone of reaction or interface boundary between the acid-reacted (degraded) and unreacted (non-degraded) core moves very slowly into the FFW solid leaving behind inert solids. The concentration of hydrogen ions contributed by the ionization of the acid must then diffuse through the degraded layer to reach the interface and react. It was concluded in the FFW deterioration (Section 3.6) and PA (Section 4.4) experiments that the primary chemical reaction associated with acid deterioration was the dissolution of calcium carbonate. The rate of ATH filler dissolution was shown (Section 4.3.4) to be much lower than calcium carbonate, consequently, this reaction was excluded from the model.

It is assumed in this model that all of the calcium carbonate will eventually dissolve by chemically reacting over a narrow zone at the interface boundary. Thus, there could exist at any time, an unreacted core of FFW material surrounded by an

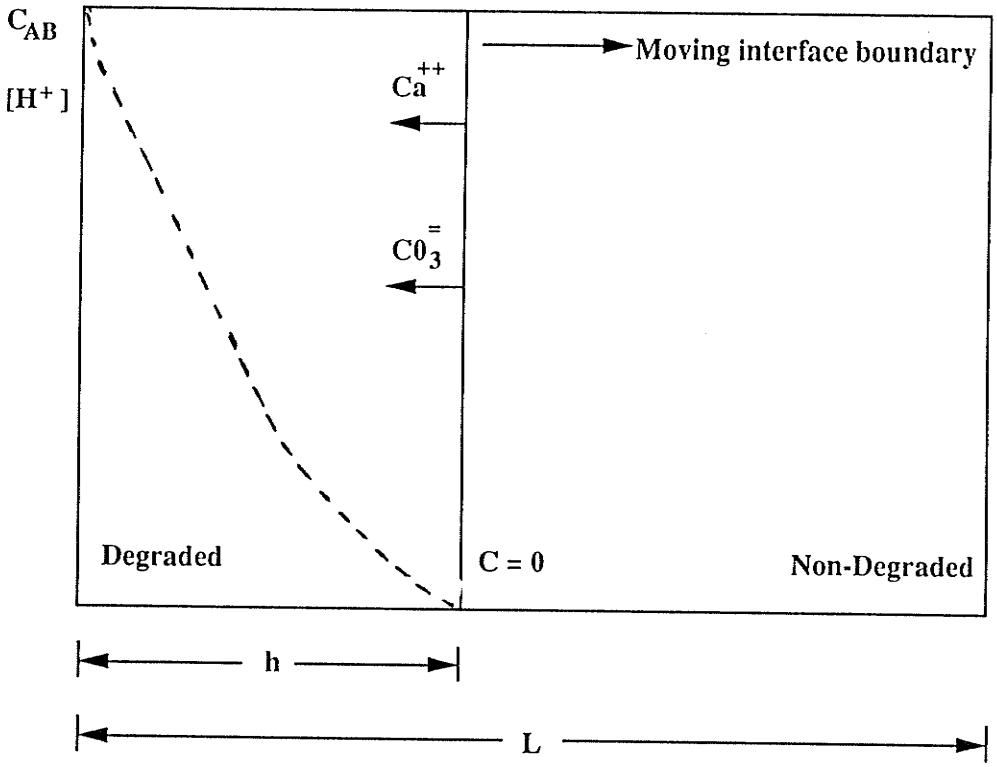

Figure 5.0 Schematic of proposed Acid Deterioration Model

envelope of inert solids such as glass, ATH, and resin particles. This assumption is supported by Balik et al. (1989) who showed that all of the $CaCO_3$ in the latex coating on painted wood substrates was removed during exposure to aqueous sulfurous acid. The removal rate decreased with increasing pH.

The rigorous mathematical solution for this model consists of solving a non-steady state diffusion problem with a moving boundary. For example, formal mathematical solutions were applied to the analogous heat conduction problem where heat flows into a semi-infinite medium (metal) and heat is evolved or absorbed at the boundary (Carslaw and Jaeger, 1959). The general problem of the moving interface boundary was solved by Danckwert (Crank, 1975) for cases where the process of diffusion caused changes which resulted in the disappearance or appearance of matter at the interface. Examples include: the melting of ice in contact with water; the diffusion of oxygen into muscle where oxygen combines with the lactic acid. In the general case of the moving boundary problem, where diffusion takes place into a semi-infinite medium and a constant concentration was maintained at surface $x = 0$, the position of the advancing boundary (h) was found to be proportional to the square root of time.

In this work, the assumption of a pseudo-steady state (PSS) condition was made to allow greater simplification of the solution to the moving boundary problem. An essential feature of the PSS assumption is that diffusion is accompanied by an irreversible chemical reaction at the interface which is so rapid compared with the rate of diffusion that it may be considered instantaneous. The condition where the rate of movement of the interface is much slower than the rate of diffusion of the reactant results in a sharp reaction boundary which moves with time through the solid. Because of this condition

it is reasonable to assume that the interface can be taken to be stationary at any time.

Using the simplified PSS approach, the diffusion problem can be readily solved to find the concentration profile that would occur behind the moving boundary. The mass flux as found from this expression is equated to the rate of disappearance of the solid reactant. A summary of assumptions used in the application of the PSS approximation to determine the rate of deterioration of FFW composites exposed to acidic environments is as follows:

1. Diffusion through the acid-degraded layer controls the rate of reaction/deterioration.
2. No chemical reaction occurs in the acid-degraded layer.
3. The rate of reaction or dissolution of calcium carbonate at the boundary is so fast it can be considered instantaneous.
4. A very narrow, well defined reaction boundary (interface) moves slowly with time toward the centre of the FFW composite.

Based on the above assumptions, the Acid Deterioration Model can be mathematically described by a second-order differential equation expressed by Fick's second law:

[33]
$$D_d \frac{\partial^2 C_A}{\partial X^2} = 0$$

Where:

D_d = diffusion coefficient in the acid-degraded layer, $mm^2.s^{-1}$

C_A = concentration of the diffusing species, $moles.cm^3$

Let the molar flux of the hydrogen ions within the degraded layer (Q_A) be expressed by Fick's law (Levenspiel, 1972):

[34] $$Q_A = -D_d \frac{\partial C_A}{\partial X}$$

Where:

Q_A = Molar flux of H^+ within the degraded layer at x = h, ($mol.m^{-2}.s^{-1}$)

Integrating across the degraded layer from the surface of the composite (x = 0) to the location of the interface (x = h), we obtain (Poggi-Varaldo, 1989):

[35] $$\int_{C_{AB}}^{O} \partial C_A = \frac{Q_A}{D_d} \int_0^h \partial X$$

Where:

C_{AB} = Concentration of H^+ ions in bulk solution at x = 0, ($moles.cm^{-3}$)

h = Distance of the interface boundary from the surface or depth of penetration in the x direction, mm

Therefore

[36] $$C_{AB} = \frac{Q_A\ (h)}{D_d}$$

Assuming steady-state conditions, the rate of reaction of H^+ at the boundary surface ($-\partial N_A/\partial t$) is equal to the mass flow (Q_A) of hydrogen ions, multiplied by the unit surface area (A) of the control volume. Thus

[37] $$(A) \left[\frac{D_d\ C_{AB}}{h}\right] = -\frac{\partial N_A}{\partial t}$$

Where:

N_A = Mass of hydrogen ions, moles.

The increase in penetration is given by the disappearance of ∂N_B moles of calcium carbonate. If we let ρ_B be the molar density of calcium carbonate in the composite and $\partial \forall$ be the control volume, we have

[38] $$-\partial N_B = -\rho_B \, \partial \forall$$

Where:

N_B = Mass of calcium carbonate, moles

ρ_B = Molar density of calcium carbonate in composite (moles.cm^{-3})

$\partial \forall$ = Control volume (∂x) (∂z) (∂h), cm^3

According to the stoichiometry of Equation 4, ∂N_A moles of hydrogen ions will react with $(b_1)N_A$ moles of calcium carbonate. Therefore

[39] $$-(b_1) \, \partial N_A = -\rho_B \, \partial \forall$$

Substituting $b_1 = 0.5$ into Eqn. [39] and rearranging gives:

[4] $$CaCO_3 + 2H^+ \rightarrow Ca^{++} + CO_2 + H_2O$$

Where $b_1 = 0.5$ (chemical reaction constant: moles of $CaCO_3$ to moles of H^+)

[40] $$\partial N_A = (2) \, \rho_B \, \partial \forall$$

Substituting $\partial \forall = (A)\,(\partial h)$ and differentiating w.r.t. time gives:

[41] $$-\frac{\partial N_A}{\partial T} = (2)\,(\rho_B)\,(A)\left[\frac{\partial h}{\partial t}\right]$$

Substituting Eqn. [41] into Eqn. [37] gives :

[42] $$\frac{D_d\ C_{AB}}{h} = (2)\ (\rho_B)\ \frac{\partial h}{\partial t}$$

And integrating over the immersion time period (t) and the depth of penetration (h) gives:

[43] $$\frac{D_d\ C_{AB}}{\rho_B} \int_0^t \partial t = (2) \int_0^h h\ \partial h$$

$$t = \left[\frac{\rho_B}{D_d\ C_{AB}}\right] h^2$$

Rearranging:

[44] $$h = (K)\ (t)^{1/2}$$

Where:

$$K = \left[\frac{D_d\ C_{AB}}{\rho_B}\right]^{1/2}$$

Equation [44] relates the depth of penetration (h) to the immersion time (t). The coefficient of proportionality, K, is a function of the density of the calcium carbonate in the FFW composite ($\rho_b = 3.0 \times 10^{-3}$ m.cm^{-3}), the diffusion coefficient in the degraded layer (D_d), and the concentration of H^+ ions in the bulk solution (C_{AB}).

A similar deterioration model has been proposed to describe the carbonation of concrete when exposed to carbon dioxide (Lin and Jou, 1991). Concrete is a porous concrete composite material in which CO_2 can diffuse inside and react with $Ca(OH)_2$ producing $CaCO_3$. According to Klopfer (1981) the depth of carbonation (h_1) can be expressed as a square root function of the carbonation coefficient (K_1) and the exposure

time (t):

[45] $$h_1 = (2K_1)^{1/2} (t)^{1/2}$$

Where:

h_1 = depth of carbonation

K_1 = carbonation coefficient

5.3 CONCLUSIONS

1. The Acid Deterioration model claims that the rate of deterioration of FFW composites in acidic environments is proportional to the square root of time. It is necessary to verify the proposed model by comparing the rate of deterioration in different acid environments.

2. The Acid Deterioration model allows one to predict the intrinsic diffusion coefficient in the acid-degraded layer (D_d) of an exposed FFW composite. The molar density, pH of the solution, and the experimental (square root) relationship between h and t must be known.

CHAPTER 6

MODEL VERIFICATION STUDY (PHASE 4)

6.1 ACID COMPARISON EXPERIMENT

6.1.1 Introduction

One of the primary objectives of this work was to verify the proposed Acid Deterioration (AD) model by comparing the rates of deterioration of FFW specimens in different acid environments. A secondary objective was to predict, in combination with the experimental data, the intrinsic diffusion coefficients in the acid-degraded layer (D_d) of these specimens.

The acid comparison (AC) experiment was designed for this purpose using the same laboratory test procedures and methods used in Chapter 4. Deterioration was measured in terms of changes in depth of penetration, loss in soluble material weight, the extent of chemical dissolution, loss in wet mechanical properties, and desorption properties for each acid environment. The same FFW test pipe, as described in Section 2.2.4, was also used in this work. The rate of deterioration of FFW composites was determined for small virgin FFW specimens exposed to sulfuric and acetic acid, under accelerated conditions of increased temperature (45°C) and low pH (2.2-2.5).

Acetic acid is an organic acid and may not necessarily affect the deterioration of FFW composites in the same way as sulfuric acid. For example, it was concluded (Section 3.6.1) that deterioration was more extensive for postcured FFW specimens immersed in acetic acid (pH 3.85) than in sulfuric acid (pH 3.96).

There are few research studies showing the effect of extreme acid conditions on the deterioration of filled FRP composites. In one unpublished laboratory study,

FiberGlas Canada (1987), evaluated the change in physical properties of various filled random-orientated chopped glass composites exposed to a 10% solution of acetic acid (ie. an initial pH of 2.25) at room temperature. Based on the findings of this study, the CSA Subcommittee on FRP Septic Tanks has revised Clause 6.3.4 of the CSA Standard CAN3-B66-M85 to include an unfilled "anti-wicking barrier" (Figure 2.1) to protect the surfaces of laminates exposed to sewage. In the literature review (Section 2.3.2), it was shown that surface above the liquid level in an anaerobic septic tank will be subject to sulfuric acid attack at pH levels as low as 2.0. In contrast, the submerged surfaces of an anaerobic septic tank will be subject to acetic acid attack at pH levels as low as 5.0. It is hoped that the results of this experiment will facilitate the establishment of a standard accelerated test procedure and lead to the revision of the current CSA Standard for filled FRP septic tanks.

6.1.2 Materials

Specimens with nominal dimensions of 133.5 mm x 38.0 mm x 4.80 mm were cut from the FFW test pipe using a diamond blade saw. A total of 120 virgin and 40 postcured specimens were prepared prior to the start of the AC experiment. The postcured specimens were prepared by drying virgin specimens in an oven at 112°C for 36 hours. The edges of all specimens were sanded and coated by brush with a corrosion-resistant polyester resin (DION COR-RES 669FR). The coating was applied at room temperature using a one percent mixture by weight of methyl ethyl ketone peroxide (MEKP) and was allowed to air dry cure for 7 days prior to immersion. The edge coating provided a visible layer of approximately 0.05 mm. Eight specimens were selected at random for immersion in each container and the remaining virgin and

postcured specimens were used for testing of initial mechanical properties in the dry state.

6.1.3 Laboratory Procedure

Three test environments: deionized water, sulfuric acid, and acetic acid were selected. The experimental operating conditions for the AC experiment are shown in Table 6.0. Virgin specimens were placed in all three environments (D25, S25, A25) and the postcured specimens were placed in deionized water (D112) only. Deionized water was selected as a control treatment. Sixteen closed top containers were filled with each solution (3 L volume) and placed in a temperature controlled chamber at 45°C (Figure 6.0).

All acid solutions were prepared using deionized water with a conductance of less than 0.2 μmhos/cm. The temperature and pH levels were checked at 2 day intervals because of some evaporation. Deionized water was added as required to maintain the level in each container at a constant 3 litre volume. Additional amounts of 1.0 N H_2SO_4 and glacial acetic acid were added intermittently to maintain the pH in the range of 2.2 to 2.3. Tests were conducted to monitor changes in specimen weight and calcium and aluminum ion concentrations in the leachate (see Chapter 3).

The extent of deterioration was quantified after 2, 4, 8, and 12 week immersion time periods. Following each immersion time period, eight specimens were removed from each of the four containers. Five of the test specimens were rinsed with distilled water and maintained in the wet state for analysis of mechanical properties. The wet mechanical properties that were measured included ultimate flexural strength, flexural modulus and indentation Barcol hardness. Two other specimens were reconditioned at

Table 6.0 Experimental Operating Conditions: AC Experiment

Specimen Type	Environment Type	Temp. (°C)	pH Condition	Conditions for Postcuring
D112	Deionized water	45	7.0	(112°C) 36 hrs
D25	Deionized water	45	7.0	room temp.*
S25	Sulfuric acid (O.10 N)	45	2.2-2.5	room temp.*
A25	Acetic acid (1.76 N)	45	2.2-2.5	room temp.*

* Specimens referred to as "virgin".

112°C for 36 hours to determine the average soluble material weight loss, and the average depth of penetration. The average depth of penetration (h) was measured using both the HC and FD (visible light) methods. The remaining specimen was used to quantify changes in diffusion properties (S_d) based on the FDSE method. A description of the HC, FD and FDSE test methods can be found in Chapter 4.0.

6.1.4 Results and Discussion

The average pH conditions for the deionized water, sulfuric acid, and acetic acid environments are shown in Table 6.1. The standard deviation for the acidic environments (S25, A25) was low ranging from 0.03 to 0.05. A plot of pH versus time (Figure 6.1) indicates little variation between weekly pH values.

Figure 6.0 Containers housed in temperature controlled chamber at 45°C

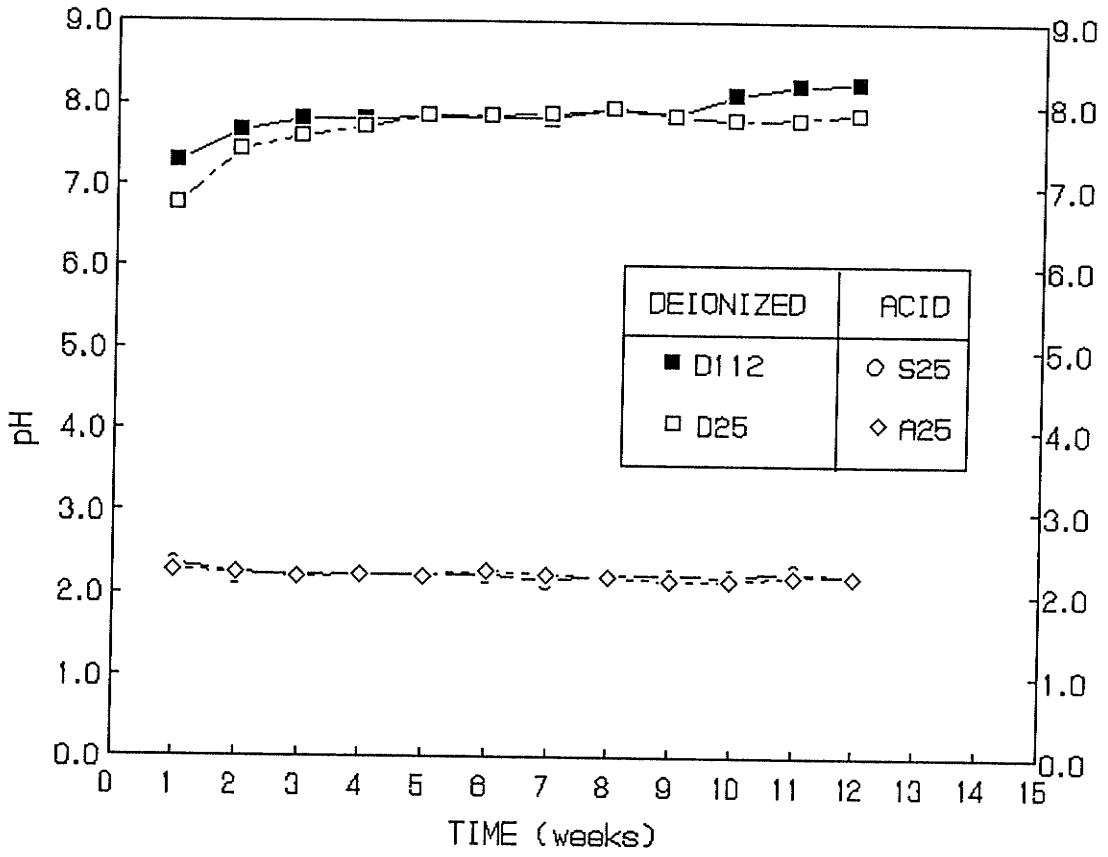

Figure 6.1 Weekly pH values: AC Experiment

Table 6.1 Average (Weekly) pH Values: AC Experiment

Specimen Condition	Number of Observations	Average pH	Standard Deviation
D112	12	7.88	0.26
D25	12	7.69	0.33
S25	12	2.23	0.05
A25	12	2.22	0.03

A summary of test results showing the extent of deterioration after 12 weeks immersion is shown in Table 6.2. A detailed tabulation of deterioration test results corresponding to other immersion time periods are presented in Appendix IV-1 to IV-4 inclusive. Regression equations were also developed to quantify the rate of deterioration of virgin FFW specimens immersed in sulfuric and acetic acid. It was assumed that the resistance to acid diffusion through the degraded FFW layer controlled the rate of deterioration, following the concepts of the AD model developed in Chapter 5.

6.1.4.1 Depth of Penetration Analysis

Changes in the depth of penetration as a function of immersion time, based on the HC and FD methods, are shown in Figures 6.2 and 6.3, respectively. In comparing the results of both methods, it is evident that there is little variation in depth of penetration among the deionized and sulfuric acid specimens. The rate of acetic acid penetration is significantly faster than for sulfuric acid. For example, after 12 weeks immersion (Table 6.2) the average h value (HC method) for acetic acid specimens was 862 μm compared to 278 μm for the sulfuric acid specimens. In comparison, the average h value (FD method) for acetic acid specimens was 1054 μm compared to

Table 6.2 Extent of Deterioration of FFW Composites After 12 Weeks Immersion: AC Experiment

Deterioration Test Parameters	Type of Environment			
	Deionized Water		Sulfuric Acid	Acetic Acid
Specimen Conditions	Postcured D112	Virgin D25	Virgin S25	Virgin A25
Gravimetric				
Material weight loss (%)	0.47 (0.01)	0.61 (0.01)	1.75 (0.07)	3.84 (0.52)
Chemical				
Calcium as $CaCo_3$ (mg. L^{-1})	128	180	1,180	5,100
Aluminum as $Al_2O_3.3H_2O$ ($mg.L^{-1}$)	< 1	< 1	208	188
Loss in Wet Mechanical Properties (%)				
Ultimate flexural strength	33.6 (4.1)	35.0 (4.8)	37.5 (8.5)	40.8 (5.9)
Flexural modulus	32.2 (5.4)	27.9 (5.0)	38.5 (7.4)	32.4 (8.8)
Barcol hardness	26.1 (7.7)	27.1 (7.2)	44.5 (9.8)	79.0 (8.4)
Diffusion Properties ($mins^{-½}$)				
Desorption slope	0.009	0.019	0.019	0.057
Microscopic Appearance				
Depth of penetration (μm)				
HC method	231 (26)	188 (37)	278 (34)	862 (89)
FD method	144 (13)	185 (15)	261 (32)	1,054 (194)

Standard deviations in brackets.

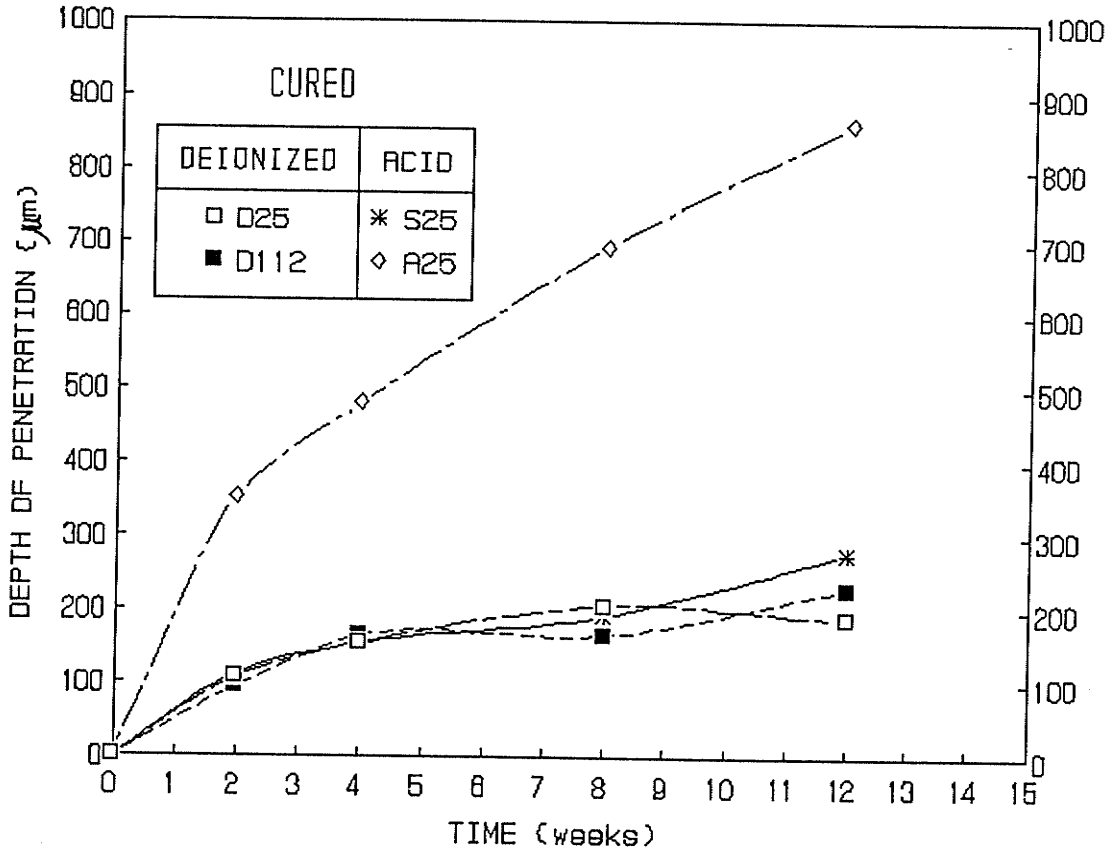

Figure 6.2 Depth of penetration as a function of immersion time: HC Method

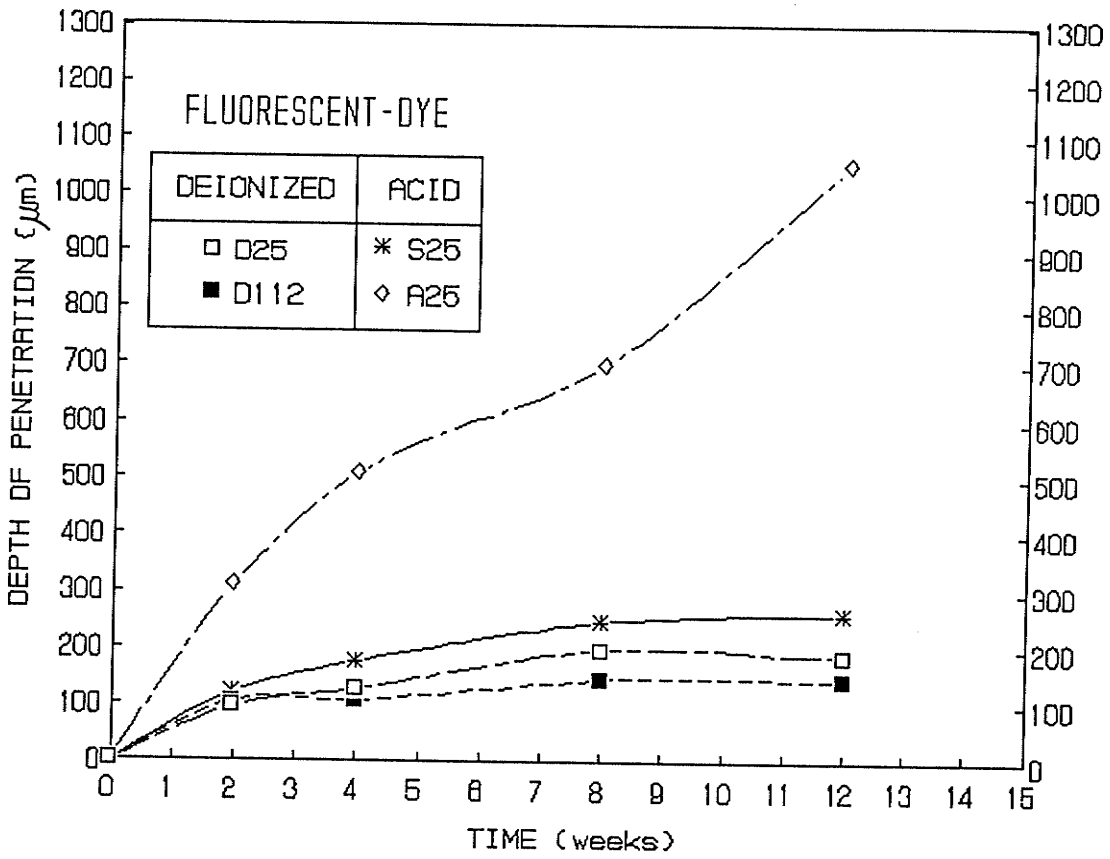

Figure 6.3 Depth of penetration as a function of immersion time: FD Method

261 μm for the sulfuric acid specimens.

Photomicrographs (x 6) taken through the thickness of typical sulfuric acid and acetic acid specimens after 4 and 12 weeks of immersion (Figures 6.4 and 6.5) show both types of acid diffusing inward primarily through the non-lined interior surface. Similar observations were made by Attioghbe and Rizkalla (1989) for concrete specimens immersed in low pH sulfuric acid solutions. Thermal drying caused the saturated layer of acid-attacked specimens to acquire a white hazy tint while, in contrast, the non-saturated layer remained a darker colour (Figure 6.4). The fluorescent dye was found to be adsorbed throughout the acid-attacked layer of the FDSE test coupons (Figure 6.5). It was evident from the photomicrographs that the desorption slope (S_d) could be used as a surrogate parameter to quantify the diffusion characteristics in the acid-attacked layer.

The AD Model claims that deterioration, as measured by depth of penetration (h) is proportional to the square root of immersion time.

[44] $$h = (K)\ (t)^{1/2}$$

A least-squares regression analyses (Table 6.3) was conducted to determine the coefficient of proportionality (K), standard error of estimate (e) and coefficient of determination (R^2) for the different acids. The high range of R^2 values (0.962 to 0.999) confirm that changes in depth of penetration (h) are proportional to the square root of immersion time for each acid condition. Similar observations were made by Lawrence (1984) who showed a linear increase in carbonation depths with the square root of time for concrete specimens.

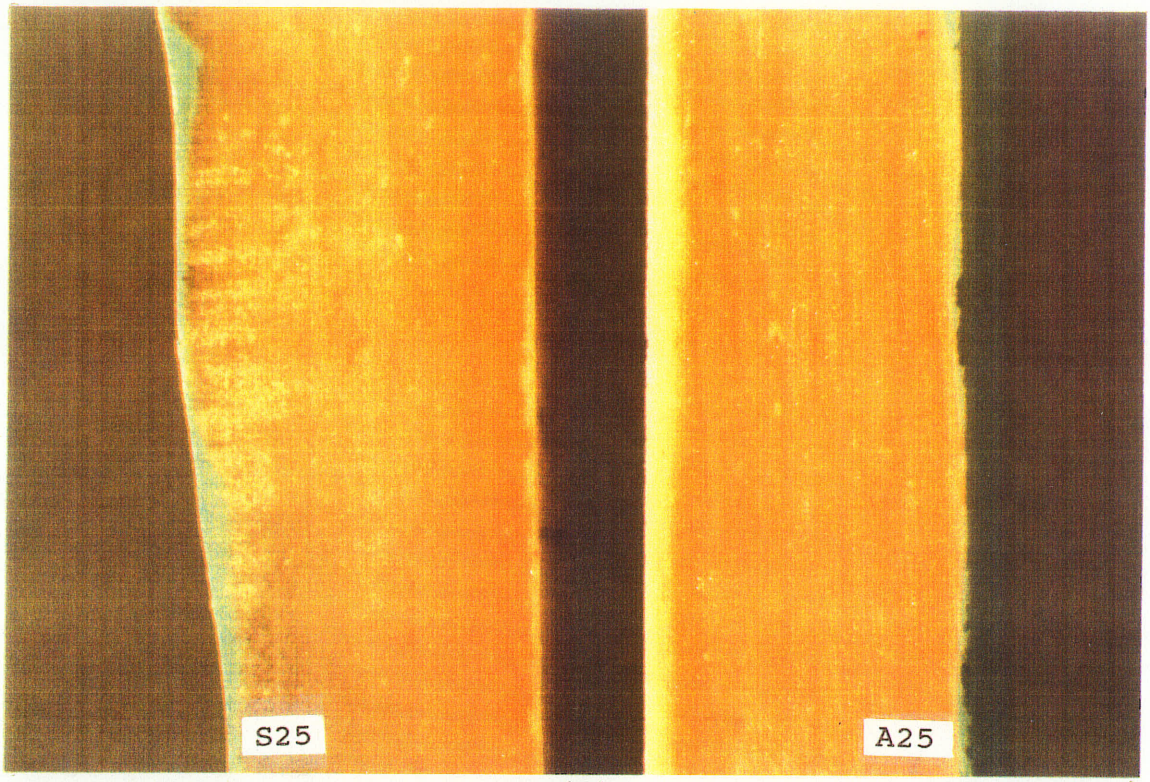

(a)

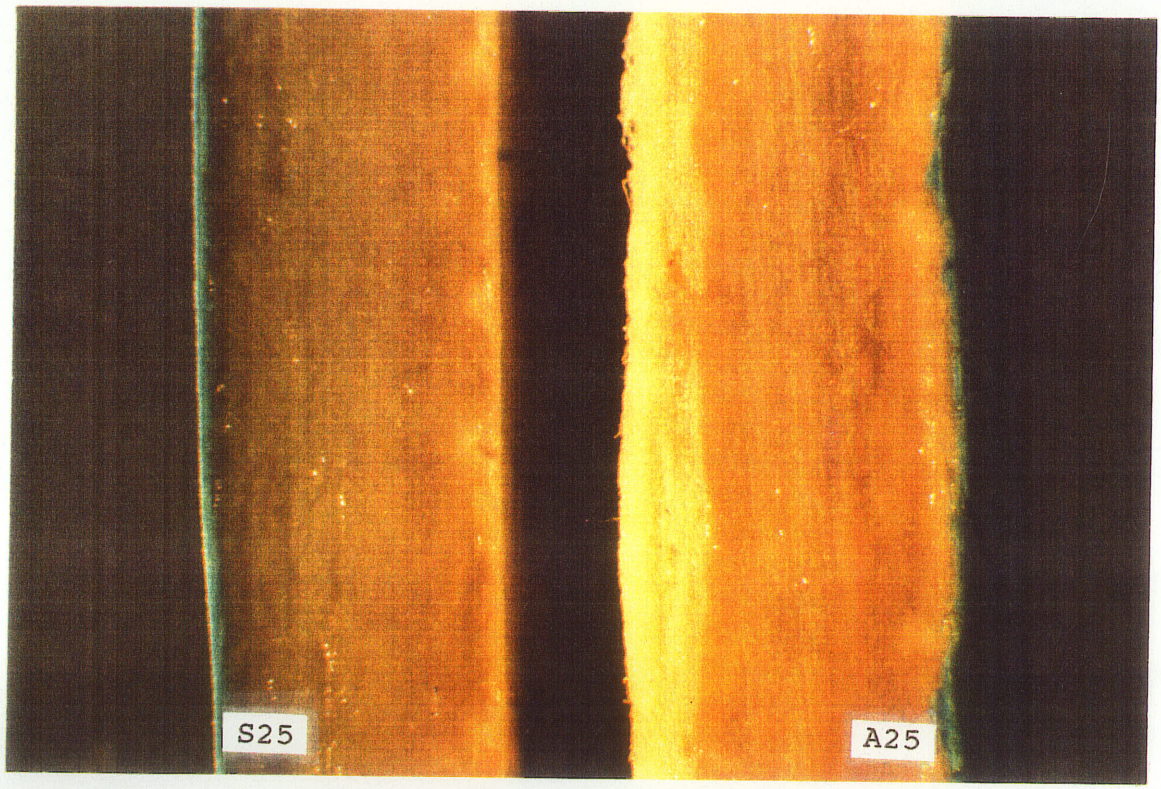

(b)

Figure 6.4 Photomicrographs of sulfuric and acetic acid specimens: HC Method (a) 4 weeks immersion (b) 12 weeks immersion

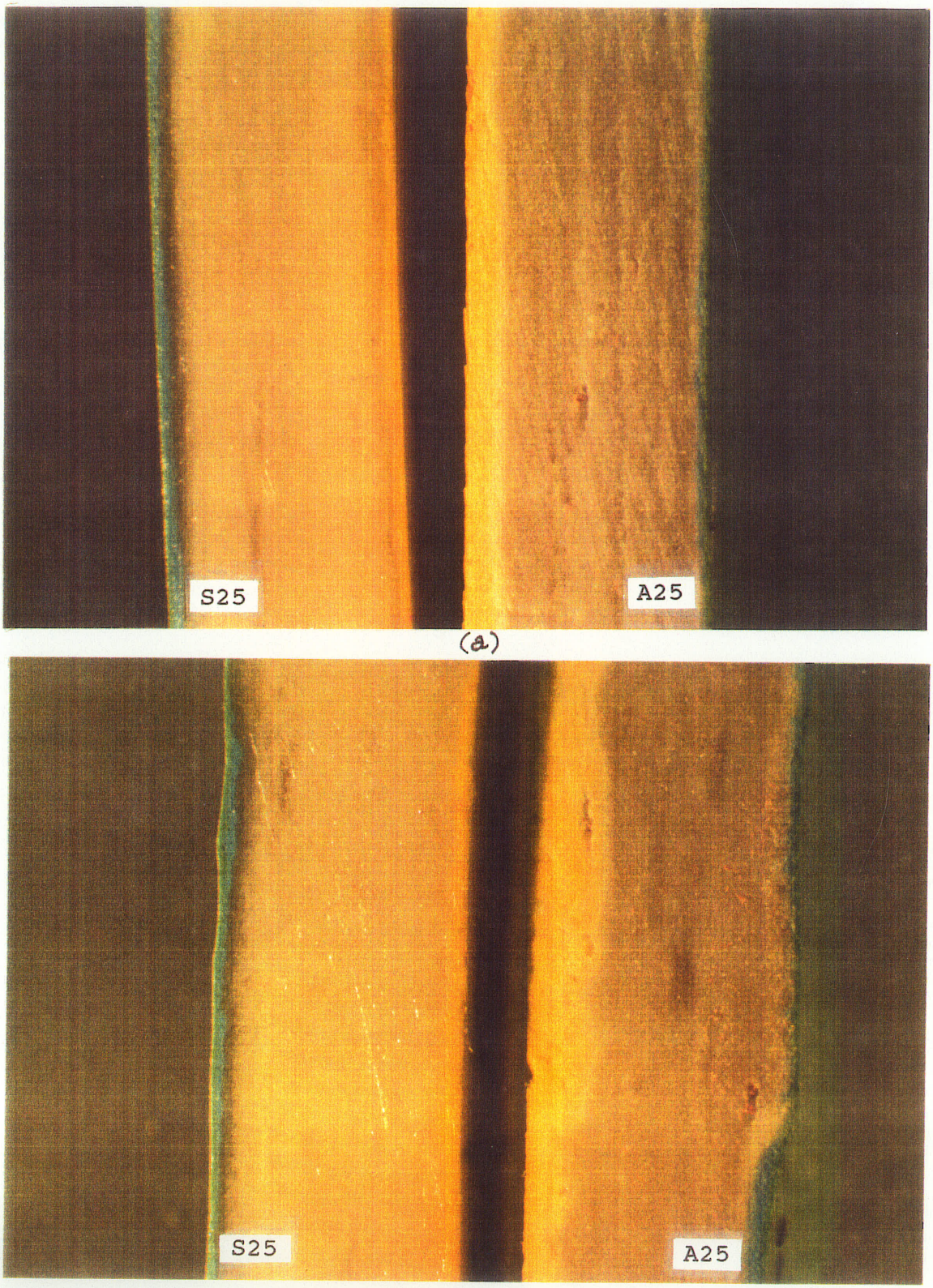

Figure 6.5 Photomicrographs of sulfuric and acetic acid specimens: FD Method (a) 4 weeks immersion (b) 12 weeks immersion

Table 6.3 Regression Analysis for Depth of Penetration:
$h = (K)(t)^{1/2}$

Depth of Penetration	Type of Environment					
h (μm)	Sulfuric Acid (S25)			Acetic Acid (A25)		
	K	e	R^2	K	e	R^2
HC method	75.9	2.7	0.982	246.7	1.5	0.999
FD method	81.6	2.9	0.980	272.7	15.1	0.962

Exterior Corrosion Liner

It was also observed, following 12 weeks immersion, that the blue polyester corrosion liner was still effective in limiting sulfuric acid penetration. However, the liner was less effective in the acetic acid environment. One explanation is that acetic acid, diffuses at a faster rate into the cross-linked (organic) polyester matrix resulting in the formation of swollen solid and gel layers. Fontano (1986) reported that in some cases cracking of the swollen solid layer may occur due to internal stresses. Photomicrographs (Figure 6.6) of the outside surfaces of the 12 week exposed liners show the formation of principle tensile stress cracks in the direction of the glass fibres for the acetic acid specimens but not the sulfuric acid specimens. Similar stress cracks were observed by Bravenic (1983) resulting from the rapid uptake of toluene and methyl ethyl ketone and swelling of cross-linked polyester resins.

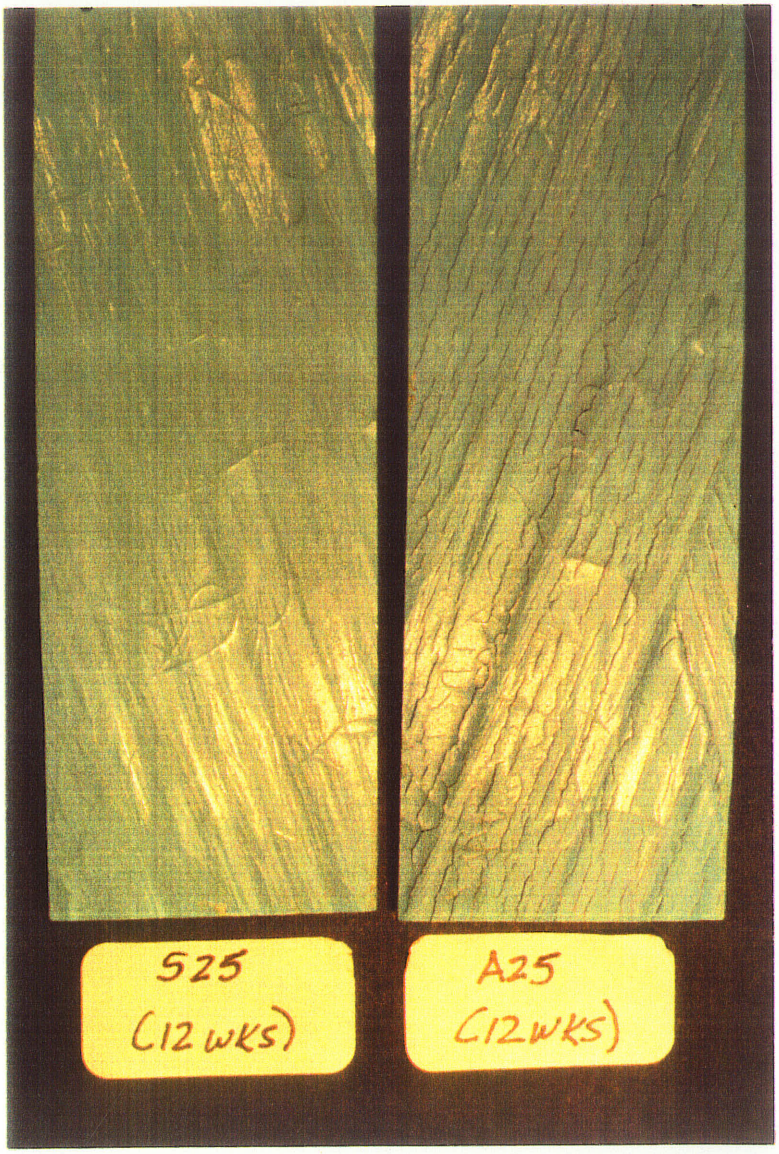

Figure 6.6 Comparison of exterior corrosion liner after 12 weeks immersion: sulfuric (S25) and acetic (A25) acid

6.1.4.2 Other Deterioration Test Results

The average values for material weight loss (W_m) were determined and plotted as a function of immersion time. Figure 6.7 shows that there is little variation in the material weight loss values for the deionized water specimens. Changes in W_m were greater for acetic acid than for sulfuric acid. For example, after 12 weeks immersion (see Table 6.2) the average material weight loss for the A25 specimens was 3.84% compared to 1.75% for the S25 specimens.

The increases in calcium and aluminum ion concentrations as a function of immersion time are shown in Figures 6.8 and 6.9, respectively. The total concentration of calcium in acetic acid leachate after 12 weeks of sample immersion was determined to be 5,100 $mg.L^{-1}$. This concentration was greater than the value of 1,180 $mg.L^{-1}$ obtained for specimens immersed in sulfuric acid. In comparison, the concentration of aluminum dissolved in acetic and sulfuric acid was only 208 and 188 $mg.L^{-1}$, respectively. The dissolution behaviour of aluminum trihydrate (ATH) appears not to be influenced by the kind of acid used. It can also be concluded, since the virgin FFW composite consisted of an equal percentage by weight of each filler constituent (Table 2.0), that calcium carbonate is considerably more soluble than ATH in low pH acidic environments.

The primary chemical reaction was the dissolution of calcium carbonate. Table 6.4 presents a comparison of total weight lost per specimen (column A) and total weight of filler constituents ($CaCO_3$ and ATH) lost per specimen (column B) after various immersion times. A reasonably close relationship was obtained between these two values for immersion times of 4, 8, and 12 weeks. The material balance and

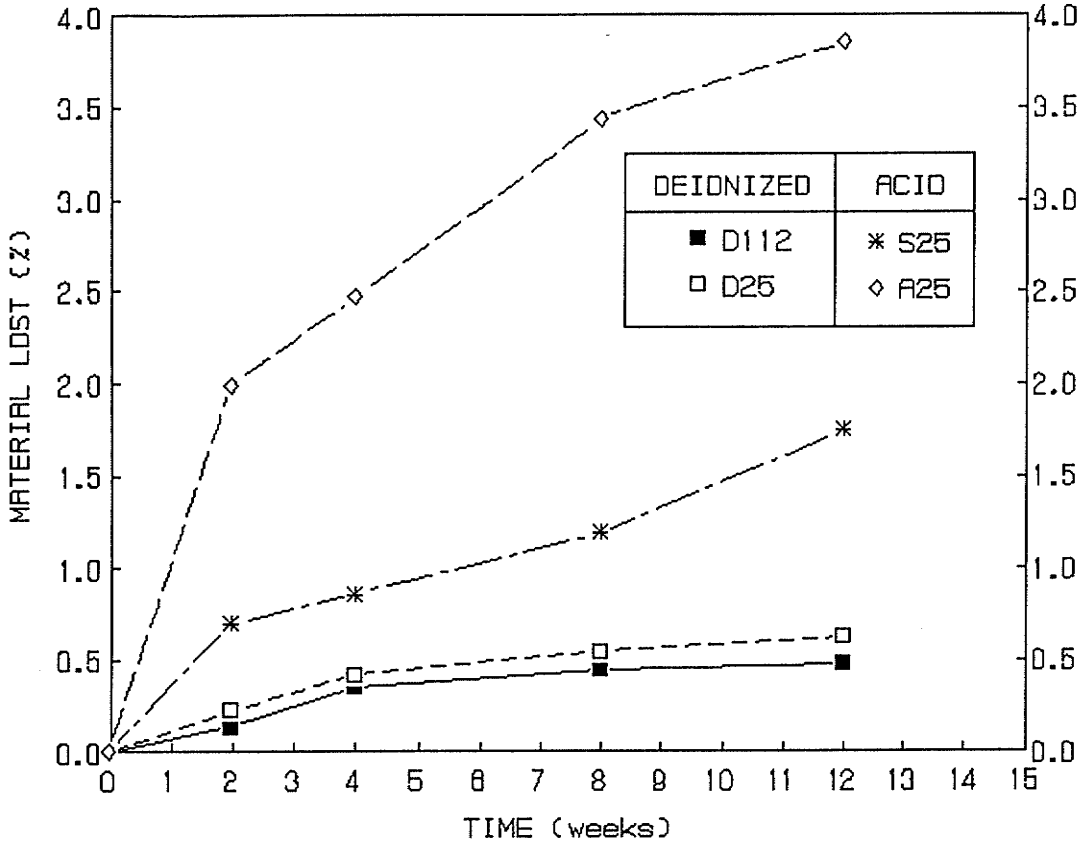

Figure 6.7 Average material weight loss (W_m) as a function of immersion time: AC Experiment

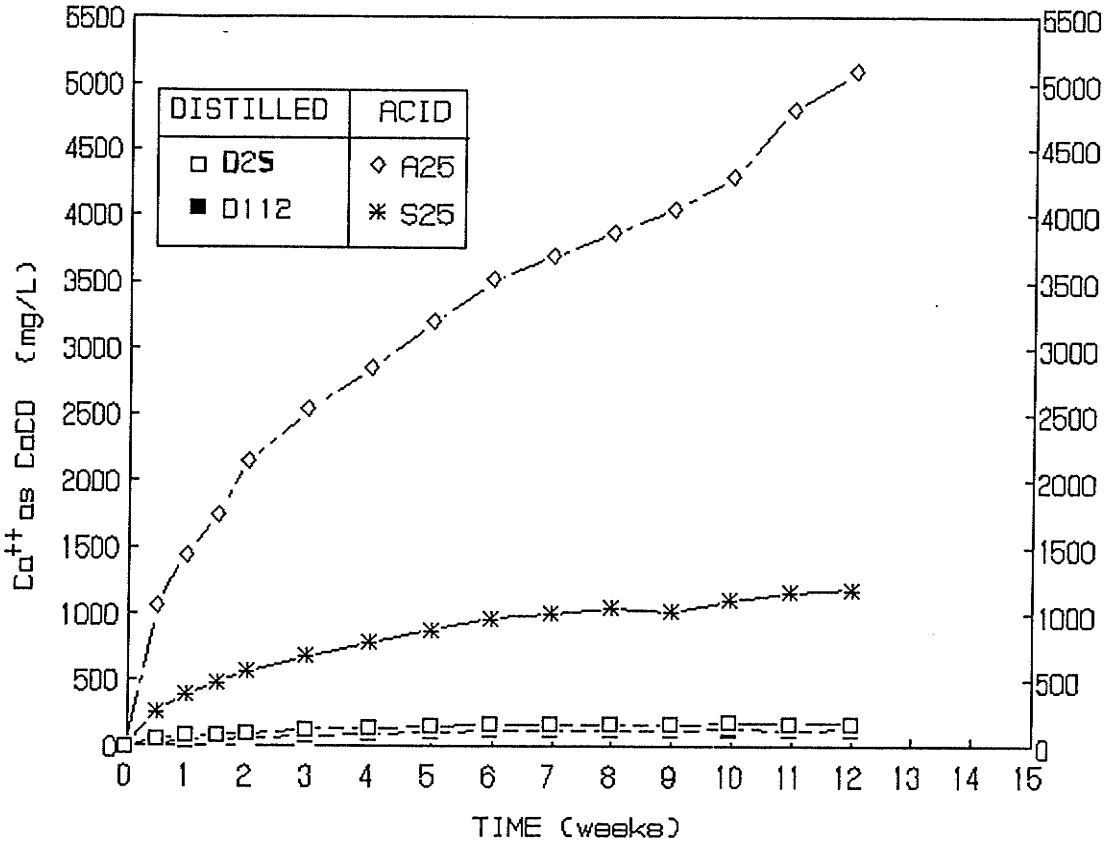

Figure 6.8 Calcium ion concentration in the leachate as a function of immersion time: AC Experiment

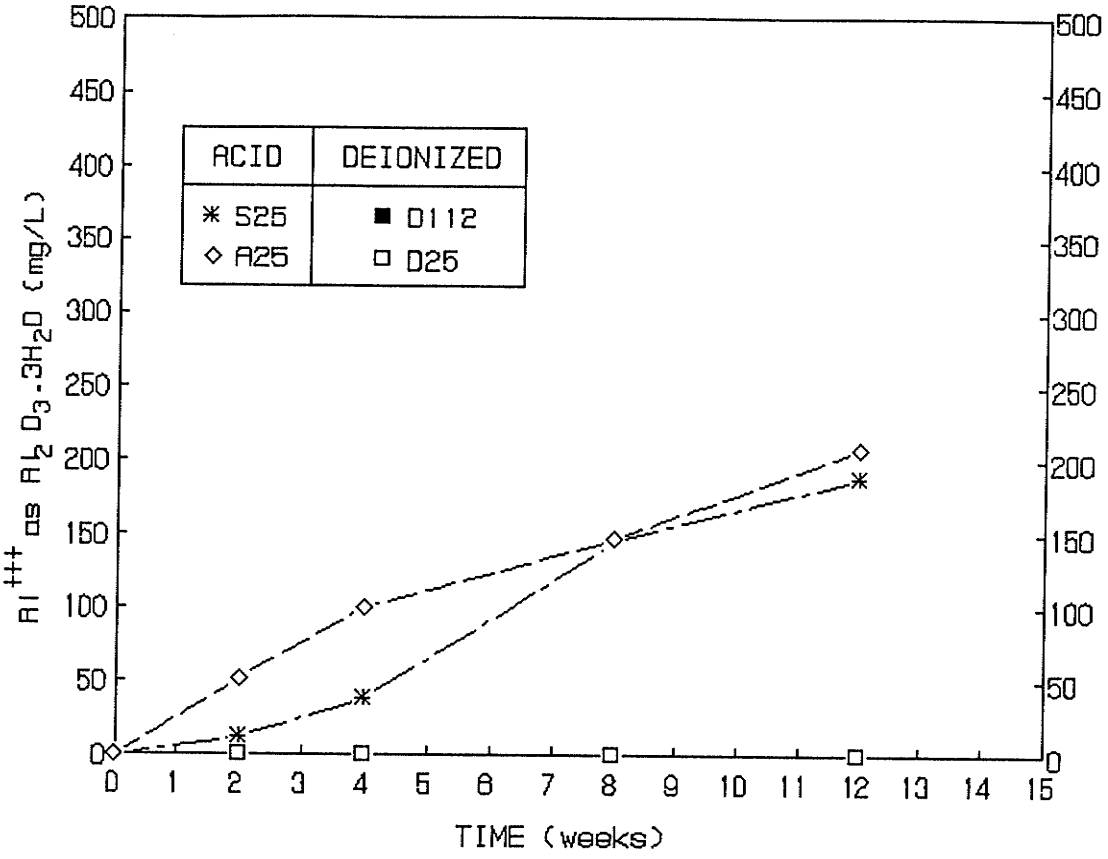

Figure 6.9 Aluminum ion concentration in the leachate as a function of immersion time: AC Experiment

Table 6.4 Material Balance Comparison of Total Material Weight Loss (Column A) vs. Estimated Filler Weight Loss (Column B)

Type of Environment	Immersion Time					
	4 Weeks		8 Weeks		12 Weeks	
	A	B	A	B	A	B
Sulfuric acid ($g.specimen^{-1}$)	0.40	0.30	0.56	0.45	0.78	0.52
Acetic acid ($g.specimen^{-1}$)	1.13	1.11	1.51	1.51	1.73	1.91

chemical analyses results indicate that the primary deterioration mechanism of virgin FFW materials exposed to acid environments is the dissolution of calcium carbonate and not polyester resin as suggested by Loos and Springer (1980) for filled SMC materials.

Changes in the mechanical properties of all wet acid immersed specimens were plotted as a function of immersion time in Figures 6.10, 6.11, and 6.12. The average initial dry mechanical properties for postcured and virgin specimens are shown in Table 6.5. All data presented were normalized with respect to the "baseline" data (identified by the subscript $_o$) and were presented as a loss (%) of the initial dry mechanical properties ($1-S/S_0$, $1-E/E_o$, $1-H/H_o$).

The losses in wet flexural properties were similar for both acids and ranged from 32.4 to 40.8 percent after 12 weeks immersion. In contrast, the reductions in hardness values were different for the two types of acid; being 44.5 percent in sulfuric acid and 79.0 percent in acetic acid (Table 6.2). A possible explanation for the difference in flexural and hardness results is that in the hardness penetration test there

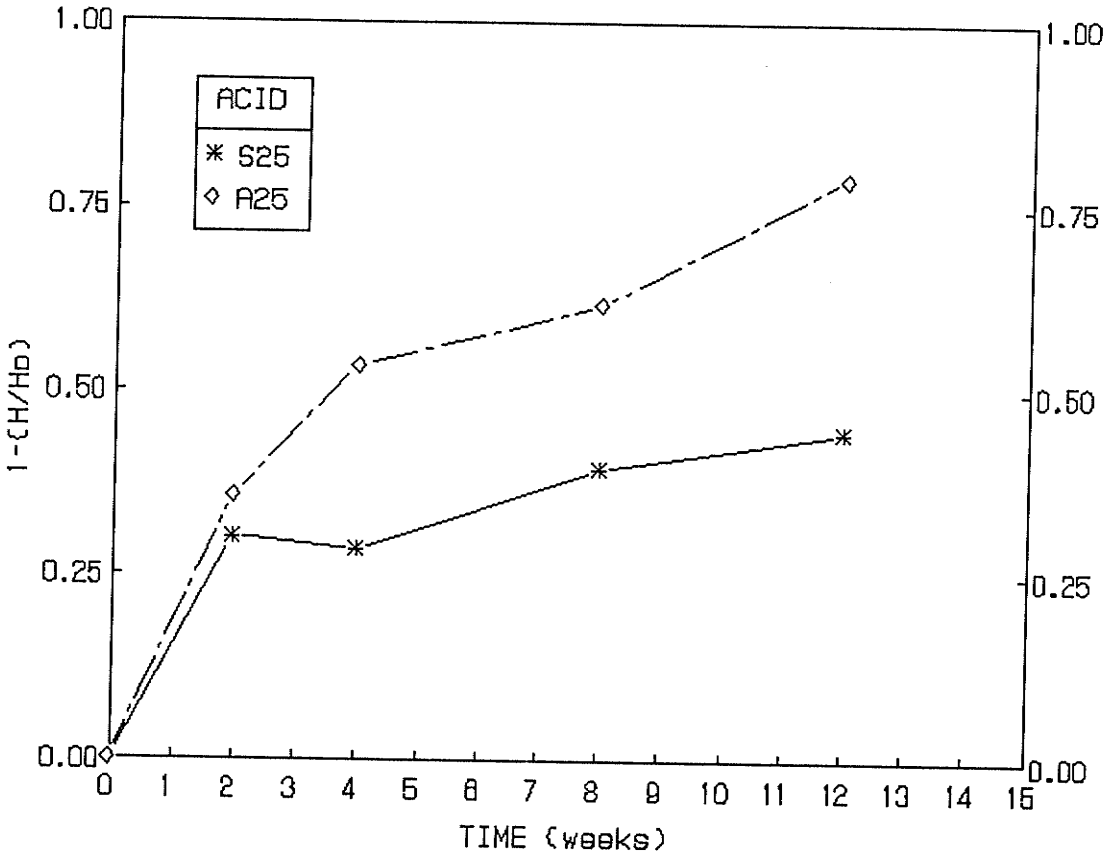

Figure 6.10 Percent reduction in wet flexural strength as a function of immersion time: AC Experiment

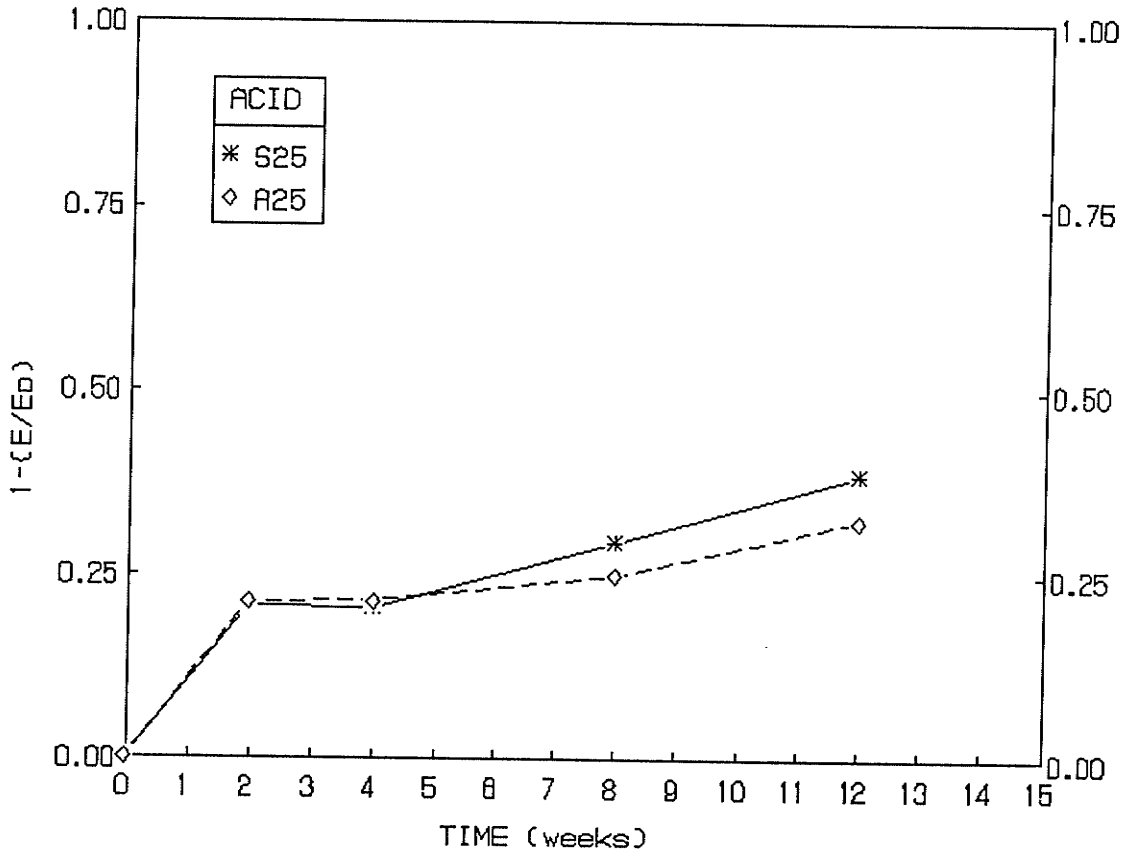

Figure 6.11 Percent reduction in wet flexural modulus as a function of immersion time: AC Experiment

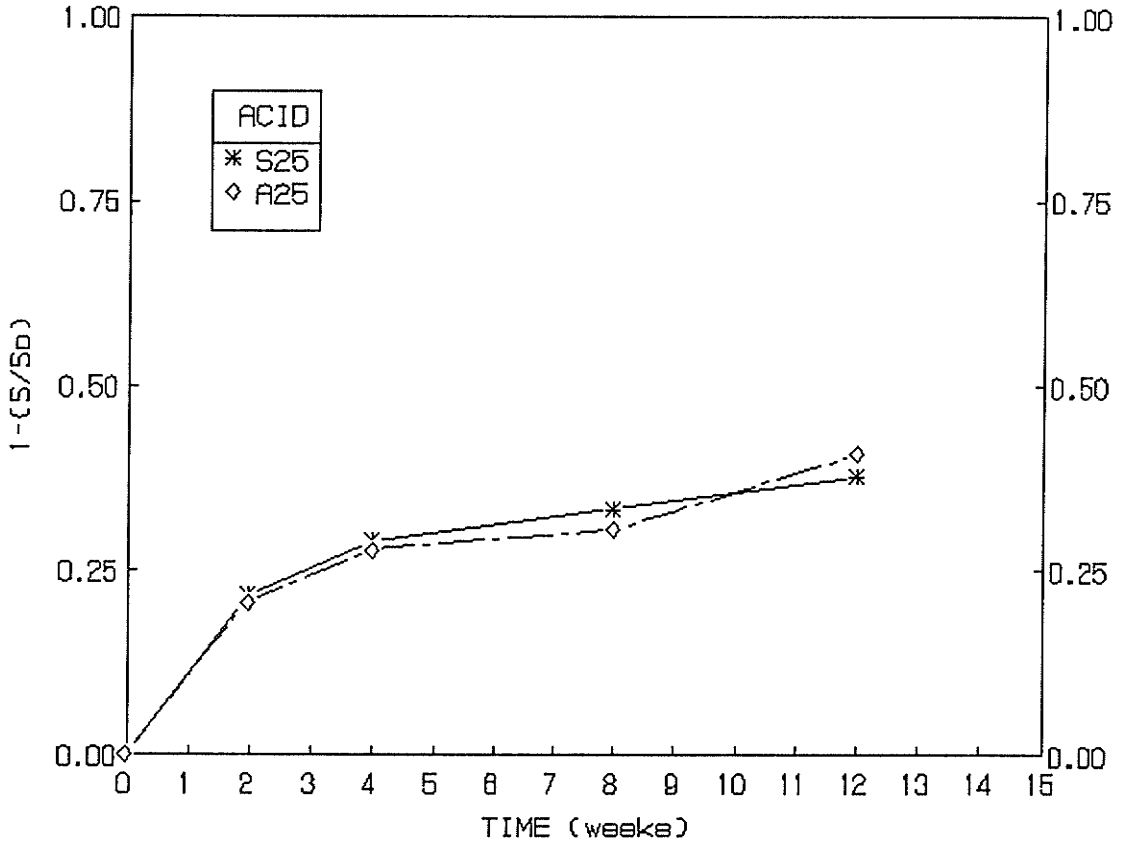

Figure 6.12 Percent reduction in wet Barcol hardness as a function of immersion time: AC Experiment

Table 6.5 Dry Mechanical Properties of Virgin and Postcured Specimens Prior to Immersion: AC Experiment

Specimen Type	Flexural Strength		Flexural Modulus		Barcol Hardness	
	(S_0)	(MPa)	(E_0)	(GPa)	(H_0)	(units)
	Mean	Standard Deviation	Mean	Standard Deviation	Unit	Standard Deviation
Virgin	311.0	19.5	21.5	1.5	59.1	3.7
Postcured	310.0	14.3	23.3	1.3	61.6	4.1

is less reliance on the part of the degraded (soft) resin/filler matrix to transfer the load to the continuous glass fibre reinforcement.

A comparison of wet flexural properties (Table 6.2) for FFW specimens immersed in acetic acid, sulfuric acid, and deionized water environments suggest little difference in results. These observations are in agreement with the results of an earlier United States (US) government industry cooperative study (GISC, 1979) which evaluated Reinforced Plastic Mortar Pipe (RPM) for water resources applications. The results of this US study showed that changes in mechanical properties of RPM specimens immersed in laboratory solutions of sulfuric acid, sodium hydroxide, synthetic soil extract, distilled and tap waters were associated primarily with physical (wetting) action rather than chemical action.

Typical FDSE (45°C) isotherms for the deionized and acidic specimens after 12 weeks immersion are shown in Figure 6.13. A summary of the FDSE results is presented in Appendix IV-4. Changes in the diffusion characteristics as measured by the desorption slope (S_d), were determined from the FDSE isotherms and plotted as a

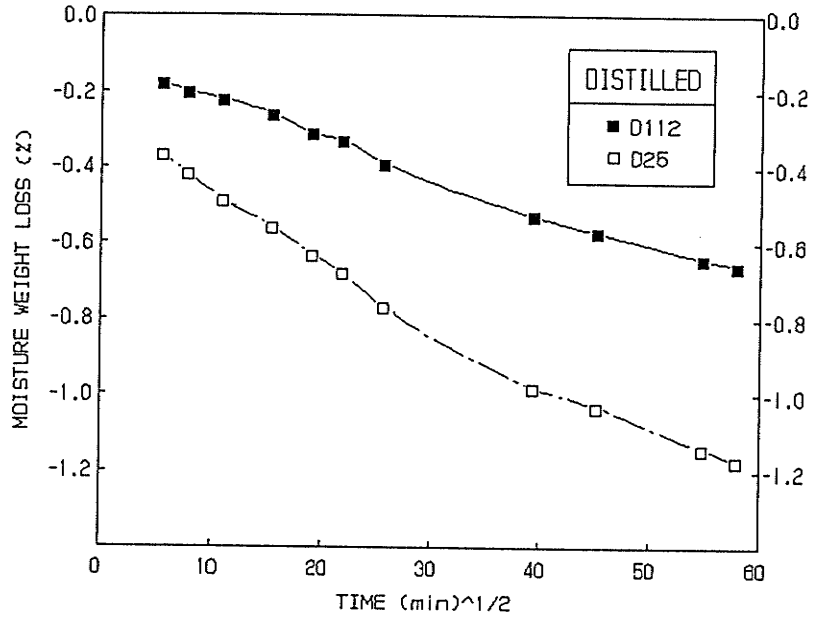

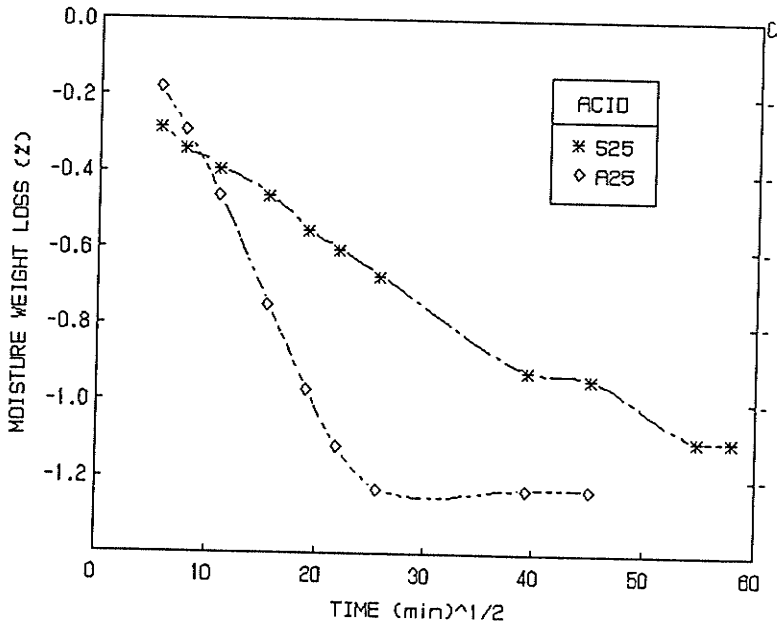

Figure 6.13 FDSE (45°C) isotherm after 12 weeks immersion
(a) deionized water (b) acidic environments

function of immersion time. Figure 6.14 shows that there is little variation in the desorption slopes for the sulfuric acid (S25) and the deionized water (D25) specimens. The desorption slope plots are similar and appear to reach an asymptote after 12 weeks immersion. The results suggest that the diffusion characteristics in the degraded layer (D_d) of the sulfuric acid specimens are similar in magnitude to that of the deionized water specimens after 12 weeks immersion.

In contrast, changes in S_d were greater for acetic acid than for the deionized and sulfuric acid specimens. For example, after 12 weeks immersion (see Table 6.2), the desorption slopes for the S25 and D25 specimens were much lower (0.019 $mins^{-1/2}$) compared to the acetic acid specimens (0.057 $mins^{-1/2}$).

Regression Analyses

Empirical equations were also developed to determine the rate of deterioration for the following deterioration test parameters: material weight loss (W_m), calcium carbonate dissolution, aluminum dissolution, ultimate flexural strength, flexural modulus, Barcol hardness, and desorption slope (S_d).

It was assumed, based on the AD model, that deterioration as measured by the above test parameters (Y) was also related to the square root of immersion time

[46]

$$Y = (A)\ (t)^{1/2}$$

Where:

Y = Deterioration test parameter.

A = rate of deterioration (regression coefficient).

t = immersion time.

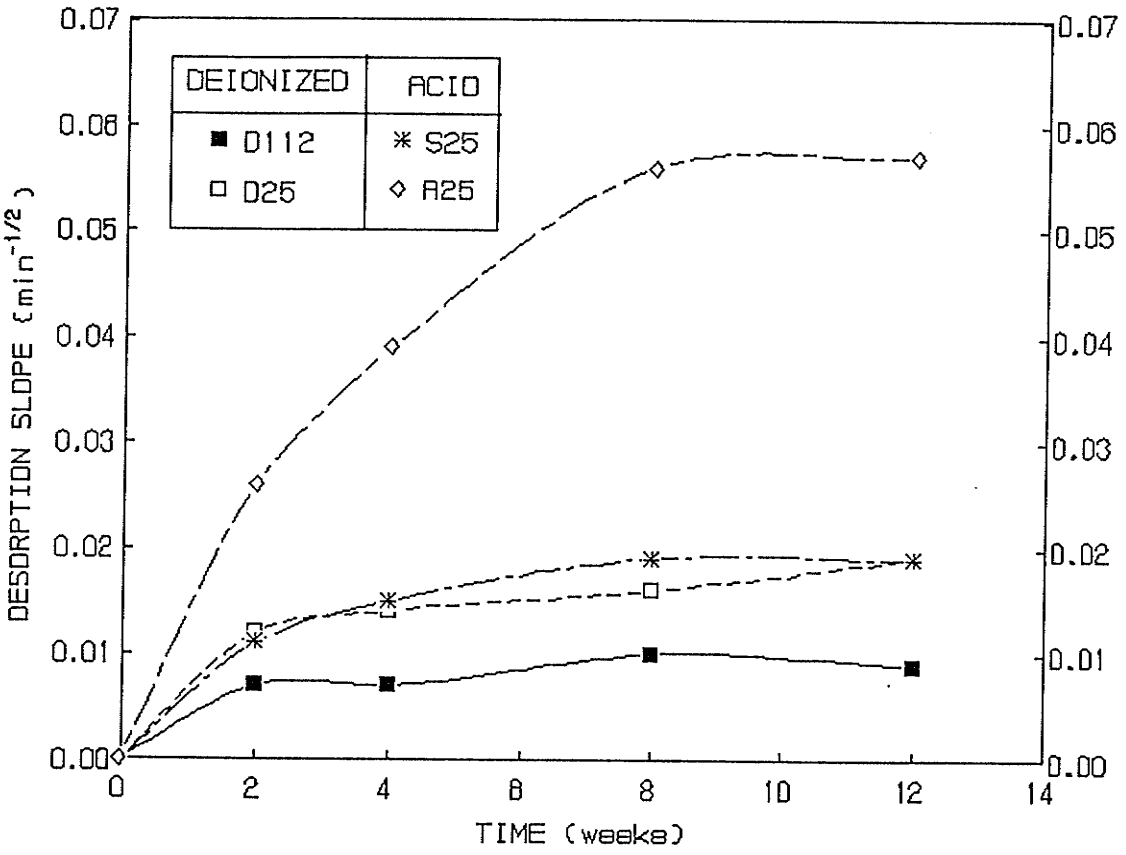

Figure 6.14 Desorption slope as a function of of immersion time: AC Experiment

A least-squares regression analyses was conducted to determine the rates of deterioration or regression coefficients (A), standard error of estimate (e) and coefficient of determination (R^2) for the various deterioration test parameters. The regressions were forced through the origin and equations obtained from the regression analyses were used to fit curves through the experimental data (Appendix IV-5 to IV-12 incl.).

Strong correlations with the square root of immersion time were observed (Table 6.6) for most of the parameters with the exception of aluminum in sulfuric acid. A comparison of the regression coefficients for each type of acid gives an indication of the relative rate of deterioration. An A_r ratio, calculated as the rate of acetic acid deterioration (A_{ac}) divided by the rate of sulfuric acid deterioration (A_s), has been defined to determine the relative rate of acid deterioration.

There is a strong correlation between W_m and the square root of time (R^2 = 0.975 and 0.979). The A_r ratio based on material weight loss is 2.5. The rate of chemical deterioration was quantified by measuring changes in the concentration of calcium rather than aluminum. The high R^2 values (0.980 and 0.994) support the AD model in that the rate of calcium carbonate dissolution is proportional to the square root of immersion time. The A_r ratio, based on calcium carbonate dissolution, is 3.9.

The R^2 values for the mechanical deterioration parameters (flexural strength, flexural modulus, Barcol hardness) ranged from 0.884 to 0.980 and suggest a strong relationship with the square root of immersion time. The A_r ratios (0.9 and 1.0) confirm that the loss in wet flexural properties is not affected by the type of acid environment. In contrast, the A_r ratio of 1.64 for Barcol hardness was much higher than values determined from wet flexural properties.

Table 6.6 Regression Analysis and A_r Ratios for Various Deterioration Test Parameters as a Function of the Square Root of Immersion Time: $Y = (A)t^{1/2}$

Deterioration Test Parameters (Y)	Type of Environment						
	Sulfuric Acid (S25)			Acetic Acid (A25)			A_r
	A_s	e	R^2	A_{ac}	e	R2	A_{ac}/A_s
Gravimetric							
Material weight loss (%)	0.47	0.02	0.975	1.18	0.04	0.979	2.5
Chemical							
Calcium as $CaCo_3$ ($mg.L^{-1}$)	363.13	5.62	0.980	1,416.69	12.67	0.994	3.9
Aluminum as $Al_2O_3.3H_2O$ ($mg.L^{-1}$)	44.50	8.04	0.766	54.30	3.33	0.956	*
Loss in Mechanical Properties							
Ultimate flexural strength (%)	0.12	0.01	0.926	0.12	0.01	0.958	1.0
Flexural modulus (%)	0.11	0.01	0.960	0.10	0.01	0.884	0.9
Barcol hardness (%)	0.14	0.01	0.900	0.23	0.01	0.980	1.6
Diffusion Characteristics ($min^{-1/2}$)							
Desorption slope (S_d)	0.0064	0.0004	0.922	0.0181	0.0008	0.972	2.8

A = regression coefficient

e = standard error of estimate for regression coefficient

R^2 = coefficient of determination

* = value not calculated due to weak relationship ($R^2 = 0.766$)

Interestingly, there is also a strong correlation between changes in diffusion characteristics, as measured by S_d, and the square root of immersion time (R^2 = 0.922 to 0.972).

6.1.4.3 Prediction of Diffusion Coefficients

Changes in wet specimen weight (M_t) were plotted as a function of the square root of immersion time (Figure 6.15). It is evident from the absorption isotherms that positive changes in weight occurred in the specimens immersed in deionized water (D112, D25), and sulfuric acid (S25), whereas, specimens immersed in acetic acid (A25), resulted in negative changes in weight. This anomalous behaviour points to extensive material loss and confirms that the weight of material loss of A25 specimens exceeded the weight of acetic acid absorbed. Similar non-Fickian behaviour of liquid transport in SMC materials was suggested by Loos and Springer (1980). These results show that the method developed by Shen and Springer (1976) cannot be used to determine diffusion coefficients for FFW specimens exposed to extreme acidic environments.

Diffusion properties were determined, however, using the method developed by Shen and Springer (1976) for virgin and postcured specimens immersed in deionized water (Table 6.7). A least-squares regression analyses was used to determine the linear slopes (S_a) from the absorption isotherms (Appendix IV-13). A comparison of the absorption slopes show that the rate of water absorption for the postcured specimens (0.44 weeks$^{-1/2}$) was approximately two-thirds the rate determined for virgin specimens (0.70 weeks$^{-1/2}$). This shows that postcuring decreases the rate of water absorption.

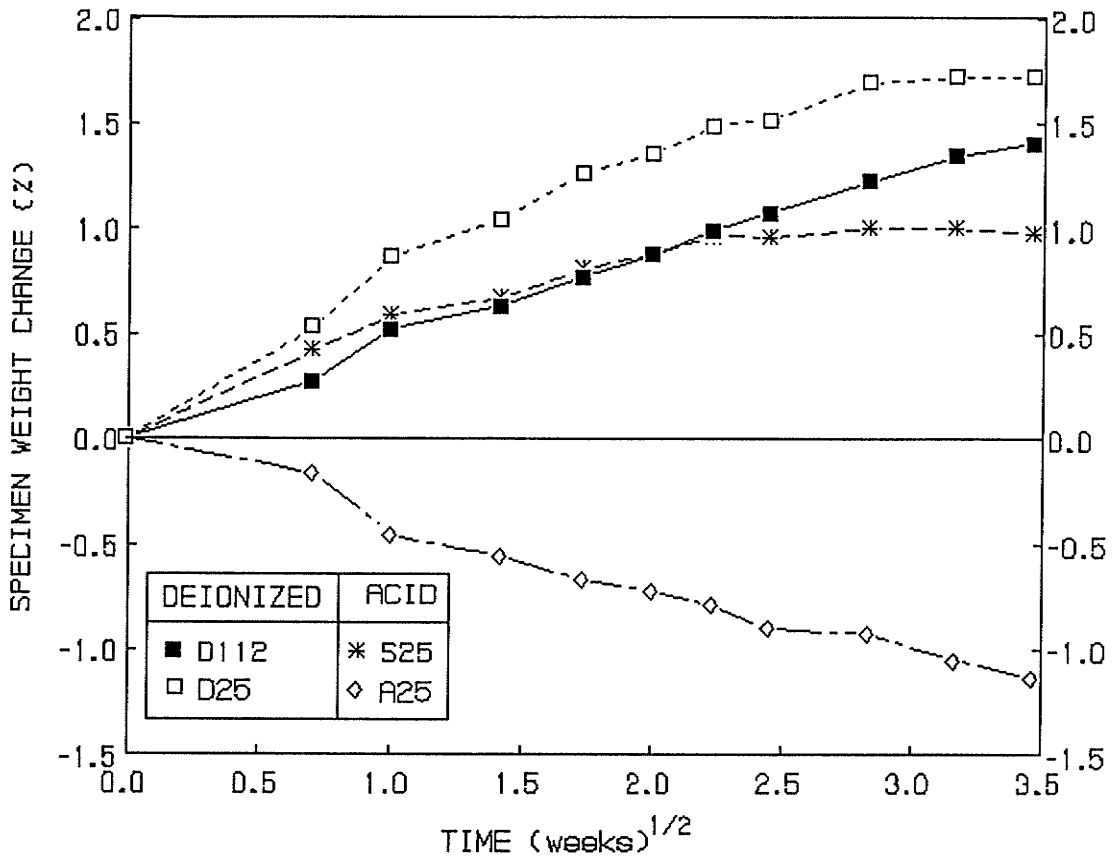

Figure 6.15 Changes in specimen weight (M_t) as a function of the square root of immersion time: AC Experiment

Table 6.7 Diffusion Properties of Virgin (D25) and Postcured (D112) FFW Specimens in Deionized Water

Specimen Type	Absorption Slope (S_a) ($weeks^{-1/2}$)	Diffusion Coefficient (D_e) ($mm^2.sec^{-1}$)	Maximum Weight Gain (M_e) (%)
D112	0.44	1.5×10^{-6}	1.88
D25	0.70	5.0×10^{-6}	1.97

The diffusion coefficients for D112 and D25 specimens were determined to be 1.5×10^{-6} and 5.0×10^{-6} mm^2/sec (see Appendix IV-14,IV-15). The lower D_e value for the postcured specimens suggests a more compact intramolecular network. The diffusivity of D112 specimens were similar to earlier results obtained in the PS study for larger FFW specimens that were postcured at 112°C for 36 hours prior to immersion in deionized water at 45°C. For example, D_e and M_e values of 1.4×10^{-6} mm^2/sec and 1.61% were reported (Section 3.3.4), respectively. It was interesting to note that the maximum percent weight gain value for D112 specimens (1.88%) is similar to that for D25 specimens (1.97%). These results suggest that the total weight gain for virgin and postcured specimens would be similar after long-term exposure in water.

Acid-Degraded (D_d) Diffusion Coefficients

The depth of penetration results were used in combination with the model parameters in Equation [44] (Section 5.2.2) to predict the diffusion coefficients in the degraded layer of the sulfuric and acetic acid specimens. Since the molar density (ρ_B), pH of the solution (C_{AB}), and the experimental relationship between (h vs. t) is known,

the intrinsic diffusion coefficients in the degraded layer (D_d) can be estimated for each acid condition.

The values of D_d of the sulfuric and acetic acid specimens were calculated to be 5.02×10^{-6} and 5.07×10^{-5} $mm^2.sec^{-1}$, respectively (see Appendix IV-16, IV-17). It is interesting to note that the intrinsic diffusion coefficient in the degraded layer of the sulfuric acid (S25) specimens was similar in magnitude to that estimated for the deionized water (D25) specimens (Table 6.7). These observations are also in agreement with the desorption slope results (see Figure 6.14).

The diffusion coefficient in the degraded layer of acetic acid specimens was predicted to be 10 times greater than that of the sulfuric acid specimens. The increase in the diffusion coefficient for acetic acid was shown to be associated with the leaching of calcium carbonate particles and the formation of tensile stress cracks.

One possible explanation for the lower diffusion coefficients associated with sulfuric acid specimens is the formation of an aluminum-calcium-sulfate gel. For example, it is possible that a crystalline hydrate ($CaSO_4$-H_2O) or gibbsite ($AL_2(OH)_6$) could form in the FFW matrix. An amorphous hydrate gel containing a significant concentration of calcium has been observed in high alumina cement pastes using transmission electron microscopic (TEM) techniques (Poon and Groves, 1988).

6.2 SUMMARY AND CONCLUSIONS

1. Photomicrographs show that acid deterioration starts primarily from the non-lined surface and moves inward with time. Strong correlations indicate that changes in depth of penetration (h) are proportional to the square root of immersion time for each acid condition. These results verify the proposed Acid

Deterioration model.

2. Other deterioration test results such as material weight lost, calcium carbonate dissolution, losses in wet mechanical properties, and desorption properties show that the rate of deterioration was a function of the square root of immersion time. These results support conclusion (1) and show that the deterioration of virgin FFW specimens exposed to extreme acidic (sulfuric and acetic) environments is a diffusion controlled process.

3. Deterioration of virgin FFW specimens in acetic acid was 1.6 to 3.9 times greater then in the sulfuric acid environment. Based on these findings, sulfuric acid is recommended as a standard laboratory test medium for FRP composites where deterioration due to sulfur oxidizing bacteria is anticipated.

4. The diffusion coefficients for deionized (postcured and virgin) water specimens, based on the method developed by Shen & Springer (1976) is estimated to be 1.5×10^{-6} and 5.0×10^{-6} $mm^2.sec^{-1}$, respectively. This method, however, could not be used to quantify diffusion coefficients of FFW composites exposed to extreme acid environments due to excessive material weight loss.

5. The intrinsic diffusion coefficients in the degraded layer of sulfuric and acetic acid specimens, based on the AD model, were estimated to be 5.02×10^{-6} and 5.07×10^{-5} $mm^2.sec^{-1}$, respectively.

6. The intrinsic diffusion coefficient in the degraded layer of the sulfuric acid (S25) specimens was similar in magnitude to that estimated for the deionized water (D25) specimens. These observations are in agreement with the desorption slope results.

CHAPTER 7

OVERALL SUMMARY AND CONCLUSIONS

A detailed list of conclusions for each phase of the research has been included at the end of each sub-chapter in Sections 3.6, 4.4, 5.3 and 6.2. This chapter summarizes the primary objectives of the research and lists the most significant conclusions.

7.1 PRELIMINARY SCREENING STUDY (PHASE 1)

One of the primary objectives of the Preliminary Screening study (Phase 1) was to identify the laboratory environment which had the most deleterious effect on postcured FFW composites. To accomplish this objective, the effects of various laboratory aqueous environments and temperature (25° and 45°C) conditions on the deterioration behaviour of postcured FFW specimens and metal (steel and galvanized) coupons were evaluated. The selection of the laboratory environments was based on a literature review and a field investigation.

Based on the preliminary screening study it was found that:

1. A laboratory operating temperature of 45°C was effective in accelerating the deterioration behaviour of large postcured FFW specimens exposed to various aqueous environments.
2. Acidic environments (pH 3.5 to 4.5) were identified, based on physical, chemical and visual indicators, to have the most deleterious effect on the postcured FFW specimens. The MIC soil environment was identified as the most corrosive environment for the steel coupons.

3. Material weight loss measurements could not be used to accurately quantify deterioration of FFW specimens in MIC soil due to soil/bacteria embedment. New analytical methods are required to quantify more accurately the deterioration of FFW composites exposed to such environments.

7.2 DEVELOPMENT OF NEW TEST METHODS (PHASE 2)

The latter phases of the experimental research program focused on the extreme acidic environments identified in Phase 1. This involved the development of new test methods for smaller FFW specimens. Test methods to measure soluble material weight loss, changes in diffusion characteristics (FDSE method) and depth of penetration (HC and FD) were developed. A Postcure Acid experiment was conducted to demonstrate the usefulness of these methods in determining the effects of postcuring on the deterioration of small FFW specimens exposed to low pH sulfuric acid environments. Based on the results of the PA experiment, it was found that:

1. The new test methods were effective in quantifying the deterioration of smaller FFW specimens in an extreme sulfuric acid environment.
2. Postcuring did not effect the deterioration of small FFW specimens at low pH (pH 2.2-2.3) conditions.
3. The primary chemical reaction associated with low pH sulfuric acid deterioration was the dissolution of calcium carbonate.

7.3 DEVELOPMENT OF AN ACID DETERIORATION MODEL (PHASE 3)

The third objective of the experimental research program was to develop a practical mathematical model to quantify the rate of deterioration of virgin FFW

composites exposed to extreme acidic environments. One particular application involves predicting the rate of deterioration of structures exposed to sewage (e.g. septic tanks). The Acid Deterioration model is based on an unreacted core model that was originally developed for gas-solid reactions. In this work the model was adapted to a physical-chemical process involving a solid-liquid interface. The moving diffusion problem is solved using a pseudo-steady state approximation. The Acid Deterioration model that was developed:

1. Claims that the rate of deterioration, as measured by the depth of penetration, is proportional to the square root of time.
2. Allows one to predict the intrinsic diffusion coefficient in the degraded layer of the acid-attacked virgin FFW composites.

7.4 MODEL VERIFICATION STUDY (PHASE 4)

The Acid Comparison (AC) experiment was designed to verify the proposed Acid Deterioration (AD) model by determining the rate of deterioration of virgin FFW specimens exposed to sulfuric and acetic acid. The experiment was conducted under accelerated conditions of increased temperature (45°C) and low pH (2.2-2.5). Deterioration was measured in terms of changes in depth of penetration, loss in soluble material weight, the extent of chemical dissolution, loss in wet mechanical properties, and changes in diffusion characteristics for each acid environment.

A secondary objective was to predict, in combination with the experimental data, the intrinsic diffusion coefficients in the acid-degraded layer (D_d) of these specimens. Based on the results of the AC experiment it was found that:

1. Strong correlations confirm that the rate of deterioration as measured by depth

of penetration and other deterioration test parameters were proportional to the square root of immersion time. These results verify the claims made in the Acid Deterioration model, and indicate that the acid deterioration is a diffusion controlled process.

3. Deterioration of virgin FFW specimens in acetic acid was 1.6 to 3.9 times greater then in the sulfuric acid environment. Based on these findings, sulfuric acid is recommended as a standard laboratory test medium for FRP composites where deterioration due to sulfur oxidizing bacteria is anticipated.

4. The intrinsic diffusion coefficients in the degraded layer of sulfuric and acetic acid specimens, based on the AD model, were estimated to be 5.02×10^{-6} and 5.07×10^{-5} $mm^2.sec^{-1}$, respectively.

CHAPTER 8

FUTURE RESEARCH AND RECOMMENDATIONS

This research has shown that acidic environments have the most deleterious effect on FFW composites. It was found that the primary chemical reaction in acidic environments (inorganic and organic) was the dissolution of calcium carbonate. These results are significant to engineers who are responsible for the design of filled FRP structures exposed to acidic (sewage) environments. ATH was found to be significantly less soluble than calcium carbonate in the environments which suggests that it would be a better filler material. Further research is required using filled FRP composite consisting of polyester resin (36%), ATH filler (32%) and reinforced with glass fibres (32%).

Sulfuric acid has been identified in the literature review as one type of acid generated in sewage environments. The results demonstrated that acetic acid is more deleterious than sulfuric acid to the FFW composite under similar low pH (2.22 to 2.23) and elevated temperature (45°C) conditions. One possible explanation is that acetic acid, diffuses at a faster rate into the cross-linked (organic) polyester matrix resulting in the formation of a swollen solid and gel layer. Further research using neat (unfilled) polyester resin specimens and the same analytical methods developed in Chapter 4.0 is required to verify this hypothesis. The feasibility of using fluorescent microscopy techniques to monitor the depth of penetration (FD method) of an advancing boundary through the thickness of the unfilled (pigmented) specimens should also be investigated.

Based on the findings of this study, sulfuric acid or hydrochloric acid is recommended as a standard laboratory test medium for filled FRP composites, where

deterioration due to sulfur oxidizing bacteria is anticipated. Further research is required to measure the rates of deterioration of FFW composites exposed to simulated anaerobic sewage environments using acetic acid (pH 5.0) as a laboratory test medium. One possible explanation for the lower diffusion coefficients associated with sulfuric acid is the formation of an aluminum-calcium-sulfate gel. Further research is required to verify the formation of this gel in sulfuric acid exposed FFW specimens.

The Acid Deterioration (AD) model was developed based on the pseudo-steady state assumption of the moving diffusion problem. The AD model should be validated for different pH concentrations using sulfuric and hydrochloric acid as immersion mediums and SMC-R25 (41.8% $CaCO_3$ and no ATH filler) as a test material. It is possible that this model is a mathematical representation of a general law of nature which could apply universally to other materials such as concrete. This is significant because the long-term durability of various materials in acidic environments could then be compared by quantifying the intrinsic diffusion coefficients (D_d) under similar standard accelerated test procedures.

In Canada, prefabricated septic tanks are manufactured in accordance with CSA Standard CAN3-B66-M85 to meet initial strength requirements. There is no standard procedure to evaluate, in a stressed or unstressed state, the accelerated deterioration behaviour of septic tank materials exposed to acidic (sewage) environments. It is hoped that this work will facilitate the establishment of a standard accelerated test procedure to measure the rate of deterioration for such materials.

CHAPTER 9

REFERENCES

AASHTO, (1988). "Soil Thermoplastic Pipe Interaction Systems", Standard Specifications for Highway Bridges, Section 18 American Association of State Highway and Transportation Officials.

ACPA, (1980). Concrete Pipe Handbook American Concrete Pipe Association, Limited Edition. pp. 6-14.

AISI, (1984). Handbook of Steel Drainage & Highway Construction Products, First Canadian Edition, American Iron and Steel Institute, p. 99.

ASCE, (1990). Sulfide in Wastewater Collection and Treatment Systems, Manual No. 69, American Society of Civil Engineers, New York.

ASTM C 581, (1983). "Standard Practice for Determining Chemical Resistance of Thermosetting Resins used in Glass Fibre Reinforced Structures Intended for Liquid Service", Annual Book of ASTM Standard, Vol. 08.01.

ASTM D 638, (1987). "Standard Test Method for Tensile Properties of Plastics", Annual Book of ASTM Standard, Vol. 08.01, Section 8.

ASTM D 790, (1986). "Standard Test Methods for Flexural Properties of Unreinforced and Reinforced Plastics and Electrical Insulating Materials", Annual Book of ASTM Standard, Vol. 08.01.

ASTM D 792, (1986). "Standard Test Method for Specific Gravity (Relative Density) and Density of Plastics by Displacement", Vol. 8.01, Section 8.

ASTM D 2583, (1987). "Standard Test Method for Indentation Hardness of rigid Plastics by means of a Barcol Impresser", Annual Book of ASTM Standard, Vol. 08.02.

ASTM D 2688, (1983). "Standard Test Methods for Corrosivity of Water in the Absence of Heat Transfer (Weight Loss Methods)".

ASTM D 3839, (1979). "Standard Practice for Underground Installation of flexible Reinforced Thermosetting Resin Pipe and Reinforced Plastic Mortar Pipe".

Atkinson A., Nickerson A.K., (1984). The diffusion of Ions through water-saturated Cement. Journal of Material Science, pp. 3068-3078.

Attiogbe, E.K., and Rizkalla, S.H. (1988). "Response of Concrete to Sulfuric Acid

Attack", ACI Materials Journal, Vol. 85, No. 6, pp.481-488.

Balik, C.M., Fornes, R.E., Gilbert, R.D. and Williams, R.S., (1989). Effects of Acid Deposition on Painted Wood Surfaces (North Carolina State University), Raleigh, NC, USA Report EPA/600-3-89/066, 48 pp. (Gov. Rep. Announce Index 89122).

Belsham, (1989). Evaluation of Methods to Quantify Degradation of a Filled GRP Composite in Corrosive Culvert Environments, B.Sc. Undergraduate Thesis, University of Manitoba.

Benefield, L.D, Judkins, J.F. and Weand, B.L., (1982). Process Chemistry for Water and Wastewater Treatment, Prentice-Hall Inc., pp. 121-125, p. 257.

Betz Inc., (1980). BETZ Handbook of Industrial Water Conditions, 3rd Edition, p. 174.

Biczok, I., (1967). Concrete Corrosion and Concrete Protection, 4th Edition, Chemical Publishing Co., New York, p. 243, 271.

Blaga, A., (1979). "Glass Fibre Reinforced Polyester Composites", Canada Building Digest, Division of Building Research, National Research Council, pp. 205(1)-205(4).

Blaga, A., (1982). "Reinforced Thermosetting Plastic Pipe", Canadian Building Digest, Division of Building Research, National Research Council, pp. 227(2)-227(3).

Bonniau, P. and Bunsell, A.R., (1984). "A comparative study of Water Absorption Theories Applied to Glass Epoxy Composites", Vol. 2, edited by G.S. Springer, Technomic Publishing Co., pp. 209-228.

Booth, G.H., Cooper, A.W. and Tiller, A.K., (1967). Br. Corr. J., Vol. 2, p. 116.

Bravenec, L.D., (1983). "Environmental Effects on the Viscoelasticity of Neat and Filled Polymeric Solids", Ph.D. Thesis, University of Delaware.

Butler, G. and Ison, H. (1966). Corrosion and its Prevention in Waters, Reinhold, New York.

Carslaw, H.S. and Jaeger, J.C., (1959). Conduction of Heat in Solids, Oxford University Press.

Carter H.G., (1978). "Fundamental and Operational Glass Transition Temperature of Composite Resins and Adhesives", Advanced Composite Materials-Environmental Effects, ASTM STP 658.

Chian, E.S., Poland, F.G., Chung, K.C. and Harper S.P., (1985). "Leachate Management and Treatment", International Conference New Directions and Research in Waste Treatment and Residuals Management, University of British Columbia, Vancouver, B.C., pp. 14-30.

Ciriscioli, P.R., Woo, I.L., Peterson, D.G., Springer, G.S. and Tang, J.M. (1987). "Accelerated Environmental Testing of Composites", Journal of Composite Materials, Vol. 21, p. 225.

Cheromisinoff, N.P. (1986). Encyclopedia of Fluid Mechanics, Vol. No. 1, Flow Phenomena and Measurement, pp.73-79.

CGSB, (1969). Standard For Process Equipment: Reinforced Polyester, Chemical Resistant, Custom-Contact Molded, Canadian Government Specification Board, Department of Defence Production, Ottawa, Canada.

Connolly, W.J. and Thornton, A.M., (1965). Modern Plastics, 43(2), p. 154.

Coytant, R.W., Barrett, E.E., Simon, R., Campbell, B.E. and Lougher E.H., (1970). "Investigation of the Reactivity of Limestone and Dolomite for Capturing SO_2 from Flue Gas", Battelle Memorial Institute, Columbus, Ohio.

Craigie, L.J., White, M.N. and Svatek, M.J., (1986). "Under Fibreglass Storage Tanks for Motor Fuels Containing High Concentrations of Alcohols, 41st Annual Conference, Reinforced Plastic Composites Institute, The Society of the Plastics Industry, Session 20-A, pp. 1-5.

Crank, J., (1965). The Mathematics of Diffusion, First Edition, Clarendon Press, London, pp. 1-4.

Crank, J., (1975). The Mathematics of Diffusion, Second Edition, Clarendon Press, Oxford, pp. 7, 18, 257, 326.

CRC Press, (1973). Handbook of Chemistry and Physics, 53rd Edition, The Chemical Rubber Company, B-77, edited by Robert W. Weast.

CSA, (1989). Private Communication, J.N. Carnegie., File No. B211-90, CSA Subcommittee on FRP Septic Tanks, Canadian Standards Association, Ontario, Canada.

CSA Standard CAN 3-B66-M85, (1985). Prefabricated Septic Tanks and Sewage Holding Tanks, pp. 1-28.

Cuadrado, R.R., Borrajo J. and Williams, R.J., (1983). On the Curing Kinetics of Unsaturated Polyesters with Styrene, Journal of Applied Polymer Science, Vol. 28, No. 2, p. 480.

Day, R.L., (1981). Reactions Between Methanol and Portland Cement Paste, Cement and Concrete Research, Vol. II., pp. 341-349.

DeIasi, R.J. and Schulte, R.L., (1984). "Moisture Detection in Composites Using Nuclear Reaction Analysis", Composite Materials: Testing and Design (Fifth Conference), ASTM STP 674, S.W. Tsai, Editor, pp. 145-150.

DeIasi, R. and Whiteside, J.B., (1978). "Effect of Moisture on Epoxy Resins and Composites", Advanced Composite Materials-Environmental Effects, ASTM STP 658, pp. 2-20.

Dexter, S.C., (1988). Metals Handbook, Ninth Edition, Volume 13, Corrosion, ASM International; Metals Park, Ohio. p. 43.

Dudgeon, C.D., (1987). "Polyester Resin", Composites: Engineered Materials Handbook, Edited by ASM, International Handbook Committee, Vol. 1. pp. 90, 92.

EPA, (1985). Design Manual for Odor and Corrosion Control in Sanitary Sewage Systems and Treatment Plants, U.S, Environmental Protection Agency, Centre for Environmental Research Information, pp. 16-17.

Feldman, R.F., (1984). "Pore Structure Damage in Blended Cements Caused by Mercury Intrusion", J. American Ceramic Society, Vol. L2, pp. 30-33.

Feldman, R.F., (1987). Diffusion Measurements in Cement Paste by Water Replacement Using Propan-2-0L, Cement and Concrete Research, Vol. 17, pp. 602-612.

Fenner, O.H., (1975). "Chemical and Environmental Properties of Plastics and Elastomers", Handbook of Plastics and Elastomers, C.A. Happer, Editor, McGraw-Hill Book Company, New York, p. 4-4.

FibreGlas Canada, (1987). Private Communication, J.B. Curry: File No. JBC-175-87, JBC-33-90.

FibreGlas Canada, (1988). Private Communication, Al Osborne, Manager of Research Division, Guelph Ontario.

Fonda, A.F. (1989). "The Professional Use of Design Fundamentals for FRP Applications", Materials Performance, Vol. 28, No. 1, p.38.

Fontana, M.G., (1986). Corrosion Engineering, McGraw-Hill, pp. 212-214, 395.

Garychuk, G.W., (1987). "Retrographic Image (PIA) Techniques for Carbonate Rock Porosity Evaluation", M.Sc. Thesis, University of Manitoba, pp. 1-8.

Gaudy, A.F. and Gaudy, E.T., (1988). Elements of Bioenvironmental Engineering, Engineering Press Inc., pp. 184-185.

Gibson, R.F., Mende, E.W. and Osborne, W.E., (1984). "The Influence of Environmental Conditions on the Vibration Characteristics of Chopped-Fibre-Reinforced Composite Materials", Vol. 2, Environmental Effects of Composite Materials, edited by G.S. Springer, pp. 79-94.

Gillat, O. and Broutman, L.J., (1977). "Effect of an External Stress on Moisture

Diffusion and Degradation in Graphite-Reinforced Epoxy Laminates", Advanced Composite Materials, Environmental Effects, ASTM STP 658, pp.61-83.

GISC, (1979). "Reinforced Thermosetting Resin Pipe", Transportation Engineering Journal of ASCE, Proceedings of the American Society of Civil Engineers, Vol. 105, No. TE2, pp. 165-183.

Grayson, M. and Eckroth, D., Ed., (1982). Encyclopedia of Chemical Technology, 3rd ed., Vol. 18, John Wiley & Sons, p.575.

Greenwood, M.E., (1975). "Buried FRP Pipe Performance Through Proper Installation", Plastic Conference November 1975, Managing Corrosion Problems with Plastics, sponsored by AICE, NACE, SPE, SPI and API., pp. 1-18.

Hamilton, W.A., (1985). "Sulphate-Reducing Bacteria and Anaerobic Corrosion", Ann. Rev. Microbiology, pp. 195-217.

Hamilton, W.S. and Maxwell, S., (1986). "Biological and Corrosion Activities of Sulphate Reducing Bacteria Within Material Biofilms", Biologically Induced Corrosion, NACE-8, Editor Stephen C. Dexter, pp. 131-132.

Hahn, H.T., (1987). "Hydrothermal Damage in Graphite 1 Epoxy Laminates", Journal of Engineering Materials and Technology, Vol. 109, pp. 3-11.

Hahn, H.T. and Kim, R.Y., (1978). "Swelling of Composite Materials", Advanced Composite Materials-Environmental Effects, ASTM STP 658, pp. 98-120.

Harvey, J.N., (1987). "An Investigation of Petrographic Image Analysis Techniques" B.Sc. Thesis, University of Manitoba, pp. 1-47.

Haviland, J.E. (1966). "Durability of Corrugated Metal Culverts", Highway Research Records, No. 242, pp. 41-64.

Hindersinn, R.R. and Witschard, Gilbert, (1978). "The Importance of Intumescence and Char in Polymer Fire Retardance", Flame Retardancy of Polymeric Materials, edited by W.C. Kurla and A.J. Papa, Markel Dekker, Inc., pp. 41-42.

Hoff, G.C., (1979). Chemical Polymer and Fibre Additives For Low Maintenance Highways, Noyes Data Corporation, pp. 176-180.

Holmes, M. and Just, D.J (1983). GRP in Structural Engineering, Applied Science Publishing, London and New York, p.42.

Holt, A.R., (1967). "Durability Design Method for Galvanized Steel Pipe in Minnesoda", Corrugated Steel Pipe Institute, Ontario, pp. 1-34.

Hughes, D.C., (1986). Concrete Research, 37 (133), pp. 227-233.

Hughes, D.C., (1987). The Use of Solvent Exchange to Monitor Diffusion Characteristics of Cement Parts containing Silica Fume, Cement and Concrete Research, Vol. 18, pp. 312-324.

Klopher, M., (1981). "The Carbonation of External Concrete and How to Combat it" One-Day Conference on the Repair of Concrete Structures (London, England: Imperial College).

Lavenda, B., (1985). "Brownian Motion", Scientific American, pp. 70-85.

Lawrence, C.D., (1984). "Transport of Oxygen Through Concrete British Ceramics Society Meeting", Imperial College, London, (April 12-13).

Levenspiel, O. (1972). Chemical Reaction Engineering, Second Edition, John Wiley & Sons, Inc., pp.357-374.

Lin, W.M. and Jou, T.W., (1991). "Corrosion of Reinforced Concrete Structures in Taiwan", Material Performance, March, pp. 38-42.

Loos, A.C., Springer, G.S., Sanders, B.A. and Tung R.W. Moisture Absorption of Polyester E Glass Composites, J. Composite Materials, Vol. 14, pp. 142-154.

Luss, D., (1968). "On the Pseudo Steady State Approximation for Gas Solid Reactions", The Canadian Journal of Chemical Engineering, Vol. 46, No. 6, pp. 154-156.

Mc Carville, W.T., (1987). "Filament Winding Resins", Composites: Engineered Materials Handbook, edited by ASM International Handbook Committee, ASM International, Vol. 1, p.135.

McCluskey, J.J. and Doherty, F.W., (1987). "Sheet Moulding Compounds", Composites: Engineered Materials Handbook, edited by ASM International Handbook Committee, ASM International, Vol. 1, p.158.

Miller, R.K., (1984). "Multi-Material Model Moisture Analysis for Steady-State Boundary Conditions", Environmental Effects on Composite Materials, edited by G.S. Springer, pp. 162-169.

Monte, S.J. and Sugerman, G., (1986). "Titanate and Zirconate Coupling Agents", Developments of 1985 - 41st Annual Conference, World of Composites, Focus 86, SPI and the Reinforced Plastics/Composites Institute and Session 26-B, p. 2.

Montgomery, J.M. Inc., (1985). Water Treatment Principles & Design, John Wiley & Sons, p. 414.

Noyce, R.W. and Ritchie, (1979). "Michigan Galvanized Metal Culvert Corrosion Study", Transportation Research Record, pp. 1-6.

Oleszkiewicz, J.A., Marstaller, T. and McCartney, D.M., (1989). "Effect of pH on Sulfide Toxicity to Anaerobic Processes", Environmental Technology Letters, No. 10, pp. 815-822.

Parrot, L.J., (1981). Effect of Drying History upon the Exchange of Pore Water with Methanol and Upon Subsequent Methanol Sorption, Behaviour in Hydrate Alite Paste. Cement and Concrete Research, Vol. II, pp. 651-658.

Parrot, L.J., Patel, R.J., Killoh, D.C. and Jennings H.M., (1984). "Effect of Age from Diffusion in Hydrated Alite Cement", J. American Ceramic Society, Vol. 67 pp. 233-237.

Patenaude, R., (1986). "Microbial Corrosion of Culvert Pipe in Wisconsin", Biologically Induced Corrosion, Proceedings of the International Conference on Biologically Induced Corrosion, NACE-8, Editor Stephen C. Dexter, pp.92-95.

Penn, L.S. (1979). "Physicochemical Characterization of Composites and Quality Control and Raw Materials", Testing and Design (Fifth Conference), ASTM STP 674, S.W. Tsai Editor, p. 528.

Perry, R.H. and Green, D. (1972). Perry's Chemical Engineering, Sixth Edition, McGraw-Hill Book Co. pp.20-11.

Pigford, R.L. and Sliger, G., (1973). "Rate of Diffusion-Controlled Reaction Between a Gas and a Porous Solid Sphere", Ind. Eng. Chem. Des. Dev., Vol. 12, No. 1, pp. 85-91.

Poon, C.S. and Groves, G.W. (1988). "TEM Observations of High Alumina Cement Paste", Journal of Material Science, Wiley, Vol. 7, pp. 243-244.

Poggi-Varalda, H. (1989). Personal Communication, University of Manitoba.

Portland Cement Association, (1987). "Effects of Substances on Concrete and Guide Protective Treatments", Concrete Information, pp. 8-21.

PostGate, J.R., (1984). The Sulphate-Reducing Bacteria, 2nd Edition, Cambridge University Press, Cambridge, p. 208.

Rao, Chanda M. and Balasubramanian, N., (1984). "A Fickian Diffusion Model for Permeable Fibre Polymer Composites", Environmental Effects on Composite Materials, edited by G.S. Springer. pp. 178-187.

Reiber, S., Ferguson, J.F. and Benjamin, M.M., (1988). "An Improved Method for Corrosion-Rate Measurement by Weight Loss", J. AWWA, Vol. 80, No. 11, pp. 41-46.

Reinhart, T.J. and Clements, L.L., (1987). "Introduction to Composites", Composites: Engineered Materials Handbook, edited by ASM International Handbook Committee,

ASM International, Vol. 1. pp.32-33.

Sargent, J.P. and Ashbee, K.G., (1984). "Very Slow Crack Growth During Osmosis in Epoxy and Polyester Resins", J. Appl. Polymer Science, Vol. 29, pp. 809-822.

Seymour, R.B. and Carraher, C.E. Jr., (1981). An Introduction to Polymer Chemistry, Marcel DeKller, New York, ISBN 0-82447-6979-1, p. 363.

Shackelford, J.F., (1988). Introduction to Materials Science for Engineers, Second Edition, Macmillan Publishing Company, pp. 134, 139, 140.

Shen, Chi-Hung and Springer, George S., (1976). "Moisture Absorption and Desorption of Composite Materials", J. Compos. Mater. 10, 2, pp. 2-20.

Shewmon, P.G., (1967). Diffusion in Solids, McGraw-Hill Book Company, p. 5.

Shirrell, C.D., (1978). "Diffusion of Water Vapour in Graphite 1 Epoxy Composites", Advanced Composite Materials- Environmental Effects, ASTM STP 658, pp. 21-42.

Smith, R.E. and Ehrlich, W.A., (1967). Soils of the Lac Du Bonnet Area, Soils Report No. 15, Manitoba Department of Agriculture.

Solem, (1988). Private Communication, Dallavia A.J., Solem, Industries Inc., A subsidiary of J.M. Huber Corporation, Fair Mount, GA 30139.

Soroka and Hzhalc, (1979). Portland Cement Paste and Concrete, MacMillan Press, London, pp. 151-154.

Springer, G.S., (1983). "Effects of Temperature and Moisture on Sheet Moulding Compounds", Journal of Reinforced Plastics and Composites, Technical Publishing Co., Inc., Vol. 2., p. 70.

Springer, G.S., (1984). "Environmental Effects on Epoxy Matrix Composites", Composite Materials: Testing and Design (Fifth Conference), ASTM STP 674, S.W. Tsai, Editor, pp. 291-312.

Springer, G.S., (1984). "Effects of Temperature and Moisture on Sheet Moulding Compounds", Vol. 2, Environmental Effects of Composite Materials, pp. 59-78.

Springer, G.S., (1984). "Model for Predicting the Mechanical Properties of Composites at Elevated Temperatures", Vol. 2, Environmental Effects of Composite Materials, edited by G.S. Springer, pp. 150-161.

Springer, G.S., Sanders, B.A. and Tung, R.W., (1980). "Environmental Effects on Glass Fibre Reinforced Polyester and Vinyl Ester Compounds", J. of Composite Materials, 14, pp. 213-232.

Standard 303C, (1985). Determination of Aluminum by Direct Aspiration into a Nitrous Oxide-Acetylene Flame, 16th Edition, APHA, AWWA, WPCF, p. 162.

Standard Methods for the Examination of Water and Wastewater, (1985; 1989). 16th and 17th Edition, APHA, AWWA, WPCF, Washington D.C.

Starkey, R.L., (1986). Biologically Induced Corrosion, Proceedings of the International Conference on Biologically Induced Corrosion, NACE-8, Editor Stephen C. Dexter, p. 351-352-P3-7.

Tiller, A.K. and Corr, T.M.I. (1986). "A review of the European Research Effort on Microbial Corrosion Between 1950 and 1984",Biologically Induced Corrosion, NACE-8, Editor Stephen C. Dexter, p. 23.

Tsai, S.W., (1979). Composite Materials: Testing and Design (Fifth Conference), ASTM STP 674, American Society for Testing Materials, Ohio, U.S.A., p. 683.

Updegraff, I.H., (1982). "Unsaturated Polyester Resins" in Handbook of Composite Materials, edited by G. Lubin, Van Nostrand Reinhold, pp. 17-37.

Watanabe, M., (1979). "Predictions of Leakage, Life and Deterioration in Water for Fibreglass Reinforced Plastic Vessels, Composite Materials Testing and Design (Fifth Conference), ASTM STP 674, S.W. Tsai, Ed., American Society For Testing and Materials, pp. 324-343.

Watanabe, M., (1979). "Effect of Water Environment on Fatigue Behaviour of Fibreglass Reinforced Plastics", Composite Materials: Testing and Design (Fifth Conference), ASTM STP 674, S.W. Tsai, Ed., American Society For Testing and Materials, pp. 344-367.

Weiz, P.B. and Goodman R.D., (1963). Combustion of Carbonaceous Deposits Within Porous Catalyst Particles, 1 Diffusion Controlled Kinetics, Journal of Catalysts, 2, pp. 397-404.

Weber, W.J., (1972). Physicochemical Processes for Water Quality Control, John Wiley & Sons, pp. 76-77.

Weng, G.J. and Sun, C.T. (1979). "Effects of Fibre Length on Elastic Moduli of Randomly-Oriented Chopped-Fibre Composites", Testing and Design (Fifth Conference), ASTM STP 674, S.W. Tsai, Ed., pp. 291-312.

Whitney, J.M., (1978). "Moisture Diffusion in Fibre Reinforced Composites", Proceedings of the 1978 International Conference on Composite Materials, American Institute of Mining, Metallurgical and Petroleum Engineers, New York, New York.

Whitney, J.M. and Brouning, C.E., (1978). "Some Anomalies Associated with Moisture Diffusion in Epoxy Matrix Composite Materials", Advanced Composite Materials-

Environmental Effect, ASTM STP 658, pp. 43-60.

Whitney, J.M., Daniel, I.M. and Pipes R.B., (1982). Experimental Mechanics of Fibre Reinforced Composite Materials, Prentice Hall Inc. pp. 237-249.

Wild, S., Arabi, M. and Rolands, G.O., (1987). "Relation Between Pore Size Distribution, Permeability, and Cementitious Gel Formatting in Cured Day-Lime Systems", Material Science and Technology, Vol. 3, pp. 1005-1010.

WPCF, (1970). Manual of Practice No. 9, Design and Construction of Sanitary and Storm Sewers, Water Pollution Control Federation, pp. 218-223.

Ye, L.C., (1989). On Fatigue Damage Accumulation and Material Degradation in Composite Materials, Composite Science and Technology, Vol. 36., pp. 339-350.

APPENDIX I

DESCRIPTION OF EXPERIMENTAL FFW COMPONENTS

A. TYPE E-GLASS FILAMENTS

E-glass is a calcium aluminoborosilicate glass with a range of major oxide constituents by weight, presented in Table I-1. Typical tensile strength and Young's modulus (stiffness) of the E-glass fibers under ambient temperature conditions are 3,450 MPa and 72.4 GPa, respectively (Watson, 1987). The specific gravity of annealed bulk E-glass fibers ranges from 2.54 to 2.62 $g.cm^{-3}$ (Miller, 1987). Silane coupling agents are used to enhance the interfacial bond between the glass fiber and polyester resins, thus improving mechanical properties and environmental durability characteristics (Reinhart, 1987).

Table I-1 Ranges for Chemical Composition of E-Glass Fibers

Constituent	Percentage by Weight
Silicon dioxide, SiO_2	52-56
Calcium oxide, CaO	16-25
Aluminum oxide, Al_2O_3	12-16
Boron oxide, B_2O_3	5-10
Magnesium oxide, MgO	0- 5
Sodium oxide, Na_2O_3	0- 2
Potassium oxide, K_2O_3	0- 2
Iron oxide, Fe_2O_3	0- 1
Minor oxides	0- 1

B. RESIN: UNSATURATED POLYESTER RESIN

The raw materials of the cured polyester resin matrix of the FFW specimens consisted of an admixture of orthophthalic resin (60-90%), a cross-linking monomer; styrene (30-50%), and various promoters, inhibitors and thixotropic agents (1-3%). The orthophthalic resin was prepared from polyhyric alcohols and polycarboxylic acids. The exact chemical formulation of the admixture was not available for disclosure. The specific gravity of the polyester resin formulation ranged from 1.1 to 1.3 g.cm^3. Typical rheological/cure properties provided by GWIL Industries are shown in Table I-2.

Table I-2 Typical Rheological/Cure Properties of filled (W1840) chopped strand FRP laminate*

Laminate Property	Measurement
Gel time (min)	20-25
Gel to peak time	40
Peak temp. (°C/°F)	28/82
Barcol hardness:	
2 hrs. after Gel	10-15
24 hrs. after Gel	45-50

* Notes: 1. All properties determined at 21°C

2. Glass/Resin/Filler ratio in percent: 25:45:30

3. Reinforcement: Type E; 3-ply 600gm chop mat

4. Filler: ATH; Resin: W1840; Initiator: 1% MEK

Table I-3 Typical Chemical Analysis: Solem ATH (SB-336)
(Solem, 1988)

Chemical Analysis	Percent by Weight*
Al_2O_3	64.90
SiO_2	0.01
Fe_2O_3	0.01
Na_2O (total)	0.35
Loss of ignition (110°C)	34.50
Free moisture (110°C)	0.20

* Solem Industries: values to be used only as a guide.

Table I-4 Typical Physical Properties: Solem ATH (SB-336)
(Solem, 1988)

Physical Properties	Range of Values
Medium particle diameter (microns)	14-16
Size less than 10 microns (%)	20-30
Bulk density - packed (gm/cm^3)	1.20
Specific gravity	2.42
Oil absorption (ml/100 gm)	23-25
Surface area (m^2/gm)	2-3
Colour reflectance (photo volt 670)	82-87

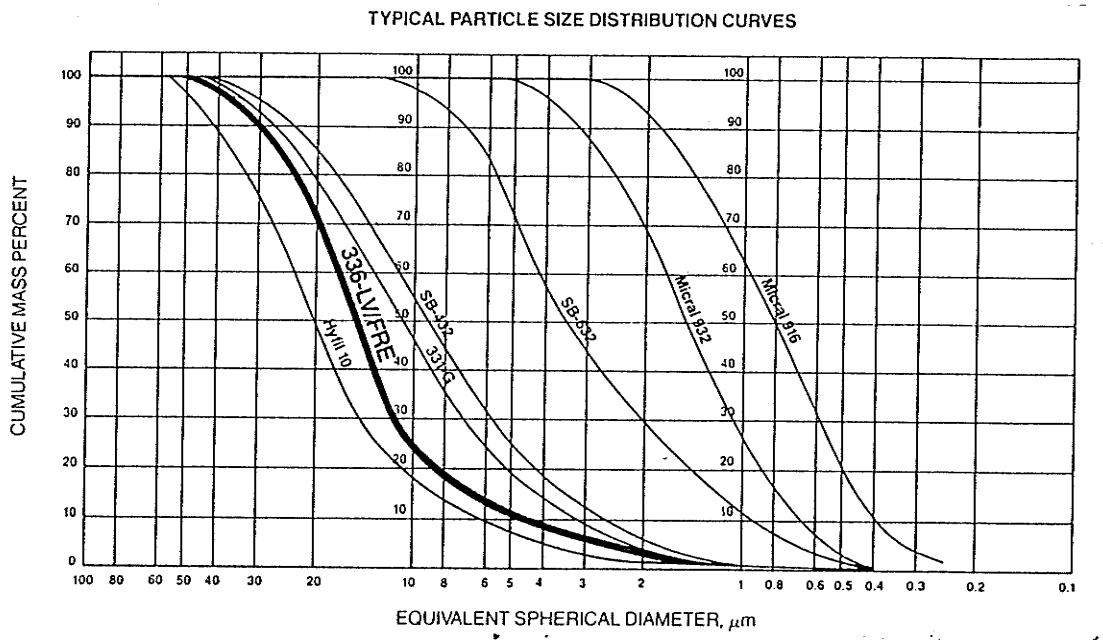

Figure I-1 Typical Solem ATH particle size distribution curves (Solem, 1988)

Table I-5 Results of Solem ATH and Aluminum Hydroxide Acid Dissolution Study: Higher pH (2.09-2.15)

Date	Time Weeks	Solem ATH		Aluminum Hydroxide	
		pH	AL^{+++} $(mg.L)^{-1}$	pH	AL^{+++} $(mg.L)^{-1}$
Jan. 22	0	2.00	0.0	2.00	0.0
Jan. 26	1.0	2.00	39.7	2.00	25.9
Feb. 2	2.0	2.00	65.8	2.00	41.8
Feb. 9	3.0	2.10	84.4	2.00	59.5
Feb. 16	4.0	2.20	98.8	2.15	69.7
Feb. 23	5.0	2.20	101.5	2.15	78.9
March 2	6.0	2.30	114.5	2.20	86.6
March 9	7.0	2.35	129.6	2.20	97.9
March 16	8.0	2.35	137.1	2.20	104.6

Table I-6 Typical Chemical Analysis: Snowhite ($CaCO_3$) (MIA Chemical, Division of FiberGlas, Canada)

Chemical Analysis	Percent by Weight
$CaCo_3$	95.0
SiO_2	2.5
$MgCO_3$	1.3
Silicates (Mg.Ca)	1.2
Fe_2O_3	0.09
$A;_2O_3$	0.03
Moisture	<0.20

Table I-7 Typical Physical Properties: Snowhite ($CaCO_3$) (MIA Chemical, Division of FiberGlas, Canada)

Physical Properties	Range of Values
Percent finer than 325/mesh	99.0
Percent finer than 200/mesh	2.7
Mean particle size (microns)	17
Hardness (Mohr's scale)	3
Linear coefficient of expansion ($°C^{-1}$)	4.3×10^{-6}
Refractive Index	1.6
Bulk density (loose) $gm.L^{-1}$	1.007
pH saturated solution	93

* Meets ASTM D-1199, Type GC, Grade II

C. THEORETICAL ANALYSIS: SATURATION CONCENTRATION OF THE ALUMINUM ION (A^{+++}_{sat}) IN AN ACIDIC SOLUTION (pH = 2.12)

$$AL(OH)_{3(s)} \rightleftarrows AL^{+3}_{(aq)} + 3OH^{-}_{(aq)} \qquad \text{[C-1]}$$

$$K_{sp} = [C_{sat}] * [OH^{-}]^3 \qquad \text{[C-2]}$$

$$K_w = [H^+]\ [OH^-] \qquad \text{[C-3]}$$

Therefore, substituting [C-3] into [C-2]

$$K_{sp} = [C_{sat}] * [K_w / H^+]^3 \qquad \text{[C-4]}$$

But $[C_{sat}] = 10^{-32.34}$ (Benefield, 1982) and $[H^+] = 10^{-2.12}$. Rearranging [C-4] and substituting:

$$\begin{aligned} [C_{sat}] &= 10^{-32.34} * [10^{-2.12} / 10^{-14}]3 \\ &= 10^{3.3} M \\ [AL(OH_3)]_{sat} &= (10^{3.3})\ (1{,}000)\ (78) = 1.6 \times 10^8\ mg/l \end{aligned} \qquad \text{[C-5]}$$

Since

$$\frac{AL}{AL(OH)_3} = 27/78 = 0.346$$

Therefore the theoretical aluminum ion concentration at pH = 2.12 is:

$$[AL^{++}]_{sat} = (0.346) * (16 \times 10^8) = 5.5 \times 10^7\ mg.l^{-1} \qquad \text{[C-6]}$$

APPENDIX II

PRELIMINARY SCREENING (PS) STUDY

A. DESCRIPTION OF HARDING SOIL

Table II-1 Harding Soil: Redox Potential (E_h)

Depth of Soil	Description of Soil	Redox Potential mv
2	moss	+155
20	SCL*	-55
40	SCL	-145

* SCL: Sandy Clay Texture

Table II-2 Harding Soil: Moisture Content (%), Wet and Dry Bulk Density

Sample No.	Culvert Location	Moisture Content (%)	Wet Density ($g.cm^{-3}$)	Dry Density ($g.cm^{-3}$)
# 89	inlet	46	1.45	0.78
# 207	centre	30	1.66	1.17
Average		38	1.56	0.98

Table II-3 Harding Soil: Sieve Analysis

Sieve Size (mm)	Percentage (%)
1. Sand(s)*	
1.0 - 2.0	3
0.5 - 1.0	7
0.25 - 0.50	17
0.10 - 0.25	15
0.05 - 0.10	6
2. Silt (Si)	27
0.05	
	25
3. Clay (C)	
0.002	

* Total sand - 48%

Table II-4 Harding Soil: Chemical Determination of Water Extract

Cations	Concentration meq.L^{-1}	Anions	Concentration meq.L^{-1}
Calcium	20.8	Bicarbonate	5.2
Magnesium	23.6	Chlorides	5.2
Sodium	35.6	Sulfates	80.0
Total Cations	80.0	Total Anions	90.4

B. DESCRIPTION OF LARGE POSTCURED FFW SPECIMENS

Table II-5 Physical Dimensions of Large Postured Specimens (Control)

Spec. No.	Spec. Desc.	Weight (grams)	Avg. Volume (cm^3)	Avg. Thickness (mm)
1	D35CF1	279.62	152.1	4.85
2	D35CF2	279.35	150.1	5.07
3	D35CT1	286.06	155.3	5.15
4	D35CT2	274.09	150.0	4.96
5	1A35CF1	282.77	152.7	4.84
6	1A35CF2	276.82	149.8	4.93
7	1A35CT1	275.44	150.8	4.98
8	1A35CT2	278.33	151.2	5.08
9	B25CF1	282.88	152.2	4.71
10	B25CF2	281.21	151.5	4.93
11	B25CT1	278.35	151.7	5.06
12	B25CT2	270.78	146.3	4.98
13	2A35CF1	274.43	150.0	5.28
14	2A35CF2	277.34	150.5	5.15
15	2A35CT1	276.71	150.4	5.02
16	2A35CT2	272.98	149.0	5.06
17	3A35CF1	286.37	155.4	5.28
18	3A35CF2	269.87	145.0	5.18
19	3A35CT1	271.27	148.0	5.14
20	3A35CT2	280.50	155.0	5.28
21	B35CF1	280.54	151.2	4.80
22	B35CF2	283.54	155.6	5.21
23	B35CT1	276.34	149.4	5.09
24	B35CT2	279.73	151.6	5.27
25	S35CF1	275.57	148.5	4.60
26	S35CF2	283.61	153.6	4.95
27	S35CT1	278.42	151.6	4.83
28	S35CT2	274.81	149.6	4.80
29	R35CT2	276.81	150.2	5.20
30	R35CF2	272.88	148.2	5.03
31	R35CT1	280.90	153.4	5.07
32	R35CT2	279.96	153.5	49.9
33	D25CF1	283.05	153.4	4.77
34	D25CF2	269.63	145.9	4.77
35	D25CT1	284.79	155.2	5.05
36	D25CT2	281.98	153.4	4.93
	Average	278.19 (4.43)*	151.1 (2.6)	5.00 (0.17)

* Brackets: standard deviation.

Table II-6 Percent Weight Loss Versus Time for Large Virgin Specimens Postured at 112°C

Postcure Time (hours)	Average Weight Loss (%)
2	0.09
3	0.14
5	0.17
12	0.23
16	0.26
20	0.27
24	0.28
30	0.30
36	0.31
42	0.32
50	0.33
60	0.34

C. LABORATORY PROCEDURE: PS STUDY

Table II-7 Preparation of Laboratory Solutions

Immersion Medium	Procedures
1. Deionized water (D25,D45)	The deionized water was prepared using a Millepore 3 barrel cartridge (pre-filter carbon, deionization system. (Initial pH = 6.75).
2. Alkaline (B25, B45)	An alkaline buffered solution was prepared by adding 29 mls of 0.65 M H_3BO_3 to 100 ml of 0.1 N na OH. (Initial buffered pH = 9.22).
3. Sulfuric Acid (1A45)	A 0.000316 N H_2SO_4 solution was prepared by adding 15.8 ml of 0.02 N stock solution to 1 L of deionized water. (Initial pH = 3.50).
4. Hydrochloric Acid (2A45)	A0.000316 N HCL solution was prepared by adding 15.8 ml of 0.02 N stock solution to 1 L of deionized water. (Initial pH = 3.49).
5. Acetic Acid (3A45)	A 0.0057 N CH_3COOH solution was prepared by adding 57 ml of 0.1 N stock solution to 1 L of deionized water. (Initial pH = 3.49).
6. Magnesium Sulfate (S45)	92.4 grams of $MgSO_4$ $7H_2$) was added to 18 L deionized water. (Initial SO_4 = 1,870 mg/L).
7. Biological (R45)	Deionized water was added to soil to produce a paste with a water content of 45.3%

D. LABORATORY PROCEDURE: SHEN AND SPRINGER (1976) METHOD

1. Prepare a specimen in the form of a thin plate.
2. Measure the weight gain of a dry specimen ($M_i = 0$) as a function of time and plot M versus $t^{1/2}$ beyond the point at which the slope of the curve is not constant ($t > t_L$).
3. Assume a value for De.
4. Select a time t, so that $t = t_1 < t_L$ where t_L is the time where the isotherm plot is concave and no longer linear.
5. Calculate $G = 1 - \exp [-7.3(t^*)^{0.75}$ where $t^* = De.t/s^2$.
6. Calculate M_e for t, where $M_e = M/G$ (use M measured at t_1).
7. Select a time t_2 so that $t = t_2 > t_1$.
8. Calculate G as before (step 5).
9. Calculate M_e as before for t_2 (step 6).
10. If the values of M_e in step 6 and 9 are equal then stop the procedure.

E. EXAMPLE CALCULATION: D_e AND M_e FOR LARGE FFW SPECIMENS IMMERSED IN DEIONIZED WATER AT 45°C.

Step 1 Determine the equation of the initial straight line portion of the 45°C plot.

X (week ½)	Y (%)	
0.00	0.00	$Y = 0.316\ X$
0.23	0.84	
0.69	2.24	
1.30	3.87	
1.39	4.69	

$\therefore$ coefficient of deformation $R^2 = 0.995$

$\therefore$ $S_a = 0.316\ \text{weeks}^{-1/2}$

Step 2 Assume $D_e = 1.4 \times 10^{-6}\ \text{mm}^2/\text{sec}$.

Step 3 $t = 2.25$ weeks $t_1 < t_L$ where $t_L \approx 14$ weeks ($M \approx 1.3$)

$M = [(2.25)\ (0.316)]^{1/2} = 0.5\%$

Step 4 Calculate G_t

(i) $t^* = D_x \cdot t/s^2$ $\quad s = 2 \cdot h = 2 \cdot 5.00\ \text{mm} \approx 10\ \text{mm}$

$t^* = (1.4 \times 10^{-6})\ (2.25)\ (7)\ (24)\ (3600)/10^2 = 0.019$ sec.

(ii) $G = 1 - \exp\ (-7.3 \cdot (t^*)^{0.75}) = 0.31$

Step 5 Determine M_m (where M_m is the maximum moisture content)

$M_m = M / G = 0.05/0.31 = 1.61\%$

$(1.3/1.47) = 0.8 > 0.6$ o.k.

Step 6 Pick $t_2 > t_1$ $\quad t_2 = 18.5$ weeks

$M_2 = (0.316)\ (18.5)^{1/2} = 1.35\%$

$t^* = 0.157$ $\qquad G = 0.84$

therefore $M_m = 1.35/0.84 = 1.61\%$

which equals the value found in step 6.

Therefore the initial estimate of D_e was correct, (i.e. $D_e = 1.4 \times 10^{-6}\ \text{mm}^2/\text{second}$).

F. FFW DETERIORATION EXPERIMENT: TEST RESULTS

Table II-8 Average Weekly pH During 27 Week Test Period FFW Deterioration Experiment

Time Weeks	TYPE OF ENVIRONMENT								
	D25	D45	B25	B45	1A45	2A45	3A45	S45	R45
1	9.29	7.68	9.23	9.26	6.08	6.20	4.97	7.85	7.80
2	8.15	7.60	9.21	9.25	5.76	5.72	3.66	7.78	-
3	7.90	7.35	9.28	9.30	5.66	5.58	3.64	7.55	7.60
4	8.18	7.33	9.28	9.23	4.49	4.35	3.75	7.55	7.60
5	7.63	7.38	9.25	9.25	4.21	4.84	3.82	7.49	7.90
6	8.10	7.38	9.25	9.27	4.01	4.93	3.82	7.55	7.60
7	8.05	7.10	9.25	9.20	3.63	4.17	3.75	7.35	-
8	7.85	7.25	9.30	9.25	3.72	4.37	3.74	7.50	7.65
9	7.95	7.25	9.32	9.28	3.67	4.26	3.81	7.60	-
10	8.15	7.15	9.32	9.25	3.67	4.18	3.87	8.25	7.50
11	7.90	7.60	9.32	9.30	3.67	4.06	3.88	7.75	-
12	8.25	7.45	9.35	9.32	3.58	3.93	3.77	7.70	7.60
13	7.95	7.50	9.32	9.22	3.43	3.74	3.79	7.65	-
14	-	-	-	-	3.79	4.78	3.79	-	-
15	8.10	7.55	9.30	9.21	3.92	4.89	3.84	7.85	7.52
16	-	-	-	-	3.63	3.77	3.84	-	-
17	7.85	7.50	9.30	9.25	3.37	3.40	3.80	8.06	7.72
18	7.48	7.55	9.25	9.20	3.64	4.04	3.80	7.50	-
19	-	-	-	-	-	-	-	-	-
20	7.80	7.65	9.30	9.20	3.80	4.50	3.85	7.60	7.78
21	7.48	8.20	9.30	9.20	3.63	4.08	3.88	7.65	-
22	7.50	7.65	9.25	9.18	3.53	3.70	3.87	7.55	7.52
23	7.63	7.68	9.28	9.15	3.65	4.00	3.87	7.55	-
24	7.68	7.72	9.28	9.20	3.38	3.36	3.79	7.55	7.8
25	7.60	7.70	9.25	9.20	3.70	3.90	3.80	7.60	-
26	7.70	7.68	9.25	9.15	3.68	3.71	3.80	7.65	7.8
27	7.65	7.70	9.30	9.25	3.70	3.80	3.80	7.70	-
Average	7.91	7.52	9.28	9.23	3.96	4.32	3.85	7.66	7.63
SD	0.38	0.23	0.03	0.04	0.73	0.70	0.24	0.19	0.28

Table II-8 Change in Material Weight Loss (W_m) for Deionized Water (D25, D45) and Sodium Hydroxide (B25, B45) Environments

Immersion Time (weeks)	Low Temperature (25°C)		High Temperature (45°C)	
	D25 (%)	B25 (%)	D45 (%)	B45 (%)
5	0.00	0.00	0.02	0.01
14	0.05	0.03	0.33	0.27
27	0.21	0.16	0.45	0.45

Table II-9 Change in Wm as a Function of Immersion Time for Acidic (1A45, 2A45, 3A45) Environments

Immersion Time (weeks)	Acidic (45°C) Environment		
	Sulfuric 1A45 (%)	Hydrochloric 2A45 (%)	Acetic 3A45 (%)
5	0.25	0.26	0.76
14	0.69	0.68	1.39
27	0.91	0.86	1.98

Table II-10 Average Weekly Calcium Ion Concentration During 27 Week Test Period

Time Weeks	Ca^{++} Concentration (mgL^{-1} as $CaCO_3$)					
	D25	D45	S45	1A45	2A45	3A45
1	22	50	10	146	156	780
2	30	74	80	227	230	916
3	50	112	160	395	389	1,155
4	56	132	188	540	532	1,320
5	66	152	226	607	622	1,513
6	67	142	221	630	648	1,560
7	80	174	200	667	703	1,710
8	84	174	200	667	703	1,710
9	86	178	264	713	725	1,800
10	84	170	262	750	760	1,860
11	96	174	260	770	827	1,957
12	100	182	270	790	840	2,007
13	104	184	274	838	900	2,100
14	-	-	-	887	920	2,350
15	112	182	266	-	-	-
16	-	-	-	800	850	2,200
17	112	182	266	-	-	-
18	112	182	284	810	860	2,450
19	-	-	-	-	-	-
20	116	176	275	810	880	2,400
21	122	180	280	850	900	2,400
22	114	176	280	830	910	2,450
23	120	176	270	840	930	2,350
24	120	180	304	890	910	2,580
25	122	178	288	860	980	2,500
26	122	180	292	880	950	2,650
27	122	180	284	920	1,000	2,550

Table II-11 Change in Specimen Volume (%) as a Function of Immersion Time for Low Temperature (D24, B25) Environments

Environment Type	Immersion Time (Weeks)		
	5	14	27
D25	-0.13	-0.13	0.19
B25	0.33	0.47	0.55
Average	0.10	0.17	0.37

Table II-12 Change in Specimen Volume (%) as a Function of Immersion Time for High Temperature (D45, B45, 1A45, 2A45, 3A45, S45) Environments

Environment Type	Immersion Time (Weeks)		
	5	14	27
D45	0.86	1.53	1.59
B45	0.91	1.40	1.53
1A45	0.98	1.13	1.65
2A45	1.00	1.27	1.67
3A45	0.96	1.32	1.66
S45	0.70	1.53	1.26
Average	0.90	1.36	1.56

Table II-13 Change in Dry Flexural Properties, Strength (S_f) and Modulus (E_f) During 52-Week Test Period

Environment Type / Test Parameter	Immersion Time (Weeks)							
	5		14		27		52	
	S_f MPa	E_f GPa	S_f MPa	E_f GPa	S_f MPa	E_f GPa	S_f MPa	E_f GPa
Low Temp.								
D25	275.3 (23.1)	17.1 (1.4)	294.6 (20.3)	17.8 (1.9)	267.7 (17.5)	17.1 (1.7)	270.8 (19.8)	17.5 (1.8)
B25	281.5 (17.5)	16.1 (1.5)	293.3 (17.4)	16.1 (1.5)	251.9 (19.0)	16.9 (1.3)	255.1 (18.7)	15.4 (0.8)
Average	278.4 (4.4)	16.6 (0.7)	294.0 (0.9)	17.0 (1.2)	259.8 (11.2)	17.0 (0.1)	263.0 (11.1)	16.5 (1.5)
D45	252.5 (17.8)	15.5 (1.5)	246.3 (18.9)	15.1 (2.1)	213.9 (14.4)	14.9 (1.1)	238.3 (13.2)	17.8 (0.7)
B45	249.1 (17.4)	15.6 (1.3)	262.2 (2.84)	16.2 (1.7)	235.3 (29.2)	15.5 (2.5)	250.1 (12.9)	17.1 (0.8)
1A45	255.3 (21.0)	15.1 (1.2)	267.7 (19.0)	16.4 (1.4)	224.9 (13.2)	15.2 (1.0)	229.4 (8.9)	16.8 (1.22)
2A45	243.6 (16.2)	15.2 (1.3)	276.7 (15.9)	16.9 (1.5)	206.3 (23.0)	14.4 (2.1)	239.1 (14.2)	17.2 (2.2)
3A45	240.1 (16.3)	15.0 (1.0)	256.7 (13.2)	15.5 (1.2)	214.6 (18.7)	15.4 (2.4)	198.9 (23.4)	16.3 (2.0)
S45	256.0 (22.8)	16.6 (2.0)	262.2 (17.9)	16.8 (1.5)	222.9 (13.1)	16.6 (1.5)	229.4 (19.9)	16.9 (1.6)
R45	251.2 (20.2)	16.2 (1.5)	278.1 (14.1)	17.9 (1.7)	237.4 (26.0)	16.2 (1.7)	234.2 (27.5)	16.3 (1.9)
Average	249.7 (5.9)	15.6 (0.6)	264.3 (11.2)	16.4 (0.9)	222.2 (11.5)	15.5 (0.7)	231.3 (16.0)	16.9 (0.5)

Standard deviations in brackets.

Table II-14 Change in Dry Tensile Properties, Strength (S_t) and Modulus (E_t) During 52-Week Test Period

Environment Type / Test Parameter	Immersion Time (Weeks)							
	5		14		27		52	
	S_t MPa	E_t GPa	S_t MPa	E_t GPa	S_t MPa	E_t GPa	S_t MPa	E_t GPa
Low Temp.								
D25	22.0 (4.1)	12.9 (1.5)	22.6 (3.2)	10.2 (1.7)	21.8 (1.7)	12.0 (1.5)	19.9 (3.1)	14.1 (6.6)
B25	25.2 (4.3)	12.1 (1.3)	25.1 (1.7)	11.7 (1.7)	22.4 (3.3)	11.2 (2.2)	20.7 (1.8)	11.2 (0.5)
Average	23.6 (2.3)	12.5 (0.6)	23.9 (1.8)	11.0 (1.1)	22.1 (0.4)	11.6 (0.6)	20.3 (0.6)	12.7 (2.1)
High Temp.								
D45	21.9 (1.6)	10.1 (1.2)	23.5 (1.9)	9.6 (1.2)	19.9 (2.8)	9.3 (1.5)	23.4 (3.1)	11.1 (0.8)
B45	20.1 (0.5)	9.5 (1.3)	17.7 (2.0)	8.8 (0.8)	24.3 (2.4)	10.3 (1.0)	24.3 (1.8)	11.2 (0.2)
1A45	22.4 (3.0)	1.06 (0.8)	19.8 (3.0)	9.7 (1.2)	23.4 (1.8)	9.8 (1.2)	18.5 (1.1)	12.2 (3.8)
2A45	23.5 (2.1)	11.8 (1.2)	23.7 (1.9)	9.5 (1.2)	21.7 (3.9)	10.2 (1.7)	19.1 (3.4)	11.6 (2.0)
3A45	18.7 (3.0)	11.0 (1.1)	20.7 (3.5)	8.6 (1.2)	22.4 (1.9)	9.7 (1.2)	23.4 (2.1)	9.3 (0.6)
S45	20.4 (2.3)	9.7 (0.8)	22.5 (2.8)	11.3 (1.7)	22.1 (2.6)	11.4 (3.0)	18.4 (5.0)	10.9 (1.6)
R45	22.0 (2.1)	9.5 (1.1)	23.1 (4.8)	9.5 (0.8)	23.4 (1.0)	10.9 (1.1)	15.1 (7.1)	11.0 (0.5)
Average	21.3 (1.6)	10.3 (0.9)	21.6 (2.2)	9.6 (0.9)	22.5 (1.4)	10.2 (0.7)	20.3 (3.4)	11.0 (0.9)

Standard deviation in brackets

Table II-15 Change in Dry Barcol Hardness (Interior Surface) During 52-Week Test Period

Environment Type	Immersion Time (Weeks)							
	5		14		27		52	
Low Temp.								
D25	59.1	(3.0)	59.5	(5.4)	60.4	(1.3)	60.6	(1.5)
B25	56.2	(6.0)	59.1	(5.2)	60.5	(3.2)	62.4	(3.8)
Average	57.7	(2.1)	59.3	(0.3)	60.5	(0.1)	61.5	(1.3)
D45	54.2	(7.4)	58.4	(2.7)	60.3	(2.5)	62.8	(2.0)
B45	57.4	(3.2)	59.9	(5.2)	61.6	(2.0)	62.8	(1.0)
1A45	59.0	(1.3)	60.0	(2.2)	56.1	(5.1)	58.0	(2.8)
2A45	57.7	(2.7)	57.2	(8.6)	54.0	(7.3)	58.8	(3.7)
3A45	57.1	(4.4)	52.4	(9.2)	50.6	(5.6)	56.2	(3.5)
S45	56.6	(2.8)	58.1	(6.8)	57.3	(4.4)	61.0	(1.8)
R45	60.8	(2.4)	61.1	(3.6)	60.4	(3.3)	60.8	(4.3)
Average	57.5	(2.0)	58.2	(2.9)	57.2	(4.0)	60.1	(2.5)

Standard deviation in brackets

Table II-16 Student t-Test Analysis: Dry Flexural Properties

Environment Comparison	Degrees of Freedom	Flexural Strength t	Flexural Modulus t	95% Confidence t (+/-)
D45 vs D25	22	-8.250	-3.532	1.717
B45 vs B25	21	-1.672*	-1.772	1.721
3A45 vs 2A45	18	0.870*	1.048*	1.734
3A45 vs 1A45	19	-1.491*	0.183*	1.729
2A45 vs 1A45	21	-2.412	-1.332*	1.721
S45 vs R45	22	-1.779	-0.624*	1.717

* Satisfies hypothesis that mean (dry) flexural properties are equal.

Table II-17 Student t-Test Analysis: Dry Tensile Properties

Environment Comparison	Degrees of Freedom	Tensile Strength t	Tensile Modulus t	95% Confidence t (+/-)
D45 vs D25	14	1.679*	3.714	1.761
B45 vs B25	14	-1.350*	1.040*	1.761
3A45 vs 2A45	12	0.409*	0.660*	1.761
3A45 vs 1A45	12	-1.045*	-0.105*	1.782
S45 vs R45	14	1.246*	-0.432*	

* Satisfies hypothesis that mean (dry) tensile properties are equal.

Table II-18 Wet Mechanical Properties of Postured Specimens After 52 Weeks Immersion

Environment Type	Flexural		Tensile		Barcol Hardness
	S_f MPa	E_f GPa	S_t MPa	E_t GPa	H units
Low Temp.					
1. D25	212.3 (23.7)	13.2 (0.9)	13.5 (4.8)	9.0 (0.3)	55.0 (1.0)
2. B25	22.94 (10.1)	14.5 (1.2)	15.6 (0.3)	6.2 (0.6)	58.8 (1.5)
Average	220.9 (12.1)	13.9 (0.9)	14.6 (1.5)	7.6 (2.0)	56.9 (2.7)
High Temp.					
1. D45	168.4 (19.9)	12.6 (1.2)	12.8 (1.6)	4.8 (0.6)	49.4 (4.8)
2. B45	176.9 (13.3)	11.8 (1.0)	10.6 (0.5)	4.8 (0.4)	52.4 (0.8)
3. 1A45	162.3 (12.4)	13.0 (0.9)	13.0 (0.6)	5.3 (0.1)	48.6 (1.7)
4. 2A45	159.8 (16.4)	12.2 (1.5)	9.5 (1.2)	5.4 (1.1)	47.8 (3.3)
5. 3A45	156.2 (17.6)	12.0 (0.7)	11.0 (1.4)	5.2 (1.6)	40.8 (5.2)
6. S45	167.1 (15.0)	13.1 (1.8)	12.0 (0.4)	4.7 (0.4)	49.2 (1.5)
7. R45	172.0 (11.2)	13.3 (0.9)	12.3 (1.4)	6.1 (0.1)	49.8 (2.3)
Average	166.1 (7.2)	12.6 (0.6)	11.6 (1.3)	5.2 (0.5)	48.3 (3.6)

Standard deviation in brackets

Table II-19 Average Weekly pH During 27-Week Test Period: Metal Corrosion Experiment

Time Weeks	Deionized Water				NaOH (Buffered)				Sulfuric Acid				MIC Soil	
	DS25	DS45	DG25	DG45	BS25	BS45	BG25	BG45	AS25	AS45	AG25	AG45	RS45	RG45
1	6.73	7.08	7.34	7.58	9.15	9.14	9.14	9.15	4.80	4.53	5.63	5.59	-	-
2	7.18	8.02	8.53	7.90	9.15	9.10	9.10	9.09	4.59	4.30	5.56	5.42	7.73	7.73
3	7.27	8.04	8.16	8.06	9.16	9.15	9.15	9.14	4.53	4.05	5.45	5.17	-	-
4	7.24	7.80	8.97	7.93	9.18	9.15	9.17	9.13	4.21	3.97	4.52	4.65	7.80	7.80
5	7.10	7.74	8.66	7.89	9.19	9.15	91.6	9.15	4.07	3.86	4.13	4.28	-	-
6	7.40	7.65	8.80	7.60	9.18	9.15	9.14	9.15	4.13	3.91	4.50	4.62	7.55	7.55
7	7.59	8.05	8.28	7.43	9.15	9.15	9.15	9.14	3.90	3.80	4.15	4.30	-	-
8	7.90	8.17	8.52	7.48	9.17	9.15	9.14	9.14	4.00	3.80	4.58	4.54	7.85	7.85
9	7.54	8.17	8.78	7.35	9.22	9.18	9.17	9.20	4.00	3.81	4.39	4.60	-	-
10	7.63	7.85	8.68	7.78	9.28	9.28	9.26	9.28	4.02	3.85	4.80	4.90	7.85	7.85
11	7.57	8.10	8.67	8.03	9.23	9.21	9.21	9.21	3.96	3.80	4.47	4.53	-	-
12	7.46	8.22	8.67	7.82	9.24	9.24	9.23	9.23	4.28	3.81	4.28	4.44	7.45	7.45
13	7.38	8.19	8.73	8.11	9.25	9.24	9.21	9.23	4.11	3.78	4.11	4.43	-	-

- continued -

Time Weeks	Deionized Water				NaOH (Buffered)				Sulfuric Acid				MIC Soil	
	DS25	DS45	DG25	DG45	BS25	BS45	BG25	BG45	AS25	AS45	AG25	AG45	RS45	RG45
14	7.28	8.09	8.33	7.63	9.23	9.22	9.19	9.23	4.96	3.66	4.96	4.49	-	-
15	7.59	8.38	8.07	7.80	9.21	9.20	9.19	9.20	3.86	3.71	4.45	4.27	-	-
16	7.78	7.83	8.54	7.83	9.24	9.23	9.22	9.23	4.05	3.87	4.77	4.61	-	-
17	7.83	7.85	8.68	7.85	9.24	9.18	9.21	9.19	3.85	3.69	4.07	4.07	-	-
18	7.25	8.10	8.55	8.10	9.22	9.20	9.20	9.20	3.86	3.68	4.04	3.98	-	-
19	-	-	-	-	-	-	-	-	3.79	3.66	3.87	3.85	-	-
20	8.10	8.45	8.45	8.45	9.20	9.23	9.20	9.23	3.77	3.66	3.89	3.84	7.10	7.10
21	8.15	8.05	7.92	7.79	9.20	9.23	9.20	9.25	3.78	3.66	3.96	3.85	-	-
22	7.55	7.80	7.60	8.50	9.20	9.20	9.20	9.20	3.75	3.64	3.86	3.75	7.25	7.25
23	8.19	8.23	8.10	8.62	9.18	9.18	9.16	9.19	3.74	3.65	3.81	3.71	-	-
24	7.95	8.35	8.00	8.65	9.20	9.22	9.20	9.22	3.71	3.60	3.79	3.65	7.80	7.80
25	8.50	7.70	8.30	8.00	9.15	9.18	9.16	9.18	3.70	3.61	3.80	3.65	-	-
26	8.30	8.30	8.55	8.55	9.15	9.18	9.12	9.18	3.73	3.73	3.75	3.67	-	-
27	7.98	7.98	8.00	8.00	9.30	9.30	9.30	9.30	3.70	3.61	3.70	3.64	7.90	7.90
Average	7.63	8.00	8.38	7.96	9.20	9.19	9.18	9.19	4.03	3.80	4.34	4.31	7.63	7.63
SD	0.42	0.29	0.39	0.35	0.04	0.05	0.04	0.05	0.34	0.21	0.56	0.55	0.28	0.28

Table II-20 Total Percent Weight Loss as a Function of Immersion Time

Environment Type	Immersion Time (weeks)			
	2	5	14	27
Deionized Water				
DS25	0.45	0.72	2.91	7.09
DS45	0.90	1.56	5.43	13.53
DG25	-	1.26	3.75	4.91
DG45	-	3.02	5.46	11.86
NaOH				
BS25	0.00	0.00	0.01	0.02
BS45	-	0.00	0.02	0.00
BG25	-	0.11	0.06	0.01
BG45	-	0.05	0.05	0.07
Sulfuric Acid				
AS25	0.50	0.88	3.25	9.41
AS45	0.76	1.40	5.57	15.56
AG25	-	0.85	3.62	7.59
AG45	-	1.30	4.20	9.27
MIC Soil				
RS45	1.43	4.32	12.15	21.13
RG45	-	4.17	4.29	4.58

APPENDIX III

DEVELOPMENT OF NEW TEST METHODS

APPENDIX III

A. POSTCURE EXPERIMENT: SMALL FFW SPECIMENS (133.5 mm x 38.0 mm x 4.80 mm)

Table III-1 Percent Weight Loss Versus Time for Small FFW Specimens Postured at 112°C

Posture Time (hrs)	Average Weight Loss (%)
2	0.15
5	0.22
18	0.30
24	0.34
30	0.37
36	0.37

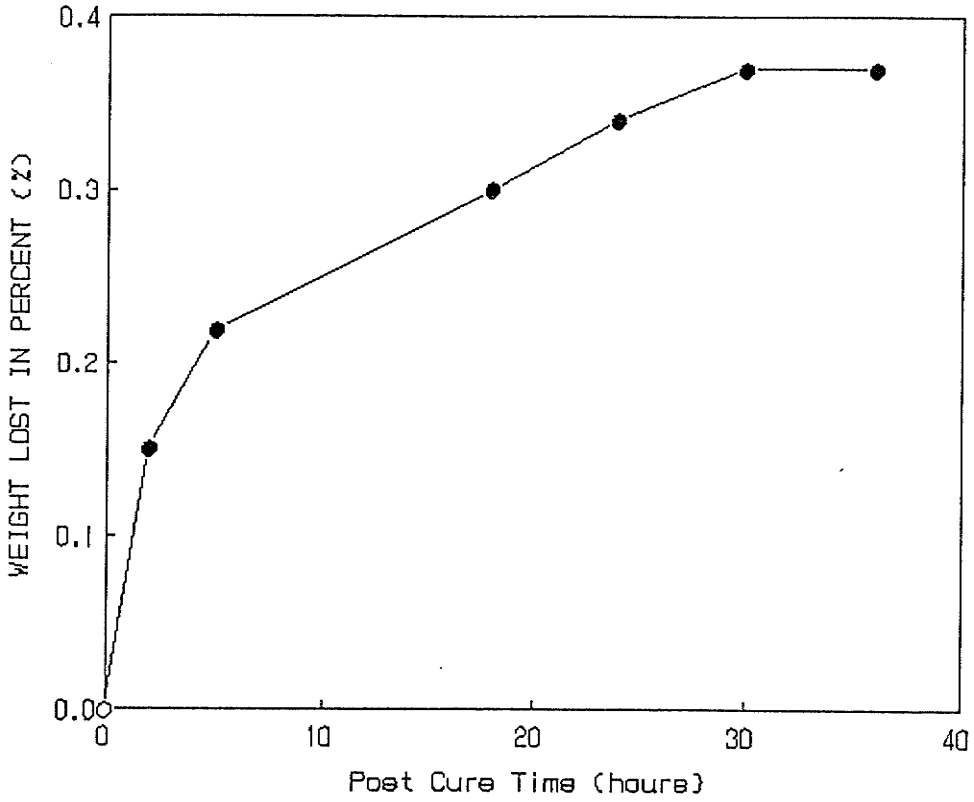

Figure III-1 Percent weight loss for small virgin FFW specimens (112°C)

B. SOLVENT ABSORPTION (SA) EXPERIMENT

The preliminary SA experiment was conducted to characterize the absorption properties of methanol and 2-propanol at 45°C and to evaluate the effect of each solvent on FFW material properties.

Materials and Procedures

Four specimens with nominal dimensions of 133.5 mm x 38.0 mm x 4.80 mm were cut using a diamond blade saw from the same FFW test pipe used in earlier studies. One postcured specimen (112°C at 36 hrs) and one virgin specimen were immersed in methanol. A second set of (2) specimens were immersed in 2-propanol. The densities of methanol and 2-propanol used in the SA tests were 0.7914 and 0.7855 $g.cm^{-3}$, respectively.

Two closed plastic containers (reactors) containing one litre of each alcohol were placed in a temperature-controlled environmental chamber at 45°C. The specimens were immersed in the heated alcohol solutions and were removed periodically and weighed on a Mettler analytical balance.

Results and Discussion

The solvent absorption isotherms for methanol and 2-propanol are shown in Figure III-2. Methanol diffused through the FWW specimens at a rate 10 times faster than 2-propanol. The initial slope of the absorption isotherm was less for postcured specimens than virgin specimens but was similar after 64 hours. The virgin specimens

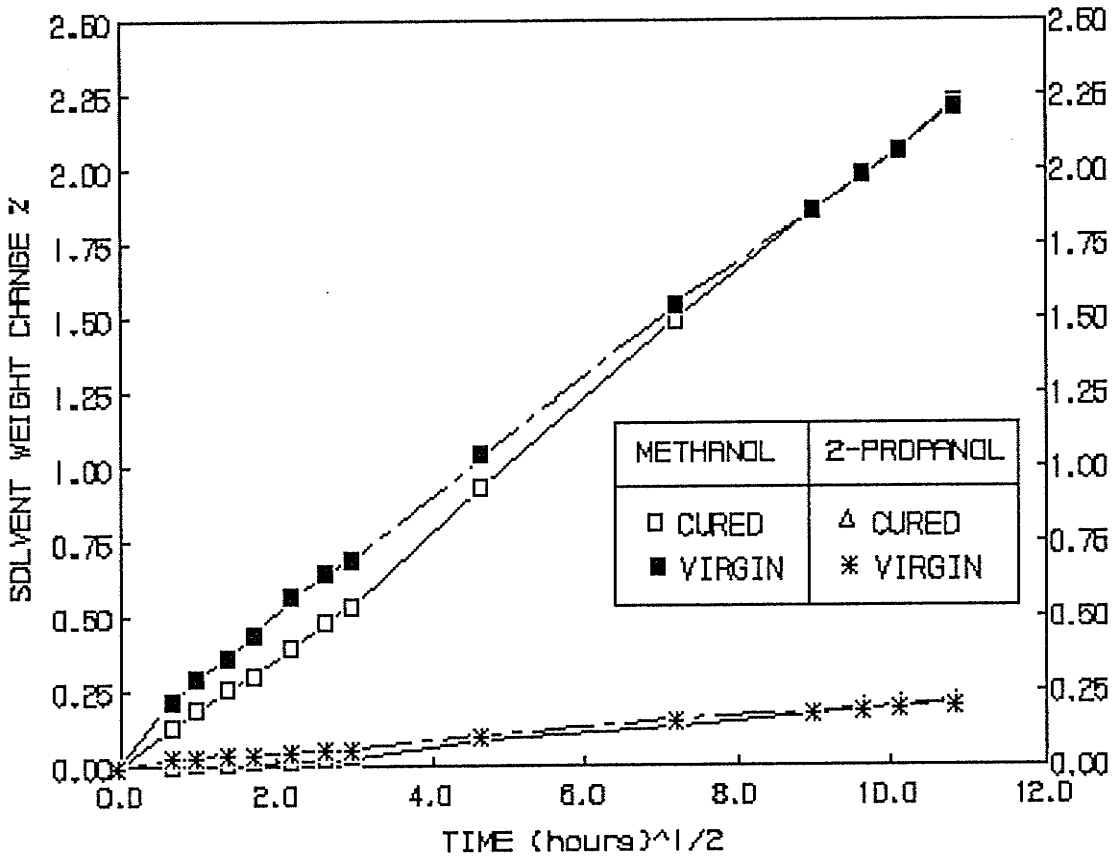

Figure III-2 Solvent absorption: methanol and 2-propanol at 45°

immersed in methanol for a period of 5 days were extremely soft and had deteriorated to the point where the specimen could be fractured by simply bending the specimen by hand. The postcured specimen immersed in methanol was whiter in appearance (see Figure III-3) which suggests a solvent-structure interaction and debonding at the interface between the glass fibres and the resin-filler matrix.

Problems were encountered during the weighing of the methanol saturated specimens. The weights of these specimens were continuously decreasing which made it difficult to obtain reliable and consistent measurements. This was attributed to rapid evaporation losses. These problems were not observed during the weighing of wet 2-propanol specimens. FFW specimens exposed to 2-propanol at 45°C were less influenced by material deterioration and weighing problems which suggest that 2-propanol is a more suitable solvent exchange medium than methanol.

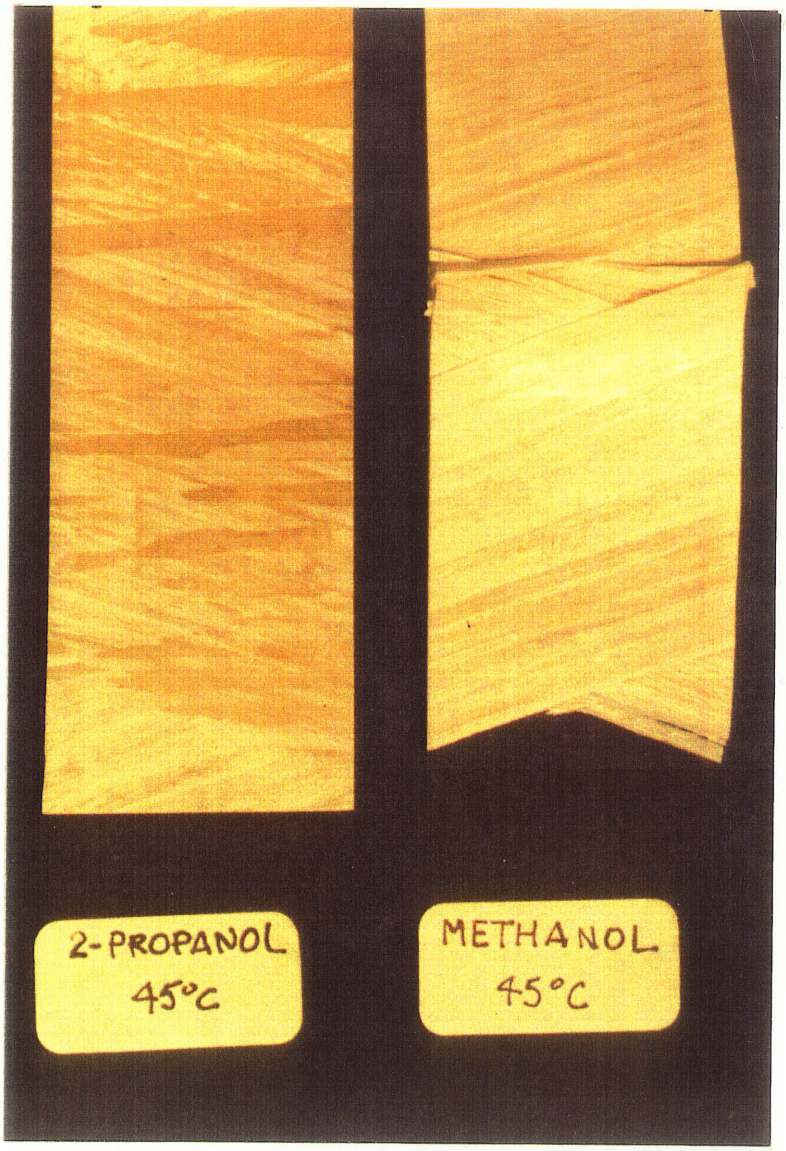

Figure III-3 Postcured FFW specimens immersed in 2-propanol and methanol at 45°C

C. FDSE PRELIMINARY EXPERIMENT

Preliminary FDSE tests were conducted to evaluate and compare the desorption behaviour characteristics of wet (45°C) virgin FFW specimens. These specimens were immersed in fluorescent greenish-yellow dye solutions of methanol and 2-propanol. Properties of this dye are presented in Table III-2.

Materials and Procedure

Two virgin specimens with nominal dimensions of 133.5 mm x 38.0 mm x 4.80 mm were immersed for 4 weeks in deionized water at 45°C. Prior to conducting the FDSE tests, 4 grams of fluorescent yellow G dye were dissolved in two plastic containers, each containing 1 L of methanol and 2-propanol. The containers were closed to prevent evaporation and placed overnight in a temperature controlled chamber at 45°C.

Following a four week (45°C) immersion period, the virgin specimens were removed and the excess surface moisture was wiped off with a cloth towel. The wet specimens were weighed, and immediately re-immersed in (45°C) solutions of methanol and 2-propanol. The FDSE tests were conducted at the same temperature as the deionized water in order to minimize temperature effects. Specimens were removed periodically from each alcohol and weight measurements were taken at different exchange times. A decrease in specimen weight indicated that the FDSE test was still incomplete and that the alcohol was still exchanging with the water in the laminate layer. The FDSE test was assumed to be complete when no further changes in specimen weight or a weight gain was observed.

Table III-2 Properties of Fluorescent-Yellow G Dye[1]

Description	Properties
Chemical Name	1 H-Benz[de] isoquinoline-1, 3 (2H)-dione 2-butyl-6-(butylamino)
Chemical Family	Quinoline dye
Colorant	Fluorescent Greenish-Yellow
Appearance	Yellow Solid
Solubility	(grams/L of solvent at 25°C) Xylene 15 2-Propanol 15 Methanol 12 Methyl Ethyl Ketone 95
Melting Point	125-126°C
Absorbance range	320-400 nm

1 Manufactured by Morton Chemical Company, Chicago, Illinois 60606 and distributed by Adrox Ltd. of St. Catharines, Ontario.

Results and Discussion

Changes in specimen weight, expressed as a percentage, were plotted as a function of the square root of exchange time and are shown in Figure III-4. The 2-propanol FDSE isotherm was well defined in comparison to the methanol FDSE isotherm. The exchange of methanol and water was complete in 5 minutes compared to an exchange time of 60 hours using 2-propanol. A characteristic linear isotherm plot for methanol was not obtained which was attributed to either high exchange rates or solvent-structure interactions. It was, however, possible to characterize the initial slope of the 2-propanol FDSE isotherm. This slope was linear for more than 60 percent of the total change in specimen weight which suggested the desorption characteristics followed Fickian counter-diffusion behaviour.

The results of the preliminary experimental investigation indicate that 2-propanol is a more suitable solvent exchange medium than methanol.

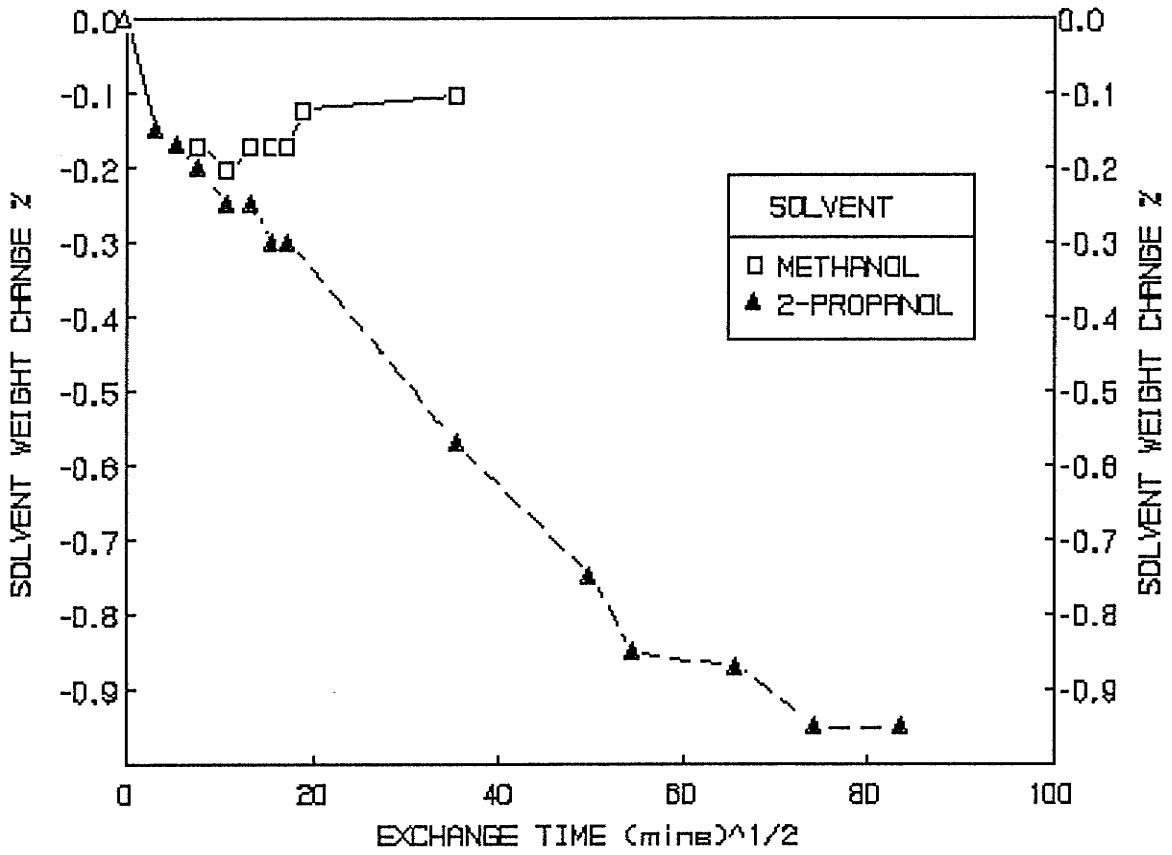

Figure III-4 FDSE (45°C) isotherm for wet FFW virgin specimens immersed in methanol and 2-propanol

D. POSTCURE ACID EXPERIMENT: TEST RESULTS

Table III-3 Specimen Weight Change (%): PA Experiment

Time (weeks)	Posture Condition			
	S55-18	S55-36	S112-18	S112-36
2	0.73 (0.11)	0.69 (0.07)	0.42 (0.10)	0.34 (0.04)
4	0.81 (0.09)	0.81 (0.05)	0.57 (0.10)	0.44 (0.05)
6	0.86 (0.10)	0.87 (0.07)	0.68 (0.12)	0.57 (0.06)
8	0.86 (0.11)	0.88 (0.10)	0.73 (0.15)	0.61 (0.07)
10	0.82 (0.10)	0.84 (0.09)	0.75 (0.15)	0.66 (0.10)
12	0.79 (0.12)	0.79 (0.10)	0.77 (0.18)	0.69 (0.11)

Table III-4 Calcium Concentration in Leachate as $CaCO_3$ ($mg.L^{-1}$): PA Experiment

Time (weeks)	Posture Condition			
	S55-18	S55-36	S112-18	S112-36
0.5	2.70	2.50	2.40	2.90
1.0	4.00	3.50	3.50	3.90
1.5	5.00	4.60	4.50	5.10
2.0	5.80	5.50	5.30	5.80
3.0	7.10	6.30	6.70	7.20
4.0	8.00	7.40	7.40	8.20
5.0	9.20	8.40	8.40	9.00
6.0	10.00	9.20	9.20	9.40
7.0	10.20	9.70	9.20	10.00
8.0	10.80	10.00	9.80	10.60
9.0	11.20	10.50	10.20	11.20
10.0	11.40	11.00	10.50	11.80
11.0	12.00	11.40	11.00	12.10
12.0	12.20	11.40	11.20	12.40

E. THEORETICAL CALCULATIONS: FORMATION OF A CALCIUM SULFITE PRECIPITATE

1. Determine the equilibrium Ca^{2+} concentration for a saturated calcium sulfate solution after the addition of 2.0×10^{-2} M H_2SO_4 to maintain a pH of 2.33.

(*i*)

$$H_2SO_4 \rightleftharpoons H^+ + HSO_4^- \quad large(Ka_1) \quad \ldots\ldots \quad E\text{-}1$$

$$HSO_4^- \rightleftharpoons H^+ + SO_4^{2-} \quad Ka_2 \quad \ldots\ldots\ldots\ldots \quad E\text{-}2$$

Assume $Ka_2 = 1.3 \times 10^{-2}$ at 45°C

$$Ka_2 = \frac{[H^+]\,[SO_4^{2-}]}{[HSO_4^-]} \quad \ldots\ldots\ldots\ldots\ldots\ldots \quad E\text{-}3$$

$$\therefore\ 1.3\ x\ 10^{-2} = \frac{[H^+]\,[SO_4^{2-}]}{[HSO_4^-]}$$

$$\therefore\ 1.3\ x\ 10^{-2} = \frac{[10^{-2.2}]\,[SO_4^{2-}]}{[HSO_4^-]}$$

but the molarity of sulfate added (c) is equal to $[HSO_4^-] + [SO_4^{2-}]$

$$\therefore\ [HSO_4^-] = C - [SO_4^{2-}]$$

$$\therefore\ 1.3\ x\ 10^{-2} = \frac{[10^{-2.2}]\,[SO_4^{2-}]}{C - [SO_4^{2-}]} \quad \ldots\ldots\ldots\ldots\ldots\ldots \quad E\text{-}4$$

(iii) the maximum amount of concentrated acid (1N H_2SO_4) added during the 12-week test was 119 ml in a 3 L volume.

$$\therefore\ C = \frac{(0.5)\ (0.119)}{3L} = 2.0\ x\ 10^{-2}\ moles/L$$

$$1.3\ x\ 10^{-2} = \frac{[10^{-2.2}]\ [SO_4^{-2}]}{[2.0\ x\ 10^{-2}] - [SO_4^{2-}]}$$

$$1.3\ x\ 10^{-2} = \frac{6.31\ x\ 10^{-3}\ [SO_4^{2-}]}{[2.0\ x\ 10^{-2}] - [SO_4^{2-}}$$

$$2.6\ x\ 10^{-4} - 1.3\ x\ 10^{-2}\ [SO_4^{2-}] = 6.31\ x\ 10^{-2}\ [SO_4^{2-}]$$

$$2.6\ x\ 10^{-4} = 1.363\ x\ 10^{-2}\ [SO_4^{2-}]$$

$$1.91\ x\ 10^{-2}M = [so_4^{2-}]$$

$$\therefore\ [Ca^{2+}] = 1.91\ x\ 10^{-2}M\ x\ (1{,}000)\ (40.08)$$

$$= 766\ mg/L$$

$$\therefore\ Ca^{2+}\ as\ mg/L\ CaCO_3 = \left[766\ x\ \frac{100}{40}\right]$$

$$= 1915\ mg/L$$

Since the maximum concentration of Ca^{2+} as $CaCO_3$ in the sulfuric acid reactor was 1,250 mg/L $\ll$ 1,915 mg/L, no $CaSO_4$ precipitation is likely to occur.

APPENDIX IV

ACID COMPARISON EXPERIMENT

APPENDIX IV

A. DEPTH OF PENETRATION: TEST RESULTS

Table IV-1 Depth of Penetration (HC Method): AC Experiment

Environment Type	Immersion Time (weeks)			
	2	4	8	12
	h (um)	h (um)	h (um)	h (um)
D112	95	165	166	231
D25	108	155	206	188
S25	112	154	192	278
A25	353	481	695	862

Table IV-2 Depth of Penetration (FD Method): AC Experiment

Environment Type	Immersion Time (weeks)			
	2	4	8	12
	h (um)	h (um)	h (um)	h (um)
D112	105	107	144	143
D25	96	127	197	185
S25	121	175	246	261
A25	312	509	700	1,054

B. OTHER DETERIORATION TEST RESULTS

Table IV-3 Change in Material Weight Loss (%) as a Function of Immersion Time: AC Experiment

Immersion Time (weeks)	Type of Environment			
	D112	D25	S25	A25
2	0.13	0.22	0.69	1.99
4	0.35	0.42	0.86	2.47
8	0.44	0.54	1.19	3.44
12	0.47	0.61	1.75	3.84

Table IV-4 Calcium Ion Concentration: AC Experiment

Time (weeks)	Ca^{++} Concentration ($mg.L^{-1}$ as $CaCO_3$)			
	D112	D25	S25	A25
0.5	20	53	264	1,060
1.0	42	76	382	1,440
1.5	53	92	481	1,736
2.0	61	97	563	2,150
3.0	81	126	675	2,550
4.0	100	141	780	2,850
5.0	106	148	880	3,200
6.0	116	168	960	3,525
7.0	115	160	995	3,700
8.0	116	162	1,040	3,870
9.0	120	168	1,020	4,050
10.0	128	184	1,100	4,300
11.0	124	180	1,160	4,800
12.0	128	180	1,180	5,100

Table IV-5 Aluminum Ion Concentration: AC Experiment

Time (weeks)	AL^{+++} Concentration ($mg.L^{-1}$ as $AL_2O_3 . 3H_2O$)			
	D112	D25	S25	A25
2	< 1	< 1	12	51
4	< 1	< 1	38	100
8	< 1	< 1	146	147
12	< 1	< 1	188	208

Table IV-6 Loss in Wet Flexural Properties: AC Experiment

Time (weeks)	D112		D25		S25		A25	
	1-S/SO	1-E/EO	1-S/SO	1-E/EO	1-S/SO	1-E/EO	1-S/SO	1-E/EO
2	0.089	0.148	0.273	0.269	0.217	0.208	0.206	0.212
4	0.224	0.204	0.253	0.215	0.290	0.205	0.277	0.215
8	0.280	0.296	0:299	0.285	0.333	0.295	0.306	0.250
12	0.336	0.322	0.350	0.279	0.375	0.385	0.408	0.324

Table IV-7 Loss in Wet Barcol Hardness: AC Experiment

Time (weeks)	D112	D125	S25	A25
	1-H/HO	1-H/HO	1-H/HO	1-H/HO
2	0.193	0.220	0.301	0.359
4	0.190	0.247	0.283	0.533
8	0.244	0.301	0.393	0.619
12	0.261	0.271	0.445	0.790

Table IV-8 Desorption Slope: AC Experiment

Environ-ment	Immersion Time (weeks)							
	2		4		8		12	
Type	Sd $(mins)^{-\frac{1}{2}}$	R^2	Sd $(mins)^{-\frac{1}{2}}$	R^2	Sd $(mins)^{-1/2}$	R^2	Sd $(mins)^{-1/2}$	R^2
D112	0.007	0.931	0.007	0.968	0.010	0.984	0.009	0.978
D25	0.012	0.994	0.014	0.976	0.016	0.992	0.019	0.976
S25	0.011	0.992	0.015	0.970	0.019	0.982	0.019	0.990
A25	0.026	0.980	0.039	0.994	0.056	0.992	0.057	0.996

C. REGRESSION ANALYSIS: AC EXPERIMENT

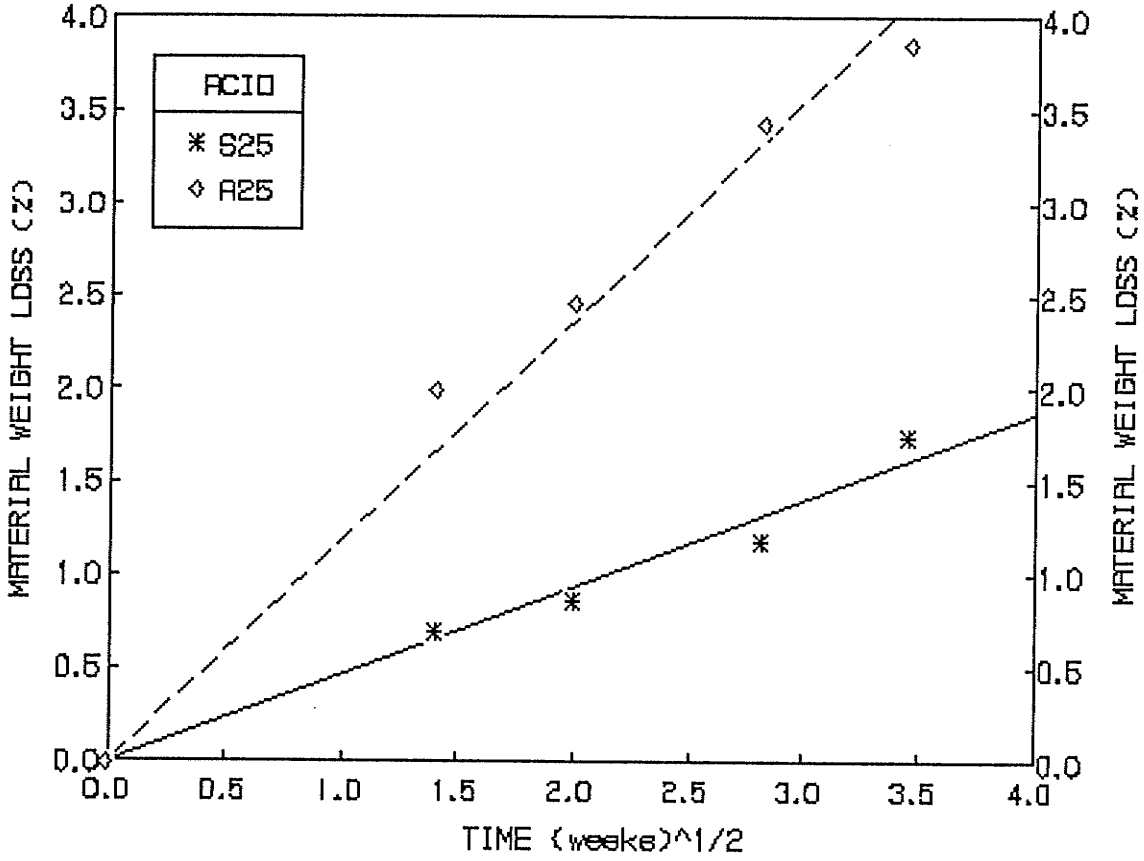

Figure IV-1 Linear regression analyses for material weight loss: S25 and A25

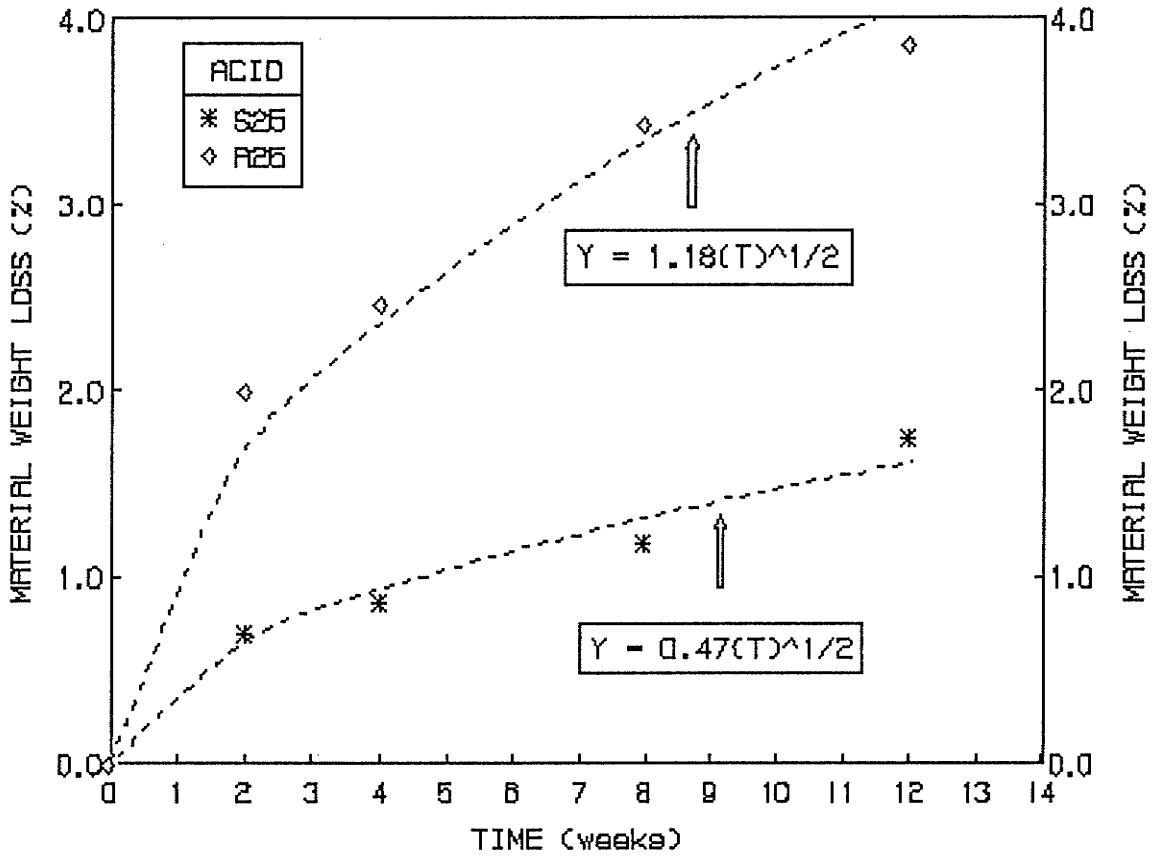

Figure IV-2 Empirical relationships for material weight loss: S25 and A25

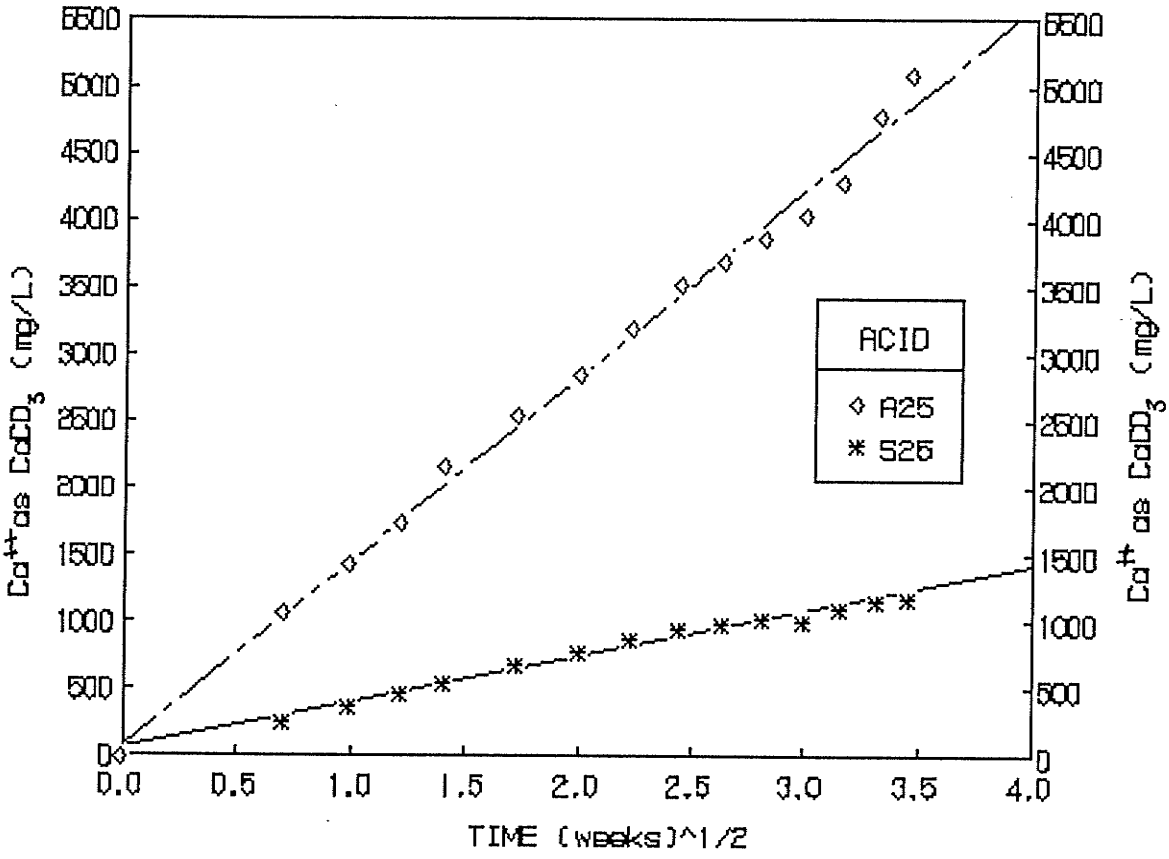

Figure IV-3 Linear regression analyses for calcium carbonate dissolution: S25 and A25

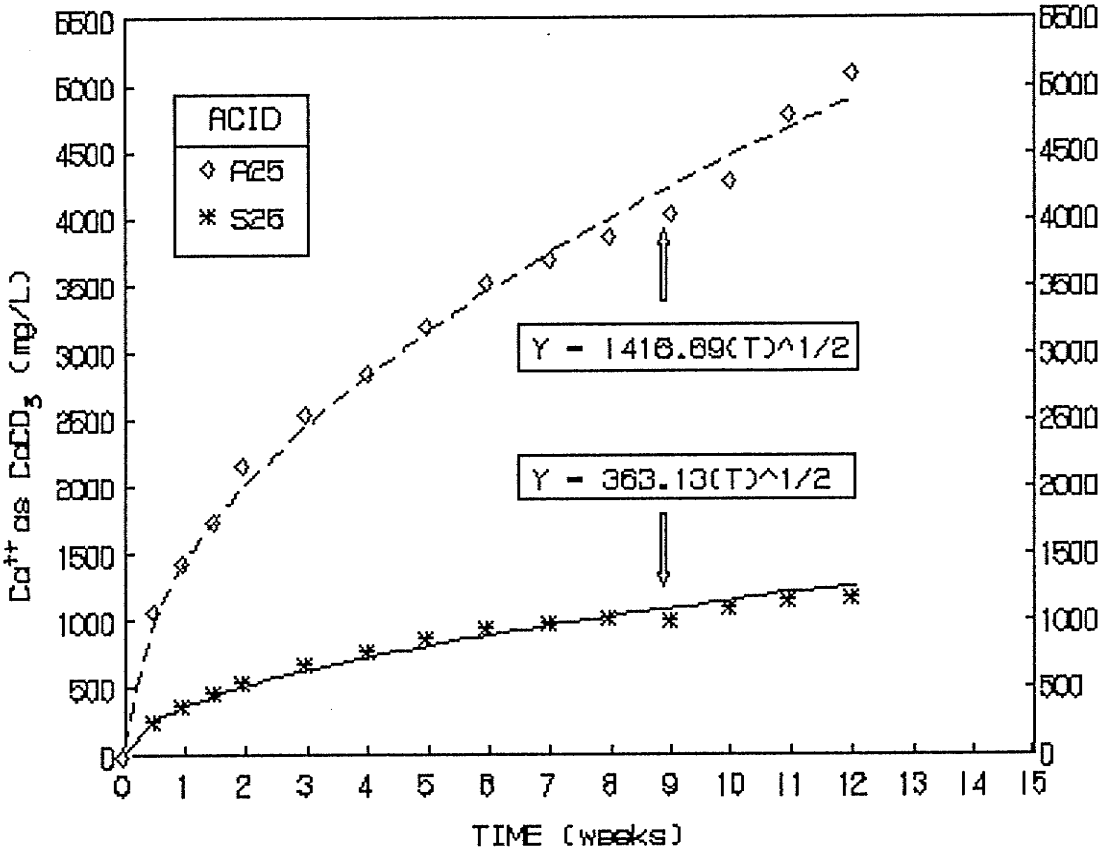

Figure IV-4 Empirical relationships for calcium carbonate dissolution: S25 and A25

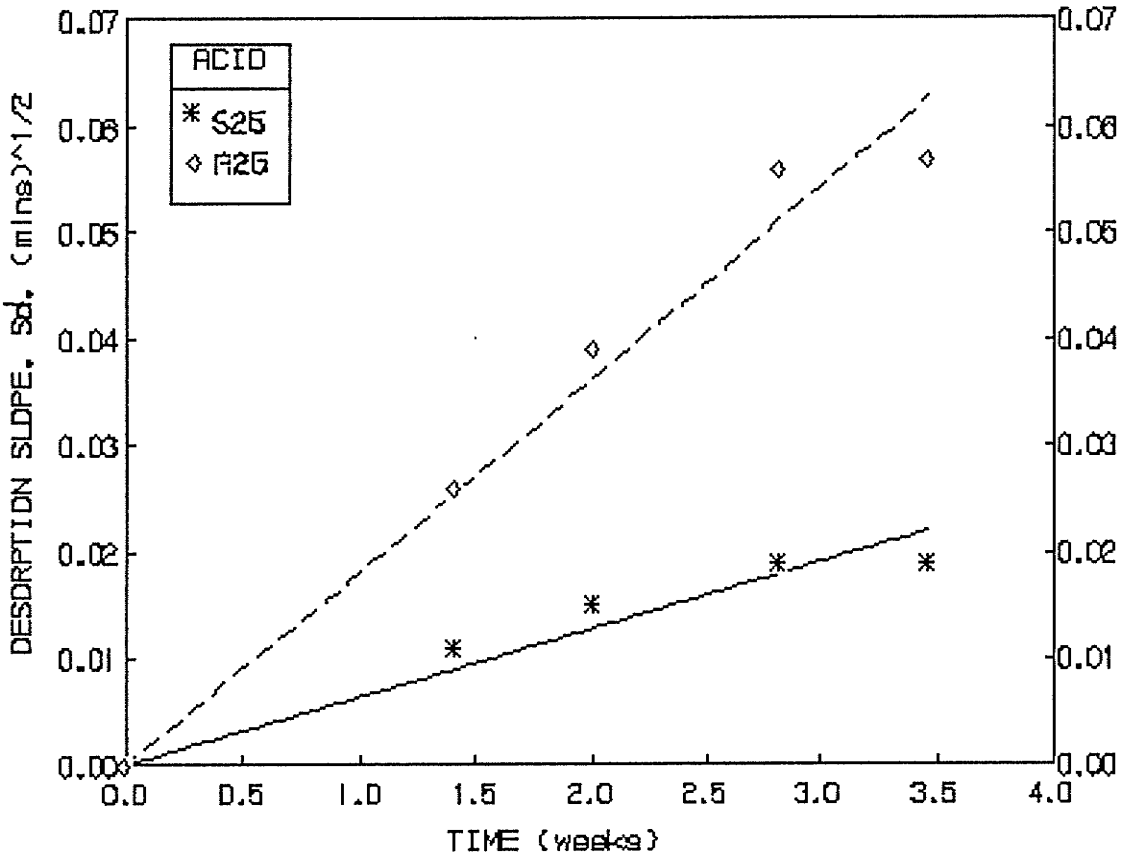

Figure IV-5 Linear regression analyses for diffusion properties: S25 and A25

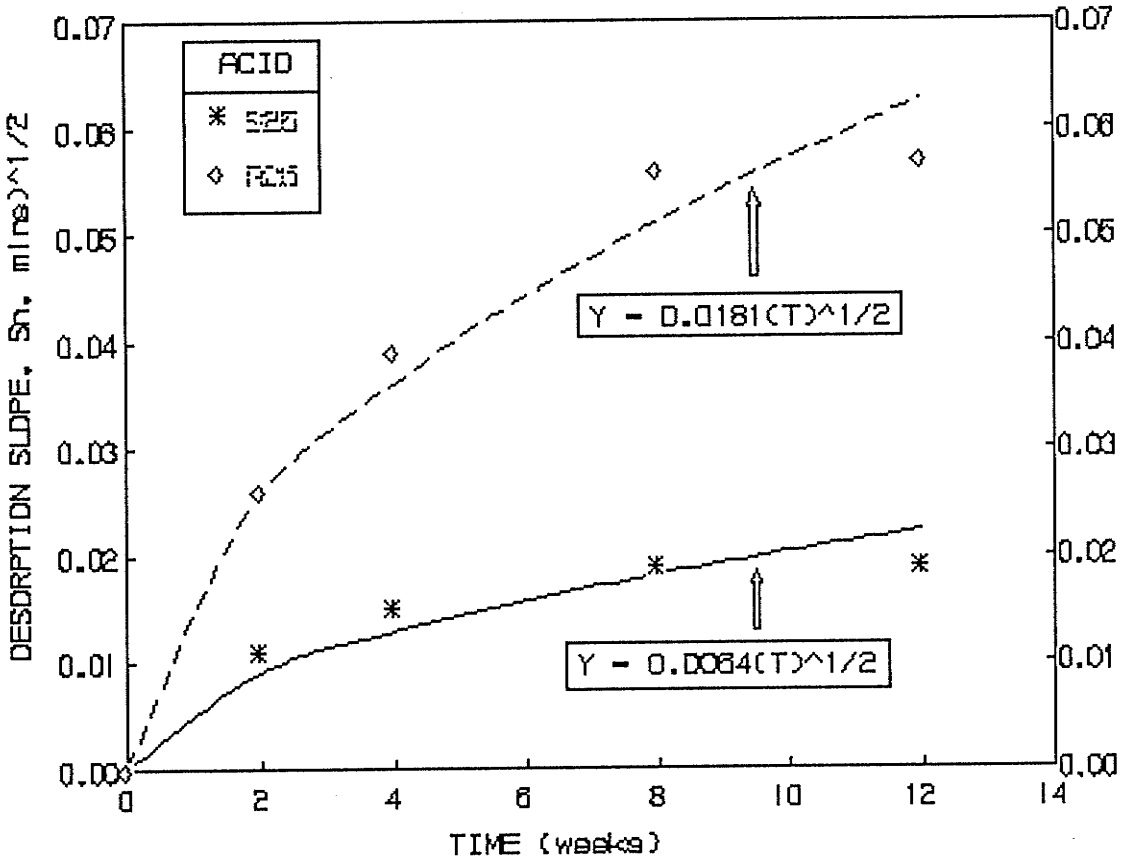

Figure IV-6 Empirical relationships for diffusion properties: S25 and A25

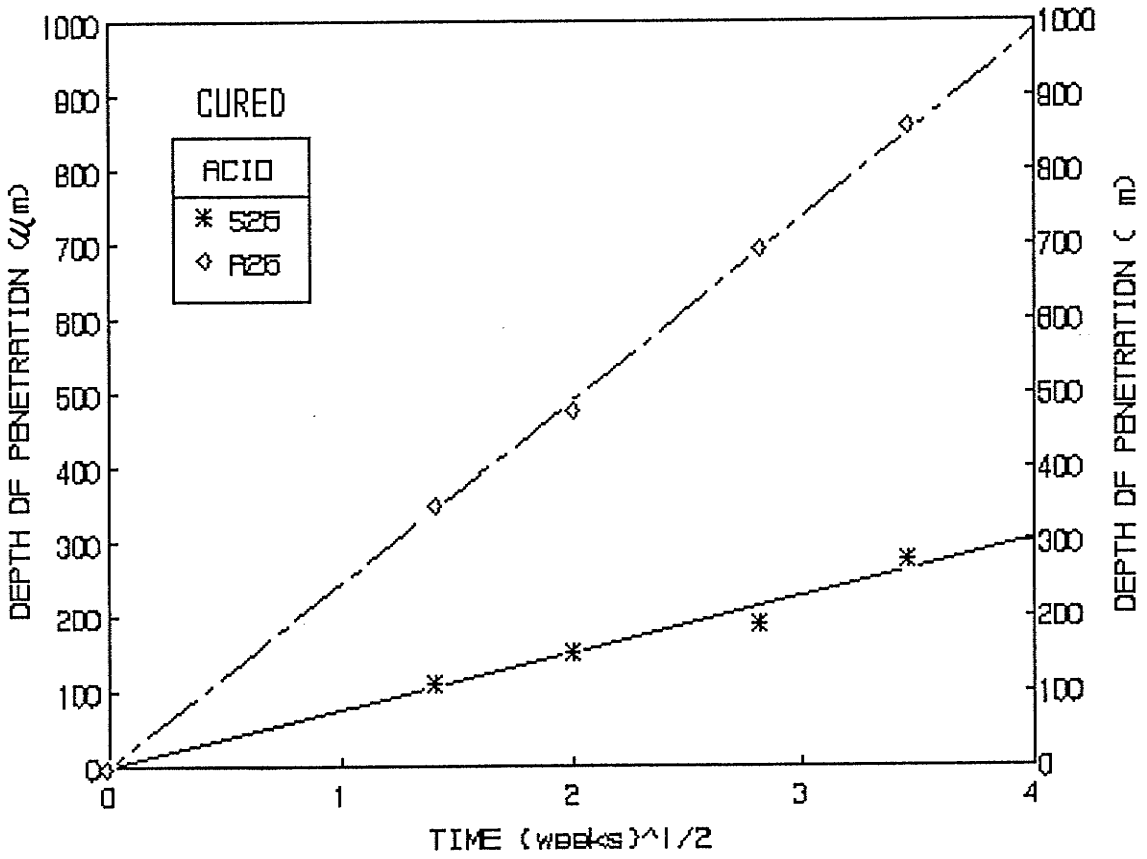

Figure IV-7 Linear regression analyses for depth of penetration (HC method): S25 and A25

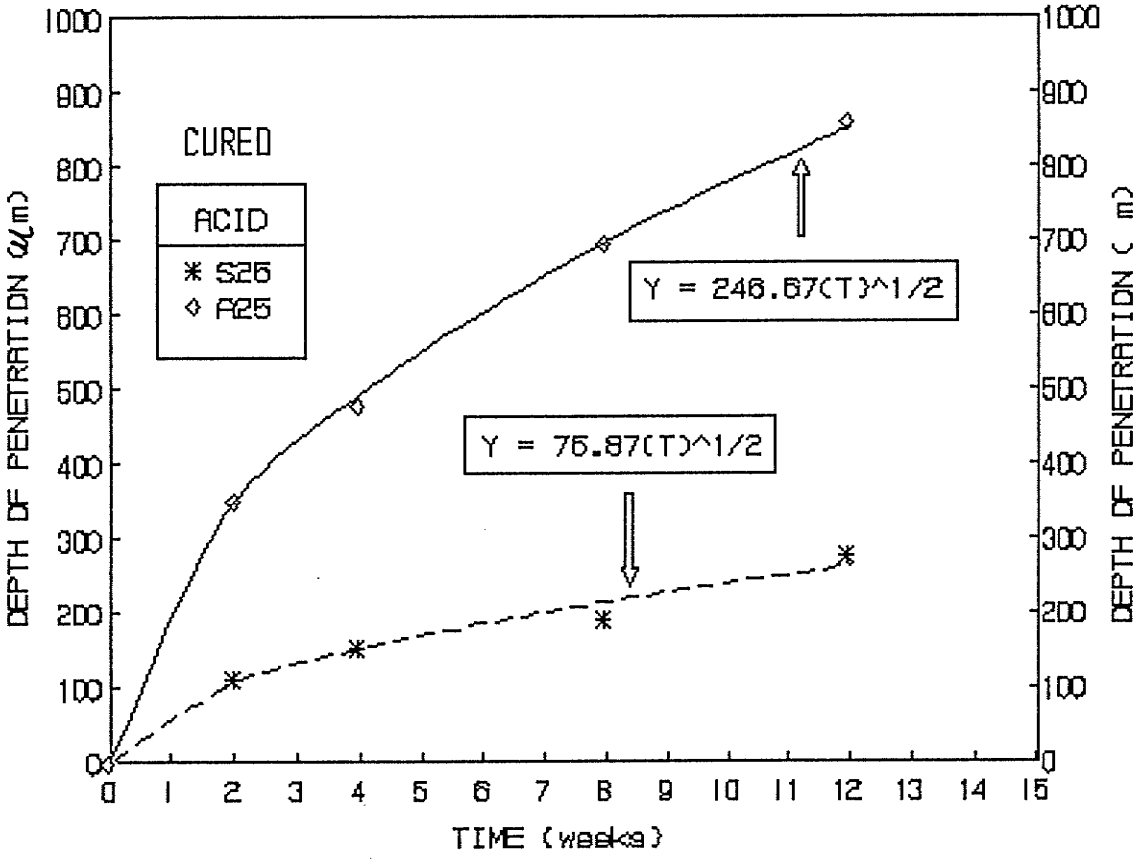

Figure IV-8. Empirical relationships for depth of penetration (HC method): S25 and A25

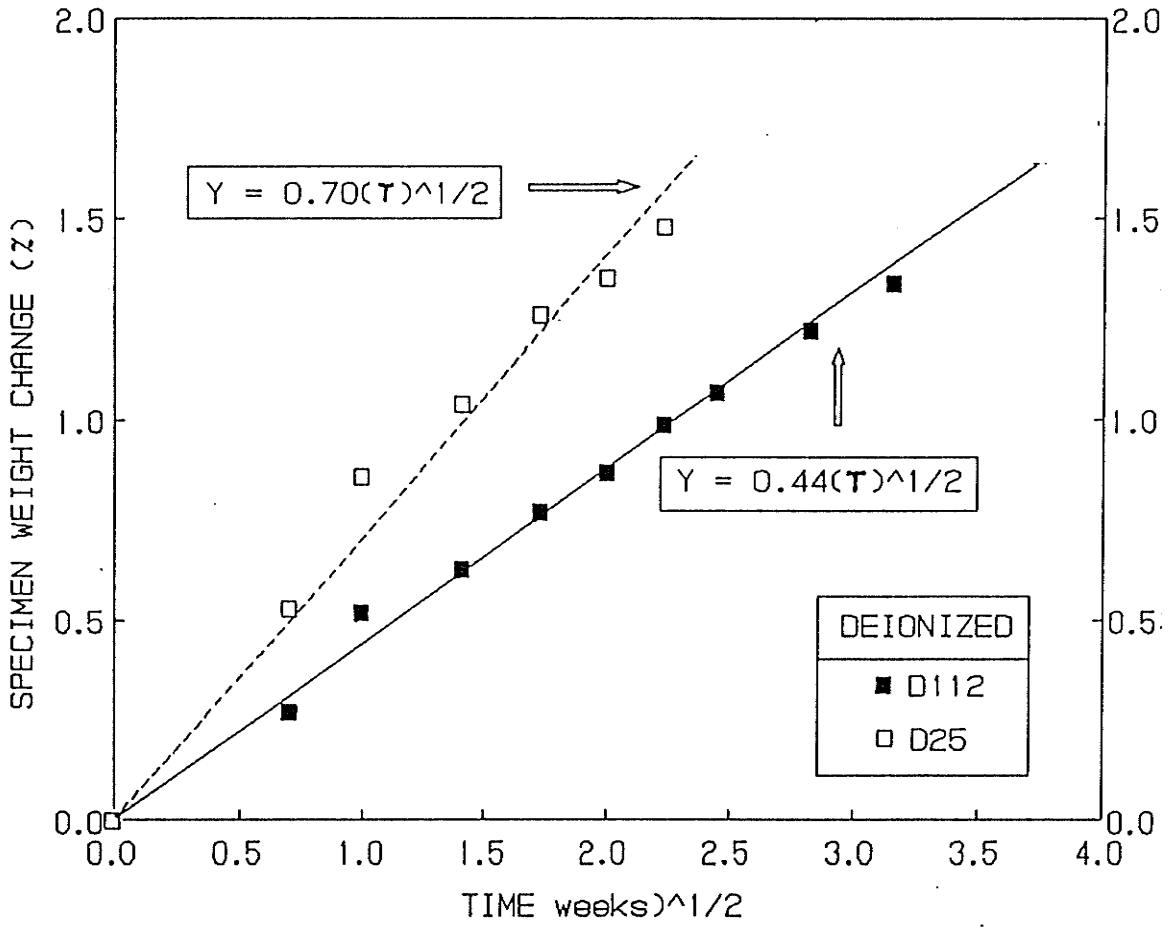

Figure IV-9 Linear regression analyses to determine absorption slopes (S_a) for deionized water specimens: AC experiment

D. DIFFUSION COEFFICIENT ANALYSIS: D25

Determination of straight line portion of the 45°C adsorption curve, as shown in Figure 6.3.

Y-Values	X-Values
0.00	0.000
0.53	0.707
0.86	1.000
1.04	1.414
1.26	1.732
1.35	2.000
1.48	2.236

r^2	=	0.933
y	=	0.703 x

Procedures as outlined by Shen and Springer:

STEP 1 Assume $D_x = 5.0 \times 10^{-6}$ mm^2/sec

STEP 2 Assume $t_1 = 5.06$ weeks ($t^1 < t_L$)

STEP 3 Calculate $M^1 = 0.703 (5.06)^{1/2} = 1.581\%$

STEP 4 Calculate $G_1 = 1 - \exp [-7.3t_1^{*(0.75)}]$

$$t_1^* = \frac{(D_x)\ (t_1)\ (7 \times 24 \times 3{,}600)}{S^2}$$

$S^2 = (2h)^2 = 92.16$ mm^2

$G_1 = 0.85$

STEP 5 Determine $M_{e_1} = M_1/G_1 = 1.581/0.85 = \underline{1.86\%}$

STEP 6 Pick $t_2{}^1 = 6.25$ weeks ($t_2 > t_L$)

STEP 7 Calculate $M_2 = 0.703 \sqrt{6.25} = 1.76\%$

STEP 8 Calculate $G_2 = 1 - \exp [-7.3t_2^{*(0.75)}]$

$$t_2^* = \frac{D_x \times t_2 \times 7 \times 24\ 3{,}600}{S^2}$$

$G_2 = 0.89$

STEP 9 Determine $M_{e_2} = M_2/G_2 = 1.76/0.89 = \underline{1.97\%}$

$M_{e_1} \approx M_{e_2}$: Therefore $D_x = 5.0 \times 10^{-6}$ mm^2/sec estimated initially was correct.

E. DIFFUSION COEFFICIENT ANALYSIS: D112

Determination of straight line portion of the 45°C adsorption curve, as shown in Figure 6.3.

Y-Values	X-Values
0.00	0.000
0.27	0.707
0.52	1.000
0.63	1.414
0.77	1.732
0.87	2.000
0.99	2.236
1.07	2.449
1.22	2.828
1.34	3.162

r^2	=	0.989
y	=	0.444 x

Procedures as outlined by Shen and Springer:

STEP 1 Assume $D_x = 1.5 \times 10^{-6}$ mm^2/sec

STEP 2 Assume $t_1 = 5.06$ weeks ($t_1 < t_L$)

STEP 3 Calculate $M_1 = 0.444\ (5.06)^{1/2} * (0.75) = 1.000\%$

STEP 4 Calculate $G_1 = 1 - \exp\ [-7.3 t_1^*]$

$$t_1^* = \frac{(D_x)\ (t_1)\ (7 \times 24 \times 3{,}600)}{S^2}$$

$S^2 = (2h)^2 = 92.16$ mm^2

$G_1 = 0.53$

STEP 5 Determine $M_{e_1} = M_1/G_1 = 1.000/0.53 = \underline{1.88\%}$

STEP 6 Pick $t_2 = 6.25$ weeks ($t_2 > t_L$)

STEP 7 Calculate $M_2 = 0.444\ (6.25)^{1/2} * (0.75) = 1.11\%$

STEP 8 Calculate $G_2 = 1 - \exp\ [-7.3 t_2^*]$

$$t_2^* = \frac{(D_x)\ (t_2)\ (7 \times 24 \times 3{,}600)}{(92.16)}$$

$G_2 = 0.59$

STEP 9 Determine $M_{e_2} = M_2/G_2 = 1.11/0.59 = \underline{1.88\%}$

$M_{e_1} \approx M_{e_2}$: Therefore $D_x = 1.5 \times 10^{-6}$ mm^2/sec estimated initially was correct.

E. ACID-DEGRADED DIFFUSION COEFFICIENTS: SULFURIC ACID (S25) SPECIMENS

$$[44]\quad k = [(D_e)\ (C_{ab})]^{1/2\,1/2} \cdot (\rho_B)^{1/2}$$

a) $K = (75.9\ \mu m \cdot wk^{1/2})\ (10^{-3}\ mm \cdot \mu m^{-1})\ (165 \times 10^{-6}\ wk \cdot sec)^{1/2}$

$= (75.9)\ (10^{-3})\ (1.29 \times 10^{-3}) = 9.79 \times 10^{-5}\ mm \cdot sec^{-1/2}$

b) $[C_{AB}] = 10^{-2.23} = 5.89 \times 10^{-3}\ M \cdot L^{-1} = 5.89 \times 10^{-6}\ M \cdot cm^{-3}$

c) $\rho_B = (1.88\ g \cdot cm^{-3} \times 0.16) = 0.3008\ g \cdot cm^{-3}$

$= 3.008 \times 10^{-3}\ M \cdot cm^{-3}$

Substituting (a) (b) and (c) into [44]

$\therefore\ 9.79 \times 10^{-5}\ mm \cdot sec^{1/2} = [(D_d)(5.89) \times 10^{-6}\ M \cdot cm^{-3})]^{1/2}\ (3.008 \times 10^{-3}\ M \cdot cm^{-3})^{1/2}$

$(D_d)^{1/2} = (9.79 \times 10^{-5})\ (22.9)$

$D_d = 5.02 \times 10^{-6}\ mm^2 \cdot sec^{-1}$

$\therefore$ The diffusion coefficient in the degraded layer of S25 specimens is predicted to be $5.02 \times 10^{-6}\ mm^2 \cdot sec.^{-1}$

F. ACID DEGRADED DIFFUSION COEFFICIENTS: ACETIC ACID (A25) SPECIMENS

[44] $$K = [(D_d)\ (C_{AB})]^{1/2}\ (\rho_B)^{\frac{1}{2}}$$

a) $K = (246.7)\ (10^{-3})\ (1.65 \times 10^{-6})^{1/2}$

$= (246.7)\ (10^{-3})\ (1.29 \times 10^{-3}) = 3.18 \times 10^{-4}$ mm . $sec^{-1/2}$

b) $[C_{AB}] = 10^{-2.22} = 6.02 \times 10^{-3}\ M.L^{-1} = 6.02 \times 10^{-6}\ M.cm^{-3}$

c) $\rho_B = 3.008 \times 10^{-3}\ M.cm^{-3}$

Substituting (a) (b) and (c) into [44]

$\therefore\ 3.18 \times 10^{-4} = [D_d)\ (6.02 \times 10^{-6})]^{1/2}\ (3.008 \times 10^{-3})^{1/2}$

$(D_d)^{1/2} = (3.18 \times 10^{-4})\ (22.4)$

$D_d = 5.07 \times 10^{-5}\ mm^2\ .\ sec^{-1}$

The diffusion coefficient in the degraded layer of A25 specimens is predicted to be $5.07 \times 10^{-5}\ mm^2\ .\ sec^{-1}$